mgr farm. Andrzej Patyra

Wpływ wtórnych metabolitów roślinnych na regulację wydzielania insuliny i mechanizm leżący u jej podstaw

Rozprawa na stopień doktora nauk medycznych i nauk o zdrowiu

w dyscyplinie nauki farmaceutyczne

Promotor: prof. dr hab. Anna Karolina Kiss

Ko-Promotor: prof. dr hab. Catherine Oiry-Cuq

Katedra i Zakład Biologii Farmaceutycznej

Obrona rozprawy doktorskiej przed Radą Dyscypliny Nauk Farmaceutycznych

Warszawskiego Uniwersytetu Medycznego

Warszawa 2023

Acknowledgements

This thesis was carried out within the Department of Pharmaceutical Biology, Faculty of Pharmacy of the Medical University of Warsaw under the supervision of Anna Karolina KISS and within the Cellular Pharmacology team (F13) of the Institut des Biomolecules Max Mousseron, Université de Montpellier under the supervision of Catherine OIRY-CUQ. I would like to extent my heartfelt appreciation to them for their invaluable guidance, encouragement, and continuous support throughout this research journey. Their expertise, patience, and insightful feedback have been instrumental in shaping the direction of my work.

I am indebted to my collaborators, Jérémie NEASTA, Michel VIGNES, Jean-François QUIGNARD, Marta DUDEK and Sylvie PERALDI-ROUX, for their tireless efforts and collaborative spirit. Their willingness to share their knowledge and engage in stimulating discussions significantly enriched my research and broadened my understanding of the subject.

I am deeply thankful to my colleagues, Justine VAILLE, Julie SCHWARTZ, and Małgorzata KOŁTUN-JASION, who participated in this study and generously shared their time and experiences. Without their cooperation, this research would not have been possible.

I extend my thanks to all my labmates and research staff for their camaraderie and helpful discussions. Their insights and collaboration have been instrumental in overcoming research challenges and has provided me with a conducive environment to pursue my academic aspirations.

I would like to thank Monika MARCINIAK, Małgorzata LIPOWSKA, Sebastian PEŁKA and Sebastian DOKTÓR for their technical assistance.

To my family, fiancée, and friends, I extend my sincerest thanks for their unwavering support, understanding, and encouragement during the challenging moments of this journey. Their love and belief in me have been a constant source of motivation. Thank you for being an essential part of this thesis work.

Funding

Phytochemical study of conifer wood extracts and pharmacological evaluations of their metabolites were funded by the National Science Centre, Poland, PRELUDIUM 20 grant 2021/41/N/NZ7/00313, entitled: “Wood from pine family (*Pinaceae*) native to Poland as a potent source of pharmacologically active lignans”; Principal Investigator: Andrzej Patyra.

NATIONAL SCIENCE CENTRE POLAND

Phytochemical study of *Angelica* L. root extracts and pharmacological evaluation of their metabolites were funded by the Ministry of Education and Science, Poland, Studenckie Koła Naukowe tworzą innowacje grant SKN/SP/533710/2022, entitled: “Searching for new innovative drugs among compounds of natural origin”; Project Manager: Sebastian Granica; Project Executive: Andrzej Patyra.

Ministry of Education and Science

French Government scholarship for doctorate degree training in Institute des Biomolecules Max Mousseron, Université de Montpellier, France, was granted to Andrzej Patyra by Campus France, N° 132828P.

RÉPUBLIQUE FRANÇAISE
Liberté
Égalité
Fraternité

CAMPUS FRANCE
POLOGNE

Two short research visits were funded by the Polish National Agency For Academic Exchange, Poland, through the PROM program “International scholarship exchange of PhD candidates and academic staff” and the STER program “Internationalization of Doctoral Schools”.

NAWA POLISH NATIONAL AGENCY FOR ACADEMIC EXCHANGE

Table of Contents

List of Figures

List of Tables

List of abbreviations

$[Ca^{2+}]_i$	intracellular calcium concentration
ACh	acetylcholine
ACS	American Chemical Society
ADP	adenosine diphosphate
AMPK	AMP-activated protein kinase
ATP	adenosine triphosphate
BK	large conductance calcium-activated potassium channels
BSA	bovine serum albumin
CaMK II	calcium/calmodulin dependent protein kinase II
cAMP	cyclic adenosine monophosphate
CC	column chromatography
CoA	coenzyme A
COSY	correlation spectroscopy
CPR1	cytochrome P450 oxidoreductase 1
CREB	cAMP response element-binding protein
CRP	C-reactive protein
DAD	diode array detector
DMSO	dimethyl sulfoxide
DP	dirigent protein
DPBS	Dulbecco's phosphate-buffered saline
DPP-4	dipeptidyl peptidase-4
EC_{50}	half maximal effective concentration
EDTA	ethylenediaminetetraacetic acid
EGTA	ethylene glycol-bis(β-aminoethyl ether)-N,N,N',N'-tetraacetic acid
EMA	European Medicines Agency
ERK	extracellular signal-regulated kinases
ESI	electrospray ionization
FCS	fetal calf serum
FRET	fluorescence resonance energy transfer
GABA	γ-aminobutyric acid
GPCR	G protein-coupled receptors
GIP	gastric inhibitory peptide
GK rat	Goto Kakizaki rat
GLP-1	glucagon-like peptide-1
GLP-1R	glucagon-like peptide-1 receptor
GLUT	glucose transporter
HbA_{1c}	glycated hemoglobin
HBSS	Hanks' balanced salt solution
HEPES	4-(2-hydroxyethyl)-1-piperazineethanesulfonic acid
hIAPP	human islet amyloid polypeptide
HMBC	heteronuclear multiple-bond correlation spectroscopy
HPLC or **LC**	high pressure liquid chromatography
HSQC	heteronuclear single quantum coherence spectroscopy
HTRF	homogenous time resolved fluorescence
IC_{50}	half maximal inhibitory concentration
IFG	impaired fasting glucose
i.g.	intragastric
IGT	impaired glucose tolerance
IK	intermediate conductance calcium-activated potassium channels
IL	interleukin
INF-γ	interferon gamma
iNOS	inducible nitric oxide synthase
IRS-1	insulin receptor substrate-1
K_{ATP}	ATP-sensitive potassium channel
K_{Ca}	calcium-activated potassium channels
KRB	Krebs-Ringer bicarbonate buffer
LPS	lipopolysaccharide
MMT	matairesinol *O*-methyltransferase
MTT	thazolyl blue tetrazolium bromide
MS	mass spectrometry
NALCN or **Na_{vi}**	sodium leak channels non-selective
NF-κB	nuclear factor kappa-light-chain-enhancer of activated B cells
NMR	nuclear magnetic resonance
OGTT	oral glucose tolerance test
OXPHOS	oxidative phosphorylation
PDX-1	pancreatic and duodenal homeobox 1
Ph. Eur.	European Pharmacopeia
PIP_2	phosphatidylinositol 4,5-bisphosphate
PKA	protein kinase A
PLR	pinoresinol/lariciresinol reductase
p.o.	per os; orally
PP	pancreatic polypeptide

PPAR-γ	peroxisome proliferator-activated receptor gamma
PSS	piperitol/sesamin synthase
REST	repressor element-1 silencing transcription factor
ROESY	rotating-frame nuclear Overhauser effect spectroscopy
RP	reversed phase
RPMI 1640	Roswell Park Memorial Institute medium
SERCA	sarco/endoplasmic reticulum Ca^{2+}-ATPase
SGLT2	sodium-glucose co-transporter 2
SID	secoisolariciresinol dehydrogenase
SK	small conductance calcium-activated potassium channels
SNARE	soluble *N*-ethylmaleimide-sensitive factor attachment proteins receptor
STZ	streptozotocin
T2DM	type 2 diabetes mellitus
TCM	Traditional Chinese Medicine
TEA	tetraethylammonium
TLC	thin layer chromatography
TNF-α	tumor necrosis factor alpha
T_r	retention time
TRP	transient receptor potential
UHPLC	ultra-high performance liquid chromatography
UV	ultraviolet
VGCC or **Ca_v**	voltage-gated calcium channels
VGKC or **K_v**	voltage-gated potassium channels
VGSC or **Na_v**	voltage-gated sodium channels
VRAC	volume-regulated anion channels
WHO	World Health Organization

Introduction

In recent decades, the prevalence of Type 2 Diabetes Mellitus (T2DM) has risen to alarming levels, evolving into a global health crisis (the only non-infectious epidemic) with profound social and economic implications. Characterized by chronic hyperglycemia and impaired insulin sensitivity, T2DM poses a multifaceted challenge that demands innovative and effective therapeutic strategies. Existing pharmaceutical interventions, though essential, often come with adverse effects and limitations, underscoring the urgent need for novel therapeutic approaches. One such approach is the utilization of plant secondary metabolites – a diverse group of bioactive compounds synthesized by plants for various ecological functions.

The investigation of plant secondary metabolites for managing T2DM offers a unique perspective, combining elements of natural product chemistry and pharmacology. The evolutionary adaptation of plants to environmental challenges has led to the development of an astonishing array of secondary metabolites, many of which exhibit bioactivity that may be harnessed to modulate critical molecular pathways involved in diabetes pathophysiology.

The most successful story of plant use in developing a first-line antidiabetic therapy is that of *Galega officinalis* L. (goat's rue, Italian fitch, French lilac) and its metabolites. In medieval Europe, the aerial parts of this plant were used in traditional medicine to address various conditions, including bubonic plague, worms, epilepsy, snake bites, and fever. Some records suggest that the plant may have been used to alleviate symptoms now attributed to T2DM, such as polyuria. Since the 17th century, it has become widely cited for treating diabetes in herbal pharmacopeias. In the following centuries, major metabolites of *G. officinalis* were identified and isolated, i.e., guanidine and its derivatives: galegine and hydroxygalegine. They were later found to possess hypoglycemic activity in animal studies. However, the dose necessary to achieve the glucose-lowering effect of natural and synthetic guanidine derivatives was too toxic for clinical use. With the rising availability of insulin in the 1930s, they were soon forgotten. The guanidines were rediscovered in the 1950s by Jean Sterne, who found that a synthetic biguanide, metformin, had a favorable glucose-lowering efficacy with minimal adverse effects compared to other derivatives. Today metformin is a first-line antidiabetic drug, listed on the World Health Organization's List of Essential Medicines, and one of the three most prescribed drugs in the USA (after atorvastatin and levothyroxine, the former being also a derivative of a natural compound).

The hypoglycemic effect of plant extracts and their metabolites may arise due to many different mechanisms and targets. In the above case of *G. officinalis* and guanidines, it was the

improvement of insulin sensitivity in peripheral tissues. Others inhibit alpha-glucosidase, alpha-amylase, and other intestinal enzyme activity, delaying glucose digestion and absorption. The metabolism of lipids and glucose may be altered, or the activity may be simply antioxidant or anti-inflammatory. Finally, plant extracts and their metabolites may target β-cell function, modulating insulin secretion. This activity is not so commonly studied as the others, yet there have been numerous reports on the insulinotropic activity of single plant metabolites, and such activity was found for some plant extracts.

Pharmacological investigations directed towards enhancing β-cell function hold paramount significance in the quest for novel antidiabetic therapies. Pancreatic β-cells are essential in regulating glucose homeostasis, serving as the primary source of insulin secretion in response to elevated blood glucose levels. This intricate process is critical in maintaining normoglycemia and preventing hyperglycemia, a hallmark of diabetes mellitus.

The strategic focus on pancreatic β-cell function stems from its crucial role in the pathophysiology of T2DM, as progressive loss of β-cell function and decreased insulin secretion occurs in the context of insulin resistance. Several critical therapeutic objectives can be achieved by identifying pharmacological agents that enhance β-cell function. Firstly, such interventions can potentiate endogenous insulin secretion, thereby improving postprandial glucose control and reducing fasting hyperglycemia. Secondly, preservation or restoration of β-cell mass and function can contribute to sustained glycemic control over time. Thirdly, attenuating β-cell stress and apoptosis, often observed in the diabetic milieu, can extend β-cell survival and function. This, in turn, could potentially delay disease progression and the need for more aggressive interventions.

State of the art

1 Pancreatic β-cell

1.1 Anatomy and histology of pancreatic β-cell in humans and rodents

Pancreatic islets, also known as islets of Langerhans, are micro-organs located in the pancreas that play a crucial role in maintaining glucose homeostasis. They are round or ovoid in shape and composed of 50 to 3000 cells divided into five major types, classified based on the primary hormone they secrete. The main hormone-secreting cell types within the islets include β-cells (insulin), α-cells (glucagon), δ-cells (somatostatin), PP-cells (pancreatic polypeptide), and ε-cells (ghrelin) [1-4].

In rodents, such as mice and rats, the islets have a well-defined structure characterized by a central core of β-cells surrounded by α-cells, δ-cells, PP-cells, and ε-cells in the periphery. β-cells comprise 60-80% of the islet cells, while α-cells make up 15-20%, δ-cells less than 10%, and PP-cells together with ε-cells less than 1% [1, 3, 5]. This core-mantle arrangement is believed to facilitate homologous interactions between β-cells and optimize insulin secretion [2, 4, 6].

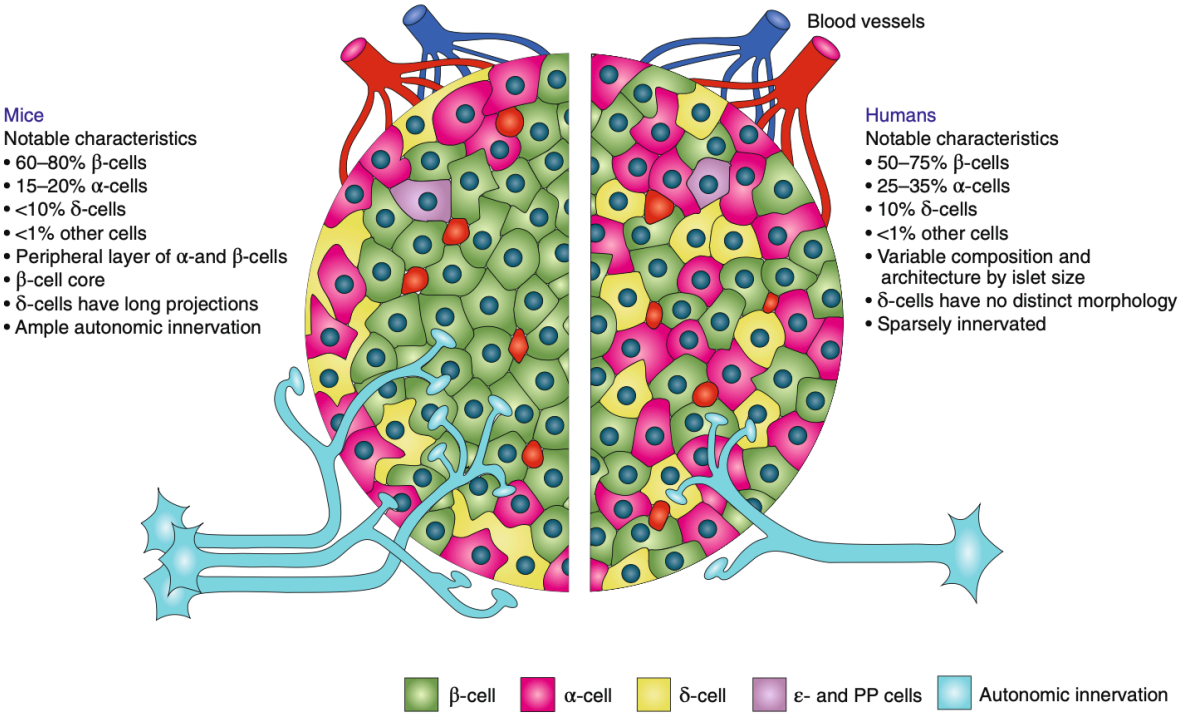

Figure 1. Pancreatic islet architecture comparison of mice and human [7].

However, human islets exhibit a different cellular organization compared to rodents. Human islets have a more scattered distribution of endocrine cells, and the α-, β-, and δ-cells appear to be

randomly distributed throughout the islet without a distinct core-mantle structure [1, 8]. The architecture of human islets is specific, facilitating close proximity of all endocrine cells to blood vessels and promoting interactions between β-cells and α-cells while also allowing for interactions among β-cells themselves [6]. Human islets also contain fewer β-cells and a higher percentage of α-cells than rodent islets. The proportion of endocrine cells within human islets can vary between individuals and different regions of the pancreas, with around 50-75% β-cells, 25-35% α-cells, 10% δ-cells and few PP and ε-cells [5, 9-11]. Studies have shown that islet structure can differ within species, depending on various physiological conditions such as diabetes, pregnancy, and obesity [8, 12].

Furthermore, interspecies comparisons have revealed variations in islet structure beyond rodents and humans. For instance, marsupial islets contain an increased presence of α-cells, and bird islets have an expanded presence of δ-cells. In some reptiles, the pancreatic tissue lacks distinct islets, and endocrine cells are dispersed throughout. These observations highlight the diversity in islet composition and architecture across different species (Figure 1) [5].

1.2 Physiology of the pancreatic β-cell

Pancreatic β-cells and neurons exhibit striking similarities in their physiology, function, gene expression, and developmental pathways, even though they do not have the exact embryological origin [13].

These similarities are evident in various aspects. For instance, the way β-cells store insulin, receive and process external stimuli, and release insulin resembles the process of neurons storing and releasing neurotransmitters. Both cell types utilize similar microvesicle assembly machinery [14-18]. Moreover, β-cells and neurons share organizational features such as cell adhesion molecules, migration signals, and associations with support cells [19-21].

The resemblance between β-cells and neurons is further emphasized by their comparable gene expression patterns [22-28]. For example, both cell types lack expression of the repressor element-1 silencing transcription factor (REST), a factor expressed in non-neuronal cells that suppresses the neuronal phenotype. REST target genes, including synaptotagmin, have been implicated in insulin expression and release. Additionally, REST regulates Pax-4, a transcription factor crucial for β-cell maturation [24]. Interestingly, several genes previously thought to be pancreas-specific, such as PDX1, HB9, and Islet-1, are transiently expressed during neural development [29, 30].

Endocrine cells, including β-cells, share certain characteristics with neurons. They can take up and decarboxylate amine precursors and produce polypeptide hormones akin to neurons [31, 32]. β-cells synthesize glutamate and employ it for intracellular signaling in glucose-responsive insulin secretion. They also express glutamic acid decarboxylase, an enzyme typically found in γ-aminobutyric acid (GABA)-secreting neurons. Furthermore, β-cells possess glutamate receptors, similar to those predominantly found in the central nervous system [14-16].

Moreover, pancreatic β-cells exhibit features resembling those of neurons, such as storing insulin in secretory granules released from synaptic-like microvesicles. β-cells can also generate action potentials like neurons, which may trigger insulin release. Additionally, neurons in the hypothalamus and β-cells respond similarly to changes in blood glucose levels. Schwann cells, major glial cells of the peripheral nervous system, surround and highly penetrate the islets, potentially serving as support cells for both islets and innervating neurons. The migration of pancreatic precursors and the association of islet cells within the islets involve molecules and mechanisms also seen in neuronal development and connectivity [17-21, 23, 27].

These remarkable similarities between β-cells and neurons highlight shared characteristics and processes, suggesting convergent functionalities and underlying molecular pathways. These similarities are necessary to understand the pancreatic β-cell's essential function, which is insulin secretion.

1.2.1 Glucose-induced insulin secretion

Insulin regulates blood glucose levels by enhancing glucose uptake and storing nutrients in muscle, fat, and liver tissues. Being the sole hormone responsible for lowering blood glucose and crucial for maintaining glucose balance, the secretion of insulin is tightly controlled. Any disturbance in this meticulously regulated process can lead to hypoglycemia or hyperglycemia, abnormal conditions characterized by low or high blood glucose levels respectively [33].

Insulin synthesis and secretion primarily occur in β-cells in response to food ingestion. While glucose is the most crucial stimulus, other nutrients and among them, amino acids like leucine [34], and free (non-esterified) fatty acids [35] can initiate insulin secretion. Many other nutrients act as potentiators or amplifiers of insulin secretion, enhancing the effects of initiators [36, 37], but cannot initiate the secretion independently. We can enumerate other amino acids like arginine, lysine,

alanine, and glutamate [38], neurotransmitters like acetylcholine (ACh) [39], incretins like glucagon-like peptide-1 (GLP-1) [40] and gastric inhibitory peptide (GIP) [41], other hormones like glucagon [42] and estrogens [43].

The primary signal for insulin secretion *in vivo* is typically neurotransmitters released upon sight or smell of food or incretins released from the gut in response to food presence. This is because resting glucose concentrations are sufficient to enable the action of these potentiators. These mechanisms prepare the body for the subsequent increase in plasma glucose levels and prevent excessive post-meal blood glucose elevation. It also explains why insulin secretion is higher in response to oral glucose than intravenous administration [44].

The process of insulin secretion in pancreatic β-cells is complex and involves electrical activity and fluctuations in intracellular calcium concentration ($[Ca^{2+}]_i$) [45]. Glucose enters the β-cell through the GLUT-1 (humans) or GLUT-2 (rodents, humans to a much smaller extent) transporters [46], and the rate-limiting step for insulin secretion is the initial phosphorylation of glucose mediated by glucokinase. This glucose metabolism generates ATP through the terminal oxidation pathway in mitochondria and thus increases the ATP/ADP ratio. This, in turn, leads to the closure of ATP-sensitive K^+ channels (K_{ATP}), resulting in membrane depolarization supported by an unidentified depolarizing conductance, possibly activity of the transient receptor potential (TRP) channels [47, 48].

When the glucose-induced depolarization reaches the threshold, β-cells display action potentials. The depolarizing phase of each action potential is mediated by the opening of voltage-gated Ca^{2+} channels (VGCC or Ca_v), with a contribution from voltage-gated Na^+ channels (VGSC or Na_v) [48, 49].

The subsequent increase in calcium triggers the exocytosis of insulin-containing vesicles through the regulation of docking and fusion processes mediated by soluble *N*-ethylmaleimide-sensitive factor attachment proteins receptor (SNARE) [50].

The repolarization phase involves rapid inactivation of VGCC and the opening of K^+ channels, primarily voltage-gated potassium channels (VGKC or K_v) and calcium-activated potassium channels (K_{Ca}), namely large conductance calcium-activated potassium channels (BK), intermediate conductance calcium-activated potassium channels (IK) and small conductance calcium-activated potassium channels (SK) [48, 49, 51].

Glucose may also directly modulate VGCC and VGKC channels, further influencing β-cell electrical activity [52, 53].

1.2.2 Ion channels and their role in insulin secretion

Ion channels play a crucial role in the activity of β-cells by controlling the flux of various ions, including potassium (K^+), sodium (Na^+), chloride (Cl^-), and calcium (Ca^{2+}), which generate both electrical and calcium signaling necessary for the secretion process (Figure 2). β-cells possess diverse channels that can be regulated at multiple levels, including transcription, translation, post-translational modifications, and intracellular trafficking. These channels allow β-cells to respond to both extracellular and intracellular signals, enabling them to finely tune their secretory activities [44, 48, 54].

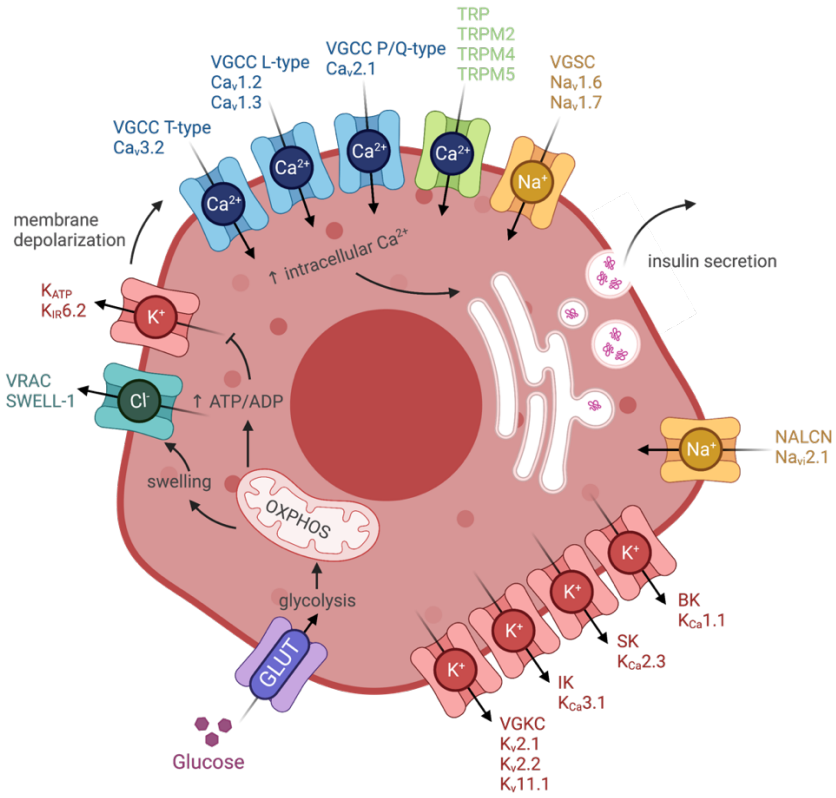

Figure 2. Ion channels that contribute to the pancreatic β-cell action potential and insulin secretion.

GLUT – glucose transporter (GLUT-1 or GLUT-2); VRAC – volume-regulated anion channels; K_{ATP} – ATP-sensitive potassium channels; VGCC – voltage-gated calcium channels; TRP – transient receptor potential channels; VGSC – voltage-gated sodium channels; BK – large conductance calcium-activated potassium channels; SK – small conductance calcium-activated potassium channels; IK – intermediate conductance calcium-activated potassium channels; VGKC – voltage-gated potassium channels; NALCN – non-selective voltage-independent sodium leak channel; OXPHOS – oxidative phosphorylation.

Over sixty different ion channels have been identified to be expressed in β-cells. These channels contribute to the regulation of insulin secretion under both physiological and pathological conditions [48].

The electrical excitability of the β-cell plasma membrane is essential for the physiological response to glucose stimulation, leading to Ca^{2+} entry and subsequent insulin secretion. The changes in the β-cell membrane potential are responsible for electrical excitability, and this potential is carefully controlled through the orchestrated opening and closing of various ion channels during the glucose stimulation [44, 48, 54].

1.2.2.1 ATP-sensitive potassium channels

ATP-sensitive potassium channels (K_{ATP}) are a type of inward-rectifying potassium channels gated by intracellular nucleotides, i.e., ATP and ADP. The K_{ATP} expressed in the β-cell is an octameric complex of 4 pore-forming $K_{ir}6.2$ subunits and four regulatory SUR1 subunits [55]. The $K_{ir}6.2$ subunits are susceptible to changes in ATP/ADP ratio and are inhibited by binding with ATP. On the other hand, the SUR1 subunits can further regulate the activity of $K_{ir}6.2$, as they possess binding sites for sulfonylureas and glinides (inhibitors), and diazoxide and magnesium-nucleotides (MgADP) complexes (activators) (Figure 3) [44, 56, 57].

At rest, the β-cell membrane potential sits near -70 to -80 mV, close to the potassium equilibrium potential, primarily due to the activities of K_{ATP} and a slight sodium leak through other small conductance channels, like the non-selective voltage-independent sodium leak channel (NALCN or Na_{vi}). When the ATP/ADP ratio increases due to glucose metabolism, K_{ATP} channels close, resulting in depolarization as the K^+ efflux is halted, but the Na^+ leak continues. Glucose metabolism also leads to β-cell swelling, activating volume-regulatory chloride current through SWELL-1, a volume-regulated anion channel (VRAC), causing Cl^- efflux and further depolarizing the membrane potential [48, 58].

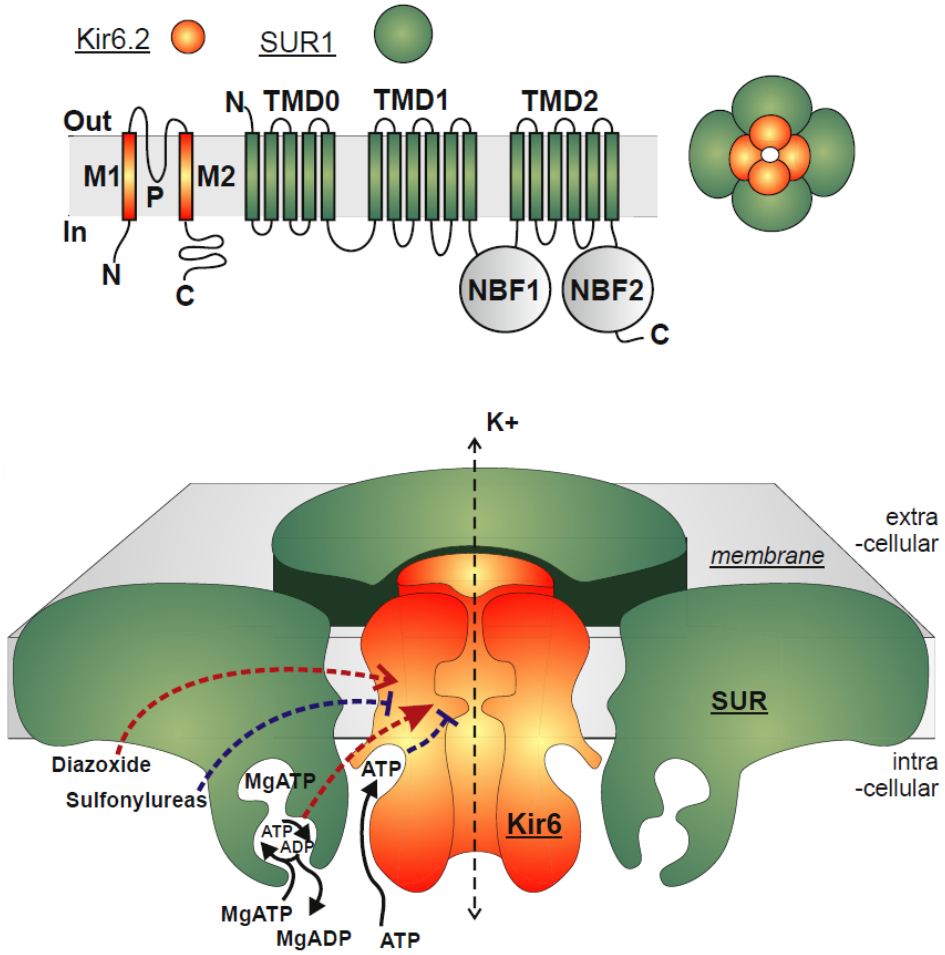

Figure 3. Schematic of ATP-sensitive potassium channel and its binding sites [59].

1.2.2.2 Transient Receptor Potential channels

TRP (transient receptor potential) channels play an essential role in insulin secretion in pancreatic β-cells [60]. These channels act as both ambient temperature sensors and modulators of cell functions. Several TRP channels, including canonical (TRPC) TRPC1, TRPC2, TRPC4 and TRPC6, vanilloid (TRPV) TRPV1, TRPV2, TRPV4 and TRPV5, and melastatin (TRPM) TRPM2, TRPM3, TRPM4 and TRPM5, have been identified in insulin-secreting cells [61].

Various stimuli, such as ligand binding, voltage changes, cell swelling, and temperature, trigger TRP channels' activation. These channels act as polymodal cellular sensors and contribute to changes in the concentration of cytosolic free Ca^{2+} by either allowing Ca^{2+} entry through the plasma membrane or modulating the membrane potential, thus affecting Ca^{2+} entry through other pathways. Consequently, TRP channels influence multiple Ca^{2+}-dependent cellular functions, including gene transcription, migration, cell death, and exocytosis [62].

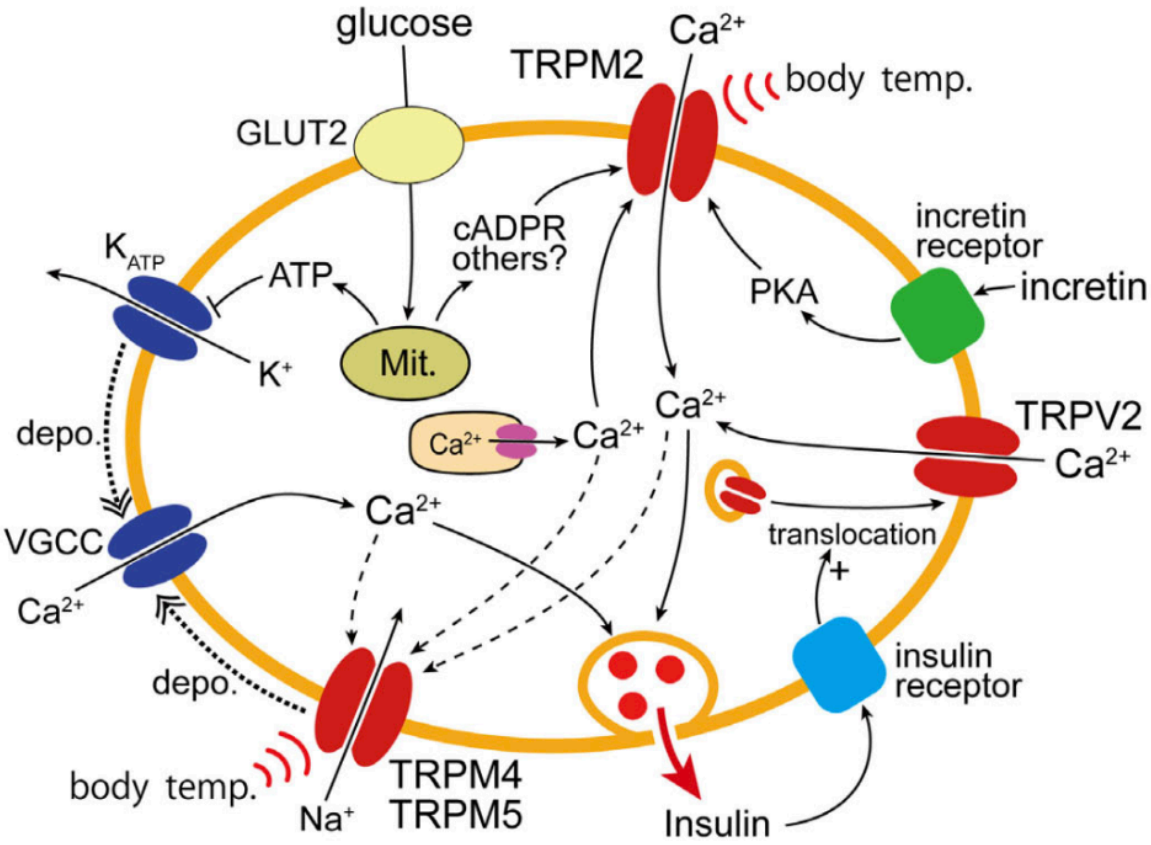

Figure 4. Transient receptor potential channels' role in insulin secretion [61].

The precise mechanisms by which TRP channels participate in insulin secretion are still being investigated. It is likely that the activation of TRP channels by different second messengers, including heat, swelling, membrane microdomain changes, arachidonic acid, cAMP, PIP_2, Ca^{2+}, and other unknown factors, influences the depolarization of β-cells, and together with the closure of K_{ATP} channels, shifts the membrane potential away from equilibrium, leading to insulin secretion (Figure 4) [61-64].

1.2.2.3 Leak sodium channels

The Na^+ leak channel, non-selective (NALCN), is a voltage-independent and tetrodotoxin-resistant sodium channel. In neurons, NALCN is responsible for the background Na^+ leak current that maintains the cells sufficiently depolarized to allow electrical activity (it counters K^+ hyperpolarizing efflux). However, in the β-cell, the NALCN forms a complex with the muscarinic acetylcholine receptor M_3 and is responsible for the depolarizing effect of the Ach [65, 66]. Its role in neurons as a counterbalance against K^+ efflux is improbable in the β-cell, as silencing the *Nalcn* gene and removing

extracellular Na^+ in pancreatic models did not affect the cell membrane resting potential (Figure 5) [67, 68].

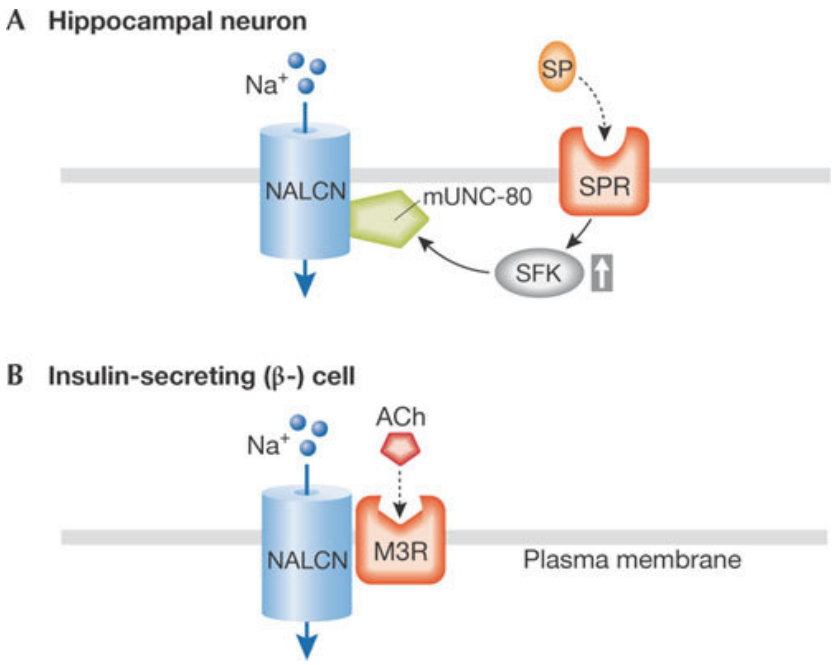

Figure 5. The non-selective voltage-independent sodium leak channel in neurons (A) and β-cells (B) [66].

1.2.2.4 Volume-regulated chloride channels

Glucose metabolism in the β-cell leads to increased cell volume, which we call swelling. To tackle this phenomenon and regulate cell volume, the β-cell expresses at low levels volume-regulated anion channels (VRAC), of which swell-activated chloride channel SWELL-1 is probably the most important. Activated by the increase in cell volume, the SWELL-1 produces Cl^- efflux, which may depolarize the cell membrane by 5-10 mV. In this context, VRAC/SWELL-1 may be essential in glucose-stimulated insulin secretion [44, 48, 69, 70].

1.2.2.5 Voltage-gated calcium channels

Voltage-gated calcium channels (VGCC) are responsible for the calcium entry into the β-cell during depolarization and consequently lead to insulin secretion. It is important to note that this extracellular source of calcium is almost entirely responsible for the rise in cytosolic Ca^{2+}. In contrast, the endoplasmic Ca^{2+} role is somewhat limited in glucose-induced insulin secretion [44, 71]. However,

it might still regulate β-cell electrical activity and is partially responsible (together with VGSC) for insulin secretion potentiated by ACh [72, 73].

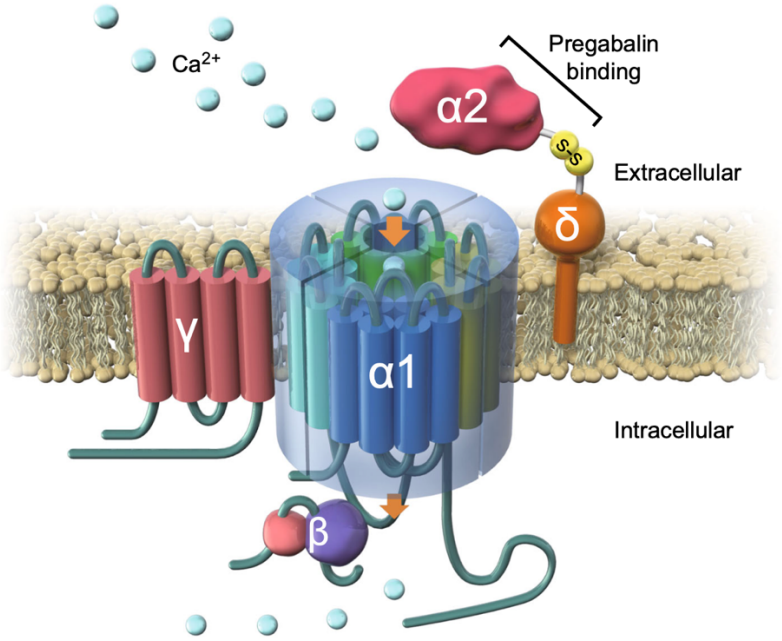

Figure 6. Structure of the voltage-gated calcium channel [74].

The VGCC consists of a large tetrameric pore-forming α_1-subunit, selective for Ca^{2+}, and three classes of auxiliary subunits, i.e., $\alpha_2\delta$, β and γ, the latter one being present only in skeletal muscle channels (Figure 6). Ten α_1-subunits were cloned and divided into five types based on their sensitivity to different blockers and the magnitude of the voltage activation [75, 76]. These types are:

- L-type calcium channels – also known as the "long-lasting". They are blocked by 1,4-dihydropyridine and are activated at high voltages. There are four channels of this type: $Ca_v1.1$, $Ca_v1.2$, $Ca_v1.3$, and $Ca_v1.4$, but only two are expressed in the β-cell, i.e., $Ca_v1.2$ and $Ca_v1.3$. They can also be blocked by verapamil and diltiazem and can be activated by (-)-(S)-BayK8644 [75] [44].
- P/Q-type calcium channels – from "Purkinje", the name of the cells where they were first discovered. They are blocked by ω-agatoxin and are activated at high voltages. The "P" and "Q" refer to alternative forms of $Ca_v2.1$, though, but usually, it is not possible to separate the P from the Q current [44, 75].

- N-type calcium channels – as “neural” or “non-L”. They are blocked by ω-conotoxin and are activated at high voltages. One channel of this type has been cloned, the $Ca_v2.2$ [44, 75].
- R-type calcium channels – from “residual”. They are blocked by SNX482 and are activated by intermediate voltages. The only representative of this group, $Ca_v2.3$, is weakly expressed in human and rodent β-cells [44, 75].
- T-type calcium channels – from “transient”. They are blocked by Z944 and activated at low voltages. In human β-cells, only $Ca_v3.2$ are present, out of the three known forms: $Ca_v3.1$, $Ca_v3.2$, and $Ca_v3.3$ [44, 75].

In the β-cell, the T-type channels, activated at about -60 mV, are probably responsible for slight cell membrane stimulation, facilitating further depolarization [49, 77]. The L-type channels, and particularly $Ca_v1.2$ together with the P/Q-type $Ca_v2.1$, are responsible for the calcium influx and rise in cytosolic Ca^{2+}, with the former more critical in high glucose concentrations [44, 49]. The role of R- and N-type channels is more ambiguous, with high discrepancies between transcriptomic (channel expression) and electrophysiological studies (current importance). The R-type channels may play a role in sustained insulin secretion and promote insulin-containing granules to the release sites, while the part of the N-type channels is not clear [44, 78].

1.2.2.6 Voltage-gated sodium channels

Voltage-gated sodium channels (VGSC) present in the pancreatic β-cell produce large tetrodotoxin-sensitive Na^+ currents. Like in other excitable cells, they and VGCC are primarily responsible for the depolarization phase of the action potential [44]. The channel consists of a large pseudotetrameric pore-forming α-subunit and one or two auxiliary β-subunits. Nine α-subunits ($Na_v1.1$ – $Na_v1.9$) and four β-subunits ($Na_vβ1$ – $Na_vβ4$) have been described [79]. In rodents, β-cells $Na_v1.7$ is predominantly expressed, while in humans, $Na_v1.6$ accounts for nearly half of all VGSC, with $Na_v1.7$, $Na_v1.3$, and $Na_v1.2$ expressed to a lesser extent. The differences exist also in the expression of the β-subunit. While in rodents, $Na_vβ1$ is dominantly expressed, in humans, $Na_vβ1$ and $Na_vβ3$ each account for about half of the transcripts [44, 80, 81].

In rodents, most VGSC ($Na_v1.7$) inactivate at very low membrane potentials, with half-maximal inactivation already at -100 mV. This implies that their role in firing action potential and, thus, insulin secretion is somewhat limited. However, the remaining 10-15% of channels ($Na_v1.3$ and $Na_v1.6$) are

sufficient to provide a depolarizing current of even higher importance than the VGCC [80]. As human β-cell express more VGSC types with higher inactivation potential, their role is much more pronounced in insulin secretion, though limited to low glucose concentrations [49, 77].

1.2.2.7 Voltage-gated potassium channels

The duration of action potentials in β-cells, found in mice and humans, is relatively brief, lasting around 5 ms in humans and 30–40 ms in mice [71, 82]. The rapid restoration of the resting potential is facilitated by the activation of voltage-gated potassium channels (VGKC). However, they are not necessary for repolarization, as the inactivation of VGCC and VGSC is sufficient to end the action potential, though in a much longer time [44, 71].

The K^+ selective pore of VGKC is built by four α-subunits which can be associated with auxiliary intracellular β-subunits. Forty different α-subunits are encoded in the genome, and additionally α-subunits forming a specific channel do not always belong to the same type, and as such heteromeric channels also exist [44, 75].

The expression of VGKC in human and mouse β-cells differ quite significantly [44]. In mice, the delayed rectifying current comes from the $K_v2.1$ and has a significant role in cell hyperpolarization [83]. The same cannot be said about human β-cells. Although they express $K_v2.2$ and $K_v1.6$ as channels that possess delayed rectifying ability, their time constant of activation is at least twice as long as the length of the action potential. Thus, the calcium-activated potassium channels play a more pronounced role in rapid repolarization in human β-cells [49, 82].

As for similarities in both species, $K_v11.1$ is dominantly expressed in humans and mice and is probably involved in action potential frequency modulation, prolonging the intervals between spikes [84].

1.2.2.8 Calcium-activated potassium channels

The repolarizing phase of the β-cell action potential relies on the involvement of calcium-activated potassium channels (K_{Ca}). Among these channels, the large conductance calcium-activated potassium channels (BK or $K_{Ca}1.1$) exhibit the highest expression in human β-cells. They can be activated by membrane depolarization and a rise in ($[Ca^{2+}]_i$), leading to calcium binding to the cytosolic

terminal COOH domain. The BK channels, being the largest and most rapidly activating potassium current during the action potential upstroke, play a crucial role in repolarizing the human β-cell action potential (as described above, VGKC is more important in mice). Inhibiting BK channels increases the amplitude of human β-cell action potentials and enhanced glucose-induced insulin secretion [44, 48, 49].

Other K_{Ca} channels, such as the small conductance calcium-activated potassium channels (SK), primarily the SK3 ($K_{Ca}2.3$) and the intermediate conductance calcium-activated potassium channels (IK or $K_{Ca}3.1$), are also present in human β-cells. Like their function in neurons, these channels regulate the frequency of β-cell action potentials. Activation of SK3 and IK occurs due to calcium influx during the action potential. It remains open after the action potential terminates, leading to after-hyperpolarization, thereby reducing the firing frequency [85-88]. The expression levels of *KCNN3* and *KCNN4*, the genes encoding SK3 and IK, respectively, are relatively low in human β-cells. Consequently, inhibition of IK modestly increases insulin secretion in human islets, while inhibition of SK3 does not have a significant effect [44, 48, 89, 90].

2 Type 2 diabetes mellitus

2.1 Definition

Type 2 diabetes mellitus (T2DM) is a chronic metabolic disorder characterized by insulin resistance and impaired insulin secretion. It is a significant global health concern with increasing prevalence and associated complications, which accounts for approximately 90% of all diabetes cases worldwide [91]. The development of T2DM involves a complex interplay of genetic, environmental, and lifestyle factors. Central to the pathogenesis of T2DM is the progressive dysfunction of pancreatic β-cells, leading to inadequate insulin secretion to counterbalance insulin resistance and subsequent hyperglycemia [92, 93]. Chronic hyperglycemia is associated with damage, dysfunction, and failure of various organs, especially the eyes (diabetic retinopathy), kidneys (diabetic nephropathy), nerves (diabetic neuropathy), heart (diabetic cardiomyopathy), and blood vessels (atherosclerotic cardiovascular disease, peripheral arterial disease) [94, 95].

2.2 Diagnosis

Diagnosis of diabetes is made based on blood glucose and glycated hemoglobin determinations, referring to the recommendations by various health organizations and authorities. Guidelines of the World Health Organization (WHO) [96, 97], American Diabetes Association [98], Polish Diabetology Society [94], and French High Authority of Health (HAS) [99] are generally in agreement that the diagnosis of T2DM should be based on random plasma glucose greater than or equal to 11.1 mmol/L (200 mg/dL), fasting plasma glucose greater than or equal to 7.0 mmol/L (126 mg/dL), or on glycated hemoglobin (HbA_{1c}) greater than or equal to 6.5% (48 mmol/mol). Furthermore, in an oral glucose tolerance test (OGTT), blood glucose levels measured after two h of a 75 g glucose load, can be used to diagnose T2DM with the same values as for random plasma glucose.

In some cases, the glucose levels measured through different tests are below the T2DM diagnosis criteria but higher than levels corresponding to normoglycemia. This state is sometimes referred to as pre-diabetes, and according to the abnormality (fasting or postprandial), it can be either called impaired fasting glycemia (IFG) or impaired glucose tolerance (IGT). The criteria to diagnose T2DM, IFG, and IGT are summarized in Table 1.

Table 1. Diagnostic criteria for T2DM, IGT, and IFG according to international recommendations.

Measurement	Polskie Towarzystwo Diabetologiczne (Polish Diabetology Society) 2023	Haute Autorité de santé (French High Authority of Health) 2014	American Diabetes Association 2021	World Health Organization 2006 / 2011
Type 2 diabetes mellitus				
Random plasma glucose	≥ 11.1 mmol/L (200 mg/dL) + symptoms	≥ 11.1 mmol/L (200 mg/dL)	≥ 11.1 mmol/L (200 mg/dL) + symptoms	≥ 11.1 mmol/L (200 mg/dL) + symptoms
Fasting plasma glucose	≥ 7.0 mmol/L (126 mg/dL)	≥ 7.0 mmol/L (126 mg/dL)	≥ 7.0 mmol/L (126 mg/dL)	≥ 7.0 mmol/L (126 mg/dL)
OGTT (2h)	≥ 11.1 mmol/L (200 mg/dL)	–	≥ 11.1 mmol/L (200 mg/dL)	≥ 11.1 mmol/L (200 mg/dL)
HbA_{1c}	≥ 6.5% (48 mmol/mol)	–	≥ 6.5% (48 mmol/mol)	≥ 6.5% (48 mmol/mol)
Impaired glucose tolerance				
OGTT (2h)	7.8 – 11.0 mmol/L (140 – 199 mg/dL)	7.8 – 11.0 mmol/L (140 – 199 mg/dL)	7.8 – 11.0 mmol/L (140 – 199 mg/dL)	7.8 – 11.1 mmol/L (140 – 200 mg/dL)
Impaired fasting glycemia				
Fasting plasma glucose	5.6 – 6.9 mmol/L (100 – 125 mg/dL)	6.1 – 6.9 mmol/L (110 – 125 mg/dL)	5.6 – 6.9 mmol/L (100 – 125 mg/dL)	6.1 – 6.9 mmol/L (110 – 125 mg/dL)

2.3 Epidemiology

The prevalence of T2DM has been rising rapidly worldwide, mainly due to the global increase in obesity, sedentary lifestyles, and unhealthy dietary patterns [91]. According to the International Diabetes Federation, approximately 537 million adults were living with diabetes in 2021, and this number is projected to reach nearly 800 million by 2045. In France, there were 3.5 million people undergoing anti-diabetic treatment in 2019 (5% of the population), and it was estimated that another million might have been unaware of their disease. According to the data of the Polish National Health Fund (NFZ), there were 2.5 million people treated for diabetes in Poland in 2017, which accounts for 8% of the adult population. However, it was estimated that only 80% of patients have been diagnosed, and thus the prevalence of this disease in the Polish population can be as high as 10% [100].

2.4 Pathophysiology

T2DM arises from a complex interplay of genetic predispositions, insulin resistance, and β-cell dysfunction, mainly due to glucotoxicity, lipotoxicity, incretin dysfunction, and chronic low-grade inflammation (Figure 7) [101].

Genetic factors play a substantial role in the development of T2DM. Multiple genes have been identified, affecting insulin signaling, β-cell function, and glucose metabolism. These genetic variations

contribute to an individual's susceptibility to T2DM and modulate the response to environmental factors. Genome-wide association studies have revealed numerous genetic loci associated with T2DM risk, providing valuable insights into the genetic basis of the disease [102].

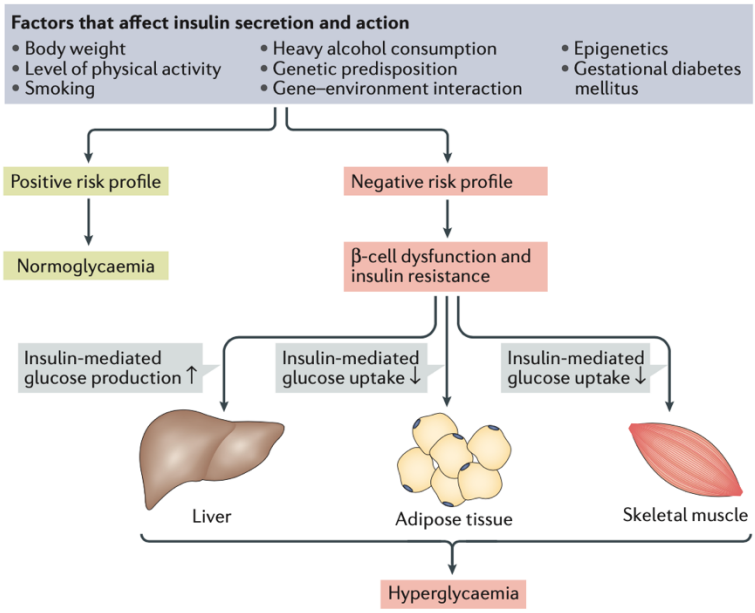

Figure 7. Pancreatic β-cell dysfunction and insulin resistance play a central role in the development of T2DM [103].

Insulin resistance is a hallmark feature of T2DM, characterized by a reduced responsiveness of target tissues to insulin [104]. Skeletal muscle, liver, and adipose tissue exhibit impaired glucose uptake and utilization, leading to hyperglycemia. Insulin resistance arises from various mechanisms, including dysregulated insulin signaling pathways, altered expression of insulin receptors, and abnormalities in intracellular glucose metabolism. Adipose tissue dysfunction, including increased release of pro-inflammatory adipokines and elevated circulating free fatty acids, further exacerbates insulin resistance, creating a vicious cycle [105].

The progressive dysfunction of pancreatic β-cells plays a pivotal role in developing T2DM [106]. Initially, β-cells compensate for insulin resistance by increasing insulin secretion. However, they fail to sustain adequate insulin production over time, resulting in persistent hyperglycemia. The impaired β-cell function involves multiple factors, including reduced insulin synthesis, altered insulin secretion dynamics, impaired proinsulin processing, and increased β-cell apoptosis. β -cell dysfunction may arise from genetic factors, oxidative stress, glucotoxicity, lipotoxicity, and chronic low-grade inflammation [107].

Chronic exposure to elevated glucose levels (glucotoxicity) and increased levels of free fatty acids (lipotoxicity) contribute to β-cell dysfunction and worsen insulin resistance [108]. Glucotoxicity occurs when β-cells are exposed to prolonged hyperglycemia, impairing insulin secretion, inducing oxidative stress, and mitochondrial dysfunction [109]. Lipotoxicity results from excessive accumulation of lipid intermediates, which disrupt insulin signaling pathways and impair β-cell function. Both glucotoxicity and lipotoxicity contribute to β-cell apoptosis, further deteriorating β-cell mass and function [110].

Incretins, such as glucagon-like peptide-1 (GLP-1), are crucial in regulating postprandial glucose homeostasis. They enhance insulin secretion, suppress glucagon release, and slow gastric emptying, collectively contributing to glycemic control. In individuals with T2DM, impaired incretin response and reduced GLP-1 secretion have been observed. This deficiency in incretin function leads to inadequate insulin secretion, compromised glucagon suppression, and impaired regulation of postprandial glucose levels. Incretin dysfunction may result from impaired incretin hormone production and release, reduced sensitivity of incretin receptors, or enhanced degradation of incretin hormones [111, 112].

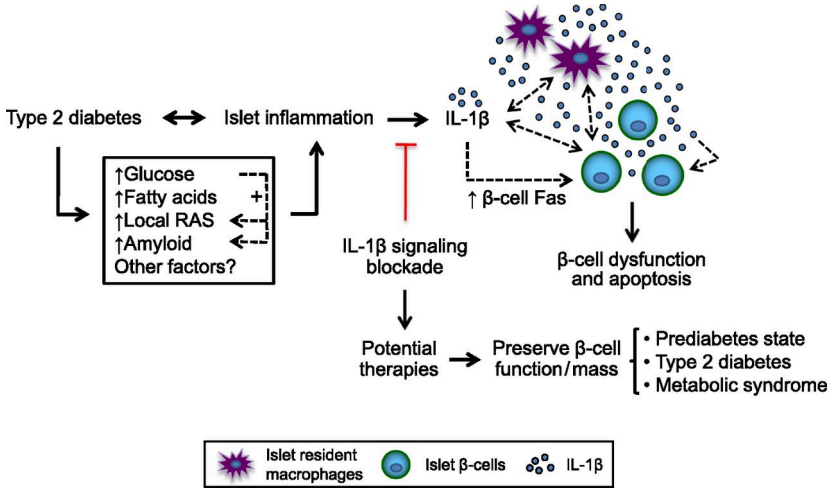

Figure 8. Role of inflammation in the development of T2DM [113].

Chronic low-grade inflammation is a prominent feature in patients with T2DM. Elevated levels of pro-inflammatory markers, such as C-reactive protein (CRP), tumor necrosis factor-alpha (TNF-α), interleukin-6 (IL-6), and other cytokines, have been observed [114]. Inflammatory processes contribute to insulin resistance by impairing insulin signaling pathways, promoting serine phosphorylation of insulin receptor substrate-1 (IRS-1), and activating stress kinases. Additionally, chronic inflammation can further worsen β-cell function and survival, exacerbating the progression of T2DM (Figure 8). This

inflammatory response may arise from various sources, including adipose tissue dysfunction, elevated circulating fatty acids, oxidative stress, and immune cell activation [115, 116].

2.5 Treatment

The initial management of T2DM involves lifestyle modifications, including dietary changes, physical activity, and weight management. These interventions are crucial in improving insulin sensitivity and glycemic control [117]. Dietary modifications may include reduced intake of simple sugars and saturated fats, increased consumption of dietary fiber, and portion control. Regular physical activity helps improve insulin sensitivity and reduces cardiovascular risk factors [118]. Weight loss, achieved through a combination of diet and exercise, is particularly important in overweight or obese individuals with T2DM [117].

2.5.1 Oral anti-diabetic agents

The biguanide metformin is the first-line oral anti-diabetic agent recommended for most patients with T2DM. It is a blood glucose levels-reducing agent, through a complex and still not entirely understood mechanism of action[119]. It primarily involves the inhibition of hepatic gluconeogenesis and glycogenolysis and the improvement of insulin sensitivity in peripheral tissues, such as liver, skeletal muscle, and adipose tissue [120, 121]. It was found to activate the AMP-activated protein kinase (AMPK), leading to metabolic adjustments in energy homeostasis [122]. This effect was connected to the inhibition of mitochondrial oxidative phosphorylation (OXPHOS) through the inhibition of mitochondrial respiratory chain complex 1 [123]. Furthermore, it limits the production of free fatty acids in adipose tissue, which contributes to improved insulin sensitivity [119]. Additionally, metformin is thought to reduce the activity of mitochondrial glycerol phosphate dehydrogenase and cAMP synthesis while also blocking glucagon's action. As a consequence, these processes enhance glucose uptake in the liver and skeletal muscles *via* the activation of glucose transporter (GLUT-4) [119]. Metformin's impact is not limited to these pathways alone. It also demonstrates an incretin effect, resulting in reduced glucose absorption in the intestines, an increase in GLP-1 concentration, and a positive influence on gut microbiota [124]. Furthermore, there are data that metformin may provide protection to pancreatic beta cells by modulating inflammatory responses and also possess cardioprotective, neuroprotective, and vasoprotective properties [119, 125, 126]. The use of metformin in T2DM is associated with a relatively favorable safety profile compared to other anti-

diabetic medications. The most common side effects are gastrointestinal in nature, including nausea, vomiting, diarrhea, and abdominal discomfort [127].

Sulfonylureas stimulate insulin secretion from pancreatic β-cells through binding to the sulfonylurea receptor (SUR1) on the β-cell membrane, leading to the closure of ATP-sensitive potassium channels (K_{ATP}) and subsequent depolarization of the cell membrane [128]. This depolarization triggers calcium influx, which promotes insulin exocytosis and enhances glucose uptake by target tissues [44, 128]. Sulfonylureas also improve glycemic control by reducing hepatic glucose production. Commonly used sulfonylureas include glibenclamide (glyburide), glipizide, glimepiride, and tolbutamide. While sulfonylureas have demonstrated efficacy in lowering blood glucose levels, their use may be associated with adverse effects, such as hypoglycemia and weight gain [129]. Despite the availability of newer anti-diabetic agents, sulfonylureas continue to be widely prescribed due to their affordability, long-term safety record, and proven efficacy in glycemic control [130]. Meglitinides (repaglinide and nateglinide), another class of insulin secretagogue agents, have the exact mechanism of action, though with a faster onset and shorter duration of the effect. Nevertheless, they possess similar adverse effects profiles, including the risk of hypoglycemia [131].

Dipeptidyl peptidase-4 (DPP-4) inhibitors (also known as gliptins), such as sitagliptin, linagliptin, vildagliptin, and saxagliptin, increase insulin secretion and reduce glucagon release by inhibiting the degradation of incretin hormones [132]. The primary function of DPP-4, a membrane enzyme, is to cleave and inactivate incretin hormones, specifically GLP-1 and GIP. GLP-1 and GIP are gut-derived peptides released in response to nutrient ingestion, and they have potent incretin effects, enhancing insulin secretion from pancreatic β-cells in a glucose-dependent manner. These incretins also suppress glucagon release from pancreatic α-cells, reduce gastric emptying, and promote satiety, collectively contributing to improved glucose control after meals. Upon release into the bloodstream, GLP-1 and GIP are rapidly degraded by DPP-4, resulting in a short half-life of these hormones. By cleaving the two incretins, DPP-4 limits their duration of action, thereby reducing their effectiveness in stimulating insulin and suppressing glucagon secretion [111, 132, 133]. DPP-4 inhibitors block the enzymatic activity of DPP-4, prolonging the action of endogenous GLP-1 and GIP and leading to enhanced glucose-dependent insulin secretion, decreased glucagon release, delayed gastric emptying, and increased satiety. These effects collectively improve postprandial glycemic control and overall glycemic management in T2DM without a significant risk of hypoglycemia. However, they primarily target the incretin system, and thus their glucose-lowering effects may not be as potent as those

achieved with other classes of anti-diabetic drugs. They are generally well-tolerated but may be associated with nasopharyngitis and upper respiratory tract infections [117, 132, 134].

Sodium-glucose co-transporter 2 (SGLT2) inhibitors, such as empagliflozin, canagliflozin, dapagliflozin, and ertugliflozin, reduce renal glucose reabsorption, leading to increased urinary glucose excretion. SGLT2 is a membrane-bound protein primarily found in the proximal tubules of the kidneys. Its essential role lies in the reabsorption of glucose from the glomerular filtrate back into the bloodstream. By reabsorbing glucose from the tubular fluid, SGLT2 plays a pivotal role in maintaining glucose homeostasis. In healthy individuals, SGLT2 reabsorbs the majority of filtered glucose, ensuring minimal glucose loss in the urine. SGLT2 inhibitors selectively block SGLT2's reabsorptive function, resulting in reduced glucose reabsorption and increased glucose excretion in the urine, known as glucosuria. By promoting the excretion of excess glucose, SGLT2 inhibitors help lower blood glucose levels, improve glycemic control, and reduce hyperglycemia-associated complications [135, 136]. Moreover, SGLT2 inhibitors may lead to additional beneficial effects beyond glycemic control. As a consequence of increased glucosuria, the body experiences osmotic diuresis, resulting in reduced blood volume and blood pressure. This diuretic effect, along with modest weight loss, may confer cardiovascular benefits in diabetic patients with hypertension and obesity, as well as in non-diabetic patients with heart failure. Thus, they are recommended for diabetic patients with heart failure. However, they can increase the risk of genital mycotic and urinary tract infections [94, 134, 137, 138].

Thiazolidinediones (also known as glitazones), such as pioglitazone and rosiglitazone, improve insulin sensitivity in adipose tissue, skeletal muscle, and the liver. They activate peroxisome proliferator-activated receptor gamma (PPAR-γ), which is primarily expressed in adipose tissue, skeletal muscles, and the liver. The activated PPAR-γ regulates the expression of various genes involved in glucose and lipid metabolism. Notably, PPAR-γ activation enhances insulin sensitivity by promoting the transcription of genes related to glucose uptake, such as GLUT-4 and adiponectin, thereby reducing blood glucose levels. In addition to their effects on glucose metabolism, thiazolidinediones also influence lipid metabolism. PPAR-γ activation results in increased expression of genes involved in fatty acid uptake and storage, leading to a decrease in circulating free fatty acids and triglycerides. Thiazolidinediones effectively lower blood glucose levels but may be associated with weight gain, fluid retention, and an increased risk of heart failure [117, 132, 134]. One significant limitation of thiazolidinediones' use is their potential to cause or exacerbate peripheral edema and congestive heart failure, particularly in patients with pre-existing cardiac conditions. As a result, they are generally contraindicated in individuals with or at risk of heart failure [134].

Alpha-glucosidase inhibitors, such as acarbose, target the enzymes known as alpha-glucosidases, which are primarily located in the brush border of the small intestine. The main function of alpha-glucosidases is to hydrolyze complex carbohydrates, such as starches and disaccharides, into simple sugars like glucose. This enzymatic activity facilitates the rapid absorption of glucose from the intestine into the bloodstream after a meal [139]. By inhibiting alpha-glucosidases, they slow down the digestion of carbohydrates, leading to a delayed and reduced absorption of glucose. The delayed carbohydrate absorption results in a blunted postprandial rise in blood glucose levels, particularly after carbohydrate-rich meals [140, 141]. Alpha-glucosidase inhibitors are generally well-tolerated but can cause gastrointestinal side effects, such as flatulence and diarrhea [117, 132].

2.5.2 Parenteral anti-diabetic agents

Glucagon-Like Peptide-1 (GLP-1) receptor agonists, also known as GLP-1 analogs, such as exenatide, dulaglutide, semaglutide, and liraglutide, mimic the effects of endogenous GLP-1 by activating GLP-1 receptors. They stimulate insulin secretion, suppress glucagon release, delay gastric emptying, and promote satiety. GLP-1 receptor agonists have shown significant efficacy in improving glycemic control and reducing body weight. They may be associated with gastrointestinal side effects, such as nausea and vomiting [40, 111].

Insulin therapy is essential for individuals with T2DM who have inadequate glycemic control despite the various anti-diabetic agents on the market. Exogenous insulin replaces the deficient endogenous insulin and improves glucose uptake in peripheral tissues. Various insulin formulations are available, including rapid-acting, short-acting, intermediate-acting, and long-acting insulins, allowing for individualized treatment regimens. Insulin therapy requires close monitoring of blood glucose levels and may be associated with the risk of hypoglycemia and weight gain [117].

3 Plant secondary metabolites as modulators of insulin secretion

Despite the development of numerous anti-diabetic medications, the side effects accompanying them, including hypoglycemia, gastrointestinal symptoms, heart failure, weight gain, edema, impaired kidney function, pancreatitis, and genital infections, present a downside to their use. The higher incidence rate of diabetes in low- and middle-income countries provides another challenge, which is the lack of availability of modern therapies or their cost being unaffordable for the majority of diabetic patients. In this context, plant extracts and their active constituents are considered an important area of seeking new anti-diabetic treatments [91, 142].

In traditional medicine systems, such as Traditional Chinese Medicine (TCM), Japanese Kampo, Indian Ayurveda, as well as African, Native American, and European traditional medicine, numerous plants were used to treat diabetes. The data on their efficacy is anecdotal, though some scientific evidence for more than 800 plants is present in the literature [142]. In many cases, the available data on plant extracts and their metabolites is somewhat limited. The effect may be only measured in terms of blood glucose, and thus the anti-diabetic effect (when found) has an unknown mechanism of action, and the active constituents responsible for the effect of the extract might be unknown.

The hypoglycemic effect of plant extracts may arise due to many different mechanisms and targets. Plant extracts, through their metabolites, may inhibit alpha-glucosidase, alpha-amylase, and other intestinal enzymes activity, delaying the digestion and absorption of glucose [143]. They can improve insulin sensitivity in peripheral tissues, like *Galega officinalis* L., which contains guanidine and its derivatives, that gave birth to the synthetic first-line drug metformin [144]. The metabolism of lipids and glucose may be altered, or the activity may be simply antioxidant or anti-inflammatory [145]. Finally, plant extracts and their metabolites may target β-cell function, modulating insulin secretion. This activity is not so commonly studied as the others, yet there have been numerous reports on the insulinotropic activity of single plant metabolites, i.e., flavonoids [146-148], lignans [149-151], coumarins [152-154] and others [155], as well as such activity, was found for some plant extracts [156-158].

3.1 Flavonoids

Flavonoids are plant secondary metabolites whose basic skeleton is built from 15 carbon atoms arranged in two benzene rings (ring A and B) joined by a propane (C_3) chain, which usually forms a heterocyclic third ring (ring C) with an oxygen atom (γ-benzopyrone) [159, 160]. They can be divided into several classes, based on the presence of two functional groups, i.e., 3-hydroxyl and 2,3-dihydro. These include flavones (2-phenylchromone), flavonols (3-hydroxyflavones), flavanones (2,3-dihydroflavones), and flavanonols (3-hydroxy-2,3-dihydroflavones). Inclusion of other compound groups to the flavonoids is dependent on the many existing definitions. Some authors include compounds lacking a heterocyclic C-ring, namely the chalcones and dihydrochalcones, and compounds in which the C-ring is 5-membered (furan) instead of the 6-membered (pyran), namely aurones and auronols. One can also distinguish isoflavonoids, which contain a 3-phenylchroman skeleton that is derived by the rearrangement of the flavonoid 2-phenylchroman skeleton. They are however almost entirely limited to the *Fabaceae* family. Finally, somewhat contentious is the inclusion of anthocyanidins, which possess the flavylium cation skeleton and flavanols (flavan-3-ols, flavan-4-ols, and flavan-3,4,-diols), which lack the carbonyl group at C4 [161] (Figure 9).

Flavonoids are widely spread in the plant kingdom, especially in the aerial parts of the plants, often giving a yellow color to flowers and fruits. They are also prominently present in the human diet. These compounds are encountered in an assortment of fruits, vegetables, grains, legumes, nuts, seeds, and beverages such as tea and wine, usually in the form of water-soluble glycosides. Flavonols are present in onion, apple, tea, lettuce, broccoli, grape, elderflower, and cabbage. Flavones can be found in celery, bell pepper, parsley, lemon, and thyme [162]. Flavanones are especially abundant in *Rutaceae* fruits, such as oranges, clementines and grapefruits [163]. Flavanonols can be encountered in black tea, red wine, cocoa, apple, and kiwi [162]. Isoflavones are almost entirely restricted to the legumes (fruits and seeds of the *Fabaceae* family), such as soybean, green bean, cowpea, chickpea and peanut [164]. Flavanols (probably the most abundant flavonoids in human diet) mostly come from black tea beverages [162]. Finally, anthocyanidins are present in red fruits and wine [165]. Interestingly some flavonoid intake in the human diet, comes not from the direct presence of a certain flavonoid, but from the processing. For example, flavanonols, rich constituents of wood, may pass into the wine vinegar during aging process in wood barrels [166].

Flavonoids, specifically flavonols, isoflavones, flavones, and flavanones, have been studied for their effects on pancreatic β-cells [160]. Animal studies have shown that quercetin (10 – 15 mg/kg,

i.p.), a flavonol, can reduce plasma glucose levels and improve glucose tolerance in diabetic rats [167]. It also protects β-cells from damage, increases insulin secretion, and enhances the activities of antioxidant enzymes [168-173]. Similar effects have been observed with other flavonols, such as kaempferol (100 mg/kg) and fisetin (10 mg/kg) [174, 175].

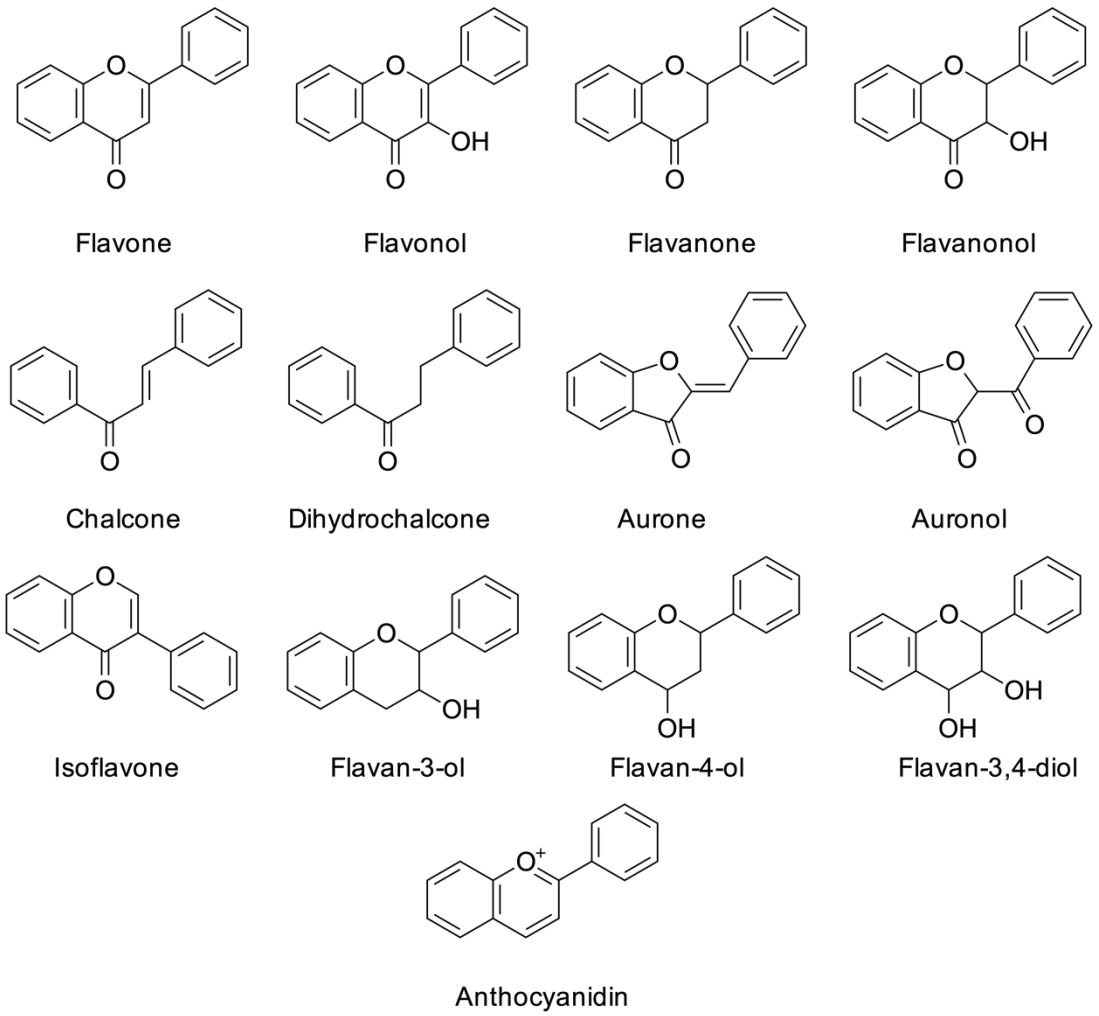

Figure 9. Flavonoid structures.

In vitro studies using insulin-secreting cell lines and isolated islets have revealed that quercetin (20 μmol/L) enhances glucose-induced insulin secretion by activation of the ERK1/2 pathway and L-type calcium channels [146, 147, 176]. It also protects β-cells from oxidative stress-induced damage and cytokine-induced cell death by inhibiting NF-κB activation and reducing the expression of inducible nitric oxide synthase (iNOS) [172, 177-179]. Other flavonols like kaempferol (10 μmol/L) have been shown to improve β-cell viability, function, and insulin synthesis through various signaling pathways, including PDX-1/cAMP/PKA/CREB and CaMK II activation [180-182]. Myricetin was found to potentiate

glucose-induced insulin secretion through activation of the GLP-1 receptor (3 μmol/L) and to protect the β-cell from human islet amyloid polypeptide (hIAPP) induced cytotoxicity (5 μmol/L) [183, 184]. Similar effects have been observed for flavonols glycosides such as rutin (50 mg/kg, i.p., and 10^{-14} mol/L (sic!)) [185].

Isoflavones, found in soybeans, have also demonstrated anti-diabetic effects. Genistein, an isoflavone, has been found to reduce blood glucose levels, increase insulin secretion, and improve β-cell mass and function in diabetic animal models (200 – 600 mg/kg, p.o.; 10 mg/kg, i.p.) and *in vitro* (0.01 – 100 μmol/L). It acts through multiple mechanisms, including inhibition of protein tyrosine kinases, activation of cAMP/PKA signaling, and suppression of NF-κB-mediated iNOS expression [186-194]. Daidzein, another isoflavone, has shown similar effects (200 mg/kg, p.o.) but to a lesser extent [192-194].

Flavones, such as apigenin and luteolin, have been reported to have anti-hyperglycemic effects. Apigenin treatment has been shown to decrease blood glucose levels in diabetic mice (0.78 mg/kg, s.c.; 4 mg/kg. i.p.) and protect β-cells from oxidative damage and cytokine-induced cell death (25 – 50 μmol/L). It also inhibits NF-κB activation and reduces the expression of iNOS [195-199]. Luteolin (2.5 – 10 μmol/L) and its glycoside luteolin-7-*O*-rutinoside (10 – 20 μmol/L) were found to protect the β-cell from high glucose-induced toxicity and to stimulate insulin secretion in INS-1 and RIN-5F cells [200, 201].

Flavanones, including naringenin, naringin (naringein 7-*O*-neohesperidoside), and hesperidin (hesperetin 7-*O*-rutinoside), have been studied for their anti-diabetic effects. These compounds (50 – 100 mg/kg, p.o.) have been found to ameliorate insulin resistance, improve β-cell function, and reduce inflammation in diabetic animal models. Naringenin (1 – 50 μmol/L) has shown protective effects on pancreatic β-cells, including the preservation of secretory granules and the downregulation of pro-inflammatory cytokines and NF-κB [176, 202-205].

3.2 Lignans

Lignans are a group of natural polyphenols (and one of the most lipophilic) located chiefly in plant cell walls, many of which are present in medical plants and in plants, being a part of the human diet. According to the recent nomenclature, lignans are dimers of two coniferyl, sinapyl, paracoumaryl, or similar alcohol monomers. Some authors restrict the term lignan only to those molecules coupled

by the central carbon of the side-chain (i.e., 8,8' or β, β' dimers). In this manner, there is a distinction between neolignans – similar compounds coupled differently (by another carbon or through oxygen bonds); norlignans – lignans that lost one of their carbon atoms from their skeleton; lignoids – compounds that have undergone skeletal rearrangement; and oligolignans – lignan condensation products – which can be divided into sequilignans (trimers) and dilignans (tetramers) [206]. Lignans were found in all plant parts, though their highest content was reported in plant wood – especially in wood knots – roots, bark, leaves, flowers, fruits, and seeds [207]. They were first identified in conifer wood, which is why they often get their names from those species, e.g., pinoresinol from *Pinus nigra* Aiton and lariciresinol from *Larix decidua* Mill. [208]. Apart from conifer wood knots (where they can accumulate in amounts up to 30% (w/w)), flaxseed and sesame seeds are considered rich but challenging sources of lignans. Lignans and neolignans formation are subject to stereoselective biosynthesis (Figure 10); thus, they are enantiomerically pure [206]. They mostly appear linked with carbohydrates, while more lipophilic aglycon-free forms can be found in wood and bark [209].

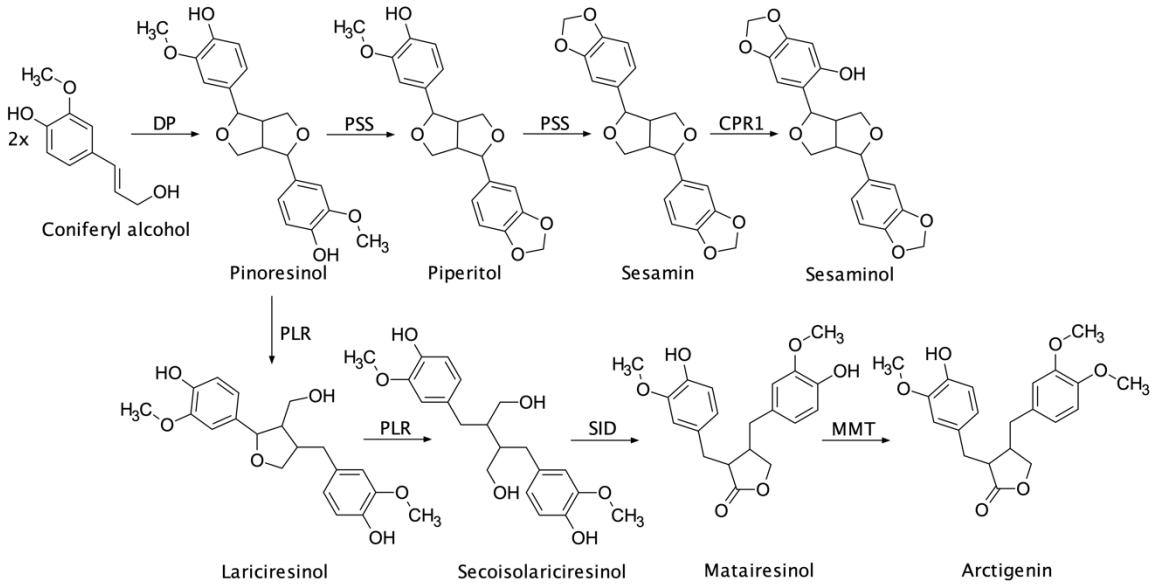

Figure 10. Biosynthetic pathway of major lignans.

DP (dirigent protein), PSS (piperitol/sesamin synthase), PLR (pinoresinol/lariciresinol reductase), CPR1 (cytochrome P450 oxidoreductase 1), SID (secoisolariciresinol dehydrogenase), MMT (matairesinol O-methyltransferase).

There is a rising interest in lignans and plants rich in these polyphenols class as more pharmacological activities are reported, such as antimicrobial, anti-inflammatory, hypoglycemic, and cytoprotective. But it's their cytotoxic activities that are best understood, and they have shed light on this group. Two anticancer drugs, etoposide, and teniposide, were derived from a potent cytotoxic

agent – podophyllotoxin from the roots of *Podophyllum peltatum* L. This led to the search for other cytotoxic metabolites among these polyphenols, with interesting finds concerning lignans and neolignans from nearly every structural subtype [210]. Interestingly, evidence from clinical and observational studies suggests that human microbiota metabolites (enterolactone, enterodiol) of dietary lignans (secoisolariciresinol, pinoresinol, lariciresinol, matairesinol, syringaresinol, medioresinol, and sesamin) are associated with reduced risk of some hormone-dependent cancers [211]. Primarily, the attention is focused on flaxseeds lignan – secoisolariciresinol diglucoside and the effect on breast and colorectal cancer development [212, 213].

There are also reports on the anti-diabetic activity of lignans and lignan-rich extracts. In a meta-analysis, lignan intake (500 μg/d) was found to reduce the risk of T2DM and cardiovascular disease [214]. Syringaresinol-4,4'-di-*O*-β-D-glucoside (25 – 75 mg/kg), an active constituent of *Eleutherococcus senticosus* Maxim. was found to increase serum insulin levels and decrease lipid markers in a streptozotocin-induced mouse model of diabetes [215]. Pinoresinol (492 μmol/L), secoisolariciresinol (25 μmol/L), secoisolariciresinol 9,9'-di-*O*-β-D-glucoside (50 μmol/L), sesamin (450 μmol/L) and lignan metabolites enterolactone (25 μmol/L) and enterodiol (25 μmol/L) were found to inhibit alpha-glucosidase activity [216-218]. Many lignans also increased insulin sensitivity due to GLUT-4 upregulation or were found to act on the adiponectin receptor [219]. However, the effect of lignans on insulin secretion was not thoroughly studied, with only single reports on their activity.

So far, only two lignans have been found to modulate insulin secretion in the pancreatic β-cell, schisandrin C (2.5 – 5.0 μmol/L) from *Schisandra chinensis* (Turcz.) Baill. fruits [149] and arctigenic acid (50 mg/kg, p.o.) from *Arctium lappa* L. fruits [150].

3.2.1 Conifer wood as a source of lignans

The *Pinaceae* family encompasses 11 genera and about 230 species, making it the largest family of conifers as well as the *Gymnospermae*. Genera include *Abies* (47 spp.), *Cathaya* (1 sp.), *Cedrus* (3 spp.), *Keteleeria* (3 spp.), *Larix* (11 spp.), *Nothotsuga* (1 sp.), *Picea* (38 spp.), *Pinus* (113 spp.), *Pseudolarix* (1 sp.), *Pseudotsuga* (4 spp.) and *Tsuga* (9 spp.). The members of this family are monoecious, resinous trees distributed widely in the Northern Hemisphere, with just one equatorial crossover species (Figure 11) [220]. Although trees from the *Pinaceae* family occupy an area of 68.4% of all forests in Poland [221], species diversity is not very large, with only a few species: *Pinus sylvestris* L. (Scots pine), *Pinus mugo* Turra (mountain pine), *Pinus ×rhaetica* Brügger (Rhaetic pine) and *Pinus*

cembra L. (Swiss pine), *Picea abies* L. (Norway spruce), *Larix decidua* Mill. (European larch) and *Larix polonica* Rac. (Polish larch), *Abies alba* Mill. (silver fir) and few introduced species, of which only *Pseudotsuga menziesii* Mirb. (Douglas fir), *Pinus strobus* L. (Weymouth pine), *Picea glauca* (Moench) Voss (white spruce), *Larix kaempferi* Lamb. (Japanese larch) and *Tsuga canadensis* Carrière (Canadian hemlock) can be found in significant numbers [222]. Most of the genera present in Poland are economically important for the timber industry, which is why they have been preferred in plantings since the XIX century [221].

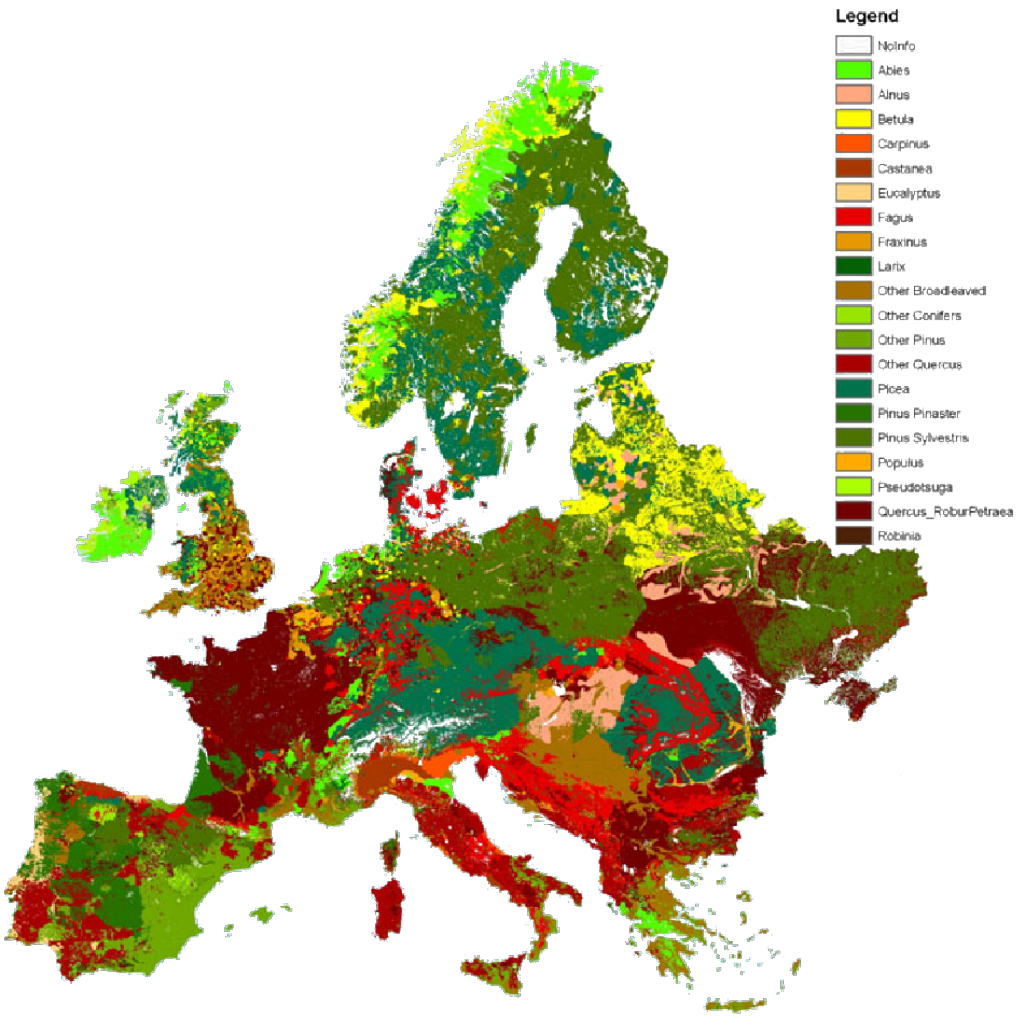

Figure 11. Map of dominant tree species in Europe [223].

With recent technological advances in the timber industry, logs and other wood products brought to sawmills are almost totally processed, leaving little to no waste. However, it is still not always the case. According to experts, the low technological level of a large part of Polish industrial

plants, the lack of financial resources for proper waste management, the state's unclear ecological policy, as well as the low level of public awareness are the reasons for the generation of substantial amounts of waste [224]. By-products from the timber industry, such as wood chips, sawdust, bark, and others, form 38.6% of the total wood flow in Europe [225]. Their high quality and solid structure could bring them many applications, yet they are mainly used to generate energy (as a biofuel) and in wood panel production [225, 226]. As more and more emphasis is placed on limiting the increase in global average temperature (i.e., global warming), with The Paris Climate Agreement, European Union's 2030 and 2050 climate strategies, a new, more responsible, and efficient approach to wood by-products is well founded.

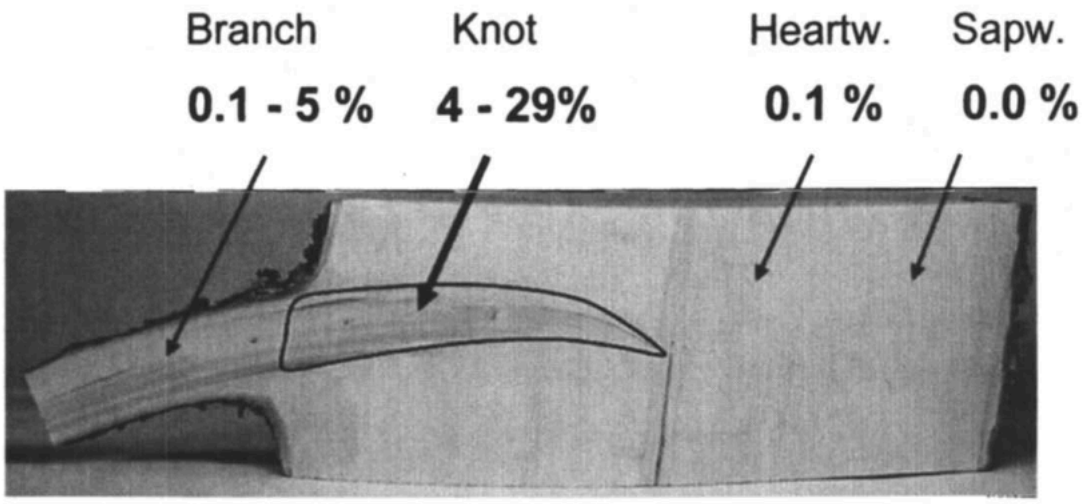

Figure 12. Typical amounts of lignans (in % w/w) in *Picea abies* trees [227].

One of such wood by-products are wood knots, which are branch bases inside a stem. They are not particularly of interest to the timber industry, as they are considered defects of the wood (fibers in this portion of wood are perpendicular to the stem), they are much harder to chip than regular wood, and their presence in wood pulp may lead to the formation of paper sheets with inferior strength, light absorption and surface properties [228]. Therefore, it is not surprising that knotwood is considered a by-product of many timber industry processes, with little applications or value up to date – most of it is burned to produce energy [228]. Knotwood and branchwood (which contain many knots on their own) have great potential for industrial applications due to their high lignan content (Figure 12). Not only can one find much higher amounts of common dietary lignans – some of them with proven dietary anti-diabetic, anti-inflammatory, antioxidant, and phytoestrogenic properties [229-232] – but also some much rarer compounds, that is, oligolignans [233], which have not yet been thoroughly studied. Only recently, a single lignan molecule 7-hydroxymatairesinol (HMRlignan) from

Picea abies wood knots has been registered as a dietary supplement [234]. Although many lignans, such as secoisolariciresinol or sesamin, have been previously found in high concentrations in oilseeds, 7-hydroxymatairesinol has been detected in the human diet quite recently, using high-resolution detection methods [235]. Both 7-hydroxymatairesinol and *Picea abies* wood knots extract were found to improve glucose metabolism, decrease insulin resistance, and indirectly inhibit adipogenesis [236].

Extracts from *Larix laricina* K. Koch inner bark have been used by the Cree people of Northern Quebec to treat symptoms related to type 2 diabetes mellitus, having its mention in their traditional pharmacopeia. Recently both *in vitro* [237, 238] and *in vivo* experiments [239] have confirmed their anti-diabetic effects, namely hypoglycemic, antioxidant, and increasing insulin sensitivity. Although the exact compound responsible for this action is not yet known, lignans such as lariciresinol and its derivatives have been isolated using bioassay-guided fractionation from this extract [240].

Many species from the *Pinaceae* family have been recognized as a rich source not only of lignans but also flavonoids and other polyphenolics. Phenolic standardized extracts from the bark of different species, such as *Pinus pinaster* Aiton (Pycnogenol, Flavangenol, Oligopin) and *Abies alba* Mill. (Abigenol), have been thoroughly studied and implemented in pharmaceutical use [241-244].

3.2.2 Other sources of lignans

3.2.2.1 Great burdock

Arctium lappa L., also known as great burdock, is a plant from the *Asteraceae* family, native to Europe and Asia. Fruits, roots, leaves and seeds are used in traditional and folk medicine (Chan *et al.*, 2011), of which dried ripe fruit (*Arctii fructus*) and root (*Arctii radix* or *Bardanae radix*) are mostly used, with their mention in Chinese Pharmacopeia and the latter being monographed by the European Medicines Agency (EMA) [245]. Pharmacological effects of *Arctium lappa* are rather known, with antioxidant, anti-inflammatory and anti-cancer properties being attributed to the plant [245, 246].

Although *Arctii fructus* has been used in traditional Chinese medicine as a remedy in T2DM for centuries, only recently it has gathered a lot of interest from researchers. Its anti-hyperglycemic effect was confirmed on *in vivo* and *in vitro* models. Yan *et al*. reported that the ethanolic extract of *Arctii fructus* lowered blood glucose levels in alloxan-induced diabetic rats [247], while Xu *et al*. observed similar effect for both water and ethanolic extracts, additionally reporting inhibitory activity towards α-glucosidase [248]. These activities were later attributed to the lignan fraction. Xu *et al*. studied total

lignan fraction of fruits extract (0.5, 1.0, and 2.0 g/kg, i.g.) on the same model and reported their glucose lowering effect for medium and higher dose in diabetic but not in normal mice [249]. The studies were continued by the same team on Goto-Kakizaki rats showing similar profile of lignan fraction to nateglinide and suggesting multiple possible mechanisms of action, i.e., by stimulation of insulin and GLP-1 secretion, and through the decrease in intestinal glucose absorption [151]. In their following study, they have identified arctigenic acid (a metabolite of arctigenin) to be the main metabolite in the rat serum after the administration of lignan fraction [150]. It must be noted here that all the above findings were reported by the same team and no other data in the literature could be found. However, other parts of the plant, such as roots and leaves, or isolated compounds, such as arctigenin, were found to improve glucose levels [250-252].

There have been numerous lignans previously identified in *Arctii fructus* lignan fraction, of which glycosides of matairesinol and arctigenin are the dominant ones, and a large variety of dimeric lappaols and arctignans present [253].

3.2.2.2 Safflower

Safflower (*Carthamus tinctorius* L.) is an annual Asteraceae family plant with characteristic inflorescence with orange or red-orange ray florets. It was cultivated in present-day China, India, Iran, and Egypt in prehistoric times and was introduced into cultivation in Europe during the Middle Ages. Due to the presence of red and orange pigments, the flowers of this species were utilized as dyes in the textile industry. However, it was replaced by aniline dyes, and its present industrial use is mainly limited to producing safflower oil and animal feed [254-256].

Apart from its industrial use, certain plant parts were used in traditional and folk medicine in Asia. In traditional Iranian medicine, flowers, seeds, and seed oil were employed as a laxative to treat rheumatism and paralysis. The fruit and leaves were utilized as analgesics, antispasmodics, and antidotes to scorpion venom. Additionally, their use as a remedy for psoriasis, vitiligo, oral ulcers, limb numbness, low mood, alopecia, and bruises with accompanying swelling in folk medicine was noted. In traditional Indian medicine, safflower treats scabies, joint inflammation, and mastalgia and enhances libido. In TCM, safflower petals were extensively used for treating conditions involving blood stasis, menstrual disorders, and wounds. In Korea, an extract from *C. tinctorius* seeds was employed to strengthen bones, prevent osteoporosis, and treat gynecological issues [254-257].

C. tinctorius has been found to contain a range of lignans, such as arctigenin, matairesinol, secoisolariciresinol, trachelogenin, and their glycosides [256]. These lignans have demonstrated potential anticancer, obesity-combating, and neuroprotective properties [210]. In an *in vitro* study on Huh7 and HEK 293T cells, it was observed that trachelogenin prevents hepatitis C virus entry into liver cells [258]. *In vitro* research on HCT-116 cells revealed the inhibitory effects of trachelogenin on cancer cell proliferation [259]. There are also reports of the antiestrogenic activity of these lignans. In this context, tracheloside (trachelogenin 4-*O*-glucoside) exhibited *in vitro* activity on Ishikawa cells, significantly reducing alkaline phosphatase activity comparable to tamoxifen [260]. Lignans in safflower fruits are among the compounds in the human diet, particularly in grain products, though their content is much smaller.

3.2.2.3 Eleutherococcus

Eleutherococcus senticosus (Rupr. & Maxim.) Maxim. (*syn*. *Acanthopanax senticosus* (Rupr. & Maxim.) Harms), also called Siberian ginseng, Shigoka, or Ciwujia, is a shrub from the *Araliaceae* family, whose roots have been used as a traditional medicine for twenty centuries. This medicinal plant is widely distributed in Asia, especially in Northeast China, North Japan and Korea, Southeast Russia, and far-east Russia [261]. The common name "Siberian ginseng" was introduced in the USA and refers to the fact that *E. senticosus* was exported for the first time from Siberia in the Soviet era. However, the local population did not use this term as they call this plant "eleutherokokk" [262]. Some authors claim that the designation "Siberian ginseng" is misleading because *E. senticosus* is only distantly related to *Panax ginseng* C.A.Mey (Asian ginseng) and *Panax quinquefolius* L. (American ginseng) and differs from them in terms of chemical composition [262, 263].

Instead of having one dominant compound or group of metabolites, *E. senticosus* root has a mixture of different constituents, of which major ones are sometimes called as "eleutherosides". Among these eleutherosides are glycosides of phenolic alcohols, lignans, coumarins, triterpenoids, and phytosterols [264]. However, they are not limited to this plant and can be found in many different species, sometimes in higher quantities than in *E. senticosus*. Most of the eleutherosides are important only from a historical perspective, except for eleutherosides B (syringin) and E (syringaresinol di-*O*-glucoside) that are marker compounds for *E. senticosus* and are considered to be responsible for its antifatigue effect [265].

In TCM, *E. senticosus* root is said to provide energy for the organism, strengthen the bones and calm the mind, and was used to treat rheumatism, hepatitis and diabetes [266, 267]. However, it was not until the 20th century that the plant gathered interest of Soviet scientists who searched for a substitute for the roots of *P. ginseng*, an adaptogen rarely found in the former Soviet Union [262]. Adaptogens are natural substances that enhance the body's non-specific resistance to stress by modulating the ability to adapt and survive. One theory states, that adaptogens' action is related to their effects on the regulation of stress hormones and key mediators of homeostasis regulation [268]. The pleiotropic action of *Eleutherococcus senticosus* roots is believed to be due to its rich content of active compounds, mainly eleutherosides (lignan derivatives, coumarins and phenylpropanoids) studied extensively for among others antioxidant, immunomodulatory, anti-inflammatory, anti-rheumatic, hepato-protective, hypolipidemic, or anticoagulant activity [269, 270].

EMA approved *E. senticosus* root in 2014 for the treatment of symptoms of asthenia such as fatigue and weakness. It was classified as traditional herbal medicine entirely based on its long-standing use [271]. The root of *E. senticosus* has been listed in European, British, Japanese, Chinese, Russian and American Pharmacopeias.

However, it is not only the adaptogenic properties of *E. senticosus* roots that have been thoroughly studied. There are also reports confirming its use to treat diabetes [272, 273]. Moreover, as mentioned before, *Eleutherococcus senticosus* root is considered a source of otherwise rare lignan, i.e., syringaresinol di-*O*-glucoside, which was studied by Zhai *et al*. for its anti-diabetic and antioxidant potential, and was found to alleviate diabetic state in STZ rats [215].

3.3 Coumarins

Coumarins are a group of cinnamic acid lactone derivatives, biosynthesized in the shikimate pathway. Chemically, they possess an α-benzopyrone (2*H*-chromen-2-one) skeleton, which can be further substituted or modified. They are usually divided into simple coumarins (substituted α-benzopyrones), isocoumarins (carbonyl group and oxygen in pyrone ring inversed), furanocoumarins (a furan ring fused to the benzene of coumarins), which can be further divided into linear (psoralen type) or angular (angelicin type) furanocoumarins, depending on how the furan ring is fused (6,7 or 7,8), and least common pyranocoumarins (a pyran ring fused to the benzene) which also can be divided into linear (xanthyletin type) or angular (seselin type) (Figure 13). They commonly occur in aglycone-

free form, though hydroxylated simple coumarins may form glycosides. Coumarins are frequently *C*- and *O*-prenylated [159].

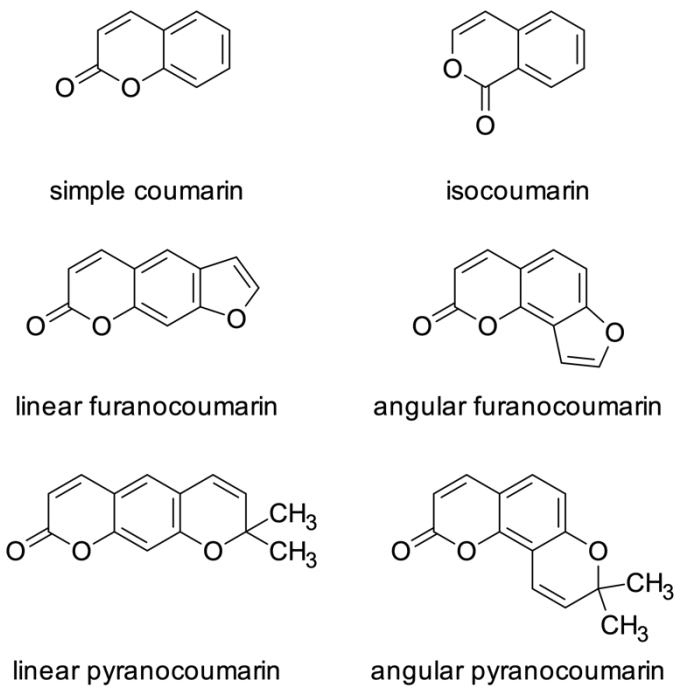

Figure 13. Coumarins structures.

Coumarins can be found in seeds, fruits, flowers, stems, leaves, and roots. They have been isolated from more than 40 different plant families, though most of them are present in just two, i.e., *Apiaceae* and *Rutaceae [274]*.

There have been numerous attempts at assessing coumarins' anti-diabetic potential, though they mostly targeted α-glucosidase [275-277]. Single studies were conducted *in vivo* and on β-cell models to evaluate the protective and insulin secretion-modulating effects of coumarins. Umbelliferone (7-hydroxycoumarin) β-D-galactopyranoside was found to increase insulin levels in streptozotocin (STZ) induced diabetic rats in doses ranging from 10 mg/kg to 40 mg/kg [278]. In another study, its aglycone (umbelliferone) induced a similar effect in alloxan-induced diabetic rats at 100 mg/kg [279]. Daphnetin (7,8-dihydroxycoumarin) was found to protect the INS-1 cells from STZ-induced β-cell death and dysfunction [280]. Ahmed *et al.* studied 13 coumarin sulfur analogs isolated from *Clutia lanceolata* Forssk on murine pancreatic islets and found that 7 of them increased glucose-induced insulin secretion, though it must be noted that the concentration used in this study was relatively high (200 µmol/L) [154]. Another coumarin, scopoletin (7-hydroxy-6-methoxycoumarin), was

able to increase glucose-induced insulin secretion through K_{ATP} and VGCC channels dependent pathway in INS-1 cells at concentrations below 20 µmol/L [153]. Imperatorin was found to increase plasma GLP-1 levels and increase insulin secretion in STZ-induced diabetic rats at 3-10 mg/kg and to modulate glucose-induced insulin secretion in INS-1 cells at 0.1 mg/mL (370 µmol/L) [152, 281]. Unfortunately, the data on the coumarins' effect on the β-cell are scarce and, in most cases, limited to high doses beyond bioavailability.

3.3.1 Selected sources of coumarins – angelica roots

Many of the previously studied coumarins were isolated or are present in the roots of *Angelica* L., as they are considered a rich source of these phytochemicals. Plants from the *Angelica* L. (*Apiaceae*) genus have been used by humans for centuries for culinary, ceremonial, and medicinal reasons. Their roots are widely used as a traditional and folk medicine around the globe and are mentioned in many pharmacopeias and medicinal systems, such as Traditional Chinese Medicine, Ayurveda, and Kampo (Figure 14).

Figure 14. Traditional medicinal use of angelica roots around the world.

Angelica archangelica L. (syn. *Angelica officinalis* Hoffm.) is native to North and Eastern Europe and Western Asia, where for centuries it has been used as a spice and a vegetable for culinary purposes [282]. Its roots in Western traditional medicine and Ayurvedic medicinal system are used as an appetite stimulant, an antispasmodic, a sedative, an anxiolytic, and as a medication for gastrointestinal

symptoms such as bloating, poor digestion, eructation, and flatulence. Its main constituents are essential oil and simple and furanocoumarins. At present, it is recognized by the United States and European Pharmacopeias and the National Formulary of India [282]. *A. archangelica* has been naturalized in Eastern North America, even though another representative of the *Angelica* genus with similar properties is naturally present there – *Angelica atropurpurea* L. [283]. Like *A. archangelica*, it has been used as a vegetable and spice. Among the Native Cultures of North America, such as the Muscogee, Cherokee, Lenape and Menominee, it was used for ceremonial, nutritional, and medicinal purposes, to treat anxiety, back pain, and gastrointestinal disorders [284]. Ceremonial and therapeutic uses of *Angelica dawsonii* S.Watson by the Blackfoot, *Angelica breweri* A.Gray by the Miwok, Paiute, Shoshoni, and Washo, *Angelica genuflexa* Nutt. by the Nuxalk and Gitxan, *Angelica lineariloba* A.Gray by the Paiute, *Angelica lucida* L. by the Aleut and Inuit, *Angelica pinnata* S.Watson by the Goshute, *Angelica tomentosa* S.Watson by the Pomo and Yana, and *Angelica venenosa* (Greenway) Fernald by the Iroquois was also noted [285, 286].

In parts of Europe, North America, and South Asia, *Angelica sylvestris* L. roots were used as an ethnomedicine. Among the Mi'kmaq of Eastern Canada, it was used to treat cough, cold and sore throat [286]. In Estonia, it was used in folk medicine to treat cancer [287], while in Pakistan, it was used to treat rheumatism and muscle pain [288]. In Pakistani and Indian Himalayan region, use of another angelica root was noted, i.e., that of *Angelica glauca* Edgew. Its roots are commonly used to treat gynecological disorders, such as dysmenorrhea, metrorrhagia, amenorrhea and polycystic ovary syndrome, and gastrointestinal disorders [289, 290].

Angelica dahurica (Hoffm.) Benth. & Hook.f. ex Franch. & Sav. is widely distributed in Korea, Northeast China, Japan, Mongolia, and Siberia. Its root contains simple and furanocoumarins, which are probably responsible for its anti-inflammatory, analgesic, and anti-oxidative properties. It has been used in TCM, Kampo, and traditional Korean medicine to treat the common cold, rhinitis, headache, toothache, and some skin diseases [291]. Korean Pharmacopoeia also mentions the root of *Angelica gigas* Nakai, which has similar properties and is used to treat common cold, headache, neuralgia, arthralgia, and gynecological disorders [292].

In China, perhaps the most known Angelica product is the root of *Angelica sinensis* (Oliv.) Diels which is also traditionally used to treat gynecological disorders, such as amenorrhea and irregular periods. Its active constituents are phthalides, organic acids, and polysaccharides [293]. Use of A. sinensis was also noted in Indonesian and Arabian traditional medicine, where it probably arrived via

trade [294, 295]. *Angelica acutiloba* (Siebold & Zucc.) Kitag. roots are sometimes used in TCM as a substitute for *A. sinensis*, *and* in Kampo to treat menstrual disorders, amenorrhea, and premenstrual syndrome [292]. Chinese Pharmacopeia also lists *Angelica anomala* Avé-Lall. to treat gynecological disorders [296].

Apart from *A. dahurica* and *A. sinensis* roots, Chinese Pharmacopeia also lists *Angelica biserrata* (R.H.Shan & Yuan) C.Q.Yuan & R.H.Shan (syn. *Angelica pubescens* Maxim. f. *biserrata* R.H.Shan et C.Q.Yuan) roots, which are used in TCM to alleviate pain, fever, and rheumatism. Coumarins are their primary constituents, probably responsible for their biological effects. It is widespread in Japan with a significantly lesser presence in mainland China and Taiwan but is not mentioned in the Japanese Pharmacopeia [297, 298]. In fact, the common Latin name of pharmacopeial plant material *Angelicae pubescentis radix* may be somehow misleading, as it applies to the roots of *A. biserrata*, sometimes considered as *A. pubescens* subspecies. *Angelica polymorpha* Maxim. is mentioned in the Chinese Pharmacopeia as a substitute of *A. pubescentis radix*.

Other species used in traditional oriental medicine include *Angelica decursiva* Franch. & Sav. (syn. *Peucedanum decursivum* Maxim.), which is also mentioned in Japanese Pharmacopeia for its anti-inflammatory effects [299], and *Angelica tenuissima* Nakai used to treat dental pain in Korean folk medicine [300].

Angelica roots are sometimes used to treat T2DM. These include *Angelica furcijuga* Kitag., *Angelica shikokiana* Makino ex Y.Yabe, *Angelica keiskei* Koidz. and *Angelica japonica var. hirsutiflora* (Liu, Chao & Chuang) T.Yamaz. [301-304].

Moreover, some of the *Angelica* L. root extracts were found to possess insulin secretagogue activity. Leu *et al.* described methanolic extract of *A. japonica var. hirsutiflora* activity to stimulate insulin secretion in HIT-T15 cells and on mouse and human islets [157]. In another study, Kim *et al.* found that Korean *Angelica reflexa* B.Y.Lee and some of its metabolites belonging to coumarins potentiated glucose-induced insulin secretion [158]. Lastly, Park *et al.* screened over 1500 plant extracts for GPR119 agonistic actions, and *A. dahurica root* extract was found to be the most active, and its effect on the modulation of insulin secretion was also established. The authors argued that coumarins may be responsible for this activity [156].

Experimental

4 Aim of the thesis

Natural products represent a tremendous structural diversity that offers a wide range of pharmacophores and a high degree of stereochemistry; thus, they play a significant role in discovering leads. Additionally, natural products may have an advantage over synthetic compounds of being natural metabolites that may be more prone to protein-protein interaction and can be more efficiently delivered to their intracellular site of action [305, 306]. Despite some skepticism about this source of therapeutics, during the period 1981-2019, 33,6 % of all new small-molecule approved drugs came from natural sources or were derived from natural sources, while another 35,2 % were natural product-inspired [307]. Technological advances and involvement of non-random screenings have revived the interest in natural products for drug discovery [305, 308].

Type 2 diabetes mellitus (T2DM) is a disease that associates insulin resistance and pancreatic β-cell dysfunction. Based on the current understanding of the pathophysiology of this disease, multiple anti-diabetic therapies have been developed to improve glycemic control and slow disease progression. Nevertheless, they have limited effectiveness and numerous side effects (i.e., digestive disorders for metformin and hypoglycemia for sulfonylureas) [309].

One possible approach targeting β-cell is using compounds that improve insulin secretion in a glucose-dependent manner, a safer strategy to help achieve glycemic goals due to the lower risk of hypoglycemia. The development of such lead molecules is still an active area of research to provide more therapeutic options in the future as the number of type 2 diabetic patients keeps growing. Moreover, knowing that β-cell dysfunction is present before the development of type 2 diabetes [310], protecting these cells also constitutes a potential approach to prevent the development of type 2 diabetes.

Research suggests that bioactive compounds (i.e., polyphenols) found in plants may help slow the aging process and reduce the risk of many chronic diseases, including type 2 diabetes mellitus. In this context, plant secondary metabolites are likely good candidates to protect β-cells against dysfunction and regulate insulin secretion since several of these well-known antioxidant compounds are now widely regarded as pharmacological agents that regulate target proteins and signaling pathways in pancreatic β-cell [311]. We can also consider data on all small-molecule anti-diabetic drugs approved in the last 40 years – again, 23% of those were drugs that came from natural sources or were derived from natural sources, and as much as 67% were natural product inspired [307].

Previous studies done at the Institut des Biomolécules Max Mousseron have shown that natural metabolites like the flavonoid quercetin or ellagitannin metabolite urolithin C potentiate glucose-induced insulin secretion through a mechanism implicating the activation of L-type voltage-gated calcium channels and ERK 1/2 pathway [147, 155, 312]. There have also been reports from other laboratories on somewhat unspecified anti-diabetic activity of other metabolites groups, with scarce reports on the insulinotropic activity of single compounds.

This led to the formulation of the **hypothesis** that plant secondary metabolites, such as flavonoids, lignans, and coumarins, may modulate the β-cell function, possibly increasing insulin secretion, considering that this activity is based on interactions between small molecules and proteins rather than on their antioxidant potential; thus, it is highly structure-dependent.

This thesis **aimed** to find a natural source of secondary plant metabolites potentially able to protect β-cell function, induce insulin secretion in a glucose-dependent manner, and elucidate their mechanism of action.

To this aim, the following **specific objectives** were set:

1. Phytochemical characterization of chosen plant extracts containing lignans, flavonoids, and coumarins to select compounds for isolation.
2. Isolation of potentially bioactive pure plant secondary metabolites and their characterization.
3. Screening *in vitro* on a β-cell model of obtained metabolite libraries for insulin secretion modulatory and protective effects.
4. Finding structure-activity relationship of active compounds on insulin secretion.
5. Elucidation of the mechanism of action of active compounds by assessing their effects on a number of key stages in insulin secretion, in particular cell electrical activity, intracellular calcium levels, and trace currents of calcium and potassium channels.

5 Materials and methods

5.1 Materials

5.1.1 Phytochemistry reagents

Table 2. Reagents used in phytochemical experiments.

Reagent	Source
Acetic acid, p.a.	POCh (Gliwice, Poland)
Acetonitrile, isocratic grade for LC	Merck (Darmstadt, Germany)
β-glucosidase from almonds, 2 U/mg	Sigma-Aldrich Chemie GmbH (Steinheim, Germany)
Cellulase from Aspergillus niger, 1.56 U/mg	Sigma-Aldrich Chemie GmbH (Steinheim, Germany)
Chlorofrom, p.a.	POCh (Gliwice, Poland)
Chloroform-d ($CDCl_3$)	Armar AG (Döttingen, Switzerland)
Diaion HP-20	Supelco Analytical (Bellefonte PA, USA)
Dichloromethane, p.a.	POCh (Gliwice, Poland)
DMSO, p.a.	POCh (Gliwice, Poland)
DMSO-d_6	Armar AG (Döttingen, Switzerland)
Ethanol, p.a.	POCh (Gliwice, Poland)
Ethyl acetate, p.a.	POCh (Gliwice, Poland)
Formic acid, ACS grade, Ph. Eur. 11th	Merck (Darmstadt, Germany)
n-Hexane, ACS grade	Merck (Darmstadt, Germany)
Methanol, p.a.	POCh (Gliwice, Poland)
Methanol, isocratic grade for LC	Merck (Darmstadt, Germany)
Methanol-d_4	Armar AG (Döttingen, Switzerland)
Sephadex LH-20	Pharmacia Fine Chemicals (Uppsala, Sweden)
Silica gel (60-200 µm)	Merck (Darmstadt, Germany)
Sulfuric acid, 95% p.a.	POCh (Gliwice, Poland)
TLC 60G F_{254} silica gel plates (20 × 20 cm)	Merck (Darmstadt, Germany)
Toluene	POCh (Gliwice, Poland)
Vanillin	Veb Laborchemie (Apolda, Niemcy)

5.1.2 Pharmacology reagents

Table 3. Reagents used in pharmacological experiments.

Reagent	Source
Bovine serum albumin (BSA)	Sigma-Aldrich Chemie GmbH (Steinheim, Germany)
Calcium chloride ($CaCl_2$)	Chempur (Piekary Śląskie, Poland)
Disodium phosphate (Na_2HPO_4)	Chempur (Piekary Śląskie, Poland)
DMSO, molecular biology grade	Sigma-Aldrich Chemie GmbH (Steinheim, Germany)
DMSO, sterile	Sigma-Aldrich Chemie GmbH (Steinheim, Germany)
Dulbecco's phosphate-buffered saline (DPBS) w/o $CaCl_2$ and $MgCl_2$	Sigma-Aldrich Chemie GmbH (Steinheim, Germany)
Fetal Calf Serum (FCS)	Eurobio Scientific (Les Ulis, France)
Fura-2-acetoxymethyl esther	Thermo Fisher Scientific (Waltham, MA, USA)
Glucose	Sigma-Aldrich Chemie GmbH (Steinheim, Germany)
L-Glutamine-penicillin-streptomycin solution	Sigma-Aldrich Chemie GmbH (Steinheim, Germany)
HEPES	Carl Roth GmbH (Karlsruhe, Germany)
HEPES 1M	Capricorn Scientific (Ebsdorfergrund, Germany)
HTRF insulin ultrasensitive dosing kit	PerkinElmer (Waltham, MA, USA)
Magnesium sulfate heptahydrate ($MgSO_4 \times 7H_2O$)	Chempur (Piekary Śląskie, Poland)
2-Mercaptoethanol 50 mM	Thermo Fisher Scientific (Waltham, MA, USA)
Monopotassium phosphate (KH_2PO_4)	Chempur (Piekary Śląskie, Poland)
Pluronic F-127	Sigma-Aldrich Chemie GmbH (Steinheim, Germany)
Poly-L-lysine hydrobromide	Sigma-Aldrich Chemie GmbH (Steinheim, Germany)
Potassium chloride (KCl)	Chempur (Piekary Śląskie, Poland)
Recombinant rat IL-1β	Thermo Fisher Scientific (Waltham, MA, USA)
Recombinant rat INF-γ	Thermo Fisher Scientific (Waltham, MA, USA)
Recombinant rat TNF-α	Thermo Fisher Scientific (Waltham, MA, USA)
RPMI-1640 w/o L-glutamine	Capricorn Scientific (Ebsdorfergrund, Germany)
Sodium bicarbonate ($NaHCO_3$)	Chempur (Piekary Śląskie, Poland)
Sodium chloride (NaCl)	Chempur (Piekary Śląskie, Poland)
Sodium pyruvate 100 mM	Thermo Fisher Scientific (Waltham, MA, USA)
Tetraethylammonium chloride (TEA)	Sigma-Aldrich Chemie GmbH (Steinheim, Germany)
Thiazolyl blue tetrazolium bromide (MTT)	Sigma-Aldrich Chemie GmbH (Steinheim, Germany)
Trypsin-EDTA HBSS	Sigma-Aldrich Chemie GmbH (Steinheim, Germany)
TWEEN 20	Sigma-Aldrich Chemie GmbH (Steinheim, Germany)
Verapamil hydrochloride	Sigma-Aldrich Chemie GmbH (Steinheim, Germany)

5.1.3 Reference compounds

Table 4. Reference compounds.

Reference compounds (analytical standards)	Source
Abietic acid	Sigma-Aldrich Chemie GmbH (Steinheim, Germany)
Angelicin	Extrasynthese (Lyon, France)
Apigenin	Extrasynthese (Genay, France)
Bergapten	Extrasynthese (Lyon, France)
Catechin	Sigma-Aldrich Chemie GmbH (Steinheim, Germany)
Chrysin	Extrasynthese (Genay, France)
Columbianetin	Phytolab GmbH (Vestenbergsgreuth, Germany)
Dihydromyricetin (ampelopsin)	Extrasynthese (Genay, France)
Dihydrokaempferol (aromadendrin)	Extrasynthese (Genay, France)
Dihydroquetcetin (taxifolin)	Extrasynthese (Genay, France)
Diosmetin	Extrasynthese (Genay, France)
Enterodiol	Previously isolated in the Department of Pharmaceutical Biology
Enterolactone	Previously isolated in the Department of Pharmaceutical Biology
Epi-catechin	Serva (Heidelberg, Germany)
Eriodictyol	Extrasynthese (Genay, France)
Esculetin	Extrasynthese (Lyon, France)
Flavanone	Extrasynthese (Genay, France)
Flavone	Extrasynthese (Genay, France)
Galangin	Extrasynthese (Genay, France)
Hesperetin	Extrasynthese (Genay, France)
Imperatorin	Extrasynthese (Lyon, France)
Isoimperatorin	Extrasynthese (Lyon, France)
Isopimpinellin	Extrasynthese (Lyon, France)
Kaempferol	Extrasynthese (Genay, France)
(Z)-Ligustilide	Extrasynthese (Lyon, France)
Luteolin	Extrasynthese (Genay, France)
Myricetin	Extrasynthese (Genay, France)
Naringenin	Extrasynthese (Genay, France)
Olivil 4'-*O*-glucoside	Previously isolated in the Department of Pharmaceutical Biology
Osthole	Extrasynthese (Lyon, France)
Oxypeucedanin	Phytolab GmbH (Vestenbergsgreuth, Germany)
Oxypeucedanin hydrate	Phytolab GmbH (Vestenbergsgreuth, Germany)
Pinobanksin	Extrasynthese (Genay, France)
Pinocembrin	Extrasynthese (Genay, France)
Psoralen	Extrasynthese (Lyon, France)
Quercetin	Sigma-Aldrich Chemie GmbH (Steinheim, Germany)
Scopoletin	Extrasynthese (Lyon, France)
Syringin	Previously isolated in the Department of Pharmaceutical Biology
Xanthotoxin	Extrasynthese (Lyon, France)

5.2 Plant material collection, treatment, and storage

Branch wood of *Pinus cembra* L., *Pinus mugo* Turra, *Pinus strobus* L., *Pinus ×rhaetica* Brügger, *Abies alba* Mill., *Picea abies* L., *Picea glauca* (Moench) Voss, *Pseudotsuga menziesii* Mirb., *Tsuga canadensis* Carrière, and *Larix kaempferi* Lamb. was collected from the Polish Academy of Sciences Botanical Garden (Powsin, Poland). Branch wood *Larix decidua* Mill. and *Larix polonica* Rac. was collected from the University of Warsaw Botanical Garden (Warsaw, Poland). *Pinus sylvestris* L. branch wood was collected from Chojnów Landscape Park (Konstancin-Jeziorna, Poland). The plant material was authenticated according to Flora Europaea by botanical gardens botanists. Voucher specimens have been deposited in the Plant Collection, Department of Pharmaceutical Biology, Medical University of Warsaw, Poland. Plant material was dried at room temperature, shredded, and freeze-dried.

Dried and shredded roots of *Angelica archangelica* L. were purchased from Nanga (Złotów, Poland). Roots of *Angelica dahurica* (Hoffm.) Benth. & Hook.f. ex Franch. & Sav., *Angelica biserrata* (R.H.Shan & Yuan) C.Q.Yuan & R.H.Shan and *Angelica sinensis* (Oliv.) Diels and whole fruits of *Arctium lappa* L. were purchased from Bozhou Zhongzheng Nature (Bozhou, China). Dried and shredded *Eleutherococcus senticosus* Maxim. roots were purchased from NatVita (Mirków, Poland). Whole fruits of *Carthamus tinctorius* L. were purchased from Polskie Ziarno (Śrem, Poland). The plant material was authenticated according to European Pharmacopoeia 11th ed. and Flora Europaea. Plant material was milled to powder and freeze-dried.

All plant material was stored at -20 °C until further use.

5.3 Extract preparation

Branch wood 90% (v/v) methanolic extracts were prepared from shredded and milled *Pinus sylvestris*, *Pinus cembra*, *Pinus mugo*, *Pinus strobus*, *Pinus ×rhaetica*, *Abies alba*, *Picea abies*, *Picea glauca*, *Pseudotsuga menziesii*, *Tsuga canadensis*, *Larix decidua*, *Larix polonica*, and *Larix kaempferi*. Each sample was weighed (5.0 g), defatted with 50 mL n-hexane, and extracted with 50 mL of 90% (v/v) aqueous methanol under reflux for 2 h. The extracts were then filtered through a filter paper, reduced in a Rotavator rotary evaporator R-100 (Buchi, Flawil, Switzerland) and lyophilized, resulting in dried methanolic extracts. These extracts were used for phytochemical profiling.

Pure methanolic extracts were prepared from branch wood of *Abies alba* (660 g) and *Pinus sylvestris* (250 g), and fruits of *Carthamus tinctorius* (500 g) and *Arctium lappa* (500 g). Briefly, the plant material was degreased with 1 L of n-hexane and extracted 3 times in a SONIC-5 ultrasonic bath (POLSONIC, Poznań, Poland) with 100% methanol at 60 °C for 2 h and evaporated to dryness on a rotary evaporator yielding 43.7 g of dry silver fir extract, 11.5 g of dry Scots pine extract, 12.8 g of dry safflower extract and 56.8 g of great burdock extract. These extracts were used for lignans isolation, and in the case of *Carthamus tinctorius* and *Arctium lappa* fruits also for phytochemical profiling.

Dried and shredded *Eleutherococcus senticosus* roots (500 g) were milled to powder, defatted with 1 L of n-hexane, and extracted 3 times in an ultrasonic bath with 70% (v/v) aqueous methanol at 60 °C for 2 h. The extract was then filtered through a filter paper, reduced in a rotary evaporator, and lyophilized, resulting in 19.3 g of dried hydromethanolic extract. It was used for phytochemical profiling and lignan isolation.

Dried and shredded roots of *Angelica archangelica* (500 g), *Angelica dahurica* (500 g), and *Angelica biserrata* (500 g) were milled to powder and extracted with 2 L of n-hexane in Soxhlet apparatus for 15 hours. The extract was the filtered through a filter paper and evaporated to dryness on a rotary evaporator, giving a residue of 14.4 g, 9.3 g and 13.0 g respectively. These extracts were used for phytochemical profiling and coumarins isolation.

Dried and shredded roots of *Angelica archangelica* (5.0 g), *Angelica dahurica* (5.0 g), *Angelica biserrata* (5.0 g) and *Angelica sinensis* (5.0 g) were milled to powder and extracted with 50 mL of 60% (v/v) aqueous ethanol under reflux for 2 h. The extracts were then filtered through a filter paper, reduced in a rotary evaporator, and lyophilized, resulting in dried ethanolic extracts. These extracts were used for pharmacological studies.

5.4 Thin Layer Chromatography (TLC)

TLC analysis was performed on glass plates coated with 60G F_{254} silica gel (Merck, Darmstadt., Germany). The plates were developed in a vertical chamber previously saturated with mobile phase for at least 15 minutes.

The mobile phase for coumarins analysis was a mixture of n-hexane and ethyl acetate (85:15, v/v) or anhydrous acetic acid, ethyl acetate and toluene (1:10:90, v/v/v). The chromatogram was

visualized and evaluated under UV light at λ_1=254 nm, λ_2=365 nm, and afterwards treated with 10% (v/v) solution of sulfuric acid in methanol, heated at 100 °C for 5 minutes and examined in daylight.

The mobile phase for lignan analysis was a mixture of dichloromethane and methanol (93:7, v/v). The chromatogram was treated with 1% (w/v) vanillin solution in concentrated sulfuric acid, heated at 100 °C for 5 minutes and examined in daylight.

5.5 Column Chromatography (CC)

Fractionation of plant extracts was performed on glass chromatography columns of different lengths and width: 30 x 10 cm, 60 x 2 cm, 40 x 3 cm, and 65 x 5 cm. They were filled with Diaion HP-20 (Supelco Analytical, Bellefonte PA, USA), Sephadex LH-20 (Pharmacia, Stockholm, Sweden), or silica gel (0.063–0.100 mm; Merck, Darmstadt., Germany). No external pressure was used (liquid flow under gravity). Fraction collection was volume-based, using the Foxy Jr. Fraction Collector (Teledyne ISCO, Lincoln NE, USA). Step gradients of water–methanol, chloroform–methanol, n-hexane–ethyl acetate and toluene–ethyl acetate were used depending on the column packing and polarity of fraction constituents. Fractions were monitored and pooled based on their TLC profiles.

5.6 Preparative Chromatography (HPLC-PREP)

Preparative HPLC was performed with a Shimadzu LC20-AP instrument (Shimadzu, Japan) using a Kinetex XB-C_{18} column (150 mm × 21.2 mm, 5 µm) (Phenomenex, Torrance, CA, USA) or a Zorbax SB-C_{18} column (150 mm × 21.2 mm, 5 µm) (Agilent, Santa Clara, CA, USA) at a flow rate of 20.0 mL/min and detection at λ_1=254 nm, λ_2=325 nm for coumarins isolation or at λ_1=254 nm, λ_2=280 nm for lignans isolation. The mobile phase consisted of 0.1% formic acid in water (A) and 0.1% formic acid in acetonitrile (B) using the following gradient: 0-60 min, 15-100% B. Water for HPLC experiments was prepared using the Milli-Q Plus system (Millipore, Billerica, MA, USA) (18.2 MΩ cm). The injection volume was 400 µL. Fraction collection was based on set retention times.

5.7 Nuclear Magnetic Resonance (NMR)

^{1}H, ^{13}C, and 2D NMR spectra (ROESY, COSY, HSQC, HMBC) were obtained on a Bruker Avance III 500 NMR spectrometer (Bruker BioSpin, Rheinstetten, Germany), operating at 500 and 126 MHz respectively, using standard pulse programs and 5 mm NMR tubes. All measurements were performed

at 295 K. Spectra were recorded in methanol-d_4, DMSO-d_6 or in $CDCl_3$. In each case, spectra were calibrated at residual solvent resonances, at 3.31 ppm for ^{1}H and 49.15 ppm for ^{13}C (methanol-d_4), 2.50 ppm for ^{1}H and 39.51 ppm for ^{13}C (DMSO-d_6) or 7.24 ppm for ^{1}H and 77.23 ppm for ^{13}C ($CDCl_3$). All isolated compounds were characterized using NMR techniques. The NMR experiments were conducted in the Centre of Molecular and Macromolecular Studies, Polish Academy of Sciences, Łódź, Poland, under the supervision of prof. Marta Katarzyna Dudek.

5.8 Liquid Chromatography with Diode Array Detector coupled with Electrospray Ionization tandem Mass Spectrometry (LC-DAD-ESI-MS/MS)

LC-DAD-ESI-MS/MS analysis was performed on a UHPLC-3000 RS system (Dionex, Dreieich, Germany) outfitted with diode array detector (Dionex, Dreieich, Germany) coupled with AmaZon SL ion trap mass spectrometer with an ESI interface (Bruker Daltonik GmbH, Bremen, Germany). Separation was performed on a Kinetex XB-C_{18} analytical column (150 mm × 2.1 mm, 1.9 µm) (Phenomenex, Torrance, CA, USA) or a Zorbax SB-C_{18} analytical column (150 mm × 2.1 mm, 1.9 µm) (Agilent, Santa Clara, CA, USA). The mobile phase consisted of 0.1% formic acid in water (A) and 0.1% formic acid in acetonitrile (B) using the following gradients: (1) 0–60 min, 15–100% B, then 10 min of equilibration or (2) 0–5 min, 0% B; 5–30 min, 0–30% B; 35–45 min, 30-50% B; 45–50 min, 50-100% B; 50–60 min, 100% B. Samples for LC-DAD-ESI-MS/MS analysis were prepared by dissolving dried extracts in 0.1% formic acid in methanol at the concentration of 10 mg/mL. Standards were prepared in the same way at the concentration of 1 mg/mL). The flow rate was 0.2 mL/min, injection volume was 5 µL, column temperature was set at 25 °C. The LC eluate was introduced into the ESI interface without splitting, and compounds were analyzed in both positive and negative ion mode with the following settings: nebulizer pressure of 40 psi, drying gas flow rate of 9 L/min; nitrogen gas temperature of 300 °C; and a capillary voltage of 4.5 kV. The mass scan ranged from 100 to 2200 m/z.

UV spectra were recorded in the range 190–400 nm. Identification of compounds was based on the UV–Vis spectra, determination of their molecular mass, and fragmentation profile, and compared to reference compounds and literature data.

5.9 Glycosides hydrolysis

To obtain trachelogenin (aglycone) from trachelogenin 4-*O*-glucoside (glycoside) an enzymatic hydrolysis was performed. The glycoside (30.0 mg) was dissolved in acetate buffer (50 mM, pH 4.5) and incubated for 24h with 3.25 U β-glucosidase and 1.56 U cellulase for each mg of the compound. Afterwards, the solution was partitioned with ethyl acetate to separate the aglycone in the organic phase from enzymes and reaction byproducts. The organic phase was evaporated to dryness on a rotary evaporator and **trachelogenin** (16.2 mg) was obtained.

5.10 Preparation of compounds and extracts solutions

Compounds and extracts that were to be used in pharmacological studies were dissolved in sterile DMSO, filtered through a 0.20 µm membrane, aliquoted and kept at -20 °C until experiment. In general, extracts were prepared to obtain a concentration of 10 mg/mL, and for compounds a concentration of 20 mmol/L.

5.11 INS-1 cell culture

INS-1 cells (rat radiation-induced insulinoma cell line) were cultured in RPMI-1640 medium supplemented with 10% heat-inactivated (30 min, 56 °C) Foetal Calf Serum, 100 U/mL penicillin, 100 µg/mL streptomycin, 2 mmol/L L-glutamine, 10 mmol/L HEPES, 1 mmol/L^{-1} sodium pyruvate and 50 µmol/L 2-mercaptoethanol, in a humidified atmosphere (5% CO_2, 37 °C). The cells used for experiments had a passage number from 29 to 42.

5.12 Insulin secretion experiments on INS-1 cells

INS-1 cells were seeded in 24-well plates pre-coated with poly-L-lysine (4×10^5 cells/well) and cultured for 5 days before insulin secretion experiments, to obtain cell confluence of about 80%. The cells were washed twice with HEPES-balanced Krebs-Ringer bicarbonate buffer (123 mmol/L NaCl, 5.4 mmol/L KCl, 1.3 mmol/L KH_2PO_4, 1.4 mmol/L $MgSO_4$, 2.9 mmol/L $CaCl_2$, 5 mmol/L $NaHCO_3$ and 20 mmol/L HEPES, adjusted to pH 7.4 with NaOH) saturated with carbon dioxide (15 min) and supplemented with 1 g/L bovine serum albumin (KRB). Then, the cells were pre-incubated for 1h (5% CO_2, 37°C) in 500 µL of KRB buffer containing 1.4 mmol/L glucose. Afterwards, the buffer was discarded, and the cells were incubated for 1h (5% CO_2, 37°C) in 500 µL of KRB buffer containing tested

compounds or extracts in the basal glucose conditions (1.4 mmol/L glucose) or stimulating glucose conditions (8.3 mmol/L glucose). To limit the measurement variations, each condition was carried out in triplicate on the same plate. Control treatments were always performed using the same amount of vehicle (DMSO) in each well.

At the end of the 1h incubation period, the supernatants were sampled and kept at -20 °C until insulin assay by the homogeneous time resolved fluorescence technology (HTRF) according to the manufacturer's instructions (PerkinElmer). Two anti-insulin anti-bodies were used; one labelled with Eu^{3+}-Cryptate (fluorescence donor) and one labelled with XL665 (fluorescence acceptor) that recognize distinct epitopes. When these two fluorophores bind to insulin molecules, the two antibodies come into proximity, allowing fluorescence resonance energy transfer (FRET) to occur between the Eu^{3+}-Cryptate and the XL665. This FRET increases proportionally with the insulin concentrations.

5.13 Insulin secretion experiments on dysfunctional INS-1 cells

INS-1 cells were seeded in 24-well plates pre-coated with poly-L-lysine (4×10^5 cells/well) and cultured for 4 days. Dysfunction was induced by culturing cells in glucotoxic condition (culture medium containing 30 mmol/L glucose) for an additional 48h. The cells were washed twice with KRB buffer and pre-incubated for 1h (5% CO_2, 37°C) in 500 µL of KRB buffer containing 1.4 mmol/L glucose.

Afterwards, the buffer was discarded, and the cells were incubated for 1h (5% CO_2, 37°C) in 500 µL of KRB buffer containing tested compounds or extracts in the basal glucose conditions (1.4 mmol/L glucose) or stimulating glucose conditions (8.3 mmol/L glucose). To limit the measurement variations, each condition was carried out in triplicate on the same plate. Control treatments were always performed using the same amount of vehicle (DMSO) in each well. At the end of the 1h incubation period, the supernatants were sampled and kept at -20 °C until insulin assay by HTRF.

5.14 Insulin secretion modulation by blocking membrane channels

INS-1 cells were seeded in 24-well plates pre-coated with poly-L-lysine (4×10^5 cells/well) and cultured for 5 days before insulin secretion experiments, to obtain cell confluence of about 80%. The cells were washed twice with KRB buffer and pre-incubated for 1h (5% CO_2, 37°C) in 500 µL of KRB buffer containing 1.4 mmol/L glucose and one of the channel blockers (20 mmol/L tetraethylammonium or 20 µmol/L verapamil). Afterwards, the buffer was discarded, and the cells

were incubated for 1h (5% CO_2, 37°C) in 500 µL of KRB buffer containing tested compounds or extracts in the basal glucose conditions (1.4 mmol/L glucose) or stimulating glucose conditions (8.3 mmol/L glucose). Control treatments were always performed using the same amount of vehicle (DMSO) in each well. Experiments were performed in duplicates. At the end of the 1h incubation period, the supernatants were sampled and kept at -20 °C until insulin assay by HTRF.

5.15 Viability of INS-1 cells

Cell viability was determined using the 3-(4,5-Dimethylthiazol-2-yl)-2,5-diphenyltetrazolium bromide (MTT) assay. INS-1 cells were seeded in 96-well plates pre-coated with poly-L-lysine (1×10^5 cells/well) and cultured for 4 days before experiments. Then, the cells were preincubated with tested compounds for 48h (5% CO_2, 37°C) in culture medium. At the end of the 48h preincubation period, cells were washed twice with KRB buffer and KRB containing 5 mg/mL MTT was added to each well. Plates were then incubated for 3 h in the dark in a humidified atmosphere (5% CO_2, 37°C). Cells were washed with DPBS, and precipitates were dissolved in 50 µL DMSO. The absorbance of the reduced intracellular formazan product was read at 492 nm on a microtiter plate reader (Tecan, Lyon, France). Experiments were performed in quadruplicate.

5.16 Cytoprotection experiments on INS-1 cells

To assess the potential of studied compounds to protect the β-cell, the INS-1 were subjected to different stress conditions, i.e., stress oxidative, glucotoxicity and inflammation.

To evaluate the protective effect of studied compounds against glucotoxicity, INS-1 cells (after 4 days of culture) were incubated with the indicated concentrations of the compound for 48h (5% CO_2, 37 °C) in culture medium supplemented with 30 mmol/L glucose. At the end of the incubation period, the cells were washed and incubated for 1h in KRB buffer under stimulating conditions (8.3 mmol/l of glucose), and the insulin secreted was quantified, as well as cell viability was assessed using MTT assay described above.

To evaluate the protective effect of studied compounds against inflammatory stress, INS-1 cells (after 4 days of culture) were incubated with the indicated concentrations of the compound for 24h (5% CO_2, 37 °C) in culture medium supplemented with either single cytokine 0.1 ng/mL IL-1β or a cytokine mixture containing 0.1 ng/mL IL-1β, 50 ng/mL TNF-α and 33 ng/mL INF-γ. At the end of the

incubation period, the cells were washed and incubated for 1h in KRB buffer under stimulating conditions (8.3 mmol/l of glucose), and the insulin secreted was quantified, as well as cell viability was assessed using MTT assay described above.

To evaluate the protective effect of studied compounds against oxidative stress, INS-1 cells (after 4 days of culture) were incubated with the indicated concentrations of the compound for 2h (5% CO_2, 37 °C) in RPMI medium. At the end of the incubation period, the cells were washed and incubated for 1h in KRB buffer under stimulating conditions (8.3 mmol/l of glucose) supplemented with 50 µmol/L hydrogen peroxide, and secreted insulin was quantified, as well as cell viability was assessed using MTT assay described above.

5.17 Image analysis of cytoplasmatic Ca^{2+} in INS-1 cells

Intracellular calcium concentration ($[Ca^{2+}]_i$) was measured using the fluorescent indicator fura-2. For this purpose, INS-1 cells grown on glass coverslips were loaded with fura-2 by a 30 min incubation at 37 °C with 1 µmol/L fura-2-AM and 0.02% pluronic F-127 in KRB buffer supplemented with 1.4 or 8.3 mmol/L glucose. $[Ca^{2+}]_i$ was monitored by videomicroscopy. After rinsing, the glass coverslip was transferred to the recording chamber mounted on an inverted microscope (Leica, DMIRB), continuously superfused with extracellular medium. Fura-2 emission was obtained by exciting alternatively at 340 and 380 nm with a rotating filter wheel (Sutter Instruments) and by monitoring emissions (F340 and F380) at 510 nm. Fluorescent signals were collected with a CCD camera (Hamamatsu), digitized, and analyzed with image analysis software (HCImage, Hamamatsu). The ratio of emissions at 510 nm (F340/F380) was recorded in cells every second. Experiments were carried out at room temperature and drug application was performed with a gravity-fed system.

The image analysis of cytoplasmatic calcium was conducted in the Pharmacochemistry of Synaptic Transmission and Neuroprotection team, Institut des Biomolécules Max Mousseron, Université de Montpellier, France, under the supervision of prof. Michel Vignes.

5.18 Electrophysiological recordings

Voltage-gated Ca^{2+} channel activities were recorded using the whole-cell patch-clamp technique with a Biologic RK400 amplifier (Biologic, France). Data acquisition and analysis were performed using the pCLAMP system (Axon Instruments, Union City, CA, USA). Currents were recorded with patch pipettes of 3–5 MΩ. Capacitive transients were electronically compensated. Residual capacitive transient and linear leakage currents were subtracted using a four sub-pulse protocol. The extracellular solution contained 130 mmol/L NaCl, 5.6 mmol/L KCl, 1 mmol/L $MgCl_2$, 1 mmol/L glucose, 10 mmol/L HEPES, 5 mmol/L $BaCl_2$, adjusted to pH 7.4 with NaOH. The pipette solution contained 130 mmol/L CsCl, 10 mmol/L EGTA, 5 mmol/L $ATPNa_2$, 2 mmol/L $MgCl_2$, 10 mmol/L HEPES, adjusted to pH 7.3 with CsOH. The holding potential was set at -65 mV, and depolarizing test pulses were applied as described. Compounds were applied to cells by pressure ejection from a glass pipette. All experiments were performed at room temperature.

Potasium channel activities were recorded using the whole-cell patch-clamp technique with the same setup and protocol as for calcium channels. However, intracellular and extracellular solution were different. The extracellular solution contained 130 mmol/L NaCl, 5.6 mmol/L KCl, 1 mmol/L $MgCl_2$, 1 mmol/L glucose, 10 mmol/L HEPES, 2 mmol/L $CaCl_2$, adjusted to pH 7.4 with NaOH. The pipette solution contained 140 mmol/L KCl, 5 mmol/L $ATPNa_2$, 2 mmol/L $MgCl_2$, 10 mmol/L HEPES, adjusted to pH 7.3 with KOH.

To measure membrane potential, INS-1 cells were incubated with a red fluorescent probe FLIPR as described by the manufacturer (Molecular Device, Paris, France) for 30 min at 37 °C in a physiological solution (130 mmol/L NaCl, 5.6 mmol/L KCl, 1 mmol/L $MgCl_2$, 1 mmol/L glucose, 10 mmol/L HEPES, 2 mmol/L $CaCl_2$, adjusted to pH 7.4 with NaOH) for measurement in real-time fluorescence by confocal microscopy (NIKON) (excitation λ: 561 nm emission λ: 605 nm, image acquisition frequency 0.20 Hz). Regions of interest were drawn around each cell to detect cellular fluorescence variations. Results are expressed as the ratio of fluorescence (fluorescence divided by initial fluorescence F/F0).

The electrophysiological experiments were conducted in Centre de Recherche Cardio-Thoracique de Bordeaux, Université de Bordeaux, France, under the supervision of prof. Jean-François Quignard.

5.19 Data and statistical analyses

The data and statistical analyses comply with the recommendations on experimental design and analysis in pharmacology [313]. All the data were analyzed using GraphPad Prism v9 software (GraphPad Software, San Diego, USA). All averaged data are expressed as mean ± Standard Error of the Mean (SEM). The group size (n) represents the number of experimental independent repeats, each carried out with distinct biological preparations. Group sizes suitable for each set of experiments were estimated to ensure adequate power and to detect a pre-specified effect based on the available literature, on pilot studies, and on previous reports [155, 312, 314]. To ensure the reliability of single values, technical duplicate and triplicate were used for insulin secretion experiments and quadruplicate for viability experiments.

Statistical analyses were run only on group size of n independent samples ≥ 3, and as follows. First, each data set was tested for normality (Shapiro-Wilk test, $p > 0.05$ = passed) and for variance homogeneity (Brown-Forsythe test, $p > 0.05$ = passed). Parametric statistical tests (t-test and ANOVAs) were used only if the data were normally distributed and there was no inhomogeneity of variance. If only one data set failed the Shapiro-Wilk test, nonparametric analyses were performed using Kruskall-Wallis test. Comparisons between multiple sets of data were performed by one-way ANOVA or Kruskall-Wallis tests with no matching. Holm-Sidak or Dunn's post hoc comparisons were conducted only if tested ANOVA or Kruskal-Wallis respectively achieved statistical significance ($p < 0.05$ = passed). The limit of statistical significance was set at $p < 0.05$ and indicated by an asterisk *.

6 Results

6.1 Phytochemical part

6.1.1 Phytochemical characterization of lignan-rich plant extracts and isolation of lignans

The aim of the phytochemical characterization of the following sixteen plant extracts was to identify and select lignans for isolation to form a compound library for subsequent pharmacological examination.

6.1.1.1 Conifer wood – phytochemistry

Through comprehensive LC-DAD-ESI-MS/MS analysis of *Pinus sylvestris* L., *Pinus cembra* L., *Pinus mugo* Turra, *Pinus strobus* L., *Pinus ×rhaetica* Brügger, *Abies alba* Mill., *Picea abies* L., *Picea glauca* (Moench) Voss, *Pseudotsuga menziesii* Mirb., *Tsuga canadensis* Carrière, *Larix decidua* Mill., *Larix polonica* Rac., and *Larix kaempferi* Lamb. branch wood methanolic extracts 40 compounds were identified or partially identified based on the elution order, UV maxima, pseudomolecular and fragmentation ions in both positive and negative ion modes and comparison to reference standards and literature data Table 5. In case of pseudomolecular ions of the same mass and fragmentation, their identity was later established through isolation and NMR analysis.

The investigated plant material contained secondary metabolites belonging to flavan-3-ols, flavonoids, lignans, sesquilignans, stilbenes, sesquiterpenes, and diterpenes. The presence of identified compounds in each studied species is presented in Table 6.

Eight compounds belonging to the group of flavan-3-ols were identified in selected wood extracts. Compounds **5** (t_r = 4.5 min) and **7** (t_r = 6.6 min) exhibited a pseudomolecular ion at m/z 289 and had identical fragmentation pattern. Based on their elution order and comparison to reference standards, these compounds were identified as catechin and epi-catechin, respectively. Whilst catechin was present in all studied plant samples, I was not able to detect epi-catechin in *P. sylvestris*, *P. mugo*, *P. ×rhaetica* and both spruces.

Four compounds **2** (t_r = 3.3 min), **3** (t_r = 3.6 min), **6** (t_r = 5.2 min) and **15** (t_r = 11.6 min) exhibited a pseudomolecular $[M-H]^-$ ion at m/z 577, which fragmented into m/z 559 $[M-H-18]^-$ - loss of water, m/z 451 $[M-H-126]^-$ from heterocyclic ring fissure fragment, m/z 407 $[M-H-170]^-$ product of retro-Diels-Alder reaction followed by the loss of water and m/z 289, which corresponds to (epi)catechin. Based on fragmentation patterns they were all characterized as type B dimeric procyanidins [315]. Previously, procyanidins B1-B4 have been isolated from the bark of *Larix gmelinii* (Rupr.) Kuzen. [316] and *Pseudotsuga menziesii* Mirb. [317]. In each plant sample at least two dimeric procyanidins B were present. Larch wood was the richest in procyanidins, containing all 4 compounds in comparison to all studied genera.

Table 5. Retention time, UV, and ESI-MS/MS data of the compounds identified in Pinaceae species wood using LC-DAD-ESI-MS/MS analysis.

	Compounds	T_r [min]	UV_{max} [nm]	ESI	Extracted ion [m/z]	Fragment ions [m/z]	Group	Presence in *Pinaceae* spp.
1.	gallocatechin	3.0	199, 277	$[M-H]^-$	305	219, 179, 137	flavan-3-ol	[318]
2.	dimeric procyanidin B (I)	3.3	230, 282	$[M-H]^-$	577	559, 451, 407, 289	flavan-3-ol	[317]
3.	dimeric procyanidin B (II)	3.6	207, 238, 280	$[M-H]^-$	577	559, 451, 407, 289	flavan-3-ol	[317]
4.	trimeric procyanidin B	4.2	199, 281	$[M-H]^-$	865	695, 577, 407, 289	flavan-3-ol	[319]
5.	catechin*	4.5	232, 278	$[M-H]^-$	289	245, 203, 179	flavan-3-ol	[320]
6.	dimeric procyanidin B (III)	5.2	238, 283	$[M-H]^-$	577	559, 451, 407, 289	flavan-3-ol	[317]
7.	epi-catechin*	6.6	279	$[M-H]^-$	289	245, 203, 179	flavan-3-ol	[319]
8.	dihydromyricetin*	7.7	213, 225, 290	$[M-H]^-$	319	301, 193, 125	flavonoid	[320]
9.	7-hydroxylariciresinol (I)**	7.8	199, 225, 279	$[M-H]^-$	375	357, 345, 327, 297	lignan	[321]
10.	*trans*-astringin	8.1	192, 218, 324	$[M-H]^-$	405	243, 225, 201, 173, 159	stilbene	[320]
11.	dihydrokaempferol*	8.4	290	$[M-H]^-$	287	259, 243, 181	flavonoid	[321]
12.	todolactol**	9.9	196, 225, 280	$[M-H]^-$	375	327, 191, 176	lignan	[320]
13.	taxifolin glucoside	10.2	196, 287	$[M-H]^-$	465	447, 437, 303, 285, 259	flavonoid	[322]
14.	*cis*-astringin	10.8	213, 319	$[M-H]^-$	405	243, 225, 201, 173, 159	stilbene	[323]
15.	dimeric procyanidin B (IV)	11.6	243, 280	$[M-H]^-$	577	559, 451, 407, 289	flavan-3-ol	[317]
16.	7-hydroxylariciresinol (II)**	11.6	198, 227, 279	$[M-H+HCOOH]^-$	421	375, 357, 345, 325	lignan	[321]
17.	piceid	11.7	216, 319	$[M-H]^-$	389	227, 185, 183, 157, 143	stilbene	[320]
18.	taxifolin*	12.4	280	$[M-H]^-$	303	285, 177	flavonoid	[321]
19.	isorhapontin	12.5	192, 218, 325	$[M-H+HCOOH]^-$	465	419, 257, 242, 241	stilbene	[320]
20.	cyclolariciresinol**	12.7	197, 283	$[M-H]^-$	359	344, 313, 189	lignan	[321]
21.	α-conidendric acid	14.0	200, 225, 280	$[M-H+HCOOH]^-$	419	373, 177	lignan	[321]
22.	7-hydroxymatairesinol**	15.0	197, 226, 280	$[M-H]^-$	373	355, 340, 311, 293, 219	lignan	[321]
23.	secoisolariciresinol**	15.3	232, 281	$[M-H]^-$	361	346, 313, 299	lignan	[321]
24.	eriodictyol*	15.4	194, 287	$[M-H]^-$	287	259, 243, 151	flavonoid	[324]
25.	myricetin*	15.7	254, 373	$[M-H]^-$	317	289, 179, 151, 137	flavonoid	[325]
26.	secoisolariciresinol guaiacylglyceryl ether	15.7	197, 280	$[M-H]^-$	557	539, 525, 521, 509, 415, 361	sesquilignan	[321]
27.	lariciresinol**	16.1	197, 200, 202, 280	$[M-H+HCOOH]^-$	405	359, 329	lignan	[321]
28.	lariciresinol guaiacylglyceryl ether	16.7	201, 225, 280	$[M-H]^-$	555	525, 507, 359, 329, 315, 195, 165	sesquilignan	[321]
29.	nortrachelogenin**	18.3	199, 225, 280	$[M-H]^-$	373	355, 327, 311, 249, 223, 191, 147	lignan	[321]
30.	pinoresinol**	19.1	201, 280	$[M-H]^-$	357	342, 327, 311, 151, 136	lignan	[321]
31.	quercetin*	19.8	208, 368	$[M-H]^-$	301	273, 179, 151	flavonoid	[326]
32.	matairesinol**	21.6	197, 281	$[M-H]^-$	357	342, 313, 298, 281, 209, 191, 147	lignan	[321]
33.	pinobanksin*	22.0	214, 284	$[M-H]^-$	271	253	flavonoid	[320]
34.	pinosylvin	26.3	223, 299	$[M-H]^-$	211	169	stilbene	[327]
35.	pinocembrin*	30.3	214, 288	$[M-H]^-$	255	213, 211	flavonoid	[327]
36.	pinobanksin 3-*O*-acetate	30.5	216, 292	$[M-H]^-$	313	271, 253	flavonoid	[328]
37.	pinosylvin monomethyl ether	33.6	212, 223, 300	$[M-H]^-$	225	210	stilbene	[327]
38.	dehydrojuvabione	41.0	224, 300	$[M+H]^+$	265	251, 233, 205, 187, 176	sesquiterpene	[321]
39.	neoabietic acid	52.0	251	$[M+H]^+$	303	257, 219, 179, 151, 123	diterpene	[327]
40.	abietic acid*	52.3	241	$[M+H]^+$	303	285, 257, 123	diterpene	[327]

* compared with reference standard; ** isolated from *A. alba* or *P. sylvestris* and identified on NMR.

Additionally, one more procyanidin was detected in all wood extracts – compound **4** (t_r = 4.2 min). The main pseudomolecular ion was at m/z 865 and fragmented into m/z 695, m/z 577, m/z 407 and m/z 289. Based on the fragmentation pattern [329] this compound was assigned as type B trimeric procyanidin (procyanidin C).

Furthermore, compound **1** (t_r = 3.0 min) gave a pseudomolecular ion at m/z 305, which fragmented into m/z 219, m/z 179 and m/z 137. This fragmentation pattern was typical for gallocatechin [315]. The presence of this flavan-3-ol were found in *A. alba*, all studies *Pinus* spp. and *Larix* spp.

A total of 10 flavonoids have been found in studied wood extracts. Most of them were present in aglycone form, with just one glycoside form detected. Compound **18** (t_r = 12.4 min) was the most abundant flavonoid in these extracts, as it was not present only in *A. alba* and *T. canadensis* and had the highest peak of all flavonoid aglycones. Compound **18** had its UV maximum at 280 nm and exhibited a pseudomolecular ion at m/z 303, which fragmented into m/z 285 and m/z 177. The compound was then identified by comparison with the reference standard and comparison to the literature data [330-332] as taxifolin (syn. dihydroquercetin). Another major flavonoid compound **13** (t_r = 10.2 min) had its UV maximum at 287 nm and its pseudomolecular ion at m/z 465 and gave a primary fragment ion at m/z 303 $[M-H-162]^-$ corresponding to the cleavage of hexose (probably glucose). Thus, compound **13** was assigned as taxifolin hexoside, which was consistent with the fragmentation pattern reported previously [330].

Four more flavanonols were detected in *Pinaceae* wood, with their UV maxima at around 290 nm. Compound **8** (t_r = 7.7 min) exhibited a pseudomolecular ion at m/z 319 and fragment ions at m/z 301 $[M-H-18]^-$ corresponding to the loss of water, at m/z 193 and m/z 125. By comparing fragmentation pattern with reference standard and literature data [333], compound **8** was assigned as dihydromyricetin (syn. ampelopsin, ampeloptin). It was found in samples from *P. mugo*, *P. rhaetica*, *L. decidua* and *L. polonica* (Table 2). Compound **11** (t_r = 8.4 min) had its pseudomolecular ion at m/z 287, which fragmented into m/z 259 $[M-H-28]^-$ corresponding to the loss of CO, m/z 243 $[M-H-44]^-$ corresponding to the loss of CO_2 and m/z 181. The fragmentation pattern matched to the literature data of dihydrokaempferol (syn. aromadendrin) [333]. Dihydrokaempferol was only found in two larch species, namely European and Polish larch (Table 2). Compound **33** (t_r = 22.0 min) exhibited a pseudomolecular ion at m/z 271 and fragment ion at m/z 253 $[M-H-18]^-$ corresponding to the loss of water. It was tentatively identified, comparing to reference compound and literature data [334] as

pinobanksin and compound **36** (t_r = 30.5 min) which exhibited a similar fragmentation pattern was assigned as pinobanksin 3-*O*-acetate, also consistent with the data found in the literature [335]. The presence of pinobanksin was not genus-specific, while pinobanksin 3-*O*-acetate was only found in *P. strobus* wood.

I have found presence of two flavanones, compound **24** (t_r = 15.4 min) and **35** (t_r = 30.3 min), which had their UV maxima at around 290 nm. Compound **24** presented a similar fragmentation pattern to that of compound **11**. Based on the elution profile and referring to the literature [336] it was tentatively assigned as eriodictyol. It was present in all larch species, Douglas fir, mountain pine, Swiss pine, and Weymouth pine. Pseudomolecular ion of compounds **35** was at m/z 255 and fragmented into m/z 213 and m/z 211. By comparison with a reference standard and literature data [337] it was assigned as pinocembrin. I have found its presence in most pine species (apart from *P. cembra*) and in Douglas fir.

I report presence of two flavonols in studied wood extracts, which were characterized by their UV maxima at around 370 nm. Compounds **25** (t_r = 15.7 min) and **31** (t_r = 19.8 min) had typical fragmentation patterns of myricetin and quercetin respectively [338], which was confirmed by comparison with reference standards. Quercetin and myricetin were found in larches and Douglas fir. Additionally, Weymouth pine contained quercetin, while myricetin was also present in mountain pine.

Lignans have been identified as major constituents in fir and pine species. Based on the LC-DAD-ESI-MS/MS analysis three compounds **9** (t_r = 7.8 min), **12** (t_r = 9.9min) and **16** (t_r = 11.6 min) had their pseudomolecular ion at m/z 375 $[M-H]^-$ and UV maxima at around 225 and 280 nm. There have been previously reported three lignan isomers in conifer wood, that could give pseudomolecular ion at m/z 375: liovil, todolactol and 7-hydroxylariciresinol [339]. Unfortunately, no ESI-MS/MS fragmentation pattern data could be found for liovil and 7-hydrolariciresinol, with just one source for todolactol [339]. Through NMR analysis (6.1.1.2) of isolates from *A. alba* wood, I was able to assign compounds **9** and **16** as 7-hydroxylariciresinol diastereoisomers, respectively. Fragmentation of m/z 375 ion corresponding to compound **12** gave m/z 327, m/z 191 and m/z 176 which was consistent with fragmentation pattern proposed for todolactol [339]. The occurrence of lignans in different conifer species was as follows: 7-hydroxylariciresinol (I) was found in silver fir and both spruces, todolactol was besides present in European and Japanese larch, Douglas fir and Canadian hemlock. 7-hydroxylariciresinol (II) was present in at least one species of each genus except spruces. LC-DAD-ESI-MS/MS analysis did not detect the signal that could correspond to liovil.

Compounds **30** (t_r = 19.1 min) and **32** (t_r = 21.6 min) exhibited pseudomolecular ions at m/z 357 $[M-H]^-$ and similar fragmentation patterns. Compound **32** gave a characteristic primary product ion for dibenzylbutyrolactone lignans $[M-H-44]^-$ at m/z 313, which corresponds to the loss of CO_2 from the lactone ring [339], and that was not observed for compound **30**. Compound **30** produced a fragment ion at m/z 342 $[M-H-15]^-$ corresponding to the loss of methyl radical, and at m/z 151 (guaiacyl) and m/z 136, which were the products of α,β-cleavage in the side chain. This fragmentation pattern was characteristic for furofuran lignans [339]. According to the fragmentation, elution order in RP-LC and comparison with literature data, compound **30** was identified as pinoresinol, while compound **32** was identified as matairesinol. Pinoresinol was only present in Scots pine wood and matairesinol could be found in nearly every plant material except silver fir and Douglas fir.

Compounds **22** (t_r = 15.0 min) and **29** (t_r = 18.3 min) exhibited their pseudomolecular ions at m/z 373 $[M-H]^-$. They both formed a fragment ion at m/z 355 $[M-H-18]^-$ corresponding to the loss of water. For compound **22** a fragment ion at m/z 311 $[M-H-62]^-$ could be found, corresponding to the loss of water and CO_2 from the lactone ring (again suggesting the compound belonged to the dibenzylbutyrolactone group). On the other hand, compound **29** did not produce a fragment ion at m/z 311; instead an ion at m/z 327 $[M-H-46]^-$ which corresponds to the loss of water and CO was observed. Both fragmentation patterns and differences among them have been previously observed [340]. According to the fragmentation and elution order in RP-LC, compound **22** was identified as 7-hydroxymatairesinol and compound **29** was identified as nortrachelogenin (syn. 8'-hydroxymatairesinol). Nortrachelogenin and 7-hydroxymatairesinol were observed in most analyzed conifer wood, only excluding mountain and Rhaetic pine for the former and additionally excluding Scots pine for the latter. Compound **21** (t_r = 14.0 min) had a pseudomolecular ion at m/z 419 $[M-H+HCOOH]^-$ which fragmented into m/z 373 $[M-H]^-$ corresponding to the loss of formate adduct. Based on literature data it was tentatively identified as α-conidendric acid [339]. It was found in silver fir, mountain pine, Weymouth pine, all larch species and Canadian hemlock.

Compound **27** (t_r = 16.1 min) had its pseudomolecular ion at m/z 405 which fragmented to m/z 359 $[M-H]^-$ corresponding to the presence of formyl adduct. I have also observed another compound **20** (t_r = 12.7 min) exhibiting its pseudomolecular ion at m/z 359 $[M-H]^-$. Differences in further fragmentation could be observed for these compounds. For peak **27** I could observe a fragment ion at m/z 329 $[M-H-30]^-$ resulting from the loss of formaldehyde. Compound **20** exhibited fragment ions at m/z 344 $[M-H-15]^-$ corresponding to the loss of methyl radical, at m/z 313 $[M-H-46]^-$ formed by the loss of methoxyl and methyl radicals and at m/z 189 which was a product of β,β-cleavage in the side

chain. Both fragmentation patterns have been previously observed [339] for lariciresinol (**27**) and cyclolariciresinol (syn. isolariciresinol) (**20**) respectively. Cyclolariciresinol was only found in silver fir, while lariciresinol was present in all larch species, silver fir, Douglas fir, Weymouth pine, Canadian hemlock, and white spruce.

Apart from cyclolariciresinol (**20**), one other butanediol lignan has been found. For compound **23** (t_r = 15.3 min) a pseudomolecular ion could be observed at m/z 361 $[M-H]^-$ and fragment ions at m/z 346 $[M-H-15]^-$ corresponding to the loss of methyl radical, at m/z 313 $[M-H-48]^-$ formed by the loss of formaldehyde and water in the diol structure and at m/z 299 $[M-H-48-15]^-$ corresponding to both rearrangements. This structure was compared to fragmentation data described in the literature [339] and identified as secoisolariciresinol. This was the dominant metabolite of silver fir and was also found in all larch and spruce species, mountain and Weymouth pine, Douglas fir, and Canadian hemlock.

Two sesquilignans have been found in conifer wood. Compound **26** (t_r = 15.7 min) exhibited a pseudomolecular ion at m/z 557 $[M-H]^-$ and fragment ions at m/z 539 $[M-H-18]^-$ corresponding to the loss of water, m/z 525 $[M-H-32]^-$, m/z 521 $[M-H-36]^-$, m/z 509 $[M-H-48]^-$ formed by the loss of formaldehyde and water in the diol structure, m/z 415 and m/z 361 $[M-H-196]^-$ corresponding to the cleavage of guaiacylglyceryl moiety. The fragmentation pattern was in accordance with the data for oligolignans isolated from Norway spruce and Scots pine knots [12]. Based on fragmentation, this compound was tentatively identified as secoisolariciresinol 4-*O*-guaiacylglyceryl ether. It was found in silver and Douglas fir, as well as all larch species and mountain pine.

Compound **28** (t_r = 16.7 min) had its pseudomolecular ion at m/z 555 $[M-H]^-$ and fragment ions at m/z 525 $[M-H-20]^-$, m/z 507 $[M-H-48]^-$ from the loss of formaldehyde and water, m/z 359 $[M-H-196]^-$ corresponding to the cleavage of guaiacylglyceryl moiety, and at m/z 329 $[M-H-196-30]^-$ resulting from the loss of formaldehyde. This compound was tentatively identified as lariciresinol 4-*O*-guaiacylglyceryl ether in accordance to previous MS/MS data [233]. It was only found in silver fir wood.

Table 6. Presence of compounds confirmed through LC-DAD-ESI-MS/MS analysis in *Pinaceae* species.

Compounds	*Abies alba*	*Pinus sylvestris*	*Pinus mugo*	*Pinus cembra*	*Pinus strobus*	*Pinus ×rhaetica*	*Larix decidua*	*Larix polonica*	*Larix kaempferi*	*Pseudotsuga menziesii*	*Tsuga canadensis*	*Picea abies*	*Picea glauca*
1. gallocatechin	+	+	+	+	+	+	+	+	+	-	-	-	-
2. dimeric procyanidin B (I)	+	+	+	+	+	+	+	+	+	+	+	+	+
3. dimeric procyanidin B (II)	+	+	+	+	+	+	+	+	+	+	+	+	+
4. trimeric procyanidin B	+	+	+	+	+	+	+	+	+	+	+	+	+
5. catechin	+	+	+	+	+	+	+	+	+	+	+	+	+
6. dimeric procyanidin B (III)	-	-	-	-	-	-	+	+	+	+	-	+	-
7. epi-catechin	+	-	-	+	+	-	+	+	+	+	+	-	-
8. dihydromyricetin	-	-	+	-	-	+	+	+	-	-	-	-	-
9. 7-hydroxylariciresinol (I)	+	-	-	-	-	-	-	-	-	-	-	+	+
10. *trans*-astringin	-	-	-	-	-	-	-	-	-	-	-	+	+
11. dihydrokaempferol	-	-	-	-	-	-	+	+	-	-	-	-	-
12. todolactol	+	-	-	-	-	-	+	-	+	+	+	+	+
13. taxifolin hexoside	-	+	+	+	+	+	-	+	+	+	-	+	-
14. *cis*-astringin	-	-	-	-	-	-	+	+	+	-	-	+	+
15. dimeric procyanidin B (IV)	-	-	-	-	-	-	+	+	+	-	-	-	-
16. 7-hydroxylariciresinol (II)	+	-	+	-	+	-	+	-	+	+	+	-	-
17. piceid	-	-	-	-	-	-	-	-	-	-	-	+	+
18. taxifolin	-	+	+	+	+	+	+	+	+	+	-	+	+
19. isorhapontin	-	-	-	-	-	-	-	-	-	-	-	+	+
20. cyclolariciresinol	+	-	-	-	-	-	-	-	-	-	-	-	-
21. α-conidendric acid	+	-	+	-	+	-	+	+	+	-	+	-	-
22. 7-hydroxymatairesinol	+	-	+	-	+	-	+	+	+	+	+	+	+
23. secoisolariciresinol	+	-	+	-	+	-	+	+	+	+	+	+	+
24. eriodictyol	-	-	+	+	+	-	+	+	+	+	-	-	-
25. myricetin	-	-	+	-	-	-	+	+	+	+	-	-	-
26. secoisolariciresinol guaiacylglyceryl ether	+	-	+	-	-	-	+	+	+	+	-	-	-
27. lariciresinol	+	-	-	-	+	-	+	+	+	+	+	-	+
28. lariciresinol guaiacylglyceryl ether	+	-	-	-	-	-	-	-	-	-	-	-	-
29. nortrachelogenin	+	+	+	-	+	-	+	+	+	+	+	+	+
30. pinoresinol	-	+	-	-	-	-	-	-	-	-	-	-	-
31. quercetin	-	-	-	-	+	-	+	+	+	+	-	-	-
32. matairesinol	-	+	+	+	+	+	+	+	+	-	+	+	+
33. pinobanksin	-	-	+	+	+	-	+	+	+	+	-	-	+
34. pinosylvin	-	+	+	-	+	-	-	-	-	-	-	-	-
35. pinocembrin	-	+	+	-	+	+	-	-	-	+	-	-	-
36. pinobanksin 3-*O*-acetate	-	-	-	-	+	-	-	-	-	-	-	-	-
37. pinosylvin monomethyl ether	-	+	+	+	+	-	-	-	-	-	-	-	-
38. dehydrojuvabione	+	-	-	-	-	-	-	-	-	-	-	-	-
39. neoabietic acid	+	+	+	+	+	+	+	+	+	+	+	+	+
40. abietic acid	+	+	+	+	+	+	+	+	+	+	+	+	+

The *Pinaceae* family, is known to be a rich source of stilbenes [28, 29, 41]. In my study I have found 6 stilbenes in conifer wood, mostly in spruce and pine species. They had characteristic UV

maxima either at around 320 nm (glycosidic form) or 300 nm (aglycone form). Compounds **10** (t_r = 8.1 min) and **14** (t_r = 10.8 min) exhibited two pseudomolecular ions at m/z 811 $[2M-H]^-$ and m/z 405 $[M-H]^-$ with similar fragmentation patterns. Primary ion at m/z 405 fragmented into m/z 243 $[M-H-162]^-$ corresponding to the cleavage of hexose and showed fragments at m/z 225 $[M-H-18]^-$ corresponding to the loss of water, m/z 201 $[M-H-42]^-$ corresponding to the losses of C_2H_2O, characteristic for stilbenoids, m/z 173 $[M-H-42-28]^-$ and m/z 159 $[M-H-42-42]^-$. Based on elution order and comparison with literature data [323, 341-343] compounds **10** and **14** were identified as *trans*-astringin (piceatannol 3-*O*-glucoside) and *cis*-astringin respectively. *Trans*-astringin was only observed in spruce species, while *cis*-astringin was also present in larch species.

Compounds **17** (t_r = 11.7 min) and **19** (t_r = 12.5 min) were only found in spruces. Main pseudomolecular ion for compound **17** was at m/z 389 $[M-H]^-$ and gave one fragment ion at m/z 227 $[M-H-162]^-$ corresponding to the cleavage of hexose and showed fragments of aglycon at m/z 185 $[M-H-42]^-$ and 183 $[M-H-42-H_2]-$ corresponding to the losses of C_2H_2O, characteristic for stilbenoids, m/z 157 $[M-H-42-28]-$ and m/z 143 $[M-H-42-42]^-$ [61]. It was tentatively identified as piceid (resveratrol 3-*O*-glucoside) in comparison with literature data [342]. Compound **19** exhibited a pseudomolecular ion at m/z 465 $[M-H+HCOOH]^-$ which showed fragment ions at m/z 419 $[M-H]^-$ corresponding to the loss of formyl adduct, at m/z 257 $[M-H-162]^-$ corresponding to the cleavage of hexose, at m/z 242 $[M-H-162-15]^-$ and at m/z 241 $[M-H-162-16]^-$ [28]. It was tentatively identified as isorhapontin (isorhapontigenin 3-*O*-glucoside).

Compounds **34** (t_r = 26.3 min) and **37** (t_r = 33.6 min) were characterized as stilbenes based on their primary pseudomolecular ion and UV maxima at around 300 nm. Comparing mass of $[M-H]^-$ ion at m/z 211 $[M-H-]^-$ and m/z at 225 $[M-H]^-$ with literature reports on stilbenes isolated previously from conifer wood and their elution order [344] these compounds were tentatively identified: **34** as pinosylvin and **37** as pinosylvin monomethyl. Moreover, compared to MS/MS data from the literature, pinosylvin (**34**) demonstrated a fragment ion at 169 m/z $[M-H-42]^-$ corresponding to the losses of C_2H_2O, characteristic for stilbenoids [341, 345]. Pinosylvin monomethyl ether (**37**) pseudomolecular ion gave a fragment ion at 210 m/z $[M-H-15]^-$ corresponding to the loss of methyl radical. Their occurrence was limited to the genus *Pinus*, with only Scots pine and mountain pine contain all the above.

I was able to identify one sesquiterpenoid and two diterpenes in conifer wood – all of them in positive ion mode. Compound **38** (t_r = 41.0 min) exhibited a pseudomolecular ion at m/z 265 $[M+H]^+$

and fragmented into m/z 251, m/z 233, m/z 205, m/z 187 m/z 176 and m/z 83. It was tentatively identified as dehydrojuvabione by comparison with MS/MS data found in literature [346]. Compounds **39** (t_r = 52.0 min) and **40** (t_r = 52.3 min) both exhibited a pseudomolecular ion at m/z 303 $[M+H]^+$ with similar fragmentation patterns: m/z 285, m/z 257 and m/z 123. Based on UV maxima, 251 nm for compound **39** and 241 nm for compound **40**, their elution order and comparing this data to the literature [347, 348] and reference standard, I was able to identify compound **39** as neoabietic acid and compound **40** as abietic acid. Dehydrojuvabione was only found in *A. alba* while both abietane type resin acids were present in all studied conifer species wood.

6.1.1.2 *Abies alba* wood – isolation

The LC-MS analysis allowed me to identify Scots pine and silver fir as the richest sources of lignans among studied conifer species, which is why their wood was chosen for compound isolation.

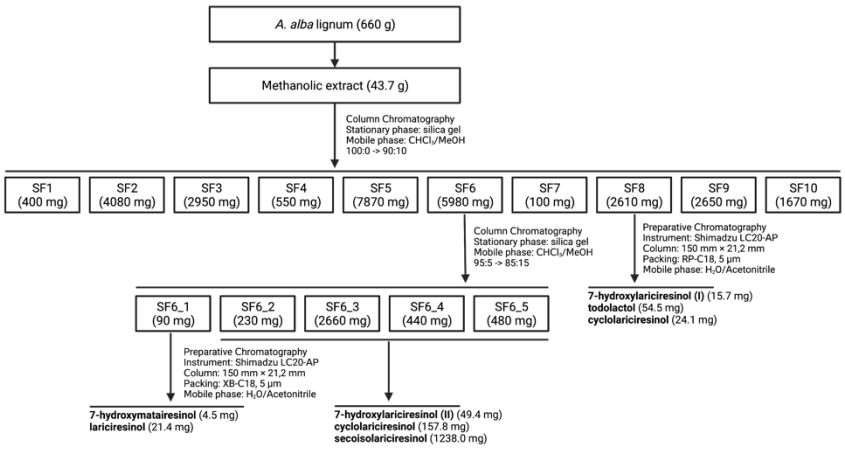

Figure 15. Scheme of *A. alba* wood methanolic extract fractionation and isolation of lignans.

The crude extract of silver fir was subjected to silica gel column chromatography (65 x 5 cm) and eluted with a $CHCL_3$-MeOH gradient (100:0 → 90:10) of 11 steps, 0.5 L each, to obtain 100 fractions of 55 mL, which were pooled into 10 main fractions (SF1-SF10) based on their TLC and LC-DAD-ESI-MS/MS profiles. Fraction SF6 (5980 mg) was rechromatographed on a silica gel column (40 x 3 cm) with $CHCL_3$-MeOH gradient (95:5 → 85:15) of 10 steps, 250 mL each, to obtain 5 fractions (SF6_1–SF6_5) of 500 mL each. Using preparative HPLC lignans were isolated from fraction SF6_1 (90 mg): **7-hydroxymatairesinol** (4.5 mg; 13.20 – 13.80 min) and **lariciresinol** (21.4 mg; 16.70 – 17.70 min), from fractions SF6_2 (230 mg), SF6_3 (2660 mg), SF6_4 (440 mg) and SF6_5 (480 mg): **7-hydroxylariciresinol**

(II) (49.4 mg; 9.65 – 10.15 min), **cyclolariciresinol** (157.8 mg; 11.00 – 11.65 min) and **secoisolariciresinol** (1238.0 mg; 14.80 – 16.00 min), and from directly from fraction SF8 (2610 mg): **7-hydroxylariciresinol (I)** (15.7 mg; 5.60 – 6.20 min), **todolactol** (54.5 mg; 6.70 – 7.50 min) and **cyclolariciresinol** (24.1 mg; 11.00 – 11.65 min). The separation and isolation are illustrated by Figure 15. All isolated compounds were characterized using NMR methods.

6.1.1.3 *Pinus sylvestris* wood – isolation

The crude extract of Scots pine was suspended in water and extracted 3 times with ethyl acetate. Ethyl acetate fraction (8.4 g) was then subjected to Sephadex LH-20 chromatography (40 x 3 cm) and eluted with methanol to obtain 34 fractions of 8 mL, which were pooled into 5 main fractions (PS-E1–PS-E5) based on their TLC and HPLC profiles. From fraction PS-E2 (110 mg), **nortrachelogenin** (9 mg; 13.30 – 14.50 min), **pinoresinol** (13 mg; 14.70 – 15.40 min), and **matairesinol** (13 mg; 17.20 – 18.10 min) were isolated using preparative HPLC. The separation and isolation are illustrated by Figure 16. All isolated compounds were characterized using NMR methods.

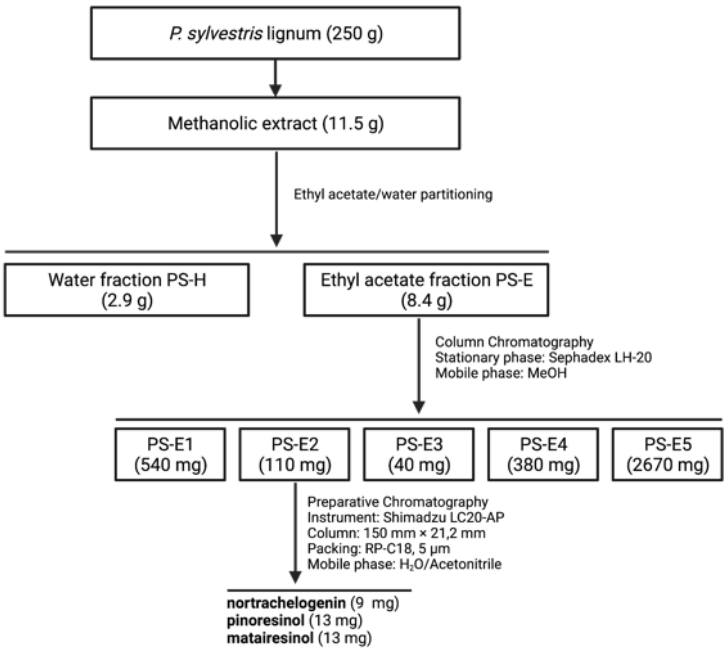

Figure 16. Scheme of *P. sylvestris* wood methanolic extract fractionation and isolation of lignans.

6.1.1.4 *Arctium lappa* fruit – phytochemistry

Through UHPLC-DAD-ESI-MS/MS analysis of *Arctii fructus* methanolic extract 25 compounds were identified or partially identified using negative and positive ion modes. The plant material was especially rich in caffeoylquinic acids and lignan glycosides (water fraction) and lignan aglycones (ethyl acetate fraction). The metabolite profile of *Arctii fructus* is shown in Table 7 and a chromatogram of water (AF-H) and ethyl acetate (AF-E) fractions is presented in Figure 17

Table 7. Retention time, UV, and MS/MS data of the compounds identified in *Arctium lappa* fruit extract using LC-DAD-ESI-MS/MS method.

Compounds	T_r [min]	UV_{max} [nm]	ESI	Extracted ion [m/z]	Fragment ions [m/z]
1. 3-*O*-Caffeoylquinic acid (neochlorogenic acid)	2.9	216, 324	$[M-H]^-$	353	191, 179, 173, 135
2. 5-*O*-Caffeoylquinic acid (chlorogenic acid)	3.8	215, 242, 324	$[M-H]^-$	353	191, 179
3. Olivil 4'-*O*-glucoside*	4.3	277	$[M-H+HCOOH]^-$	583	537, 375, 195
4. 4,5-Di-*O*-caffeoylquinic acid	12.4	211, 287, 325	$[M-H]^-$	515	353, 335, 299, 255, 203, 173
5. 3,5-Di-*O*-caffeoylquinic acid	13.1	214, 230, 327	$[M-H]^-$	515	353, 191, 179, 173
6. 3,4-Di-*O*-caffeoylquinic acid	14.0	201, 215, 326	$[M-H]^-$	515	353, 299, 255, 203, 173
7. Matairesinol 4-*O*-glucoside**	14.5	229, 279	$[M-H]^-$	519	357, 342, 313, 298, 281, 209, 147
8. Lappaol H	15.0	234, 283	$[M-H]^-$	749	731, 713, 683, 665, 607, 589, 465
9. Lappaol C / Isolappaol C / Lappaol E / Arctignan A	15.6	280	$[M-H]^-$	553	535, 517, 505, 411
10. Arctigenin 4-*O*-glucoside**	16.8	279	$[M-H]^-$	535	371
11. Lappaol C / Isolappaol C / Lappaol E / Arctignan A	17.3	281	$[M-H]^-$	553	535, 517, 505, 411
12. Lappaol C / Isolappaol C / Lappaol E / Arctignan A	17.5	280	$[M-H]^-$	553	535, 517, 505, 411
13. Lappaol C / Isolappaol C / Lappaol E / Arctignan A	17.8	281	$[M-H]^-$	553	535, 517, 505, 411
14. Arctignan B / Arctignan C	20.0	280	$[M-H]^-$	551	533, 521
15. Arctignan B / Arctignan C	20.3	281	$[M-H]^-$	551	535, 517, 505, 411, 357
16. Matairesinol**	21.6	281	$[M-H]^-$	357	342, 313, 298, 281, 209, 191, 147
17. Lappaol A / Hedyotol A / Isolappaol A	23.9	282	$[M-H]^-$	535	517, 505
18. Lappaol A / Hedyotol A / Isolappaol A	24.1	282	$[M-H]^-$	535	517, 505
19. Arctigenin**	25.2	281	$[M-H]^-$	371	356, 313, 295, 209, 147
20. Lappaol F	25.5	285, 330	$[M-H]^-$	713	695, 683, 677, 665
21. Lappaol B	26.7	281	$[M-H+HCOOH]^-$	595	549, 531, 519, 505, 283
22. 7,8-Didehydroarctigenin	27.6	284, 336	$[M-H]^-$	369	353, 217, 203, 174
23. Viridissimaol E	33.4	285, 332	$[M-H]^-$	739	724, 707, 679, 589, 544, 513
24. Diarctigenin	33.6	285	$[M+H]^+$	743	725, 507, 489, 285, 271, 253
25. Neoarctin A	35.3	280	$[M+H]^+$	743	725, 507, 369, 247

* compared with reference standard; ** isolated from this plant material and identified on NMR.

Peaks **1** (t_r = 2.9 min), **2** (t_r = 3.8 min), **4** (t_r = 12.4 min), **5** (t_r = 13.1 min), and **6** (t_r = 14.0 min), were characterized by UV maxima at around 325 nm, which is typical for hydroxycinnamic acid derivatives.

Compounds **1** and **2** exhibited their pseudomolecular ion at m/z 353 $[M-H]^-$ and a fragment ion at m/z 191 $[M-H-162]^-$ which corresponds to quinic acid ion after cleavage of caffeoyl moiety (162 Da). Both compounds were characterized as caffeoylquinic acids and assigned based on their differences in fragmentation and elution order. Peak **1** had additionally secondary fragment ions at m/z 179 (caffeic acid ion), m/z 173 (quinic acid-H_2O ion) and m/z 135 which was a result of losing CO_2 by the caffeic acid ion. Thus, compound **1** was identified as 3-*O*-caffeoylquinic acid. For compound **2** secondary peak at m/z 179 (caffeic acid ion) as observed and was thus identified as 5-*O*-caffeoylquinic acid [349-352].

Compounds **4**, **5** and **6** all exhibited their pseudomolecular ion at m/z 515 $[M-H]^-$ and a fragment ion at m/z 353 $[M-H-162]^-$, a caffeoylquinic acid ion, resulting via the loss of a hexosyl or caffeoyl moiety. For peak **4** I observed fragment ions at m/z 335 $[M-H-162-18]^-$ corresponding to the loss of caffeoyl moiety followed by the loss of water, at m/z 299 $[M-H-18-162-18-18]^-$ corresponding to the loss of water, caffeoyl moiety and followed by the loss of two additional water molecules, at m/z 255 formed by subsequent loss of carbon dioxide, at m/z 203 resulting probably from the loss of C_4H_4, and at m/z 173 $[M-H-162-162-18]^-$ corresponding to a quinic acid ion after losing a molecule of water. It (**4**) was assigned as 4,5-di-*O*-caffeoylquinic acid. Compound **5** had MS^3 base peaks at m/z 191, m/z 179 and m/z 173 and was identified as 3,5-di-*O*-caffeoylquinic acid. Compound **6** also exhibited ions at m/z 299, m/z 255, m/z 203 and m/z 173 (all described above) and was assigned as 3,4-di-*O*-caffeoylquinic acid [353, 354].

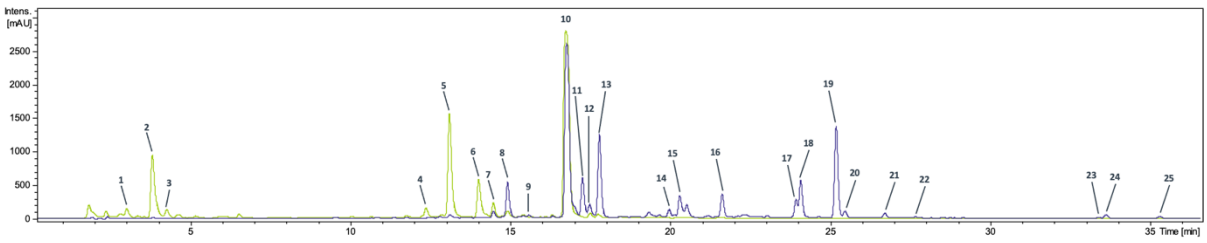

Figure 17. LC-DAD chromatogram of *A. lappa* fruit obtained at 280 nm.

Green trace – water fraction (AF-H); blue trace – ethyl acetate fraction (AF-E).

Compound **16** (t_r = 21.6 min) exhibited a pseudomolecular ion at m/z 357 $[M-H]^-$ and gave a characteristic primary product ion for dibenzylbutyrolactone lignans $[M-H-44]^-$ at m/z 313, which corresponds to the loss of CO_2 from the lactone ring [339]. It was later isolated and identified as matairesinol. Compound **7** (t_r = 14.5 min) which exhibited a pseudomolecular ion at m/z 519 $[M-H]^-$ and produced fragment ions typical for matairesinol was isolated and identified as matairesinol 4-*O*-glucoside.

Compound **3** (t_r = 4.3 min) exhibited a pseudomolecular ion at m/z 583 $[M+HCOOH-H]^-$ and fragment ions at m/z 537 $[M-H]^-$ corresponding to the loss of the HCOOH adduct, at m/z 375 $[M-H-162]^-$ corresponding to the cleavage of hexose and at m/z 195 $[M-H-162-180]^-$. Thus, compound **3** was assigned as olivil 4'-*O*-glucoside, which was confirmed by comparison with reference standard and literature data [355]. To the best of my knowledge, it is the first report on the presence of this compound in *Arctii fructus*.

Compound **8** (t_r = 15.0 min) exhibited a pseudomolecular ion at m/z 749 $[M-H]^-$ and fragment ions at m/z 731 $[M-H-18]^-$ from the loss of H_2O, at m/z 713 $[M-H-18-18]^-$ from the loss of two H_2O, at m/z 683 $[M-H-18-18-30]^-$ from the loss of two H_2O and CH_2O moiety, at m/z 665 $[M-H-18-18-30-18]^-$ from the subsequent loss of another H_2O, at m/z 607 $[M-H-142]^-$ from condensation and loss of $C_7H_{10}O_4$, at m/z 589 $[M-H-142-18]^-$ from subsequent loss of H_2O, and at m/z 465. It was assigned as lappaol H [356].

Compounds **9** (t_r = 15.6 min), **11** (t_r = 17.3 min), **12** (t_r = 17.5 min) and **13** (t_r = 17.8 min) all exhibited a pseudomolecular ion at m/z 553 $[M-H]^-$ and fragment ions at m/z 535 $[M-H-18]^-$ from the loss of H_2O, m/z 517 $[M-H-18-18]^-$ from the loss of two H_2O, m/z 505 $[M-H-18-18-12]^-$ from the loss of two H_2O and a carbon, and m/z 411 $[M-H-142]^-$ from the loss of $C_7H_{10}O_3$. There are 4 compounds identified in *Arctii fructus* that give this fragmentation pattern and I was not able to distinguish them. Thus, these peaks have been tentatively assigned together as arctignan A, lappaol C, isolappaol C or lappaol E [356, 357]. A similar situation was encountered with compounds **17** (t_r = 23.9 min) and **18** (t_r = 24.1 min) which produced ions down by one H_2O molecule. They were assigned as lappaol A, hedyotol A or isolappaol A [356].

Compounds **14** (t_r = 20.0 min) and **15** (t_r = 20.3 min) exhibited a pseudomolecular ion at m/z 551 $[M-H]^-$ but differed in its fragmentation. It was not possible to distinguish two isomers from one another and thus they were assigned as arctignan B or arctignan C [356].

Compound **19** (t_r = 25.2 min) exhibited a pseudomolecular ion at m/z 371 $[M-H]^-$ and fragment ions at m/z 356, m/z 313, m/z 295, m/z 209 and m/z 147. Although this fragmentations hasn't been explained, it is characteristic for arctigenin [339]. A similar fragmentation pattern down by 2 Da could be seen for compound **22** (t_r = 27.6 min) which was assigned as 7,8-didehydroarctigenin [356]. Compound **10** (t_r = 16.8 min) produced a pseudomolecular ion at m/z 535 $[M-H]^-$ and fragmented into an ion at 371 $[M-H-162]^-$ corresponding to the cleavage of hexose. It was identified as arctigenin 4-*O*-glucoside (arctiin).

Compound **20** (t_r = 25.5 min) exhibited a pseudomolecular ion at m/z 713 $[M-H]^-$ and fragment ions at m/z 695 $[M-H-18]^-$ from the loss of H_2O, at m/z 683 $[M-H-18-12]^-$ from the subsequent loss of carbon, at m/z 677 $[M-H-18-18]^-$ from the loss of two H_2O, and at m/z 665 $[M-H-18-12-18]^-$ from the loss of two H_2O and carbon. It was identified as lappaol F [356].

Compound **21** (t_r = 26.7 min) exhibited a pseudomolecular ion at m/z 595 $[M-H+HCOOH]^-$ and fragment ions at m/z 549 $[M-H]^-$ from the cleavage of formyl adduct, m/z 531 $[M-H-18]^-$ from the loss of H_2O, m/z 519 $[M-H-18-12]^-$ from the subsequent loss of carbon, m/z 505 and at m/z 283. It was assigned as lappaol B [356].

Compound **23** (t_r = 33.4 min) exhibited a pseudomolecular ion at m/z 739 $[M-H]^-$ and fragment ions at m/z 724, m/z 707, m/z 679, m/z 589, m/z 544 and at m/z 513. Its fragmentation resembled that of diarctigenin-2H. In the literature there is only one compound described that could match this fragmentation, and that is a dimer of arctigenin and 7,7-didehydroarctigenin – viridissimaol E [358].

Compound **24** (t_r = 33.6 min) and **25** (t_r = 35.3) exhibited a pseudomolecular ion at m/z 741 $[M+H]^+$ but differed in fragmentation pattern. Compound **24** produced fragment ions at m/z 725 $[M+H-18]^+$ from the loss of H_2O, at m/z 507 $[M+H-236]^+$ from the loss of $C_{13}H_{16}O_4$, at m/z 489 $[M+H-236-18]^+$ from the subsequent loss of H_2O, at m/z 285 $[M+H-458]^+$ from the loss of $C_{25}H_{30}O_8$, at m/z 271 $[M+H-458-14]^+$ from the subsequent loss of CH_2 radical, and at 253 $[M+H-458-30-2]^+$ from the loss of $C_{25}H_{30}O_8$, a methoxy group (30 Da) and condensation (2H = 2 Da). It was assigned as diarctigenin [356]. Compound **25** produced fragment ions at m/z 725 $[M+H-18]^+$ from the loss of H_2O, at m/z 507 $[M+H-236]^+$ from the loss of $C_{13}H_{16}O_4$, at m/z 369 $[M+H-374]^+$ from the loss of $C_{21}H_{26}O_6$, and at m/z 247 $[M+H-374-122]^+$ from the subsequent loss of $C_7H_6O_2$. It was identified as neoarctin A [356]. These two compounds were identified in positive ion mode, due to lack of literature data on fragmentation in the negative ion mode.

6.1.1.5 *Arctium lappa* fruit – isolation

Phytochemical characterization of great burdock fruit extract showed presence of multiple lignans and lignan glycosides. Based on these findings it was decided to isolate the most abundant compounds in the plant material.

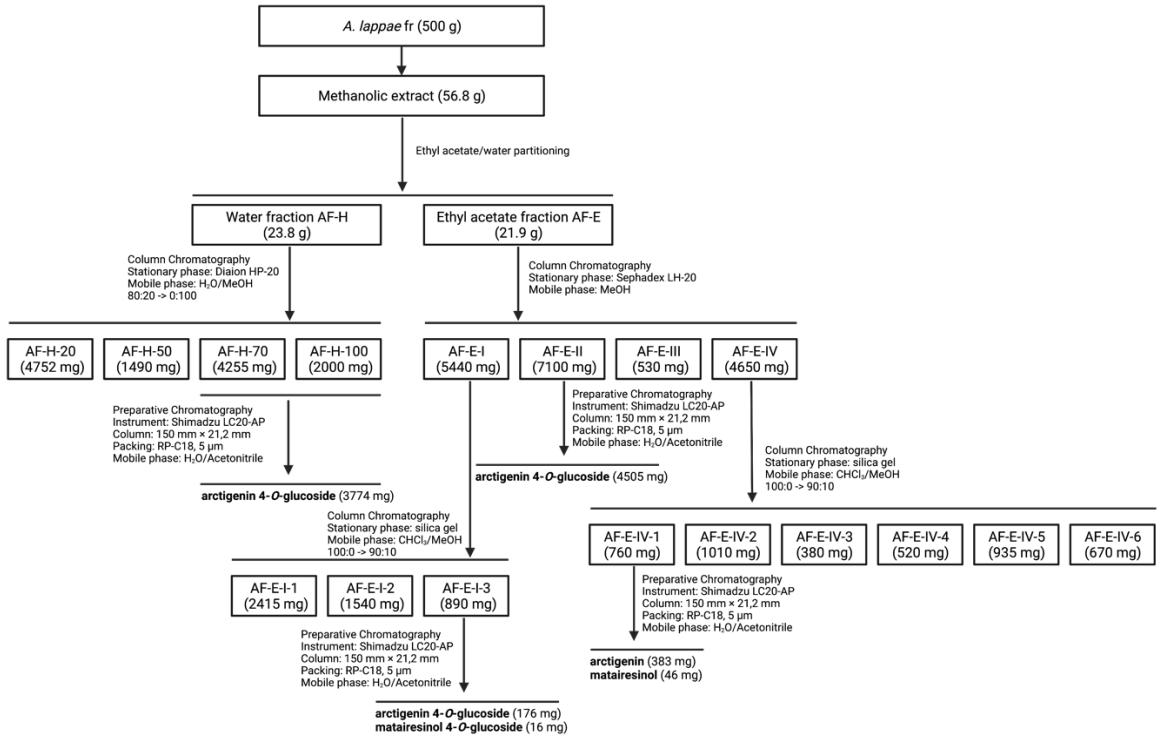

Figure 18. Scheme of *A. lappa* fruit methanolic extract fractionation and isolation of lignans.

The crude extract of great burdock was suspended in water and extracted 3 times with ethyl acetate. The water fraction (23.8 g) was then subjected to Diaion HP-20 chromatography (30 x 10 cm) and eluted with a methanol/water gradient (0:100 → 100:0) of 5 steps, 1 L each, to obtain 5 fractions (AF-0, AF-20, AF-50, AF-70 and AF-100). From fractions AF-70 (4255 mg) and AF-100 (2000 mg) **arctigenin 4-*O*-glucoside** (3774 mg; 14.00 – 15.60 min) was isolated using preparative HPLC. The ethyl acetate fraction (21.9 g) was divided into 4 parts and each part was subjected to Sephadex LH-20 chromatography (40 x 3 cm) and eluted with methanol to obtain 25 fractions of 12 mL, which were pooled into 4 main fractions (AF-EI–AF-EIV) based on their TLC and HPLC profiles. Fraction AF-E-I (5400 mg) was rechromatographed on a silica gel column (60 × 2) with a chloroform/methanol gradient (100:0 → 90:10) of 6 steps, 500 mL each. Ninety-six fractions of 30 mL each were collected and pooled into 3 main fractions (AF-E-I-1–AF-E-I-3) based on their TLC profiles. From fraction AF-E-I-3 (890 mg)

arctigenin 4-*O*-glucoside (176 mg; 14.00 – 15.60 min) and **matairesinol 4-*O*-glucoside** (16 mg; 12.00 – 12.35 min) were isolated using preparative HPLC. From fractions AF-E-II (7100 mg) **arctigenin 4-*O*-glucoside** (4505 mg; 14.00 – 15.60 min) was isolated using preparative HPLC. Fraction AF-E-IV (4650 mg) was rechromatographed on a silica gel column (60 × 2) with a chloroform/methanol gradient (100:0 → 90:10) of 6 steps, 500 mL each. One hundred six fractions of 30 mL each were collected and pooled into 6 main fractions (AF-E-IV-1–AF-E-IV-6) based on their TLC profiles. From fraction AF-E-IV-1 (760 mg) **arctigenin** (383 mg; 25.2 – 27.2 min) and **matairesinol** (46 mg; 20.90 – 22.00 min) were isolated using preparative HPLC. The separation and isolation are illustrated by Figure 18. All isolated compounds were characterized using NMR methods.

6.1.1.6 *Carthamus tinctorius* fruit – phytochemistry

Through UHPLC-DAD-ESI-MS/MS analysis of *Carthami fructus* methanolic extract 14 compounds were identified or partially identified using negative ion mode. The plant material was especially rich in serotonin hydroxycinnamic acid amides and lignan aglycones and glycosides. The metabolite profile of *Carthami fructus* is shown in Table 8 and a chromatogram obtained at 280 nm is presented in Figure 19.

Compound **1** (t_r = 11.3 min) exhibited a pseudomolecular ion at m/z 483 $[M-H]^-$ which fragmented into m/z 321 $[M-H-162]^-$ characteristic for *N*-coumaroylserotonin hexoside. Based on presented data it is not possible to determine the exact structure of sugar moiety and its binding site. However, a *N*-coumaroylserotonin 5-*O*-glucoside was previously isolated from safflower [359]. Compound **7** (t_r = 16.7 min) exhibited a pseudomolecular ion at m/z 321 $[M-H]^-$ and produced fragment ions at m/z 201 and at m/z 145 $[M-H-176]^-$ corresponding to serotonin. It was identified as the aglycone of compound **1**, i.e., *N*-coumaroylserotonin [360]. Similarly, compound **11** (tr = 20.5) exhibited a pseudomolecular ion at m/z 641 $[M-H]^-$ and produced fragment ions at m/z 521, m/z 478, m/z 401 and at m/z 358, and was tentatively identified as a dimer of compound **7**, i.e., 4,4'-bis(*N*-coumaroyl)serotonin based on the previous data on its presence in *Carthami fructus* (no previous MS data available) [359].

Compound **2** (t_r = 12.0 min) exhibited a pseudomolecular ion at m/z 513 $[M-H]^-$ which fragmented into m/z 351 $[M-H-162]^-$ characteristic for *N*-feruloylserotonin hexoside. Based on presented data it is not possible to determine the exact structure of sugar moiety and its binding site. However a *N*-feruloylserotonin 5-*O*-glucoside was previously isolated from safflower [361]. Compound

8 (t_r = 17.3 min) exhibited a pseudomolecular ion at m/z 351 $[M-H]^-$ and produced fragment ions at m/z 336, m/z 201, m/z 161, and at m/z 135. It was identified as the aglycone of compound **2**, i.e., *N*-feruloylserotonin (moschamine) [360]. Similarly, compound **13** (t_r = 20.8) exhibited a pseudomolecular ion at m/z 701 $[M-H]^-$ and produced fragment ions at m/z 565, m/z 551, m/z 522, m/z 508, m/z 401, m/z 358 and at m/z 315, and was tentatively identified as a dimer of compound **8**, i.e., 4,4'-bis(*N*-feruolyl)serotonin (bismoschamine) based on the previous data on its presence in *Carthami fructus* (no previous MS data available) [359].

Table 8. Retention time, UV, and MS/MS data of the compounds identified in *Carthamus tinctorius* fruit extract using LC-DAD-ESI-MS/MS method.

Compounds	T_r [min]	UV_{max} [nm]	ESI	Extracted ion [m/z]	Fragment ions [m/z]
1. *N*-Coumaroylserotonin 5-*O*-glucoside	11.3	223, 292	$[M-H]^-$	483	321
2. *N*-Feruloylserotonin 5-*O*-glucoside	12.0	220, 293	$[M-H]^-$	513	351
3. Matairesinol 4-*O*-pentosylhexoside	14.1	280	$[M-H]^-$	651	519, 487, 357
4. Matairesinol 4-*O*-glucoside***	14.9	279	$[M-H]^-$	519	357, 342, 313, 298, 209, 147
5. Trachelogenin 4-*O*-glucoside**	15.2	279	$[M-H]^-$	595	387, 357, 339
6. Secoisolariciresinol***	15.3	279	$[M-H]^-$	361	346, 313, 299
7. *N*-Coumaroylserotonin	16.7	224, 293	$[M-H]^-$	321	201, 145
8. *N*-Feruloylserotonin	17.3	222, 313	$[M-H]^-$	351	336, 201, 161, 135
9. Unknown compound	18.1	268, 331	$[M-H]^-$	591	307, 283, 268
10. Acacetin 7-*O*-glucuronide	19.5	268, 326	$[M-H]^-$	459	283, 175
11. 4,4'-Bis(*N*-coumaroyl)serotonin	20.5	220	$[M-H]^-$	641	521, 478, 401, 358
12. 4-[*N*-coumaroylserotonin-4'-yl]-*N*-feruloylserotonin	20.6	221, 313	$[M-H]^-$	671	551, 535, 521, 508, 492, 478, 401, 358, 315
13. 4,4'-Bis(*N*-feruloyl)serotonin	20.8	220, 314	$[M-H]^-$	701	565, 551, 522, 508, 401, 358, 315
14. Trachelogenin	22.2	275	$[M-H]^-$	387	339, 329, 249, 193
15. Matairesinol***	22.3	281	$[M-H]^-$	357	342, 313, 298, 281, 209, 191, 147

* compared with reference standard; ** isolated from this plant material and identified on NMR; *** compared with compound isolated from another plant material from this study.

Compound **12** (t_r = 20.6 min) exhibited a pseudomolecular ion at m/z 671 $[M-H]^-$ which fragmented into m/z 551, m/z 535, m/z 521, m/z 508, m/z 492, m/z 478, m/z 401, m/z 359 and m/z 315. It was tentatively identified as a dimer of compounds **7** and **8**, i.e., 4-[*N*-coumaroylserotonin-4'-yl]-*N*-feruloylserotonin based on the previous data on its presence in *Carthami fructus* (no previous MS data available) [359].

One flavonoid was found in *Carthami fructus* extract, that is compound **10** (t_r = 19.5 min). It exhibited a pseudomolecular ion at m/z 459 $[M-H]^-$ and produced fragment ions at m/z 283 [M−H-

176]$^-$ from the loss of glucuronic moiety and at m/z 175. It was identified as acacetin 7-*O*-glucuronide [362].

Compound **15** (t_r = 22.3 min) exhibited a pseudomolecular ion at m/z 357 [M−H]$^-$ and gave a characteristic primary product ion for dibenzylbutyrolactone lignans [M−H−44]$^-$ at m/z 313, which corresponds to the loss of CO_2 from the lactone ring [339]. According to the fragmentation, elution order in RP-LC and comparison with compound isolated from *A. lappa* it was identified as matairesinol. Compound **3** (t_r = 14.1 min) which exhibited a pseudomolecular ion at m/z 651 [M−H]$^-$ and fragment ions at m/z 519 [M−H−132]$^-$ corresponding to the cleavage of a pentose, m/z 487 and at m/z 357 [M−H−132−162]$^-$ corresponding to the cleavage of a pentose and a hexose, was identified as matairesinol 4-*O*-pentosylhexoside based on literature data [363]. Similarly, compound **4** (t_r = 14.9 min) which exhibited a pseudomolecular ion at m/z 519 [M−H]$^-$ and produced fragment ions typical for matairesinol was identified by comparison with compound isolated from *A. lappa* as matairesinol 4-*O*-glucoside.

For compound **6** (t_r = 15.3 min) a pseudomolecular ion could be observed at m/z 361 [M−H]$^-$ and fragment ions at m/z 346 [M−H−15]$^-$ corresponding to the loss of methyl radical, at m/z 313 [M−H−48]$^-$ formed by the loss of formaldehyde and water in the diol structure and at m/z 299 [M−H−48−15]$^-$ corresponding to both rearrangements. This structure was compared to fragmentation data described in the literature [339], and with compound isolated from *A. alba* and identified as secoisolariciresinol.

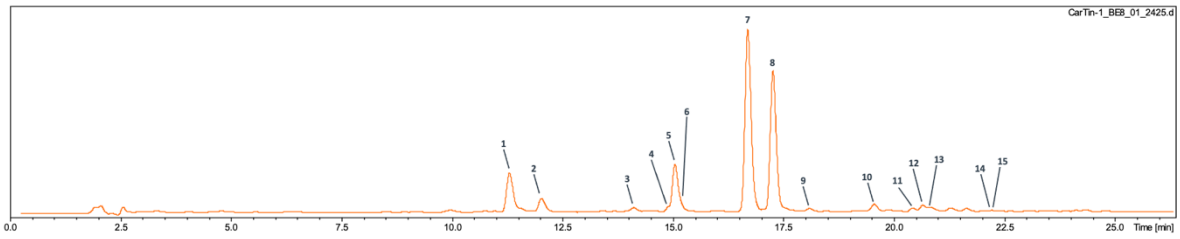

Figure 19. LC-DAD chromatogram of *C. tinctorius* fruit obtained at 280 nm.

Compound **14** (t_r = 22.2 min) exhibited a pseudomolecular ion at m/z 387 [M−H]$^-$ and fragmented into m/z 339, m/z 329, m/z 249 and m/z 193. This fragmentation was characteristic for trachelogenin [339]. Compound **5** (t_r = 15.2 min) exhibited a pseudomolecular ion at m/z 595 [M−H]$^-$ and fragmented into m/z 387 [M−H−162]$^-$ corresponding to the cleavage of hexose, m/z 357 and m/z 339. It was isolated and identified as trachelogenin 4-*O*-glucoside based on literature data [364].

6.1.1.7 *Carthamus tinctorius* fruit – isolation

Phytochemical profiling of safflower fruit extract showed presence of a rare lignan glycoside, i.e., trachelogenin 4-O-glucoside, which was selected for isolation. The crude extract of safflower was subjected to Diaion HP-20 chromatography (30 x 10 cm) and eluted with a methanol/water gradient (0:80 → 100:0) of 4 steps, 1 L each, to obtain 4 fractions (CT-20, CT-50, CT-70 and CT-100). Fraction CT-70 (4400 mg) was rechromatographed on a silica gel column (60 × 2) with a chloroform/methanol gradient (100:0 → 80:20) of 11 steps, 200 mL each. Thirty-eight fractions of 60 mL each were collected and pooled into 6 main fractions (CT-70-1–CT-70-6) based on their TLC profiles. From fractions CT-70-4 (1852 mg) and CT-70-5 (625 mg) **trachelogenin 4-*O*-glucoside** (339 mg; 11.65 – 12.50 min) was isolated using preparative HPLC. The separation and isolation are illustrated by Figure 20. Isolated lignan was characterized using NMR methods.

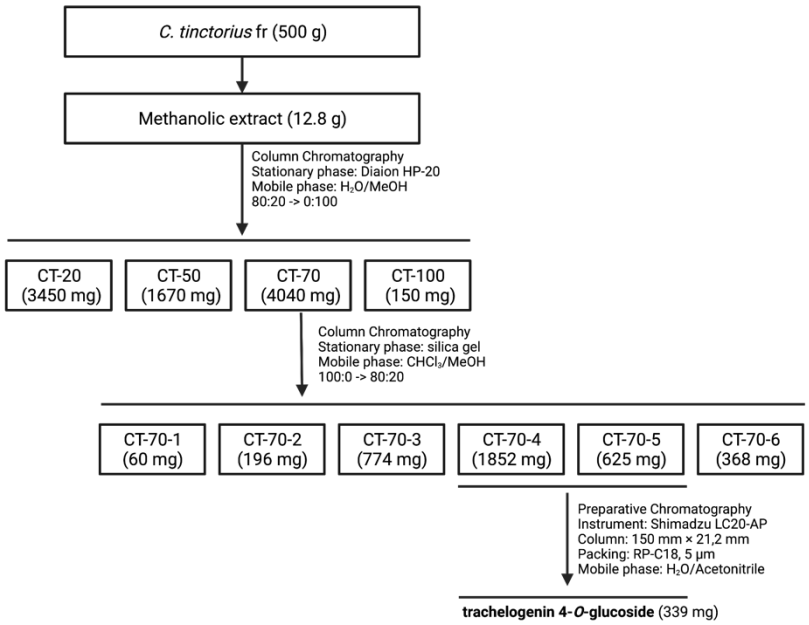

Figure 20. Scheme of *C. tinctorius* fruit methanolic extract fractionation and isolation of a lignan.

6.1.1.8 *Eleutherococcus senticosus* root – phytochemistry

Through UHPLC-DAD-ESI-MS/MS analysis of *Eleutherococci radix* 36 compounds were identified or partially identified using both positive and negative ion modes. The plant material was especially rich in syringin, caffeoylquinic acids and lignans in their aglycone and glycosidic form. The

metabolite profile of *Eleutherococcus* root is shown in Table 9 together with 7 unidentified compounds and a chromatogram obtained at 280 nm is presented in Figure 21.

Peak **1** (t_r = 20.0 min) exhibited a pseudomolecular ion at m/z 315 $[M-H]^-$ and fragment ions at m/z 153 $[M-H-162]^-$ and m/z 109 characteristic for protocatechuic acid hexoside [365]. Based on presented data it is not possible to determine the exact structure of sugar moiety and its binding site. However a protocatechuic acid 3'-*O*-β-D-glucopyranoside was previously isolated from the bark of *Eleutherococcus senticosus* [366].

Compound **2** (t_r = 21.8 min) with a similar fragmentation pattern was thus identified as protocatechuic acid, which was consistent with literature data [367]. The main pseudomolecular ion obtained from compound **3** (t_r = 22.7 min) was at m/z 329 $[M-H]^-$ and fragmented into m/z 167 $[M-H-162]^-$. Based on this and comparing to the literature [368], compound **3** was identified as vanillic acid 4-*O*-hexoside. All three compounds have been previously found in stems of *Eleutherococcus senticosus* [369], but there were no reports of their presence in the roots.

A major compound **9** (t_r = 27.3 min) exhibited a pseudomolecular ion at m/z 417 $[M-H+HCOOH]^-$ and fragment ions at m/z 371 $[M-H]^-$ corresponding to the loss of formyl adduct and at m/z 209 $[M-H-162]^-$ from the loss of hexosyl moiety. It was identified as syringin (eleutheroside B), by comparison with literature data [370] and reference standard; one of the compounds used for *E. senticosus* roots standardization [371].

Compound **15** (t_r = 30.7 min) had its main pseudomolecular ion at m/z 415 $[M-H+HCOOH]^-$ and fragment ions at m/z 369 $[M-H]^-$ corresponding to the loss of formyl adduct and at m/z 207 $[M-H-162]^-$ from the cleavage of hexose. It was assigned as sinapaldehyde 4-*O*-glucoside [370], which was reported for the first time in *Eleutherococci radix* by Slacanin *et al.* [372].

Peaks **4** (t_r = 24.1 min), **5** (t_r = 24.6 min), **6** (t_r = 25.4 min), **7** (t_r = 26.2 min), **8** (t_r = 26.4 min), **10** (t_r = 27.8 min), **11** (t_r = 28.3 min), **13** (t_r = 29.7 min), **17** (t_r = 31.5 min), **23** (t_r = 34.4 min), **27** (t_r = 35.5 min), **32** (t_r = 37.3 min), **33** (t_r = 37.9 min) and **34** (t_r = 38.2 min) were characterized by UV maxima at around 325 nm, which is typical for hydroxycinnamic acid derivatives.

Table 9. Retention time, UV, and MS/MS data of the compounds identified in *Eleutherococcus senticosus* root extract using LC-DAD-ESI-MS/MS method.

Compounds	T_r [min]	UV_{max} [nm]	ESI	Extracted ion [m/z]	Fragment ions [m/z]
1. Protocatechuic acid 3-*O*-glucoside	20.0	199, 212	$[M-H]^-$	315	153, 109
2. Protocatechuic acid	21.8	202, 215, 259, 293	$[M-H]^-$	153	109
3. Vanillic acid 4-*O*-glucoside	22.7	210, 250, 290	$[M-H]^-$	329	167
4. 5-*O*-(4'-*O*-Caffeoyl glucosyl)quinic acid	24.1	210, 285, 325	$[M-H]^-$	515	353, 341, 323, 191, 179, 173
5. 3-*O*-Caffeoylquinic acid	24.6	201, 324	$[M-H]^-$	353	191, 179, 135
6. 5-*O*-(4'-*O*-Feruoyl glucosyl)quinic acid	25.4	200, 230, 290, 320	$[M-H]^-$	529	367, 337, 191, 173
7. 5-*O*-(3'-*O*-Caffeoyl glucosyl)quinic acid	26.2	205, 322	$[M-H]^-$	515	353, 341, 323, 191, 179
8. 4-*O*-Feruoyl-5-*O*-caffeoylquinic acid	26.4	325	$[M-H]^-$	529	367, 193, 173
9. Syringin*	27.3	218, 264	$[M-H+HCOOH]^-$	417	371, 209
10. 5-*O*-Caffeoylquinic acid	27.8	216, 325	$[M-H]^-$	353	191
11. 4-*O*-Caffeoylquinic acid	28.3	213, 325	$[M-H]^-$	353	191, 179, 173
12. Isofraxidin 7-*O*-glucoside	29.0	206, 293	$[M-H+HCOOH]^-$	429	383, 221
13. Caffeic acid	29.7	213, 240, 290, 323	$[M-H]^-$	179	135
14. Olivil 4'-*O*-glucoside	30.2	278	$[M-H+HCOOH]^-$	583	537, 375, 195
15. Sinapaldehyde 4-*O*-glucoside	30.7	201, 311	$[M-H+HCOOH]^-$	415	369, 207
16. Pinoresinol 4,4'-di-*O*-glucoside	31.1	200, 277	$[M-H+HCOOH]^-$	727	681, 519, 357
17. 1,3-Di-*O*-caffeoylquinic acid	31.5	202, 281, 320	$[M-H]^-$	515	353, 335, 191, 179
18. Syringaresinol 4,4'-di-*O*-glucoside**	32.2	206, 225, 270, 324	$[M-H+HCOOH]^-$	787	741, 579, 417
19. Unidentified	32.5	202, 275	$[M-H+HCOOH]^-$	613	567, 405, 357
20. Secoisolariciresinol 9-*O*-glucoside	33.1	199, 219, 275	$[M-H]^-$	523	361, 346, 313, 179
21. Unidentified	33.6	206	$[M-H]^-$	531	339, 295, 229
22. Unidentified	33.8	205, 273	$[M-H+HCOOH]^-$	613	567, 404, 357, 165
23. 3,5-Di-*O*-caffeoyl-4-*O*-feruloylquinic acid	34.4	211, 320	$[M-H]^-$	691	529, 367, 193, 173
24. 5,5'-Dimethoxylariciresinol 4-*O*-glucoside	34.7	202, 279	$[M-H]^-$	581	419, 389, 223
25. Unidentified	34.9	202, 332	$[M-H]^-$	567	403, 357, 339, 329
26. Ciwujiatone 4-*O*-glucoside	35.1	202, 275	$[M-H]^-$	595	433, 387, 369, 357
27. 3,4-Di-*O*-caffeoyl-5-*O*-feruloylquinic acid	35.5	208, 325	$[M-H]^-$	691	529, 367, 353, 327, 193, 173
28. Unidentified	36.2	205, 332	$[M-H]^-$	371	327, 295, 261
29. Medioresinol 4'-*O*-glucoside	36.5	210, 275	$[M-H]^-$	549	387, 372, 341, 181, 151
30. Matairesinol 4-*O*-glucoside***	36.7	202, 275	$[M-H]^-$	519	357
31. Syringaresinol 4-*O*-glucoside	37.0	206, 277, 315	$[M-H]^-$	579	417, 402, 181
32. 4,5-Di-*O*-caffeoylquinic acid	37.3	211, 287, 325	$[M-H]^-$	515	353, 335, 299, 255, 203, 173
33. 1,5-Di-*O*-caffeoylquinic acid	37.9	214, 290, 328	$[M-H]^-$	515	353, 335, 191, 179
34. 3,5-Di-*O*-caffeoylquinic acid	38.2	214, 230, 327	$[M-H]^-$	515	353, 191, 179, 173
35. Medioresinol	38.6	205, 279, 325	$[M-H+HCOOH]^-$	423	387, 357, 343, 313, 191
36. Unidentified	38.9	206, 280, 320	$[M-H]^-$	561	369, 351, 187
37. 3,4-Di-*O*-caffeoylquinic acid	39.4	201, 215, 326	$[M-H]^-$	515	353, 299, 255, 203, 173
38. Secoisolariciresinol***	40.0	202, 281	$[M-H]^-$	361	346, 343, 298, 191, 165
39. Unidentified	41.3	205, 279	$[M-H]^-$	531	351, 339, 215, 191
40. Savinin	41.5	211, 278	$[M+H]^+$	353	335, 321, 289, 191, 167
41. Medioresinol 4'-*O*-guaiacylglycerol ether	43.8	213	$[M-H]^-$	583	535, 387, 369
42. Pinoresinol***	45.8	206, 281	$[M-H]^-$	357	341, 327, 313, 295, 267, 177
43. Matairesinol***	48.5	209, 279	$[M-H]^-$	357	342, 311, 295, 288, 209, 147

* compared with reference standard; ** isolated from this plant material and identified on NMR; *** compared with compound isolated from another plant material from this study.

Compounds **4**, **7**, **17**, **32**, **33** and **34** all exhibited their pseudomolecular ion at m/z 515 $[M-H]^-$ and a fragment ion at m/z 353 $[M-H-162]^-$, a caffeoylquinic acid ion, resulting via the loss of a hexosyl or caffeoyl moiety. Elution order would imply that caffeoylquinic acids hexosides should have lower retention times than dicaffeoylquinic acids [349-352]. Indeed, peaks of isomers **4** and **7** presented a typical caffeoylquinic acids hexoside fragmentation: m/z 341 $[M-H-174]^-$ corresponding to the cleavage of quinic acid moiety, m/z 323 $[M-H-174-18]^-$, as above but followed by loss of water, m/z 191 $[M-H-162-162]^-$ from the loss of hexosyl and caffeoyl residues, and m/z 179 $[M-H-162-174]^-$ a caffeic acid ion. Compound **4** as identified as 5-*O*-(4'-*O*-caffeoyl glucosyl)quinic acid and compound **7** as 5-*O*-(3'-*O*-caffeoyl glucosyl)quinic acid, comparing to the fragmentation pattern described in the literature [351].

Fragmentation of remaining peaks was slightly different from the above. For peaks **17**, **32** and **33** a fragment ion at m/z 335 $[M-H-162-18]^-$ corresponding to the loss of caffeoyl moiety followed by the loss of water was observed. Compound **17** exhibited also ions at m/z 191 and m/z 179 (described above) and was assigned as 1,3-di-*O*-caffeoylquinic acid. Compound **32** had its remaining fragment ions at m/z 299 $[M-H-18-162-18-18]^-$ corresponding to the loss of water, caffeoyl moiety and followed by the loss of two additional water molecules, at m/z 255 formed by subsequent loss of carbon dioxide, at m/z 203 resulting probably from the loss of C_4H_4, and at m/z 173 $[M-H-162-162-18]^-$ corresponding to a quinic acid ion after losing a molecule of water. Compound **32** was identified as 4,5-di-*O*-caffeoylquinic acid. Compound **33** exhibited remaining fragment ions at m/z 191 and m/z 179 and was assigned as 1,5-di-*O*-caffeoylquinic acid. Compound **34** had MS^3 base peaks at m/z 191, m/z 179 and m/z 173 and was identified as 3,5-di-*O*-caffeoylquinic acid. Identification of this compounds was based on fragmentation pattern described in the literature [349-352].

Compounds **5**, **10** and **11** all exhibited their pseudomolecular ion at m/z 353 $[M-H]^-$ and a fragment ion at m/z 191 $[M-H-162]^-$ which corresponds to quinic acid ion after cleavage of caffeoyl moiety (162 Da). All these compounds were characterized as caffeoylquinic acids and assigned based on their differences in fragmentation and elution order. Peak **5** had secondary fragment ions at m/z 179 (caffeic acid ion) and m/z 135 which was a result of losing CO_2 by the caffeic acid ion. Thus, compound **5** was identified as 3-*O*-caffeoylquinic acid. For compound **10** no secondary fragment ions were observed and it was assigned as 5-*O*-caffeoylquinic acid. Lastly, compound **11** had its secondary peaks at m/z 179 (caffeic acid ion) and m/z 173 (quinic acid-H_2O ion) and was thus identified as 4-*O*-caffeoylquinic acid [349-352].

Compounds **6** and **8** presented fragmentation typical for feruoylquinic acid hexosides. They exhibited their main pseudomolecular ion at m/z 529 and a fragment ion at m/z 367 $[M-H-162]^-$ corresponding to the cleavage of hexose. Compound **6** had its remaining fragment ions at m/z 337 $[M-H-192]^-$ from the cleavage of quinic acid moiety, at m/z 191 $[M-H-162-176]^-$ from the loss of feruoyl and hexosyl moieties, and at m/z 173 from subsequent loss of water. Compound **8** exhibited fragment ions at m/z 193 (ferulic acid ion) and m/z 173. Based on the differences in fragmentation and comparing it to the literature [349-352], compound **6** was identified as 5-*O*-(4'-*O*-feruoyl glucosyl)quinic acid and compound **8** as 4-*O*-feruoyl-5-*O*-caffeoylquinic acid.

Compound **13** exhibited its pseudomolecular ion at m/z 179 and a fragment ion at m/z 135 from the loss of CO_2 and was identified as caffeic acid [373].

Peaks **23** and **27** had their pseudomolecular ion at m/z 691 and exhibited fragmentation pattern characteristic for dicaffeoylferuloylquinic acids. Both compounds exhibited fragment ions at m/z 529 $[M-H-162]^-$ from the loss of one caffeoyl moiety, at m/z 367 $[M-H-162-162]^-$ from the loss of two caffeoyl moieties, at m/z 193 (ferulic acid ion) and m/z 173 (quinic acid-H_2O ion). For compound **27** additional secondary peaks could be observed at m/z 353 $[M-H-162-176]^-$ from the loss of one caffeoyl and feruoyl moiety and at m/z 327. Compound **23** was identified as 3,5-di-*O*-caffeoyl-4-*O*-feruloylquinic acid and compound **27** as 3,4-di-*O*-caffeoyl-5-*O*-feruloylquinic acid. The fragmentation pattern for the above hydroxycinnamic acid derivatives was consistent with the literature data [349-352].

Although some of the hydroxycinnamic acids identified in the present study have been previously found in *Eleutherococci radix* and most of them were present in other parts of the plant (such as stem), to the best of my knowledge, this is the most comprehensive study to date concerning the qualitative composition of hydroxycinnamic acids in *Eleutherococcus senticosus* root. The root seems to be particularly rich in these phytochemicals, as they represent the biggest diversity of structures among all constituents, as wells as their UV chromatogram peeks area are the largest, which could imply their significant quantity.

Peak **12** (t_r = 29.0 min) exhibited a pseudomolecular ion at m/z 429 $[M+HCOOH-H]^-$ and fragment ions at m/z 383 $[M-H]^-$ corresponding to the loss of the HCOOH adduct, at m/z 221 $[M-H-162]^-$ corresponding to the cleavage of hexose. Based on fragmentation, UV maxima and comparison with literature [374], compound **12** was identified as isofraxidin 7-*O*-glucoside (Eleutheroside B1). It

was the only coumarin identified in the plant extract. Isofraxidin and its glucoside are among key components of *Eleutherococci* root [372]. It is worth noting, that only glucoside of isofraxidin was found in this plant extract, and its UV peak area suggest rather limited quantity of this secondary metabolite.

Lignans were identified as one of the dominant metabolites in *Eleuetherococcus* root. Compound **14** (t_r = 30.2 min) exhibited a pseudomolecular ion at m/z 583 $[M+HCOOH-H]^-$ and fragment ions at m/z 537 $[M-H]^-$ corresponding to the loss of the HCOOH adduct, at m/z 375 $[M-H-162]^-$ corresponding to the cleavage of hexose and at m/z 195 $[M-H-162-180]^-$. Thus, compound **14** was assigned as olivil 4'-*O*-glucoside, which was confirmed by comparison with reference standard and literature data [355]. To the best of my knowledge, it is the first report on the presence of this compound in *Eleutherococci* root.

Compound **16** (t_r = 31.1 min) exhibited a pseudomolecular ion at m/z 727 $[M+HCOOH-H]^-$ and fragment ions at m/z 681 $[M-H]^-$ corresponding to the loss of the formate adduct, at m/z 519 $[M-H-162]^-$ and 357 $[M-H-162-162]^-$ corresponding to the cleavage of first and second hexose, respectively. The compound was tentatively identified as pinoresinol 4,4'-di-*O*-glucoside [375], which was previously identified in *Eleutherococcus senticosus* stem [369].

A major lignan compound **18** (t_r = 32.2 min) exhibited a pseudomolecular ion at m/z 787 $[M+HCOOH-H]^-$ and fragment ions at m/z 741 $[M-H]^-$ corresponding to the loss of the HCOOH adduct, at m/z 579 $[M-H-162]^-$ and 417 $[M-H-162-162]^-$ corresponding to the cleavage of first and second hexose, respectively. The compound was tentatively identified by comparison with literature data [375] as syringaresinol 4,4'-di-*O*-glucoside (*syn*. Eleutheroside D, Eleutheroside E, Liriodendrin), which was previously identified in *Eleutherococcus senticosus* root [264, 375]. The fragment ion at m/z 579 was also present for compound **31** (t_r = 37.0), with a similar fragmentation pattern: m/z 417 $[M-H-162]^-$ again corresponding to the cleavage of hexose, m/z 402 $[M-H-162-15]^-$ corresponding to the loss of methyl group and m/z 181 $[M-H-162-236]^-$. Based on this, compound **31** was identified as syringaresinol 4-*O*-glucoside (*syn*. Eleutheroside E1, Acanthoside B) [375], reported previously in this plant material by He *et al.* [375]. A distinct peak for syringaresinol aglycone (*syn*. Lirioresinol B) was not found. Syringaresinol and its glucosides are rare compounds among already rare class of polyphenols, i.e., lignans. *Eleutherococci radix* is considered a significant source of these phytochemicals, though, their concentration in comparison with other constituents is rather limited.

Compound **20** (t_r = 33.1 min) exhibited a pseudomolecular ion at m/z 523 $[M-H]^-$ and fragment ion at m/z 361 $[M-H-162]^-$ corresponding to the cleavage of hexose, m/z 346 $[M-H-162-15]^-$ corresponding to the loss of methyl group, m/z 331 $[M-H-162-30]^-$ corresponding to the demethoxylation, m/z 313 $[M-H-162-48]^-$ corresponding to the demethoxylation and dehydratation, and m/z 179 $[M-H-162-182]^-$ and m/z 165 $[M-H-162-196]^-$ both assigned as the products of lignan β-β bond cleavage. The compound was then identified by comparison with reference standard as secoisolariciresinol 9-*O*-glucoside. Compound **38** exhibited a pseudomelucalar ion at m/z 361 $[M-H]^-$ and a similar fragmentation pattern to the secoisolariciresinol 9-*O*-glucoside. The compound **38** was then identified by comparison with a compound isolated from *A. alba* and literature data [339] as aglycone of the compound **20** – i.e., secoisolariciresinol.

Compound **24** (t_r = 34.7 min) exhibited a pseudomolecular ion at m/z 581 $[M-H]^-$ and fragment ions at m/z 419 $[M-H-162]^-$ corresponding to the cleavage of hexose, at m/z 389 $[M-H-162-30]^-$ corresponding to the loss of two methyl radicals and at m/z 223. The compound was tentatively identified as 5,5'-dimethoxylariciresinol 4-*O*-glucoside, which was previously identified in *Eleutherococcus senticosus* stem [369].

A minor compound **26** (t_r = 35.1 min) exhibited a pseudomolecular ion at m/z 595 $[M-H]^-$ and fragment ions at m/z 433 $[M-H-162]^-$ corresponding to the cleavage of hexose, at m/z 387 $[M-H-162-46]^-$ corresponding to concerting loss of CO_2 and water, at m/z 369 $[M-H-162-64]^-$ and at m/z 357 $[M-H-162-76]^-$. The compound was tentatively identified as ciwujiatone 4-*O*-glucoside, which was previously identified in *Eleutherococcus senticosus* stem [369].

Compound **35** (t_r = 38.6 min) exhibited a pseudomolecular ion at m/z 423 $[M+HCOOH-H]^-$ and fragment ions at m/z 387 $[M-H]^-$ corresponding to the loss of the HCOOH adduct, at m/z 357 $[M-H-30]^-$ corresponding to the demethoxylation, at m/z 343 $[M-H-44]^-$ corresponding to the loss of CO_2, m/z 313 $[M-H-74]^-$ and m/z 191 $[M-H-196]^-$ assigned as the product of β-β bond cleavage. The compound was tentatively identified as medioresinol [339]. A different fragmentation pattern could be seen for compound **29** (t_r = 36.5 min) which exhibited a pseudomolecular ion at m/z 549 $[M-H]^-$ and fragment ions at m/z 387 $[M-H-162]^-$ corresponding to the cleavage of hexose, at m/z 372 $[M-H-162-15]^-$ corresponding to the loss of methyl radical, at m/z 341 $[M-H-162-46]^-$, m/z 181 assigned as syringyl and m/z 151 assigned as guiacyl moieties Compound **29** was identified as medioresinol 4'-*O*-glucoside [375]. The main pseudomolecular ion obtained for peak **41** (t_r = 43.8 min) was at m/z 583 $[M-H]^-$ and fragmented into m/z 387 $[M-H-196]^-$ which corresponds to the cleavage

of guaiacylglycerol and m/z 369 [M−H−196−18]$^-$ corresponding to the loss of water. Compound **41** was tentatively identified as medioresinol 4'-*O*-guaiacylglycerol ether, which was previously identified in *Eleutherococcus senticosus* stem [369].

Compound **30** (t_r = 36.7 min) exhibited a pseudomolecular ion at m/z 519 [M−H]$^-$ and fragment ion at m/z 357 [M−H−162]$^-$ corresponding to the cleavage of hexose. The compound was then identified by comparison with a compound isolated from *A. lappa* as matairesinol 4-*O*-glucoside.

One of the compounds characterized by UV maxima at 211 and 278, i.e., compound **41** (t_r = 41.5) couldn't be analyzed in negative ion mode due to low sensitivity. However, it exhibited a protonated species in positive ion mode at m/z 353 [M+H]$^+$ and fragment ions at m/z 335 [M+H−18]$^+$ as a result of losing water yielding an acylium ion, at m/z 321, m/z 289, m/z 191 and m/z 167. Due to the lack of negative ion mode spectrum, it was supposed that compound **40** was a lignan lacking phenolic groups and tentatively identified as savinin [339], which was previously identified in *Eleutherococcus senticosus* stem [376].

Compounds **42** (t_r = 45.8 min) and **43** (t_r = 48.5 min) exhibited pseudomolecular ions at m/z 357 [M−H]$^-$ and quite similar fragmentation patterns. According to the elution order in RP-LC and comparison with compounds isolated from *P. sylvestris* and literature data [339], compound **42** was identified as pinoresinol, while compound **43** was identified as matairesinol.

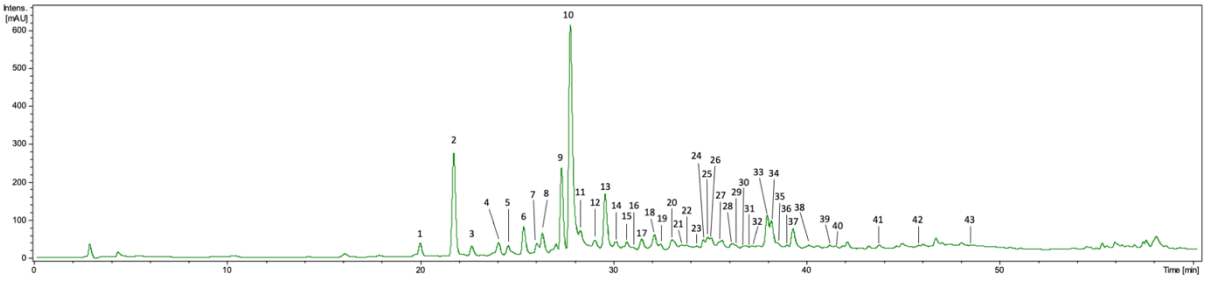

Figure 21. LC-DAD chromatogram of *E. senticosus* root obtained at 280 nm.

Eleutherococcus senticosus roots were extracted and subjected to UHPLC-DAD-ESI-MS/MS analysis. The focus of analysis was on qualitative data of secondary metabolites of *E. senticosus* roots. Through this analysis 36 secondary metabolites were identified or tentatively assigned, of which three have not been described in the entire genus (**13**, **23**, **27**), one was previously found in another *Eleutherococcus* spp. but has not been described in *E. senticosus* (**35**), and finally twelve have been

only previously found in other parts of the studied plant (**2**, **4**, **6**, **7**, **8**, **17**, **20**, **24**, **26**, **30**, **40**, **41**). On the other hand, I was not able to detect some of the metabolites that were previously described and isolated from this plant material. A comprehensive summary my findings in reference to the previous studies is available in Table 10. Most notably, I did not detect in our sample any other coumarins apart from isofraxidin 7-*O*-glucoside (**12**). I presume, that this may be due to their low concentration, below my level of detection.

Table 10. Summary of literature investigation of *Eleutherecoccus senticosus* root secondary metabolites.

No	Compound	Literature investigation
	Phenolic acids and their derivatives	
13	Caffeic acid	
-	Coniferaldehyde	
-	Coniferaldehyde 4-*O*-glucoside	
-	Coniferin	
-	Coniferyl alcohol	
-	Ferulic acid	
-	Gentisic acid	
-	p-Coumaric acid	
-	p-Hydroxybenzoic acid	
1	Protocatechuic acid	
2	Protocatechuic acid 3-*O*-glucoside	
-	Quinic acid	
15	Sinapaldehyde 4-*O*-glucoside	
-	Sinapyl alcohol	
-	Syringic acid	
9	Syringin	
-	trans-Cinnamaldehyde	
-	Vanillic acid	
3	Vanillic acid 4-*O*-glucoside	
	Caffeoylquinic acids	
-	1-*O*-Caffeoylquinic acid	
17	1,3-Di-*O*-caffeoylquinic acid	
33	1,5-Di-*O*-caffeoylquinic acid	
5	3-*O*-Caffeoylquinic acid	
27	3,4-Di-*O*-caffeoyl-5-*O*-feruloylquinic acid	
37	3,4-Di-*O*-caffeoylquinic acid	
23	3,5-Di-*O*-caffeoyl-4-*O*-feruloylquinic acid	
34	3,5-Di-*O*-caffeoylquinic acid	
11	4-*O*-Caffeoylquinic acid	
8	4-*O*-Feruoyl-5-*O*-caffeoylquinic acid	
32	4,5-Di-*O*-caffeoylquinic acid	
7	5-*O*-(3'-*O*-Caffeoyl glucosyl)quinic acid	
6	5-*O*-(4'-*O*-Feruoyl glucosyl)quinic acid	
4	5-*O*-(4'-*O*-Caffeoyl glucosyl)quinic acid	
10	5-*O*-Caffeoylquinic acid	

No	Compound	Literature investigation
	Lignans	
24	5,5'-Dimethoxylariciresinol 4-*O*-glucoside	
-	7,8-dihydrodehydrodiconiferyl alcohol	
-	7,8-trans-dihydrodehydrodiconiferyl alcohol 4-*O*-glucoside	
-	Asarinin	
26	Ciwujiatone 4-*O*-glucoside	
-	Dehydrodiconiferyl alcohol	
43	Matairesinol	
30	Matairesinol 4-*O*-glucoside	
35	Medioresinol	
-	Medioresinol 4,4'-di-*O*-glucoside	
29	Medioresinol 4'-*O*-glucoside	
41	Medioresinol 4'-*O*-guaiacylglycerol ether	
14	Olivil 4'-O-glucoside	
42	Pinoresinol	
-	Pinoresinol 4-O-glucoside	
16	Pinoresinol 4,4'-di-*O*-glucoside	
40	Savinin	
38	Secoisolariciresinol	
20	Secoisolariciresinol 9-*O*-glucoside	
-	Sesamin	
-	Syringaresinol	
31	Syringaresinol 4-*O*-glucoside	
18	Syringaresinol 4,4'-di-*O*-glucoside	
	Coumarins	
-	4-Methylesculetin	
-	6,7-dihydroxy-4-methylcoumarin	
-	6,7,8-Trimethoxycoumarin	
-	Esculin	
-	Fraxetin	
-	Fraxidin	
-	Fraxinol	
-	Isofraxidin	
12	Isofraxidin 7-*O*-glucoside	
-	Scoparone	

Legend

- Detected in study, no literature reports
- Detected in study + reports on presence in *Eleutherococcus* spp.
- Detected in study + reports on presence in other parts of *E. senticosus*
- Detected in study + reports on presence in roots of *E. senticosus*
- Reports only in literature on presence in roots of *E. senticosus*

6.1.1.9 Eleutherococcus senticosus root – isolation

The LC-MS analysis of *E. senticosus* root showed limited availability of lignans in the extract. Nevertheless, one of these compounds – syringaresinol 4,4'-di-*O*-glucoside is a rare lignan with some

unspecified hypoglycemic properties, which is why a decision was made to isolate it regardless of its low content in the plant material.

The crude extract of *Eleutherocci radix* was suspended in water and extracted 3 times with ethyl acetate. The water fraction (8.9 g) was then subjected to silica gel (60 × 2) chromatography and eluted with a chloroform/methanol gradient (100:0 → 0:100) of 11 steps, 1000 mL each. Seventy-seven fractions of 150 mL each were collected and pooled into 9 main fractions (ES-H1–ES-H9) based on their TLC profiles. Fraction ES-H7 (450 mg) was rechromatographed on Sephadex LH-20 column (40 x 3 cm) and eluted with methanol to obtain 96 fractions of 4.5 mL, which were pooled into 5 main fractions (ES-H7A–ES-H7E) based on their TLC profiles. From fraction ES-H7A (100 mg) **syringaresinol 4,4'-di-*O*-glucoside** (4 mg; 21,00 – 21,70) was isolated using preparative HPLC. The separation and isolation are illustrated by Figure 22. Isolated lignan was characterized using NMR methods.

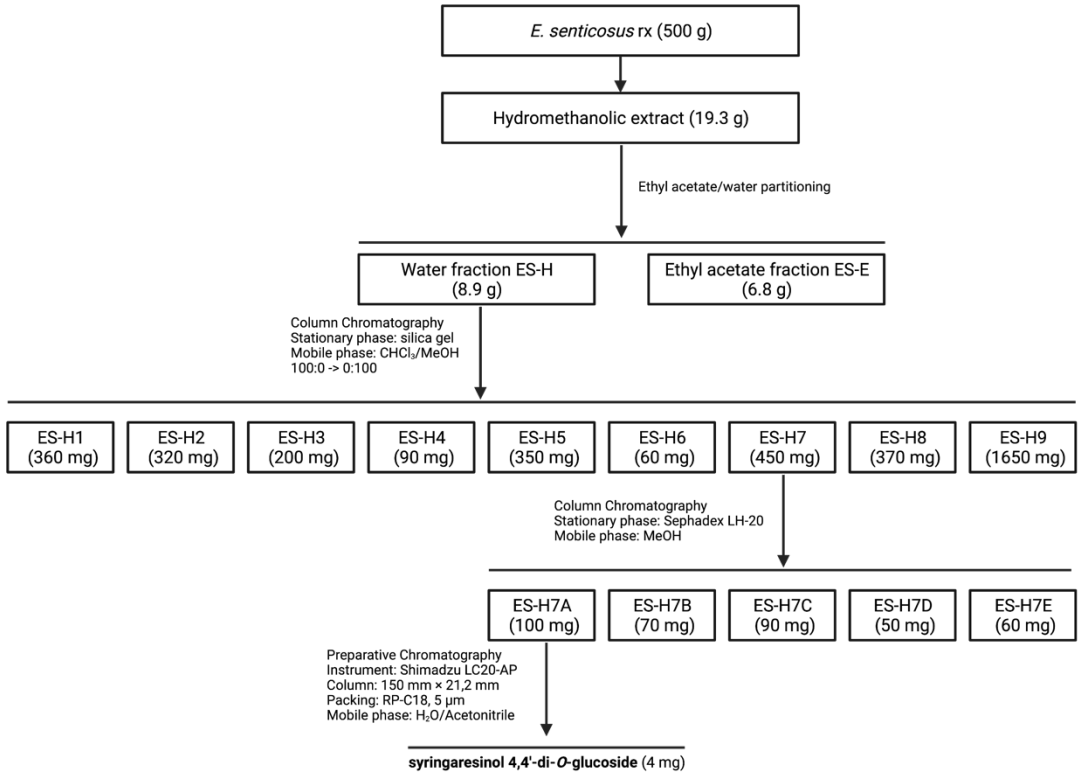

Figure 22. Scheme of *E. senticosus* root hydromethanolic extract fractionation and isolation of a lignan.

6.1.2 Phytochemical characterization of *angelica* roots extracts

Angelicae archangelicae radix, *Angelicae dahuricae radix*, *Angelicae pubescentis radix* and *Angelicae sinensis radix* are pharmacopeial plant materials coming from the roots of distinct angelica species (i.e., *A. archangelica*, *A. dahurica*, *A. biserrata* and *A. sinensis* respectively). Although metabolite content of these plant materials is somewhat varied, as they are standardized for the content of different secondary metabolites, Ph. Eur. 11th provides a common TLC method for their characterization, based on the presence or absence of three compounds – osthole, imperatorin and (Z)-ligustilide. The TLC analysis confirmed the presence of osthole and imperatorin in *A. archangelica* root, as well as excluded the presence of (Z)-ligustilide. Similar chromatogram, with some distinct zones (described in Ph. Eur. 11th) was observed for *A. biserrata* root, though the zone for imperatorin was hardly observable due to the low content of this coumarin in this plant material (its presence is not mandatory for confirmation of the origin of this root). For *A. dahurica* root only zone for imperatorin was observed and for *A. sinensis* root the presence of (Z)-ligustilide was confirmed. These finding were later proved by LC-DAD-ESI-MS/MS analysis.

Further, for a more comprehensive analysis of angelica roots from different species, LC-DAD-ESI-MS/MS analysis was performed, which was supported by isolation of some of the compounds and their characterization through NMR analysis (Chapter 6.1.3). Through this analysis I was able to identify or partly identify 41 compounds. Most of them were simple or furanocoumarins, apart from one phthalide and one sesquiterpene. The metabolite profiles of studied angelica roots are shown in Table 11 and chromatograms obtained at 254 nm are presented in Figure 23.

Compound **1** (t_r = 9.5 min) exhibited its pseudomolecular ions at m/z 193 $[M+H]^+$ and m/z 215 $[M+Na]^+$. It was assigned as scopoletin based on comparison of UV, retention time and MS signals with reference compound. Compound **2** (t_r = 12.4 min) exhibited its pseudomolecular ions at m/z 179 $[M+H]^+$, m/z 201 $[M+Na]^+$ and at m/z 379 $[2M+Na]^+$. Its retention time was compared with that of a reference standard for esculetin, but they didn't match. Thus, it was assigned as unknown coumarin.

Compounds **3** (t_r = 15.5 min), **17** (t_r = 25.1 min) and **22** (t_r = 27.6 min) exhibited their pseudomolecular ions at m/z 287 $[M+H]^+$, m/z 309 $[M+Na]^+$, m/z 573 $[2M+H]^+$ and at m/z 595 $[2M+Na]^+$. Based on elution order and comparison with reference standards, compound **3** was assigned as pabularinone, compound **17** as pabulenol and compound **22** as oxypeucedanin.

Table 11. Retention time, UV, and MS/MS data of the compounds identified in *Angelicae* roots.

Compounds	T_r [min]	UV_{max} [nm]	Extracted ion [m/z]	Fragment ions [m/z]	Species	Ref.
1. Scopoletin*	9.5	225, 342	193 $[M+H]^+$ 215 $[M+Na]^+$	137	AA	[377]
2. Unknown coumarin	12.4	220, 339	179 $[M+H]^+$ 201 $[M+Na]^+$ 379 $[2M+Na]^+$	147	AA	[377]
3. Pabularinone	15.5	264, 306	287 $[M+H]^+$		AD	[378]
4. Columbianetin**	16.8	207, 218sh, 260, 328	247 $[M+H]^+$ 269 $[M+Na]^+$ 493 $[2M+H]^+$ 515 $[2M+Na]^+$	175	AB	[377, 379]
5. Oxypeucedanin hydrate**	17.1	220, 266sh, 311	305 $[M+H]^+$ 327 $[M+Na]^+$ 631 $[2M+Na]^+$	203 286, 267	AA, AD	[283, 378]
6. Byakangelicin**	17.8	219, 268, 314	335 $[M+H]^+$ 357 $[M+Na]^+$ 691 $[2M+Na]^+$		AD	[378]
7. Psoralen**	19.9	217, 243, 294, 325sh	187 $[M+H]^+$ 209 $[M+Na]^+$ 395 $[2M+Na]^+$		AA, AD, AB	[377, 378]
8. Angelicin**	20.7	246, 300	187 $[M+H]^+$ 209 $[M+Na]^+$ 395 $[2M+Na]^+$		AA	
9. Angelol A / Angelol D / Angelol G / Isoangelol A	20.9	204sh, 219, 328	377 $[M+H]^+$ 399 $[M+Na]^+$ 775 $[2M+Na]^+$		AB	[379]
10. Xanthotoxin**	21.3	217, 245, 301	217 $[M+H]^+$ 239 $[M+Na]^+$ 433 $[2M+H]^+$ 455 $[2M+Na]^+$		AA, AD, AB	[283, 377, 378]
11. Angelol A / Angelol D / Angelol G / Isoangelol A	21.3	219, 247sh, 263sh, 302	377 $[M+H]^+$ 399 $[M+Na]^+$ 775 $[2M+Na]^+$		AB	[377, 379]
12. Angelol A / Angelol D / Angelol G / Isoangelol A	23.2	220, 326	377 $[M+H]^+$ 399 $[M+Na]^+$ 775 $[2M+Na]^+$		AB	[379]
13. Angelol C	23.7	220, 268, 317	379 $[M+H]^+$ 401 $[M+Na]^+$	361, 347, 278, 259, 219, 207	AB	[379]
14. Bergapten**	23.8	220, 249, 267, 312	217 $[M+H]^+$ 239 $[M+Na]^+$ 433 $[2M+H]^+$ 455 $[2M+Na]^+$		AA, AD, AB	[283, 377, 378]
15. Isopimpinellin**	24.0	221, 249, 268, 313	247 $[M+H]^+$ 269 $[M+Na]^+$ 493 $[2M+H]^+$ 515 $[2M+Na]^+$		AA, AD	[283, 378]
16. Suberenol	24.9	217, 261, 325	261 $[M+H]^+$ 283 $[M+Na]^+$ 543 $[2M+Na]^+$	243, 217, 189	AB	[377]
17. Pabulenol	25.1	220, 267, 313	287 $[M+H]^+$ 309 $[M+Na]^+$ 595 $[2M+Na]^+$	224	AD	[377, 378]
18. Neobyakangelicol**	25.1	220, 267, 313	317 $[M+H]^+$ 339 $[M+Na]^+$	224	AD	[378]
19. Osthenol**	25.7	256, 325	231 $[M+H]^+$ 253 $[M+Na]^+$ 483 $[2M+Na]^+$	201, 189, 175	AA	[283, 377]
20. Bisabolangelone**	26.1	247	271 $[M+Na]^+$ 519 $[2M+Na]^+$		AB	
21. Byakangelicol	27.4	221, 268, 312	317 $[M+H]^+$ 339 $[M+Na]^+$ 633 $[2M+H]^+$ 655 $[2M+Na]^+$	299, 233	AD	[378]

Compounds	T_r [min]	UV_{max} [nm]	Extracted ion [m/z]	Fragment ions [m/z]	Species	Ref.
22. Oxypeucedanin*	27.6	220, 248, 308	287 $[M+H]^+$ 309 $[M+Na]^+$ 573 $[2M+H]^+$ 595 $[2M+Na]^+$	203	AA, AD	[283, 378]
23. Columbianetin acetate**	27.8	202, 259, 326	289 $[M+H]^+$ 311 $[M+Na]^+$ 577 $[2M+H]^+$ 599 $[2M+Na]^+$	187	AB	[377, 379]
24. Heraclenol-2'-*O*-angelate**	28.9	217, 247, 301	387 $[M+H]^+$ 409 $[M+Na]^+$ 795 $[2M+Na]^+$	369, 269, 203 342, 225, 207, 185	AA	[283]
25. Byakangelicin-2'-*O*-angelate**	30.7	220, 246sh, 267, 309	417 $[M+H]^+$ 439 $[M+Na]^+$ 855 $[2M+Na]^+$	399, 299, 231, 167	AA	[283]
26. Vaginidiol-2'-*O*-angelate**	32.1	220, 267, 313	345 $[M+H]^+$ 367 $[M+Na]^+$		AA	
27. Byakangelicin-2'-*O*-isovalerate**	32.6	221, 269, 313	419 $[M+H]^+$ 441 $[M+Na]^+$ 859 $[2M+Na]^+$	383, 339, 255, 239, 209, 187	AA	[283]
28. Imperatorin**	33.2	218, 247, 261sh, 301	271 $[M+H]^+$ 293 $[M+Na]^+$ 536 $[2M+Na]^+$	203	AA, AD, AB	[283, 377, 378]
29. (Z)-Ligustilide*	33.9	281, 324, 350	191 $[M+H]^+$ 381 $[2M+H]^+$	173	AS	[293]
30. Osthole**	34.8	203, 221, 324	245 $[M+H]^+$ 267 $[M+Na]^+$ 489 $[2M+H]^+$ 511 $[2M+Na]^+$	189	AA, AB	[283, 377]
31. Cnidilin**	34.9	222, 269, 313	301 $[M+H]^+$ 323 $[M+Na]^+$ 623 $[2M+Na]^+$	233	AD	[377, 378]
32. Phellopterin**	36.0	221, 268, 312	301 $[M+H]^+$ 323 $[M+Na]^+$ 623 $[2M+Na]^+$	254	AA, AD	[283, 377, 378]
33. Isoimperatorin**	36.4	221, 249sh, 269sh, 310	271 $[M+H]^+$ 293 $[M+Na]^+$ 563 $[2M+Na]^+$	259, 224, 203	AA, AD, AB	[283, 378]
34. Suberosin	36.9	221, 330	245 $[M+H]^+$ 267 $[M+Na]^+$ 511 $[2M+Na]^+$		AD	[378]
35. Columbianadin I	37.0	210, 259sh, 326	329 $[M+H]^+$ 351 $[M+Na]^+$ 657 $[2M+H]^+$ 679 $[2M+Na]^+$	229, 187	AB	[377, 379]
36. Columbianadin II**	37.3	210, 259sh, 326	329 $[M+H]^+$ 351 $[M+Na]^+$ 657 $[2M+H]^+$ 679 $[2M+Na]^+$	229, 187	AB	[377, 379]
37. Dihydrocolumbianadin I	37.8	219, 260sh, 326	331 $[M+H]^+$ 353 $[M+Na]^+$ 661 $[2M+H]^+$ 683 $[2M+Na]^+$	229, 187	AB	[379]
38. Dihydrocolumbianadin II	38.1	219, 260sh, 326	331 $[M+H]^+$ 353 $[M+Na]^+$ 661 $[2M+H]^+$ 683 $[2M+Na]^+$		AB	[379]
39. Isoedultin**	38.3	218, 321	409 $[M+Na]^+$ 795 $[2M+Na]^+$		AA	
40. Archangelicin**	45.3	202, 217, 321	449 $[M+Na]^+$ 875 $[2M+Na]^+$		AA	[283]
41. 2'-Angeloyl-3'-isovaleryl vaginate**	47.1	202, 217, 321	451 $[M+Na]^+$ 879 $[2M+Na]^+$		AA	[283]

AA – *Angelica archangelica*; AD – *Angelica dahurica*; AB – *Angelica biserrata*; AS – *Angelica sinensis*.
* compared with reference standard; ** isolated from angelica root and identified on NMR.

Compounds **4** (t_r = 16.8 min) and **15** (t_r = 24.0 min) exhibited their pseudomolecular ions at m/z 247 $[M+H]^+$, m/z 269 $[M+Na]^+$, m/z 493 $[2M+H]^+$ and at m/z 515 $[2M+Na]^+$. They were compared to reference standards and identified: compound **4** was assigned as an angular furanocoumarin columbianetin and compound **15** as a linear furanocoumarin isopimpinellin.

Compound **5** (t_r = 17.1 min) exhibited its pseudomolecular ions at m/z 305 $[M+H]^+$, m/z 327 $[M+Na]^+$ and at m/z 631 $[2M+Na]^+$. It was tentatively identified as oxypeucedanin hydrate. Similarly, compound **6** (t_r = 17.8 min) exhibited its pseudomolecular ions at m/z 335 $[M+H]^+$, m/z 357 $[M+Na]^+$ and at m/z 691 $[2M+Na]^+$. It was tentatively assigned as byakangelicin.

Compounds **7** (t_r = 19.9 min) and **8** (t_r = 20.7 min) exhibited their pseudomolecular ions at m/z 287 $[M+H]^+$, m/z 209 $[M+Na]^+$ and m/z 396 $[2M+Na]^+$. Their UV and MS spectra did not allow me to distinguish the obvious two candidates, that is linear furanocoumarin psoralen and angular furanocoumarin angelicin. Both compounds were assigned by comparison with reference standards as psoralen and angelicin respectively.

Compounds **9** (t_r = 20.9 min), **11** (t_r = 21.3 min) and **12** (t_r = 23.2 min) exhibited their pseudomolecular ions at m/z 377 $[M+H]^+$, m/z 399 $[M+Na]^+$ and m/z 775 $[2M+Na]^+$. They are 4 compounds previously described in *Angelica* species that could give these signals, namely angelol A, angelol D, angelol G and isoangelol A. The three signals together were assigned as angelol A, angelol D, angelol G or isongelol A.

Compounds **10** (t_r = 21.3 min) and **14** (t_r = 23.8 min) exhibited their pseudomolecular ions at m/z 217 $[M+H]^+$, m/z 239 $[M+Na]^+$, m/z 433 $[2M+H]^+$ and m/z 455 $[2M+Na]^+$. Their UV and MS spectra did not allow me to distinguish the obvious two candidates, that is 5-*O*-methoxy or 8-*O*-methoxy substituted psoralen. Both compounds were assigned by comparison with reference standards as xanthotoxin (methoxalen) and bergapten respectively.

Compound **13** (t_r = 23.7) exhibited its pseudomolecular ions at m/z 379 $[M+H]^+$ and at m/z 401 $[M+Na]^+$. The $[M+H]^+$ ion fragmented into ions at m/z 361 $[M+H-18]^+$ from the loss of H_2O, and few minor ions at m/z 347, 278, 259, 219 and 207. Comparing with literature data it was assigned as angelol C.

Compound **16** (t_r = 24.9 min) exhibited its pseudomolecular ions at m/z 261 $[M+H]^+$, m/z 283 $[M+Na]^+$ and m/z 543 $[2M+Na]^+$. The $[M+H]^+$ ion fragmented into ions at m/z 243 $[M+H-18]^+$ from the loss of H_2O, m/z 217 $[M+H-44]^+$ and at m/z 189 $[M+H-72]^+$. Based on literature data it was assigned as suberenol.

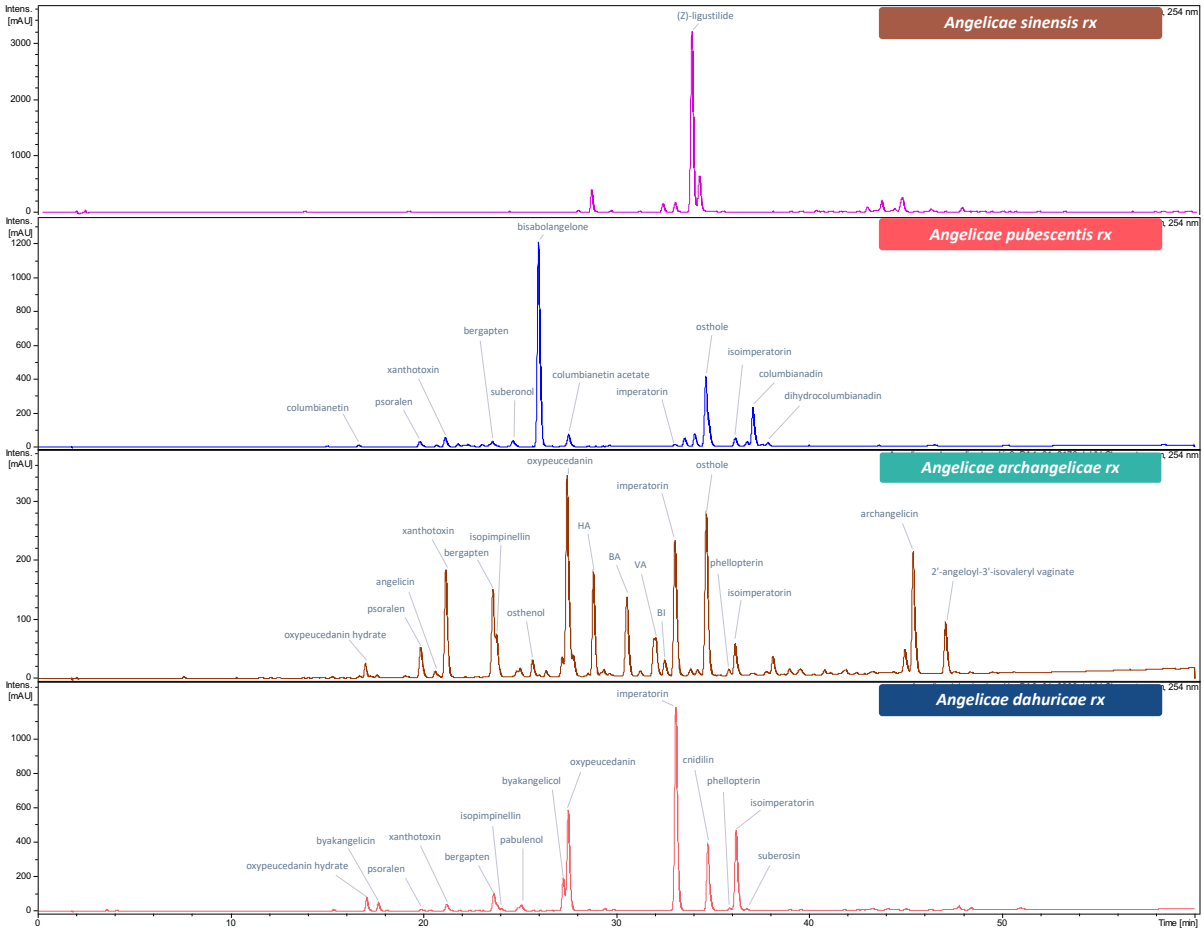

Figure 23. Chromatograms of angelica roots n-hexane extracts obtained at 254 nm.

HA – heraclenol-2'-*O*-angelate; BA – byakangelicin-2'-*O*-angelate; VA – vaginidiol-*O*-angelate; BI – byakangelicin-2'-*O*-isovalerate.

Compounds **18** (t_r = 25.1 min) and **21** (t_r = 27.4 min) exhibited their pseudomolecular ions at m/z 317 $[M+H]^+$ and m/z 339 $[M+Na]^+$, with the latter exhibiting also ions at m/z 633 $[2M+H]^+$ and m/z 655 $[2M+Na]^+$. The identity of these two compounds was confirmed later through isolation and NMR analysis (Chapter 6.1.3). Compound **18** was identified as neobyakangelicol, while compound **21** rapidly degraded after isolation giving signals and ions typical for byakangelicin (**6**). Assessing that the cause of this degradation could be hydrolysis of the oxirane group in acidic eluent and judging from the product, compound **21** was assigned as byakangelicol.

Compound **19** (t_r = 25.7 min) exhibited its pseudomolecular ions at m/z 231 $[M+H]^+$, 253 $[M+Na]^+$ and m/z 483 $[2M+Na]^+$. It was tentatively identified as osthenol.

Compound **20** (t_r = 26.1 min) exhibited its pseudomolecular ions at m/z 271 $[M+Na]^+$ and m/z 519 $[2M+Na]^+$. It was isolated from *A. biserrata* roots and through NMR analysis identified as the only found sesquiterpene – bisabolangelone (Chapter 6.1.3).

Compound **23** (t_r = 27.8 min) exhibited its pseudomolecular ions at m/z 289 $[M+H]^+$, m/z 311 $[M+Na]^+$, m/z 577 $[2M+Na]^+$ and m/z 599 $[2M+Na]^+$. It was tentatively assigned as columbianetin acetate.

Compounds **24** (t_r = 28.9 min) and **39** (t_r = 38.3 min) exhibited their pseudomolecular ions at m/z 409 $[M+Na]^+$ and m/z 795 $[2M+Na]^+$, with the former exhibiting also ion at m/z 387 $[M+H]^+$. Both compounds were isolated from the roots of *A. archangelica* roots (Chapter 6.1.3) and identified through NMR analysis as heraclenol-2'-*O*-angelate (**24**) and isoedultin (**39**).

Compound **25** (t_r = 30.7 min) exhibited its psuedomolecular ions at m/z 417 $[M+H]^+$, m/z 439 $[M+Na]^+$ and m/z 855 $[2M+Na]^+$. Based on literature data it was tentatively identified as byakangelicin-2'-*O*-angelate.

Compound **26** (t_r = 32.1 min) exhibited its psuedomolecular ions at m/z 345 $[M+H]^+$ and at m/z 367 $[M+Na]^+$. It was isolated and based on NMR analysis (Chapter 6.1.3) it was assigned as vaginidiol-2'-*O*-angelate.

Compound **27** (t_r = 32.6 min) exhibited its psuedomolecular ions at m/z 429 $[M+H]^+$, m/z 442 $[M+Na]^+$ and m/z 859 $[2M+Na]^+$. Based on literature data it was tentatively identified as byakangelicin-2'-*O*-isovalerate.

Compounds **28** (t_r = 33.2 min) and **33** (t_r = 36.4 min) exhibited their pseudomolecular ions at m/z 271 $[M+H]^+$, m/z 293 $[M+Na]^+$ and m/z 536 $[2M+Na]^+$, both producing fragment ion from the $[M+H]^+$ at m/z 203. The peaks represented two major coumarins in *A. archangelica* and *A. dahurica* roots, with the peak **28** being significantly more abundant. Based on elution order and comparison

with reference standards, compound **28** was identified as imperatorin (8-*O*-isoprenyloxypsoralen) and compound **33** as isoimperatorin (5-*O*-isoprenyloxypsoralen).

Peak **29** (t_r = 33.9 min) which was present only in A. sinensis root had its UV spectra different from that of coumarins, with UV_{max} at 281, 324 and 350 nm. It exhibited pseudomolecular ions at m/z 191 $[M+H]^+$ and at m/z 381 $[2M+H]^+$. Based on literature data and comparing with reference standard it was assigned as (Z)-ligustilide.

Compounds **30** (t_r = 34.8 min) and **34** (t_r = 36.9 min) exhibited their pseudomolecular ions at m/z 245 $[M+H]^+$, m/z 267 $[M+Na]^+$ and at m/z 511 $[2M+Na]^+$, with the former additionally exhibiting a $[2M+H]^+$ ion at m/z 489. Based on elution order and comparison with reference standards, compound **30** was identified as osthole and compound **34** as suberosin. Characteristic absence of osthole in *A. dahurica* roots was also observed.

Compounds **31** (t_r = 34.9 min) and **32** (t_r = 36.0 min) exhibited their pseudomolecular ions at m/z 301 $[M+H]^+$, m/z 323 $[M+Na]^+$ and at m/z 623 $[2M+Na]^+$. Their retention times and UV spectra were similar. Compound **31** was identified as cnidilin (5-*O*-isoprenyloxy-8-*O*-methoxypsoralen) and compound **32** as phellopterin (8-*O*-isoprenyloxy-5-*O*-methoxypsoralen).

Compounds **35** (t_r = 37.0 min) and **36** (t_r = 37.3 min) exhibited their pseudomolecular ions at m/z 329 $[M+H]^+$, m/z 351 $[M+Na]^+$, m/z 661 $[2M+H]^+$, and at m/z 683 $[2M+Na]^+$. Their retention times and UV spectra were similar. They were tentatively assigned as enantiomers of columbianadin. Similarly, compounds **37** (t_r = 37.8 min) and **38** (t_r = 38.1 min) exhibited their ions 2 Da higher, which could be explained by the presence of isovaleryl moiety instead of angeloyl one. Thus, they were tentatively assigned as enantiomers of dihydrocolumbianadin.

Compound **40** (t_r = 45.3 min) exhibited its psuedomolecular ions at m/z 449 $[M+Na]^+$ and at m/z 875 $[2M+Na]^+$. It was tentatively assigned as archangelicin.

Compound **41** (t_r = 47.1 min) exhibited its psuedomolecular ions at m/z 451 $[M+Na]^+$ and at m/z 879 $[2M+Na]^+$. It differed only by 2 Da from compound **40**, presenting similar UV spectra and retention time. It was tentatively assigned as 2'-angeloyl-3'-isovaleryl vaginate, which is an archangelicin with angeloyl moiety at 3' replaced with isovaleryl one. This was later confirmed by NMR analysis of an isolate from *A. archangelica* (Chapter 6.1.3).

6.1.3 Coumarins isolation

Though LC-MS analysis three roots were chosen as sources for coumarins isolation, *A. archangelica*, *A. dahurica* and *A. biserrata*.

Angelica archangelica root n-hexane extract was subjected to silica gel column chromatography (65 × 5) and eluted with a chloroform/methanol gradient (100:0 → 90:10) of 11 steps, 0.5 L each, to obtain 100 fractions of 55 mL, which were pooled into 8 main fractions (AAH1–AAH8) based on their TLC profiles. From fraction AAH4 (1880 mg), **psoralen** (5.5 mg; 15.25 – 16.60 min), **bergapten** (11.7 mg; 18.75 – 20.20 min), **imperatorin** (5.0 mg; 24.25 – 25.5 min), **osthole** (112.2 mg; 28.70 – 30.30 min) and **isoimperatorin** (9.4 mg; 30.50 – 31.60 min) were isolated using preparative HPLC. Using the same technique, **oxypeucedanin hydrate** (5.5 mg; 12.40 – 13.40 min) and **isopimpinellin** (9.9 mg; 18.80 – 20.00 min) were isolated from fraction AAH5 (2570 mg). Fraction AAH6 (4050 mg) was rechromatographed on a silica gel column (60 × 2) with a n-hexane/ethyl acetate gradient (90:10 → 75:25) of 4 steps, 750 mL each. One hundred forty-four fractions of 20 mL each were collected and pooled into 5 main fractions (AAH6A–AAH6E) based on their TLC profiles. Using preparative chromatography **isoimperatorin** (3.2 mg; 30.50 – 31.60 min) was purified from fraction AAH6B (320 mg), **imperatorin** (0.6 mg; 24.25 – 25.50 min), **osthole** (9.0 mg; 28.70 – 30.30 min), **phellopterin** (0.8 mg; 30.35 – 31.10 min), **archangelicin** (110.4 mg; 38.60 – 40.00 min) and **2'-angeloyl-3'-isovaleryl vaginate** (97.2 mg; 40.10 – 41.75 min) were isolated from fraction AAH6C (820 mg) and **xanthotoxin** (9.3 mg; 16.40 – 18.50 min), **bergapten** (2.2 mg; 18.75 – 20.20 min), **osthenol** (22.1 mg; 20.50 – 22.20 min), **vaginidiol-*O*-angelate** (16.5 mg; 23.30 – 24.1 min), **imperatorin** (12.4 mg; 24.25 – 25.5 min) and **isoedultin** (24.5 mg; 31.80 – 33.20 min) were isolated from fraction AAH6D (1630 mg). Fraction AAH7 (2620 mg) was rechromatographed on a silica gel column (60 × 2) with a n-hexane/ethyl acetate gradient (90:10 → 75:30) of 5 steps, 750 mL each. Four hundred fractions of 10 mL were collected and pooled into 6 main fractions (AAH7A–AAH7F). Preparative chromatography was used to obtain **angelicin** (64.0 mg; 16.00 – 16.70 min) from fraction AAH7B (80 mg), **isoedultin** (64.0 mg; 31.80 – 33.20 min) from fraction AAH7D (160 mg), **heraclenol-2'-*O*-angelate** (68.2 mg; 21.40 – 22.40 min), **byakangelicin-2'-*O*-angelate** (102.2 mg; 22.50 – 23.50 min) and **byakangelicin-2'-*O*-isovalerate** (14.4 mg; 23.90 – 24.70 min) from fraction AAH7F (680 mg). The separation and isolation are illustrated by Figure 24. All isolated compounds were characterized using NMR methods.

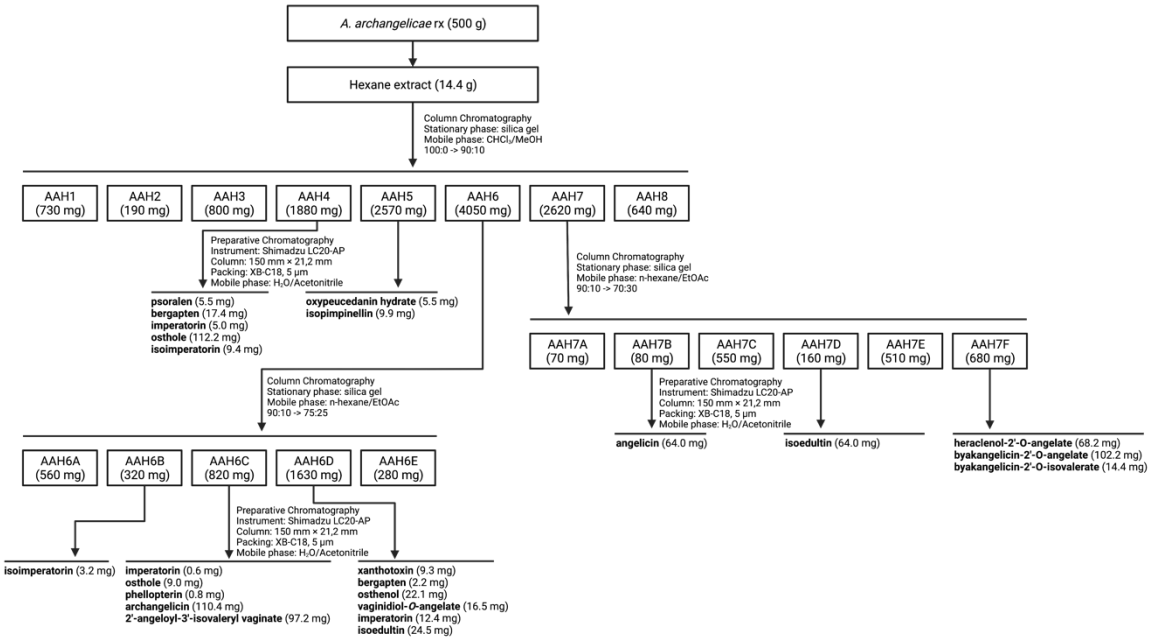

Figure 24. Scheme of *A. archangelica* root hexane extract fractionation and isolation of coumarins.

Angelica dahurica root n-hexane extract was subjected to silica gel column chromatography (65 × 5) and eluted with a chloroform/methanol gradient (100:0 → 50:50) of 26 steps, 250 mL each, to obtain 100 fractions of 65 mL, which were pooled into 4 main fractions (ADH1–ADH4) based on their TLC profiles. Preparative chromatography was used to obtain **psoralen** (0.3 mg; 15.25 – 16.60 min), **bergapten** (13.1 mg; 18.75 – 20.20 min) and **isoimperatorin** (135.9 mg; 30.50 – 31.60 min) from fraction ADH1 (1000 mg) and **xanthotoxin** (1.2 mg; 16.40 – 18.50 min), **bergapten** (13.5 mg; 18.75 – 20.20 min), **imperatorin** (206.7 mg; 24.25 – 25.5 min), **cnidilin** (3.3 mg; 28.80 – 30.40 min) and **isoimperatorin** (12.1 mg; 30.50 – 31.60 min) from fraction ADH2 (970 mg). Fraction ADH3 (3900 mg) was rechromatographed on a silica gel column (60 × 2) with a n-hexane/ethyl acetate gradient (100:0 → 70:30) of 7 steps, 750 mL each. Three hundred forty-eight fractions of 15 mL were collected and pooled into 8 main fractions (ADH3A–ADH3H). Preparative chromatography was used to purify and isolate **phellopterin** (6.3 mg; 30.35 – 31.10 min) from fraction ADH3B (360 mg), **imperatorin** (173.7 mg; 24.25 – 25.5 min) and **cnidilin** (221.2 mg; 28.80 – 30.40 min) from fraction ADH3C (830 mg), and a mixture (3:1) of **neobyakangelicol** and **pabulenol** (10.6 mg; 19.90 – 21.50 min) and **byakangelicin**

(5.5 mg; 11.50 – 12.40 min) from fraction ADH3F (130 mg). The separation and isolation are illustrated by Figure 25. All isolated compounds were characterized using NMR methods.

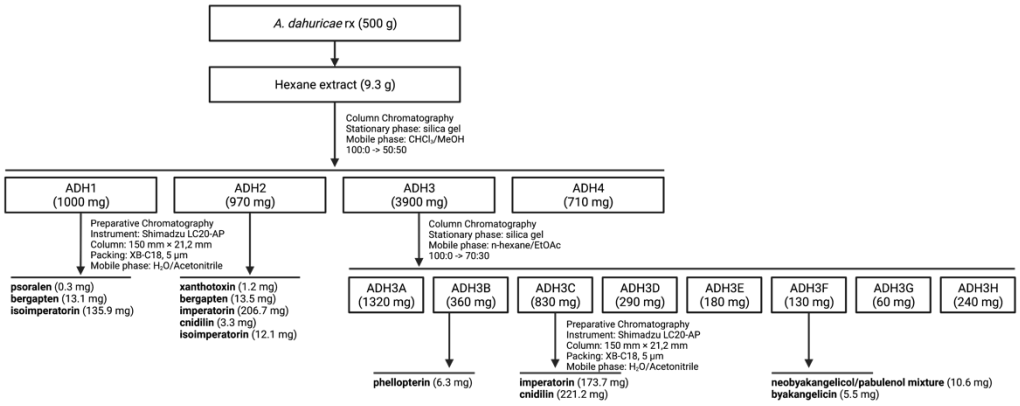

Figure 25. Scheme of *A. dahurica* root hexane extract fractionation and isolation of coumarins.

Angelica biserrata root (*Angelicae pubescentis radix*) n-hexane extract was subjected to silica gel column chromatography (65 × 5) and eluted with a chloroform/methanol gradient (100:0 → 70:30) of 16 steps, 400 mL each, to obtain 100 fractions of 65 mL, which were pooled into 5 main fractions (APH1–APH5) based on their TLC profiles. Fraction APH4 (6320 mg) was rechromatographed on a silica gel column (60 × 2) with a toluene/ethyl acetate gradient (99:1 → 70:30) of 14 steps, 500 mL each. Seven hundred fractions of 10 mL were collected and pooled into 11 main fractions (APH4A–APH4K). Preparative chromatography was used to purify and isolate **columbianadin** (108.9 mg; 32.45 – 33.60 min) from fraction APH4D, **columbianetin acetate** (30.7 mg; 21.6 – 22.5 min) from fraction APH4G (470 mg), **bisabolangelone** (23.7 mg; 20.65 – 21.75 min) from fraction APH4I (590 mg), and **columbianetin** (14.2 mg; 12.10 – 12.90 min) from fraction APH4J (20 mg). The separation and isolation are illustrated by Figure 26. All isolated compounds were characterized using NMR methods.

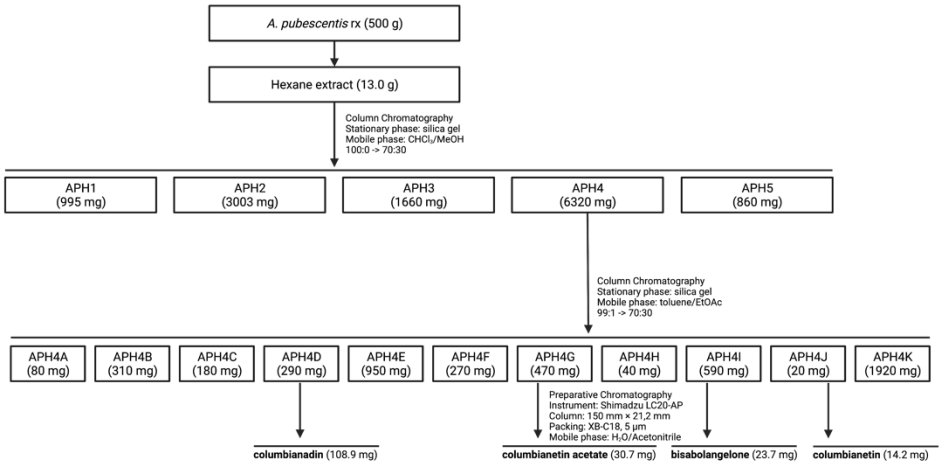

Figure 26. Scheme of *A. biserrata* root (*A. pubescentis radix*) hexane extract fractionation and isolation of coumarins.

6.2 Pharmacological part

6.2.1 Flavonoids

6.2.1.1 Screening of flavonoids on insulin secretion

The main objective of pharmacological part of this thesis was to study structurally diverse plant secondary metabolites from three groups, i.e., the flavonoids, lignans and coumarins, for their modulatory activity *in vitro* on the β-cell function on the INS-1 β-cell line. Through phytochemical characterization of plant extracts and isolation of potentially active pure compounds, two libraries were formed: one of lignans and one of coumarins. As flavonoids are widely commercially available, there was no need to isolate these plant metabolites and instead, the library was acquired from chosen suppliers.

Flavonoids also differed from other two metabolite groups in that their activity in the studied context was somewhat better described. The possibility to refer to previous results was considered a good starting point and thus, it was decided to commence the pharmacological studies with this group.

Eighteen flavonoids were assessed for their potential to modulate glucose-induced insulin secretion. The compounds were chosen to obtain a more comprehensive relationship between structure and activity. For this purpose, four flavonols (quercetin, kaempferol, myricetin, and galangin), five flavones (flavone, luteolin, diosmetin, chrysin, and apigenin), four flavanonols (taxifolin,

aromadendrin, ampelopsin, and pinobanksin) and five flavanones (naringenin, pinocembrin, flavanone, eriodictyol, and hesperetin) were studied. A screening concentration of 20 μmol/L was chosen based upon previous studies carried out at Institut des Biomolécules Max Mousseron, as it corresponds to the maximal effect of quercetin on insulin secretion [146]. As a flavonoid with confirmed insulinotropic effect, quercetin was used as a positive control. As expected, glucose induced insulin secretion in a concentration-dependent maner on the INS-1 β-cell line (Figure 27). The stimulating effect of glucose was observed relative to basal condition (1.4 mmol/L glucose) by a 2- to 3-fold increase in insulin secretion. After one hour incubation, insulin concentration in the cell supernatant treated with 1.4 mmol/L glucose was 23.27 ± 0.7886 ng/mL, while in the supernatants treated with 8.3 mmol/L glucose was 53.54 ± 1.453 ng/mL.

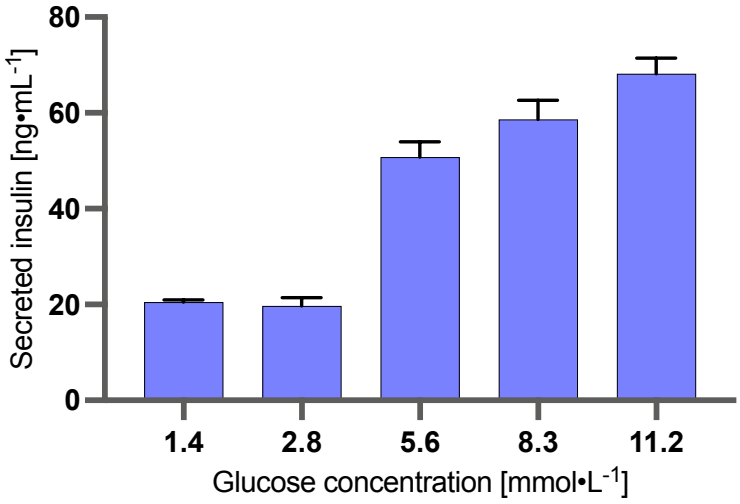

Figure 27. Glucose effect on insulin secretion.

The screening experiment was carried out in 8.3 mmol/L glucose, an intermediate stimulating concentration appropriate to examine the potential stimulatory effect of a compound, essentially to avoid any possible saturation of the system that could mask a pharmacological action.

Four of the studied flavonoids were able to significantly increase 8.3 mmol/L glucose-induced insulin secretion, namely quercetin (220.8 ± 12.31 %), kaempferol (166.7 ± 4.233 %), apigenin (150.7 ± 25.69 %), and chrysin (145.6 ± 15.31 %), while one compound, galangin (29.17 ± 3.983 %) significantly decreased glucose-induced insulin secretion (Figure 28).

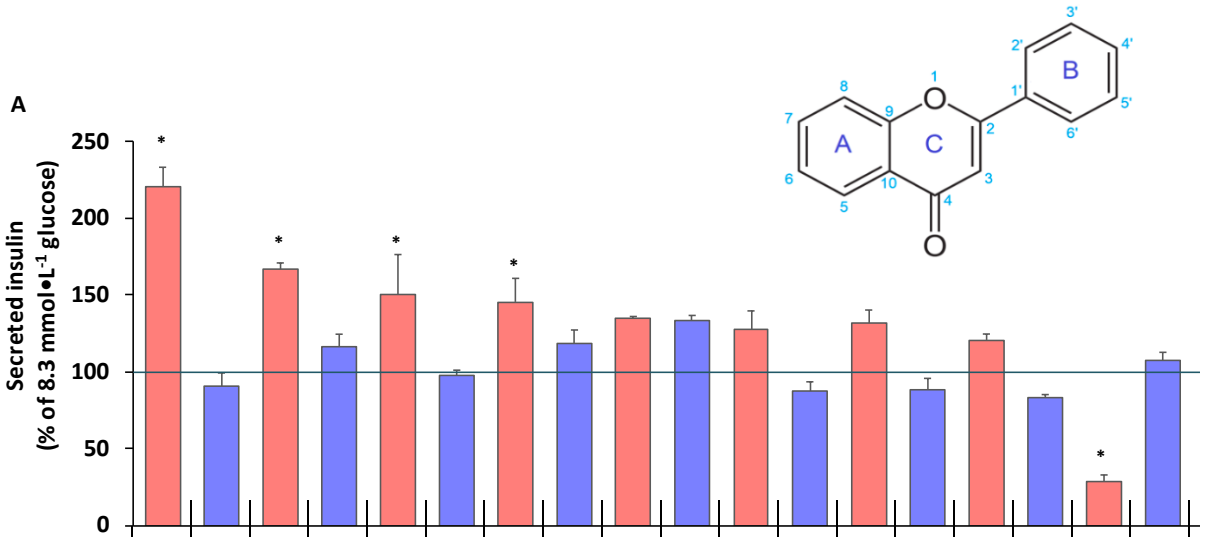

	Quercetin	Taxifolin	Kaempferol	Aromadendrin	Apigenin	Naringenin	Chrysin	Pinocembrin	Flavone	Flavanone	Luteolin	Eriodictyol	Myricetin	Ampelopsin	Diosmetin	Hesperetin	Galangin	Pinobanksin
2-3	=	–	=	–	=	–	=	–	=	–	=	–	=	–	=	–	=	–
3’	OH	OH									OH	OH	OH	OH	OH	OH		
4’	OH	OH	OH	OH	OH	OH					OH	OH	OH	OH	OCH3	OCH3		
5’													OH	OH				
3	OH	OH	OH	OH									OH	OH			OH	OH
5	OH	OH	OH	OH	OH	OH	OH	OH			OH	OH	OH	OH	OH	OH	OH	OH
7	OH	OH	OH	OH	OH	OH	OH	OH			OH	OH	OH	OH	OH	OH	OH	OH

Figure 28. Modulation of glucose-induced insulin secretion by flavonoids.

(A) The bar graph depicts the mean ± SEM of insulin secretion as a percentage of 8.3 mmol/L glucose-induced insulin secretion after 1h incubation of INS-1 cells with 20 μmol/L flavonoids; *$p < 0.05$ different from 0 μmol/L of flavonoids with one-way ANOVA followed by Holm–Sidak test, n = 3. (B) Structure of studied flavonoids.

All active compounds (both increasing or decreasing insulin secretion) belonged to the flavones and flavonols subclasses of flavonoids. When comparing active flavone with a corresponding flavanone or flavonol with a corresponding flavanonol (the sole difference was the lack of the double bond between C2 and C3), the effect was lost entirely. The effect of hydroxylations on the flavone structure and their exact position seems much more ambiguous. For example, a negative modulator of insulin secretion galangin is hydroxyl substituted at C3, C5, and C7, but one additional hydroxyl substitution at C4’ (kaempferol) or removal of substitution at C3 (chrysin) produces a positive modulation. This might suggest that positive and negative effects on insulin secretion modulation come from different molecular targets; thus, the evaluation of the structure-activity relationship should be based on the effect on the molecular target and not solely on the cell function.

6.2.2 Lignans

6.2.2.1 Screening of lignans on insulin secretion

The phytochemical studies of conifer wood, *A. lappa* and *C. tinctorius* fruits, and *E. senticosus* roots allowed me to indicate potentially active lignans for isolation, which was subsequently performed using chromatography techniques. All isolated compounds were characterized by NMR and their purity (> 95 %) and amount was deemed sufficient for pharmacological studies. Eleven isolated lignans in aglycone form, isolated from the fruits of *A. lappa* (arctigenin), fruits of *C. tinctorius* (trachelogenin), wood of *P. sylvestris* (pinoresinol, matairesinol, nortrachelogenin) and wood of *A. alba* (7-hydroxymatairesinol, 7-hydroxylariciresinol, lariciresinol, cyclolariciresinol, secoisolariciresinol, todolactol), four lignan glycosides, isolated from the fruits of *A. lappa* (arctigenin 4-*O*-glucoside, matairesinol 4-*O*-glucoside), fruits of *C. tinctorius* (trachelogenin 4-*O*-glucoside) and roots of *E. senticosus* (syringaresinol 4,4'-di-*O*-glucoside), and two lignan metabolites (enterolactone, enterodiol) were studied for their potential to modulate insulin secretion on the INS-1 β-cell line, in glucose-stimulating condition (8.3 mmol/L glucose) at 20 μmol/L.

Three out of seventeen screened compounds significantly decreased insulin secretion, while none of them was able to increase it (Figure 29).

The compounds able to decrease glucose-induced insulin secretion were trachelogenin (55.08 ± 16.03 %), nortrachelogenin (37.09 ± 11.52 %) and arctigenin (29.29 ± 4.587 %). Studied glycosides did not modulate insulin secretion (data not shown).

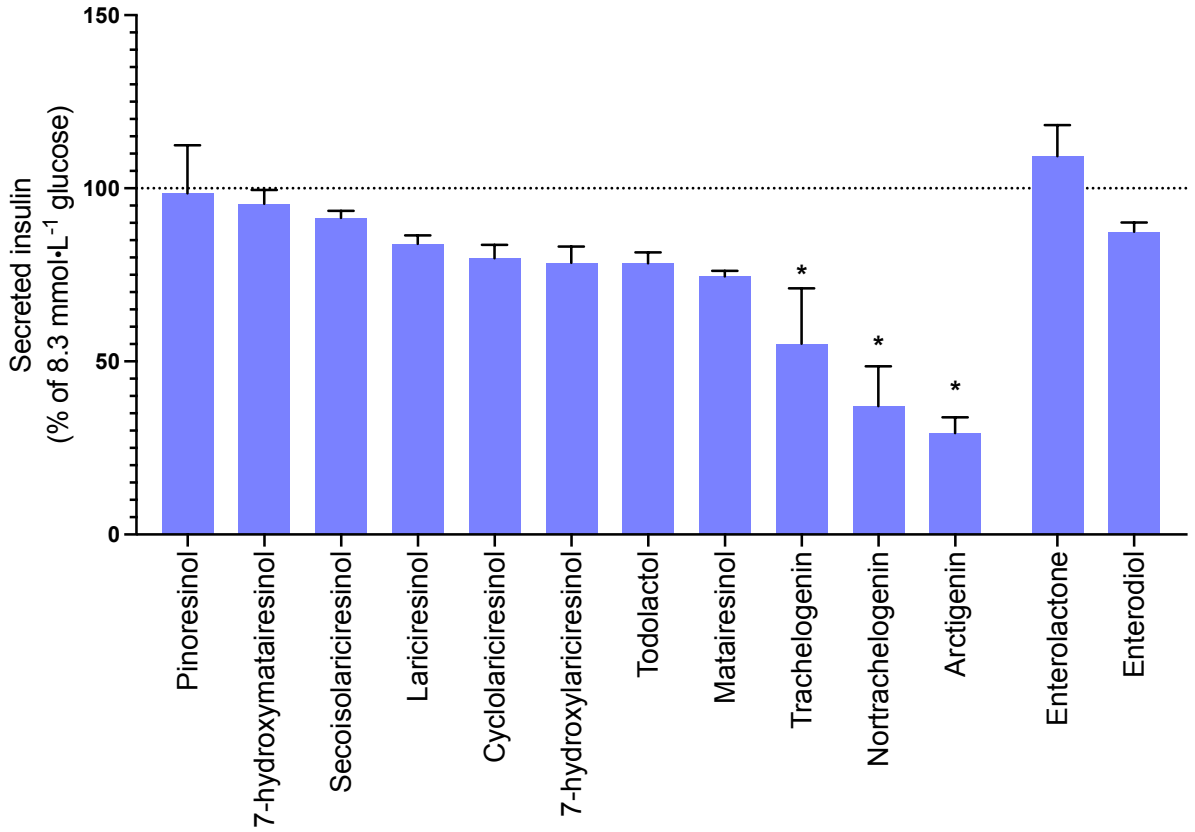

Figure 29. Effects of lignan aglycones and metabolites (20 μmol/L) on insulin secretion in glucose stimulating condition (8.3 mmol/L glucose) in INS-1 cells.

The bar graph depicts the mean ± SEM of insulin secretion as a percentage of 8.3 mmol/L glucose-induced insulin secretion after 1h incubation of INS-1 cells with 20 μmol/L lignan aglycones and metabolites; *$p < 0.05$ different from 0 μmol/L of lignans with one-way ANOVA followed by Holm–Sidak test, n = 3.

6.2.2.2 Evaluation of lignans toxicity in β-cells

To exclude any potential cytotoxic effect of studied lignans on the used cell model, i.e., INS-1, cell viability after 48 h of incubation with tested compounds was assessed using the MTT assay (Figure 30).

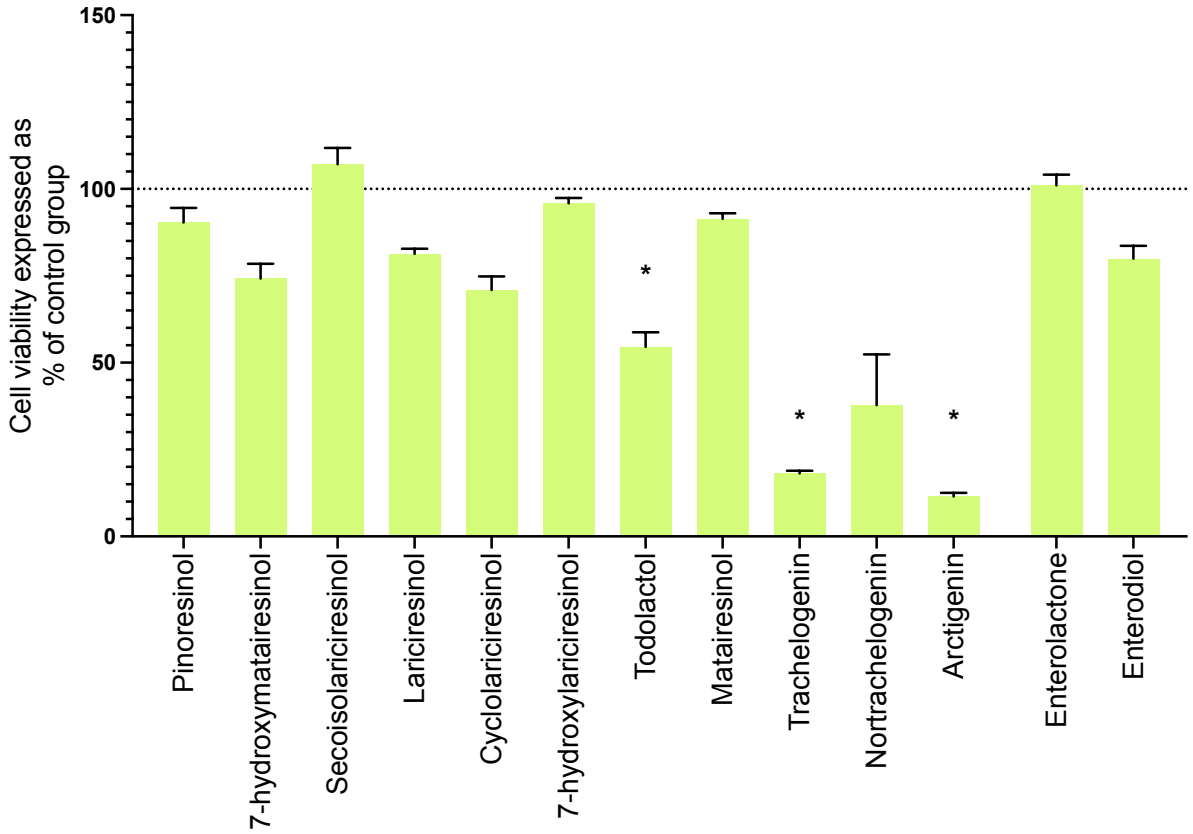

Figure 30. Effects of lignans on cell viability after 48 h incubation at 20 μmol/L.

The bar graph depict the mean ± SEM of cell viability in % of intraassay control; *$p < 0.05$ different from 0 μmol/L of lignans with Welch and Brown-Forsythe ANOVA followed by Dunnett T3 test, n = 3.

Todolactol (54.56 ± 4.209 %), trachelogenin (18.13 ± 0.7922 %) and arctigenin (11.52 ± 1.055 %) significantly decreased viability of the INS-1 cells, while a non-significant but still quite visible decrease was observed for nortrachelogenin (37.80 ± 14.60 %). These results might indicate that the decrease in insulin secretion caused by trachelogenin, nortrachelogenin and arctigenin could have arisen from toxicity of these compounds on this cell model.

6.2.2.3 Protection of β-cells by lignans

In another study carried out in the Department of Pharmaceutical Biology, some lignans were found to significantly reduce pro-inflammatory cytokines secretion induced by lipopolysaccharide (LPS) in monocytes/macrophages isolated from human peripheral blood. Because of chronic low-grade inflammation in patients with T2DM can further worsen β-cell function and survival, exacerbating the progression of the disease, I evaluated the effect of pro-inflammatory cytokine on cell viability and β-cell in the INS-1 model by incubating the cells for 24h with IL-1β.

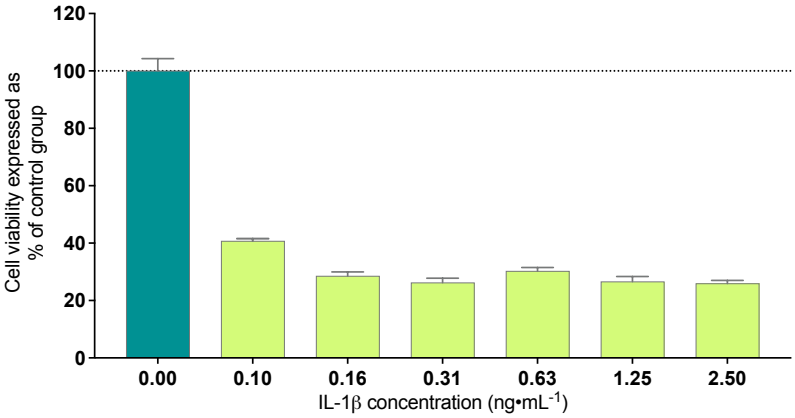

Figure 31. IL-1β effect on β-cell viability after 24 h incubation.

All studied concentrations of IL-1β decreased cell viability (Figure 31) and glucose-induced insulin secretion by more than 50 % (Figure 32). For subsequent protection studies, it was decided to use the lowest concentration of IL-1β, that is 0.1 ng/mL.

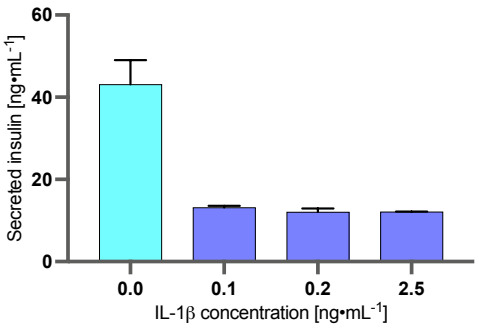

Figure 32. IL-1β effect on glucose-induced insulin secretion after 24h incubation.

The protective effect of lignans on the β-cell was studied by simultaneous incubation of 0.1 ng/mL of IL-1β with 20 μmol/L of all non-toxic lignans (arctigenin, trachelogenin, nortrachelogenin, todolactol and lignan metabolites were not studied) (Figure 33).

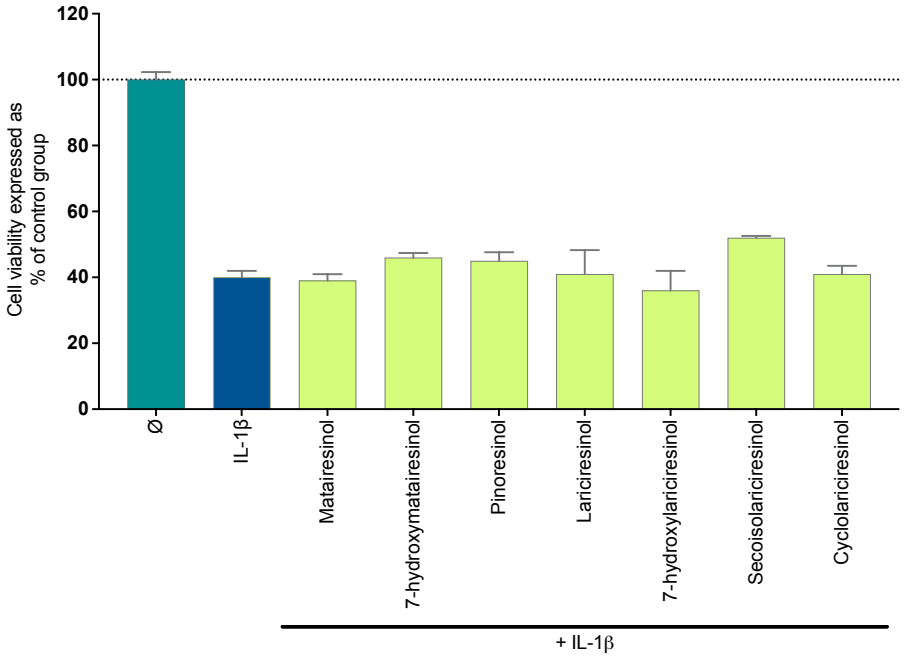

Figure 33. Lignans protective effect against IL-1β induced cell death.

The bar graph depicts the mean ± SEM of cell viability in % of intraassay control; *p < 0.05 different from 0 μmol/L of lignans + 0.1 ng/mL IL-1β with one-way ANOVA followed by Holm–Sidak test, n = 3.

None of the studied lignans had any protective effects against IL-1β induced cell death.

6.2.3 Coumarins

6.2.3.1 Screening of angelica roots extracts on insulin secretion

Ethanolic root extracts of four pharmacopeial plants from the genus *Angelica* L., namely: *A. archangelica*, *A. dahurica*, *A. sinensis* and *A. biserrata* were studied for their potential to modulate insulin secretion. The experiment was carried out in 8.3 mmol/L glucose-stimulating condition for extracts concentration ranging from 1.6 to 50.0 μg/mL (Figure 34).

None of the concentrations of *A. sinensis* root extract was able to modulate insulin secretion, while increase in insulin secretion for certain concentrations of three other extracts was observed (Figure 34).

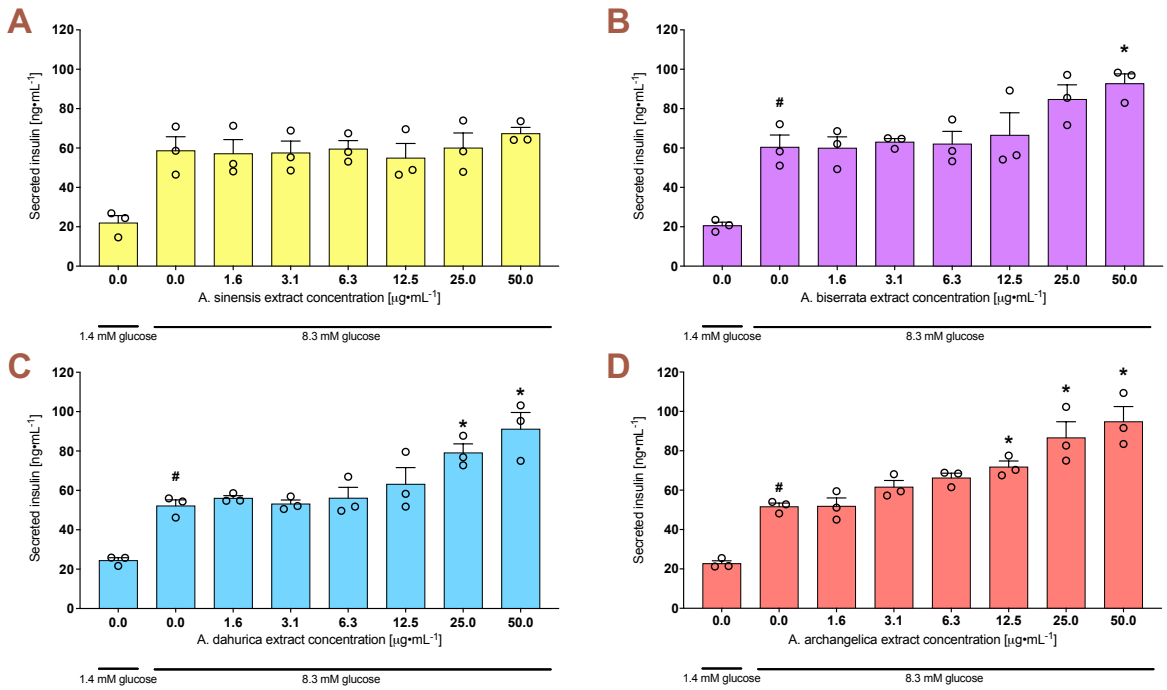

Figure 34. Modulation of insulin secretion in glucose-stimulating condition after 1h incubation with angelica root extracts.

The bar graphs depict the mean ± SEM of insulin secretion in ng/mL; (A) – *A. sinensis* root extract; (B) – *A. biserrata* root extract; (C) – *A. dahurica* root extract; (D) – *A. archangelica* root extract;*p < 0.05 different from 0.0 µg/mL of extract in 8.3 mmol/L glucose (#) with one-way ANOVA followed by Holm–Sidak test, n = 3.

As expected, 8.3 mmol/L glucose significantly increased insulin secretion. None of the concentrations of *A. sinensis* root extract was able to modulate glucose-induced insulin secretion (Figure 34A). In contrast, a significant increase in glucose-induced insulin secretion was observed for 50.0 µg/mL of *A. biserrata* extract (secreted insulin of 92.74 ± 4.915 vs. 60.47 ± 6.162 ng/mL) (Figure 34B), for 25.0 and 50.0 µg/mL of *A. dahurica* extract (79.14 ± 4.480 and 91.16 ± 8.384 vs. 52.16 ± 3.017 ng/mL respectively) (Figure 34C), and for 12.5, 25.0 and 50.0 µg/mL of *A. archangelica* extract (71.81 ± 2.992, 86.60 ± 8.126 and 94.80 ± 7.657 vs. 51.68 ± 1.781 ng/mL respectively) (Figure 34D). The insulinotropic effect was observed to follow a dose dependency. As only extracts containing coumarins (as described in chapter 6.1.2) were able to modulate insulin secretion, it was decided henceforth to study the effects of pure coumarins present in studied species.

6.2.3.2 Screening of coumarins on insulin secretion

Twenty-three coumarins isolated from the roots of *A. archangelica*, *A. dahurica* and *A. biserrata* were screened for their insulinotropic effect at 20 µmol/L in 8.3 mmol/L glucose-stimulating condition. Out of the 23 tested compounds, 6 were able to significantly increase insulin secretion (Figure 35).

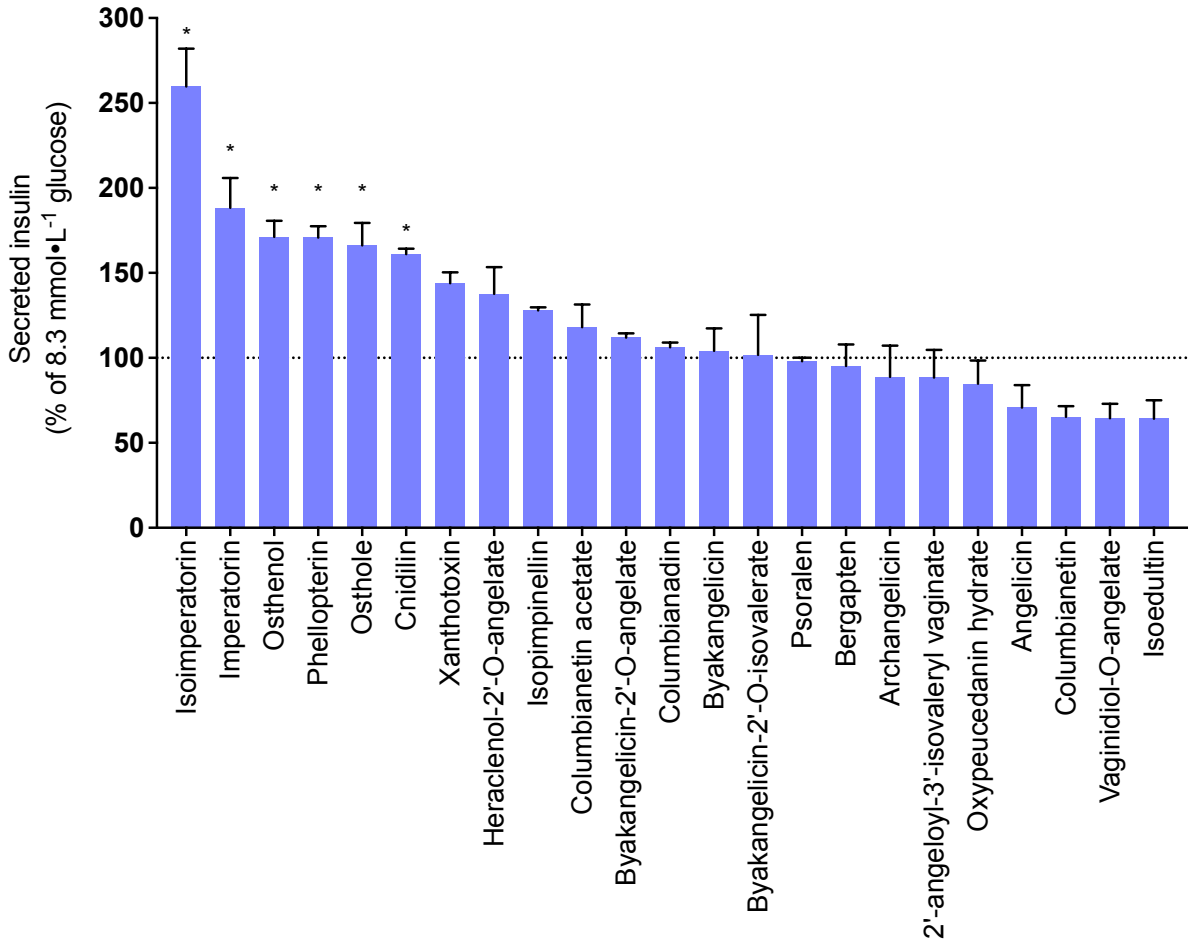

Figure 35. Effects of coumarins (20 µmol/L) on insulin secretion in glucose stimulating condition (8.3 mmol/L glucose) in INS-1 cells.

The bar graph depicts the mean ± SEM of insulin secretion as a percentage of 8.3 mmol/L glucose-induced insulin secretion after 1h incubation of INS-1 cells with 20 µmol/L coumarins; *$p < 0.05$ different from 0 µmol/L of coumarins with one-way ANOVA followed by Holm–Sidak test, n = 3.

The compounds able to amplify glucose-induced insulin secretion were isoimperatorin (259.7 ± 22.29 %), imperatorin (188.3 ± 17.64 %), osthenol (171.3 ± 9.371 %), phellopterin (170.8 ± 6.718), osthole (166.2 ± 13.27 %) and cnidilin (161.1 ± 3.237 %).

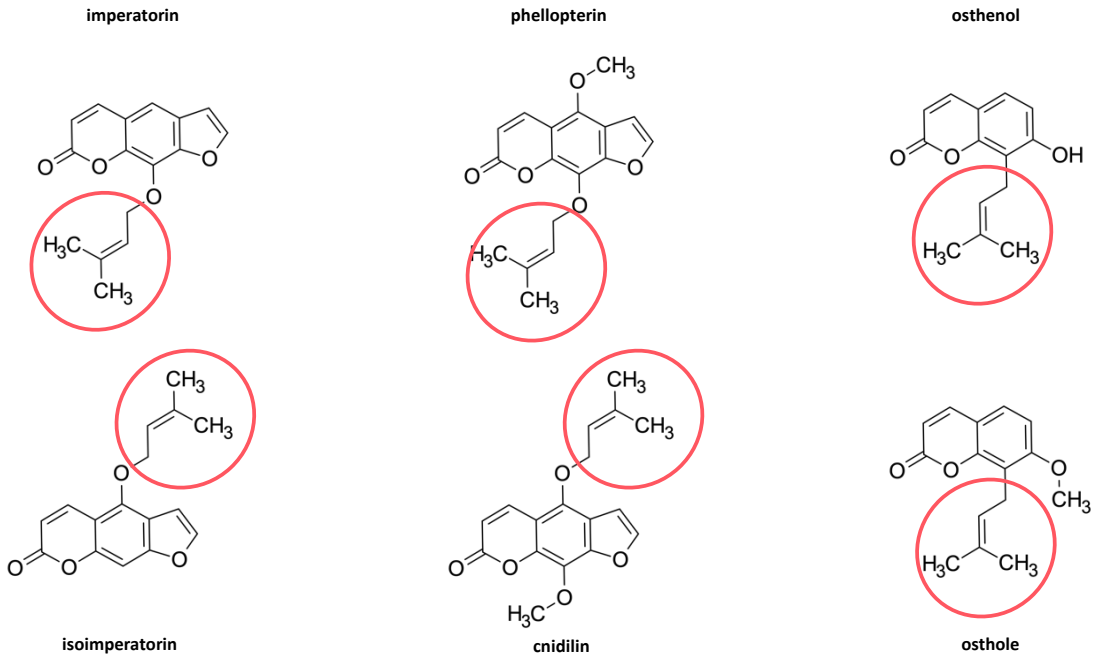

Figure 36. Structures of active coumarins with isoprenyl sidechain marked.

Based on these results, assumptions were made on structure activity relationship. It seems that insulinotropic activity is determined by an isoprenyl sidechain attached to the coumarin (Figure 36), while the nature of the heterocyclic coumarin ring may vary (both simple and furanocoumarins). Neither the position of substitution (both C5 and C8) nor its character (*C*-prenylation and *O*-prenylation) seem to be important for this activity. However, any substitution or prolongation of the isoprenyl sidechain leads to loss of function (Figure 37).

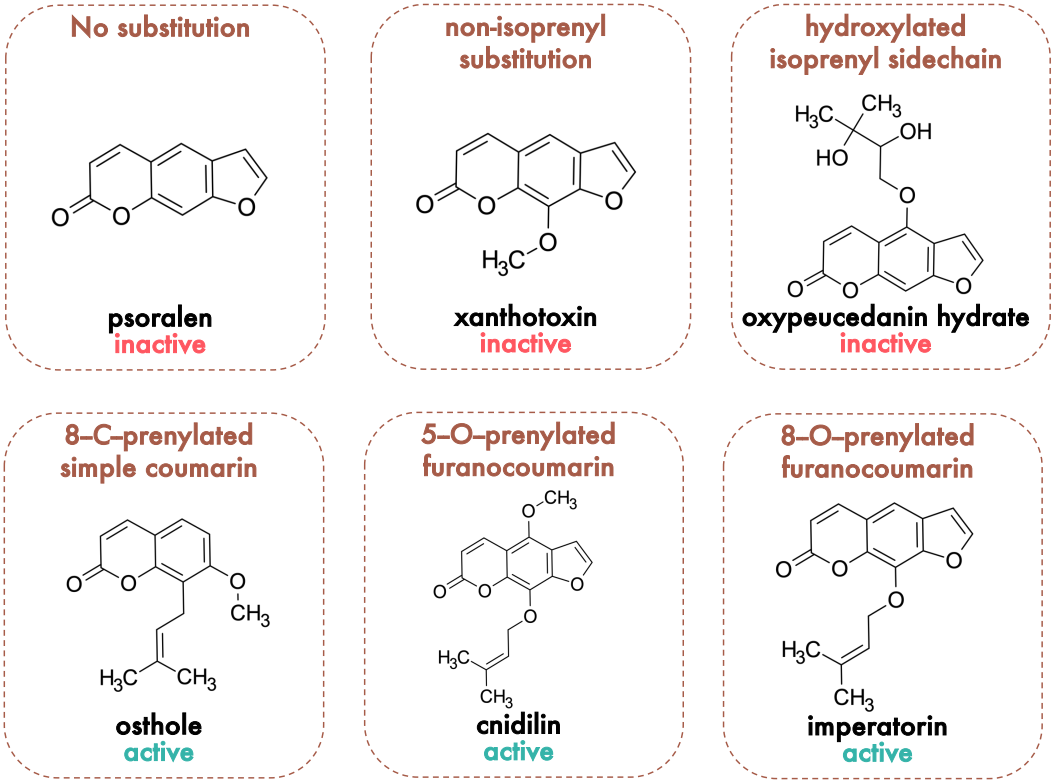

Figure 37. Structures of active coumarins compared to inactive structures.

It was decided that two most active compounds, namely isoimperatorin and imperatorin, would be further evaluated, together with an inactive compound most closely resembling their structure, i.e., psoralen, to use as a negative control. These compounds were tested in rising concentrations (from 5 to 40 µmol/L) in both basal (1.4 mmol/L) and glucose-stimulating (8.3 mmol/L) conditions. As expected, compared to 1.4 mmol/L glucose, 8.3 mmol/L glucose induced a significant insulin secretion (24.2 ± 1.2 ng/mL and 50.7 ± 1.4 ng/mL respectively).

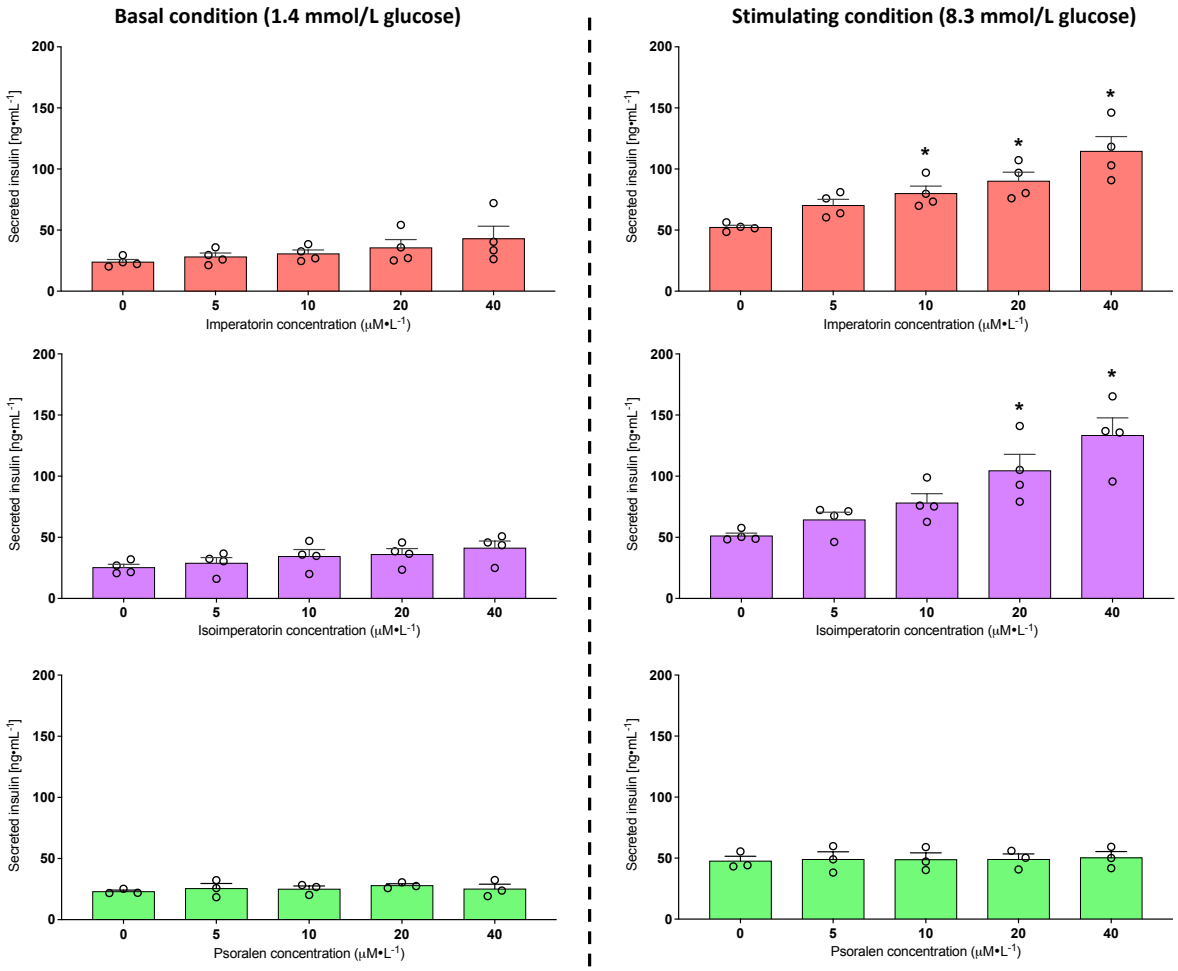

Figure 38. Effects of imperatorin, isoimperatorin and psoralen on basal (left) and glucose-induced (right) insulin secretion.

The bar graphs depict the mean ± SEM of basal (left) and glucose-induced (right) insulin secretionin ng/mL; *p < 0.05 different from 0 µmol/L of coumarins with one-way ANOVA followed by Holm–Sidak test, n = 4 (for psoralen n = 3).

In basal glucose condition none of the 3 compounds at any concentration was able to significantly increase insulin secretion (Figure 38 left). In glucose-stimulating condition imperatorin significantly increased glucose-induced insulin secretion in a concentration-dependent manner (80.00 ± 6.028, 90.11 ± 7.275 and 114.6 ± 11.94 vs. 52.28 ± 1.611 ng/mL for 10, 20 and 40 µmol/L respectively), as well as isoimperatorin (104.6 ± 13.28 and 133.4 ± 14.33 vs. 51.28 ± 2.185 ng/mL for 20 and 40 µmol/L respectively). Psoralen was inactive regardless of concentrations (Figure 38 right).

In T2DM, chronic hyperglycemia, inflammation and oxidative stress lead to β-cell dysfunction, increase apoptosis, and down-regulate insulin gene expression. To study potential of coumarins to exert their insulinotropic effect on cells more closely reassembling those in diabetic state, a

dysfunction was induced through incubation in glucotoxic (30 mmol/L glucose, 48 h) condition. As expected, in glucotoxic conditions, we observed a strong decrease in 8.3 mmol/L glucose-induced insulin secretion (44.53 ± 2.491 % of insulin secretion in non-glucotoxic condition).

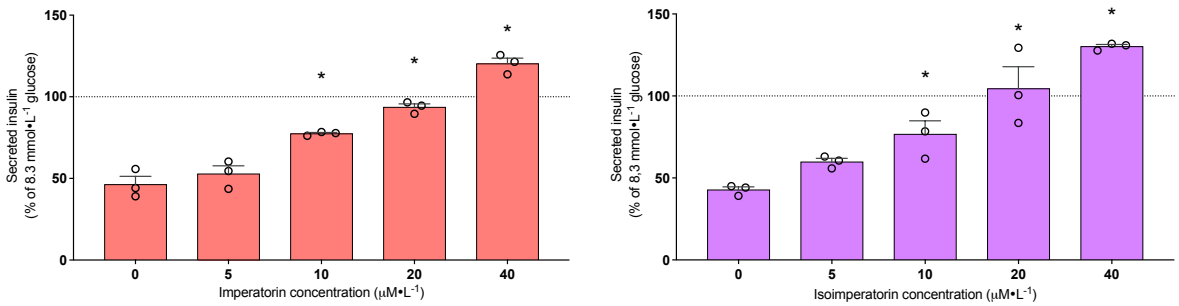

Figure 39. Effects of imperatorin and isoimperatorin on glucose-induced (8.3 mmol/L) insulin secretion in dysfunctional INS-1 cells.

The bar graphs depict the mean ± SEM of insulin secretion as a percentage of 8.3 mmol/L glucose-induced insulin secretion after 1h incubation of INS-1 cells with various concentrations of coumarins; *p < 0.05 different from 0 μmol/L of coumarins with one-way ANOVA followed by Holm–Sidak test, n = 3

In the dysfunctional INS-1 cells imperatorin and isoimperatorin were able to significantly increase insulin secretion in glucose-stimulating condition (Figure 39). In glucose-stimulating condition 10, 20 and 40 μmol/L imperatorin significantly increased insulin secretion in a concentration dependent manner (77.46 ± 0.6843, 93.61 ± 2.089 and 120.3 ± 3.449 % respectively), as well as 10, 20 and 40 μmol/L isoimperatorin (76.70 ± 8.179, 104.5 ± 13.38 and 130.2 ± 1.234 % respectively). As before, psoralen did not modulate glucose-induced insulin secretion in dysfunctional INS-1 cells (data not shown).

6.2.3.3 Evaluation of coumarins toxicity in β-cells

To exclude any potential cytotoxic effect of studied coumarins on used cell model, i.e., INS-1, cell viability after 48 h of incubation with various concentrations of tested compounds was assessed using MTT assay (Figure 40).

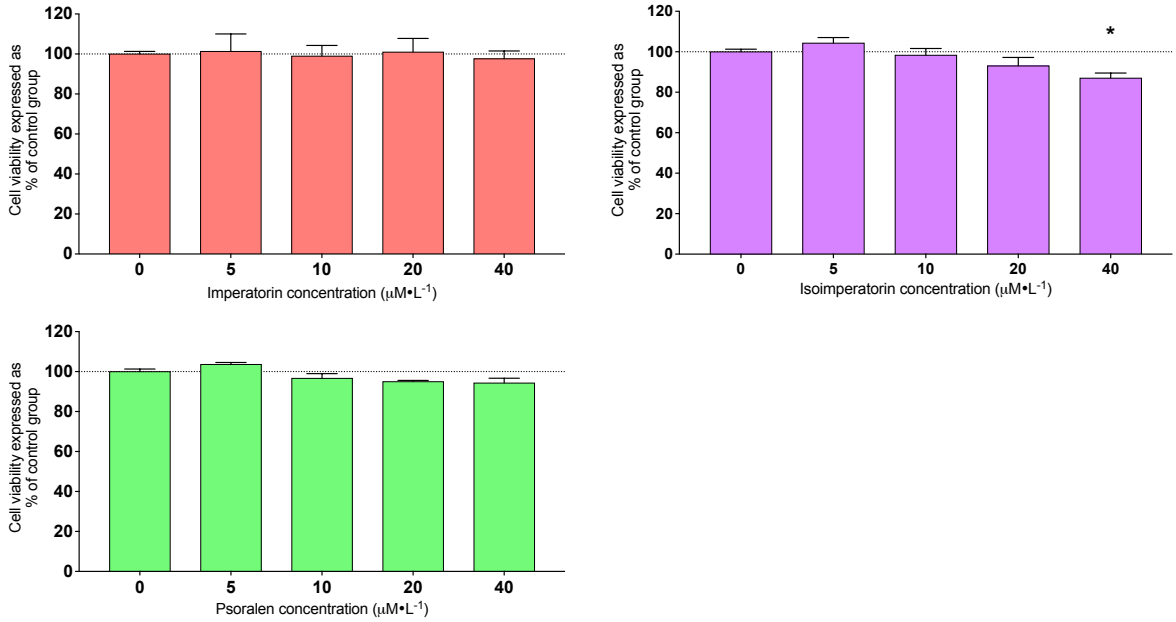

Figure 40. Effects of coumarins on cell viability.

The bar graphs depict the mean ± SEM of cell viability in % of intraassay control; *p < 0.05 different from 0 μmol/L of coumarins with one-way ANOVA followed by Holm–Sidak test, n = 3.

As shown in Figure 40, only the highest concentration of isoimperatorin, i.e., 40 μmol/L was found to be slightly cytotoxic (87.00 ± 2.517 %). Other studied compounds did not induce cytotoxicity at studied concentrations (5-40 μmol/L). Nevertheless, it was decided not to exclude 40 μmol/L of isoimperatorin from further experiments.

6.2.3.4 Protective effects of coumarins on the β-cell

Another approach was implemented to evaluate if coumarins can protect the β-cell from dysfunction induced by incubation in oxidative stress (50 μmol/L hydrogen peroxide, 1 h) (Figure 41) or glucotoxic (30 mmol/L glucose, 48 h) (Figure 42) conditions.

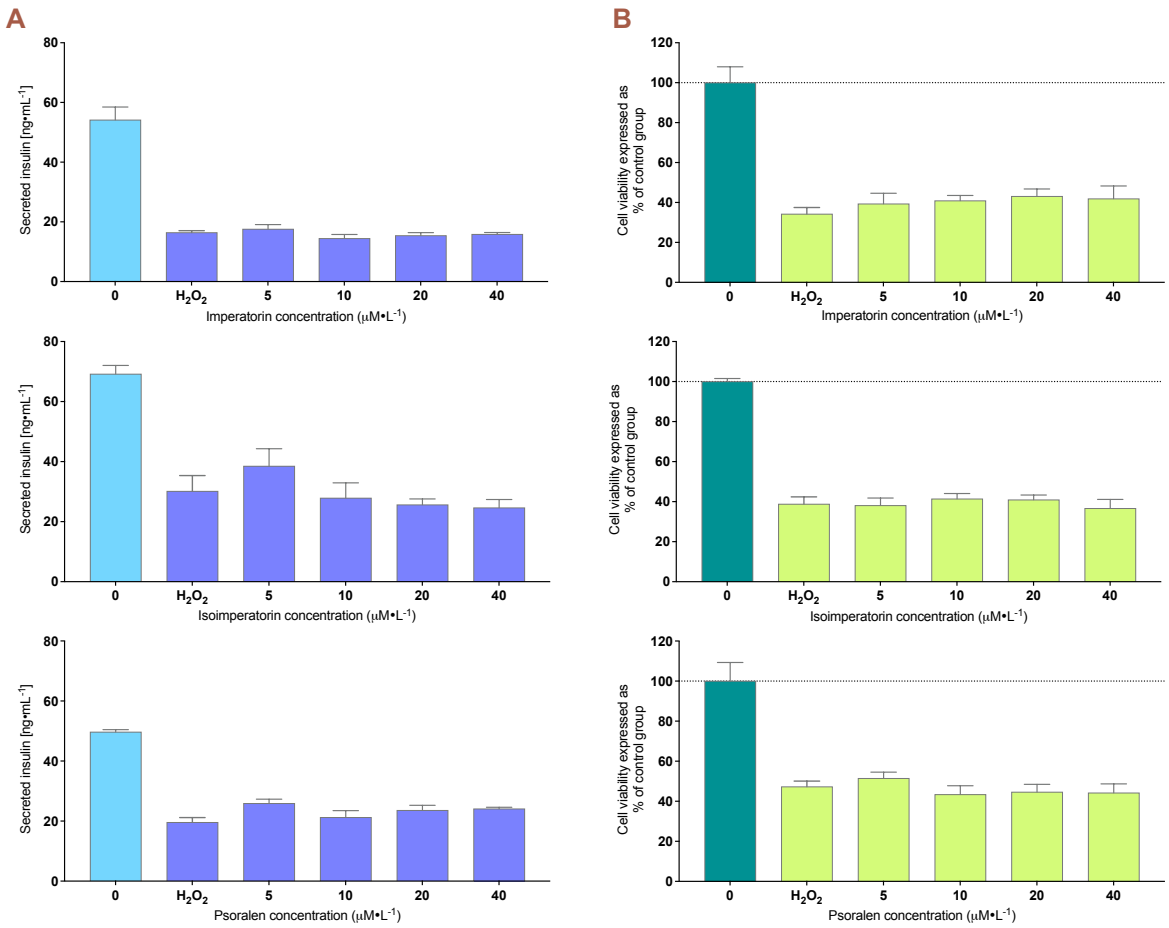

Figure 41. Effect of imperatorin, isoimperatorin or psoralen on H_2O_2- induced dysfunction on insulin secretion (A) and cell viability alteration (B).

The bar graphs depict the mean ± SEM of insulin secretion in ng/mL (A) and mean ± SEM of cell viability in % of intraassay control (B); *p < 0.05 different from 0 µmol/L of coumarins + 50 µmol/L H_2O_2 with one-way ANOVA followed by Holm–Sidak test, n = 3 (A), n = 4 (B).

As expected, in H_2O_2 conditions, we observed a strong decrease in 8.3 mmol/L glucose-induced insulin secretion (57.67 ± 3.319 vs. 22.06 ± 2.606 ng/mL in the absence and presence of H_2O_2, respectively) (Figure 41A). In the same way, H_2O_2 induced a strong decrease in cell viability (40.13 ± 2.335 % of insulin secretion in the absence of H_2O_2) (Figure 41B).

Two-hour preincubation with imperatorin, isoimperatorin, or psoralen did not protect the cell from oxidative stress-induced dysfunction and cell death, whatever the concentration.

A 48 h incubation with 30 mmol/L glucose lead to a significant decrease in insulin secretion by about half (Figure 42). Again, 48 h simultaneous preincubation with one of the coumarins and 30 mmol/L glucose did not protect the cell from glucotoxicity induced dysfunction.

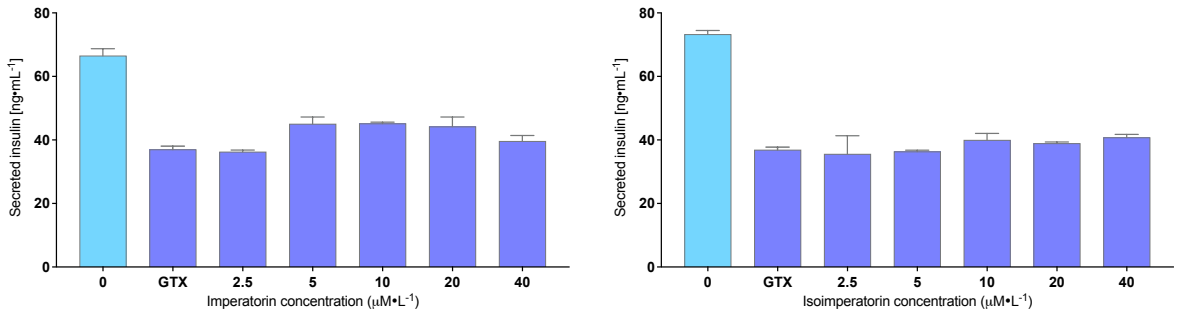

Figure 42. Coumarins protective effect on the β-cell insulin secretion against glucotoxicity.

The bar graphs depict the mean ± SEM of insulin secretion in ng/mL; *p < 0.05 different from 0 μmol/L of coumarins + 30 mmol/L glucose with one-way ANOVA followed by Holm–Sidak test, n = 3.

6.2.3.5 Mechanisms of action of coumarins on insulin secretion in β-cells

Various approaches were implemented to elucidate mechanism of action of active coumarins, i.e., imperatorin and isoimperatorin. As calcium in the β-cell plays a pivotal role in insulin secretion, I found it necessary to study effect of these compounds on the changes in intracellular Ca_{2+} ($[Ca_{2+}]_i$) in pancreatic β-cell. Moreover, as cell membrane depolarization also plays an important role in β-cell function, we assessed the impact of imperatorin on membrane potential. The change in intracellular calcium levels was evaluated using the ratiometric fluorescent Ca^{2+} indicator Fura-2AM and the membrane potential was studied in real-time fluorescence by confocal microscopy with a fluorescent probe FLIPR. It was found that 20 μmol/L imperatorin was able to increase the membrane potential and intracellular calcium in comparison with vehicle (Figure 43). Both effects were correlated in term of kinetic. It was decided to study the effects of coumarins on intracellular calcium in greater detail.

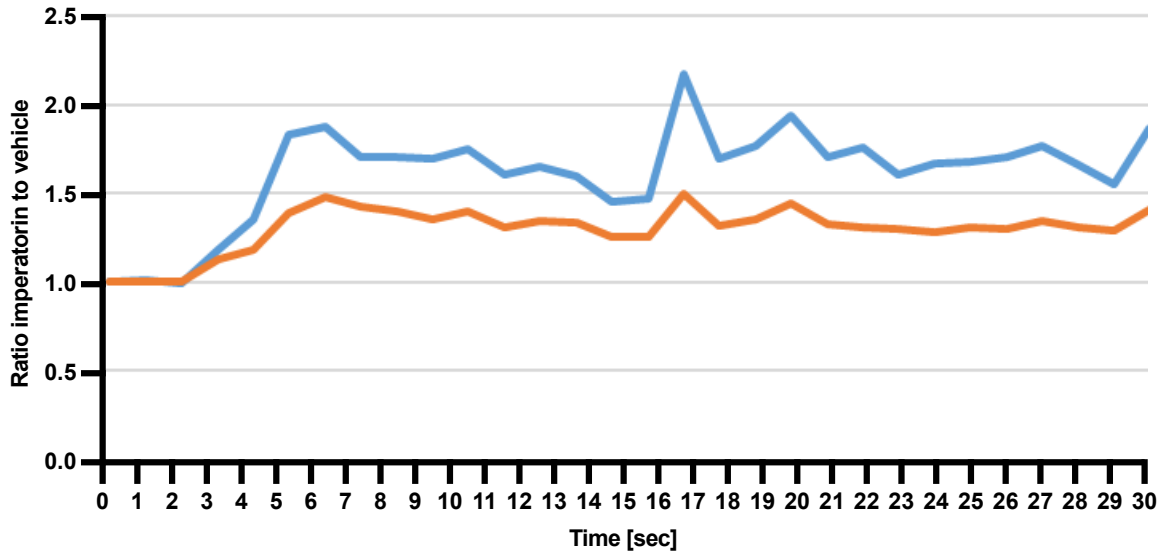

Figure 43. Exploratory study of Imperatorin effect on membrane potential (orange) and intracellular calcium (blue).

The curves depict the ratio of 20 µmol/L imperatorin to vehicle.

Then, I investigated whether imperatorin, isoimperatorin or psoralen induced a change in intracellular calcium levels using the ratiometric fluorescent Ca^{2+} indicator Fura-2AM. First, variations of fluorescence ratio (F340/F380) in response to 20 µmol/L imperatorin, isoimperatorin, psoralen and 30 mmol/L KCl (positive control) in basal condition (1.4 mmol/L glucose) were recorded in INS-1 cells, and are shown on Figure 44.

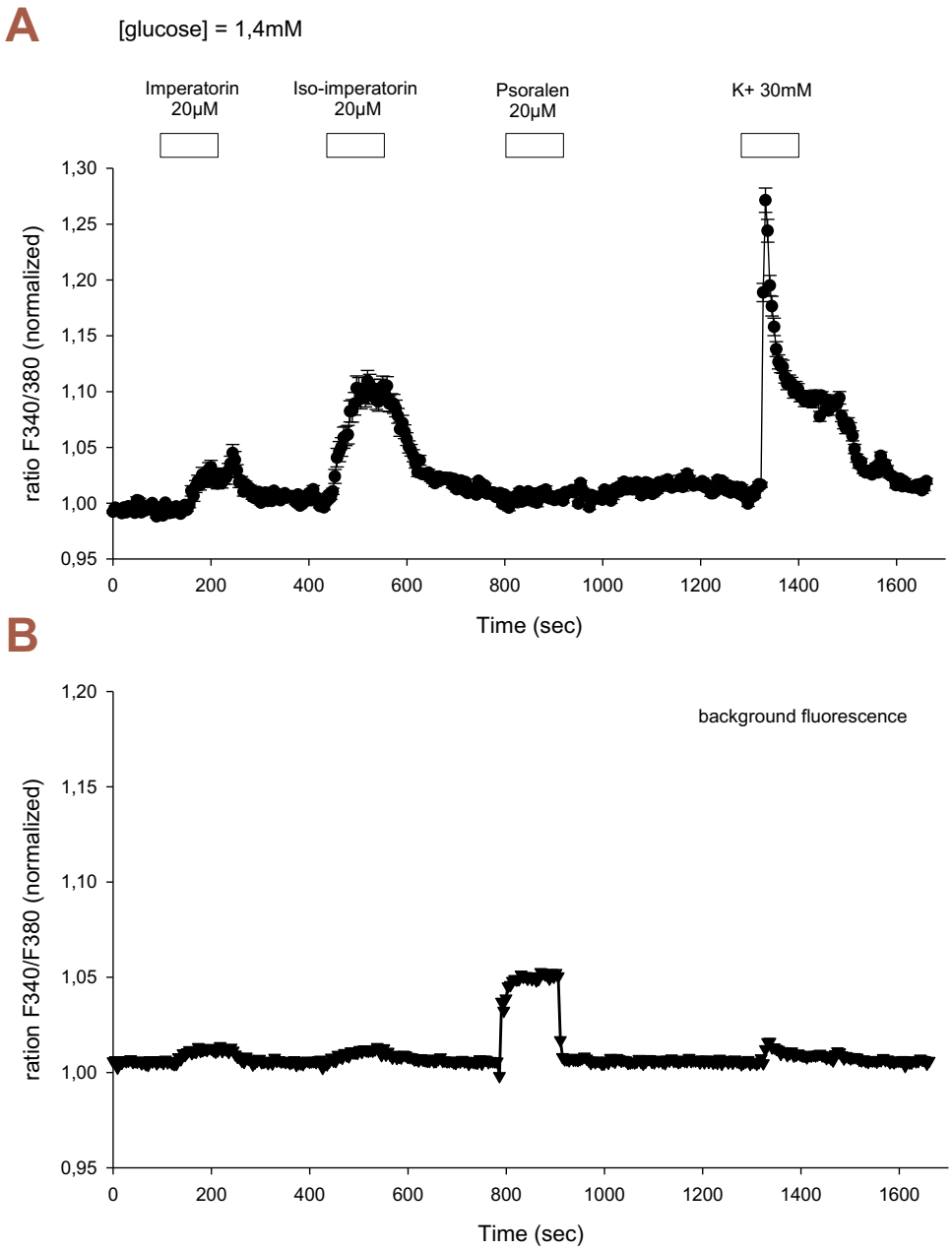

Figure 44. Effects of imperatorin, isoimperatorin and psoralen on intracellular calcium level and background fluorescence.

(A) Plotted data depict the mean ± SEM of normalized fluorescent ratio under different conditions (B) The graph represents the mean ± SEM of background fluorescence. 30 mmol/L KCl as positive control.

As expected, the depolarizing agent KCl (30 mmol/L) induced an immediate and strong $[Ca^{2+}]_i$ rise, as illustrated by the increase in F340/F380 Fura-2AM fluorescence ratio. Imperatorin and isoimperatorin (20 µmol/L) were able to induce a rapid and highly reproductible increase in $[Ca^{2+}]_i$, while psoralen displayed no effect (Figure 44A). To exclude effect of coumarins possible autofluorescence, background fluorescence was assessed. Only psoralen showed a small

autofluorescence capability (at studied wavelengths), but the magnitude of this effect did not affect the results (Figure 44B).

Next, imperatorin and isoimperatorin were tested for their effect on $[Ca^{2+}]_i$ in rising concentrations (from 1 to 30 µmol/L) in basal condition (1.4 mmol/L glucose).

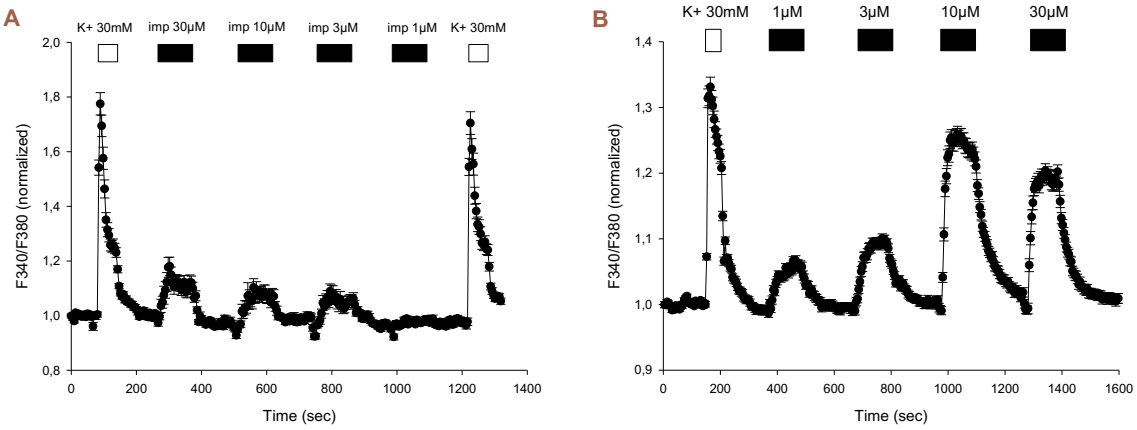

Figure 45. Concentration effects of imperatorin and isoimperatorin on intracellular calcium level.

Plotted data depict the mean ± SEM of normalized fluorescent ratio under various concentrations of imperatorin (A) and isoimperatorin (B) in basal condition (1.4 mmol/L glucose). Plotted data depict the mean ± SEM of normalized fluorescent ratio. 30 mmol/L KCl as positive control; n = 3 for isoimperatorin, n = 2 for imperatorin.

Isoimperatorin followed a concentration-dependency, with the effect already visible at 1 µmol/L and obtaining maximal effect at 10 µmol/L (Figure 45B). Imperatorin showed a similar profile (Figure 45A). The concentration-effect of isoimperatorin was also studied on intracellular calcium level in 8.3 mmol/L glucose condition (Figure 46). Isoimperatorin at 10 and 30 µmol/L seems to be more effective in the presence of a stimulating concentration of glucose. Nevertheless, the half maximal effective concentration (EC_{50}) calculated under these two experimental conditions appeared to be identical (3 µmol/L).

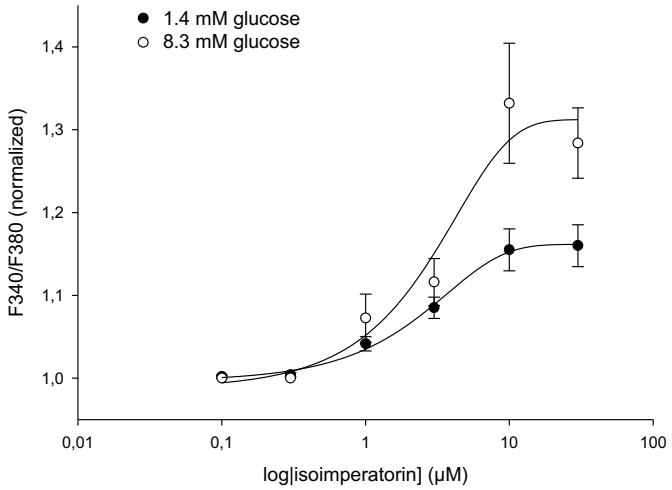

Figure 46. Concentration-effects curves for isoimperatorin on intracellular calcium level in basal and stimulated conditions.

Plotted data depict concentration-response curves of normalized fluorescent ratio in response to isoimperatorin. Values represent the means ± SEM from 3 experiments. Next, the mechanism involved in the increase of $[Ca^{2+}]_i$ was analyzed. As depolarization dependent Ca^{2+} influx through voltage-gated calcium channels (VGCC) is essential for insulin secretion, I evaluated if imperatorin-mediated rise of $[Ca^{2+}]_i$ comes from activation of VGCC. The electrophysiological properties of whole-cell Ca^{2+} currents in INS-1-cells were studied with the patch-clamp method using Ba^{2+} as the charge carrier. Ba^{2+} was used as the charge carrier so that the T-type Ca^{2+} channel currents could be identified and separated from the L-type Ca^{2+} channel currents, as the inactivation kinetics of the latter are much slower than that of the former under these conditions (Figure 47).

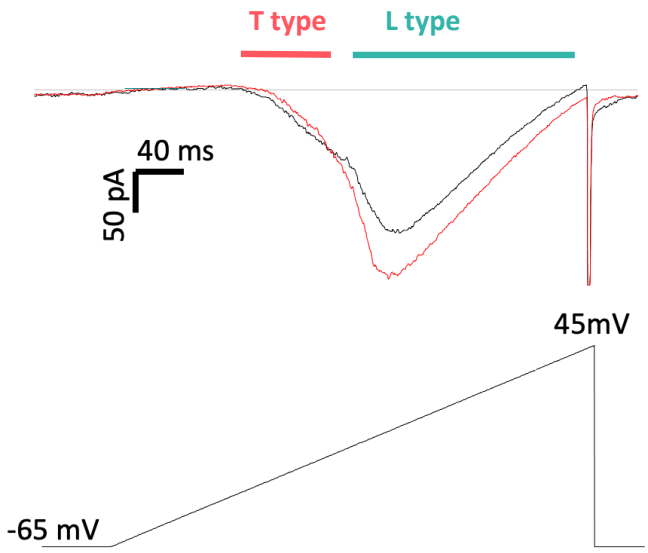

Figure 47. Effects of imperatorin on L-type and T-type Ca^{2+} channel currents in the INS-1 cells.

Typical traces of L- and T-type Ca^{2+} current stimulated by a ramp depolarization in the absence (black trace) or presence (red trace) of 20 µmol/L imperatorin. Current was stimulated by a ramp depolarization from -65 mV to 45 mV before or 1 minute after the addition of 20 µmol/L imperatorin.

It was observed that 20 µmol/L imperatorin increased inward currents at potentials for which L-type current is predominant while a small inhibitory effect could be seen at potentials for which T-type current is predominant (Figure 48). This was subsequently evaluated in one step experiments, which have confirmed above findings (Figure 48). The L-type calcium current was stimulated by a step depolarization from -65 mV to 0 mV before or 1 minute after the addition of 20 µmol/L imperatorin, and the T-type current was stimulated by a step depolarization from -65 mV to -35 mV. Imperatorin enhanced L-type current at test potential of 0 mV (Figure 49 A) whereas it inhibited the T-type current measured at -35 mV (Figure 49 B). Electrophysiological data for isoimperatorin followed the same pattern (data not shown).

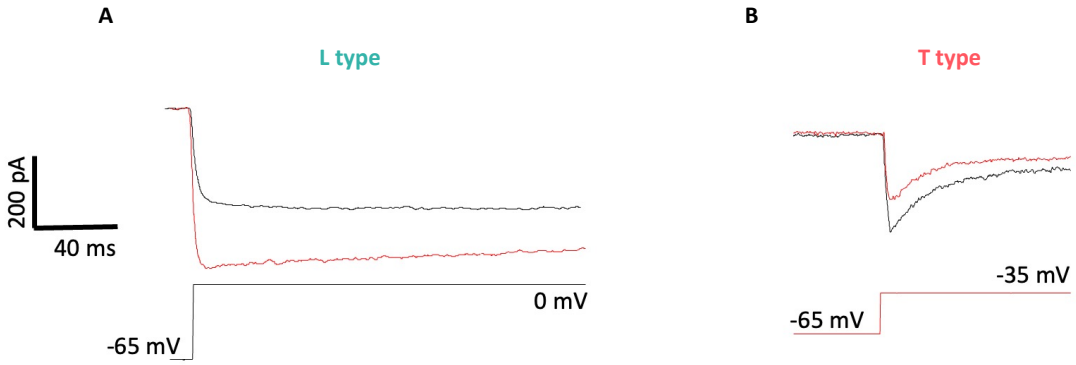

Figure 48. Effects of imperatorin on L- and T-type Ca^{2+} channel currents in INS-1 cells.

Typical traces of the L-type (A) and T-type (B) calcium currents in a step depolarization experiments in the absence (black trace) or presence (red trace) of 20 µmol/L imperatorin.

I then hypothesized that the insulin-secreting activity of coumarins relied, at least in part, on its capacity to enhance L-type Ca^{2+} currents. This possibility was tested by determining the effect of coumarins on glucose-induced insulin secretion in the presence of the Ca^{2+} channels inhibitor verapamil at 20 µmol/L, a concentration described to ensure efficient inhibition of L-type Ca^{2+} currents in accordance with their IC_{50} (Figure 49).

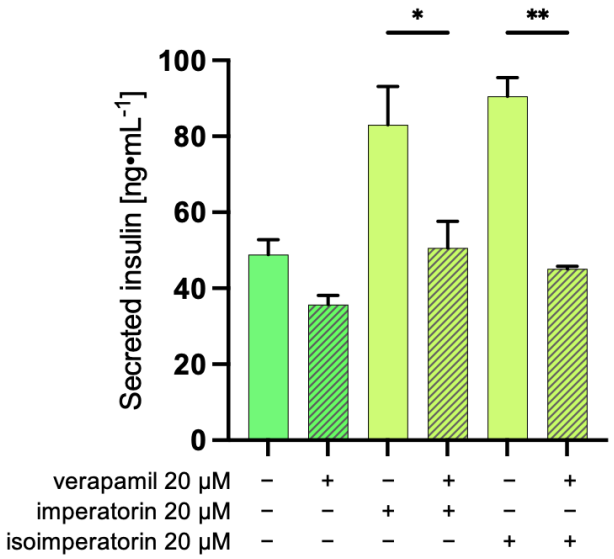

Figure 49. Coumarins effect on glucose-induced insulin secretion in the presence of VGCC blocker (verapamil).

The bar graph depicts the mean ± SEM of insulin secretion in ng/mL induced by 8.3 mmol/L glucose in the absence or presence of 20 µmol/L imperatorin, isoimperatorin and verapamil; *$p < 0.05$, **$p < 0.01$ with one-way ANOVA followed by Holm–Sidak test, n = 3.

As expected, and shown in Figure 49, imperatorin and isoimperatorin at 20 µmol/L enhanced 8.3 mM glucose-induced insulin secretion, but this effect was not observed in the simultaneous presence of 20 µmol/L verapamil.

A similar approach was used to assess the involvement of VGCCs in coumarins-induced elevation of intracellular calcium. It was observed that the effect of 10 µmol/L isoimperatorin was much weaker when INS-1 cells were co-incubated with 20 µmol/L verapamil. After washing the cells and reintroducing 10 µmol/L isoimperatorin, the elevation of $[Ca^{2+}]_i$ was equivalent to the one before co-incubation with verapamil, suggesting that inhibitory effect was reversed and cells function was maintained (Figure 50). A similar profile was observed for 10 µmol/L imperatorin (data not shown).

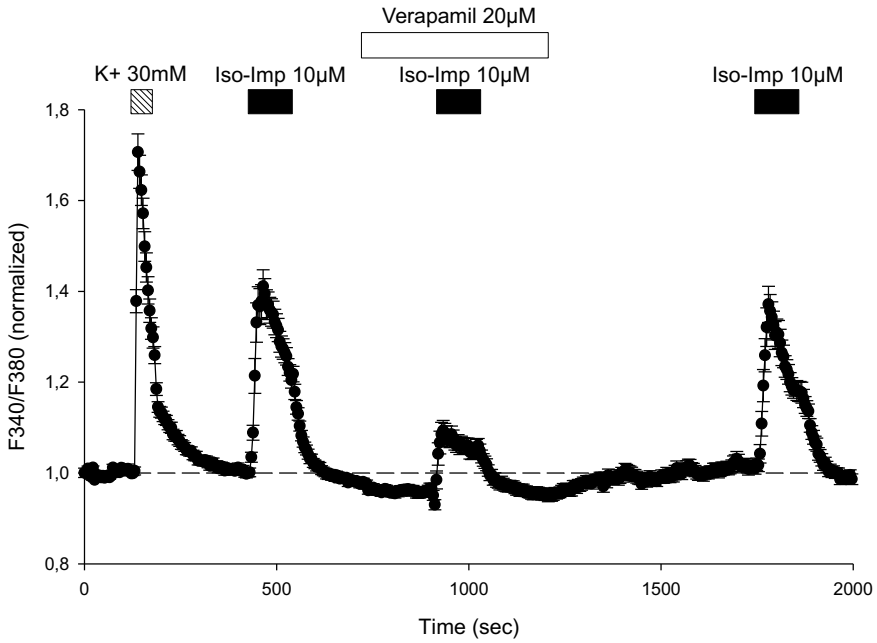

Figure 50. Isoimperatorin effect on intracellular calcium levels in the presence of VGCC blocker (verapamil).

Typical trace of isoimperatorin and verapamil effect on intracellular calcium levels depicted as the mean ± SEM of normalized fluorescent ratio in 8.3 mmol/L glucose condition. 30 mmol/L KCl as positive control.

As voltage-gated potassium channels were also suspected of playing a role in coumarins effect on insulin secretion, I evaluated isoimperatorin and imperatorin effect on $[Ca^{2+}]_i$ in the presence of tetraethylammonium (TEA), a VGKC blocker.

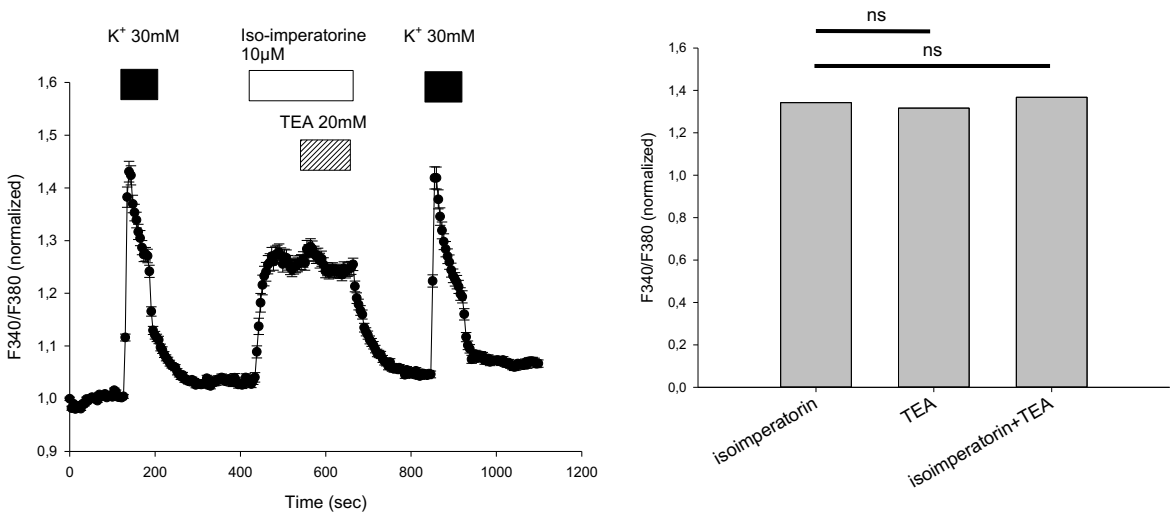

Figure 51. Isoimperatorin effect on intracellular calcium levels in the presence of VGKC blocker (TEA).

Plotted data depict the mean ± SEM of normalized fluorescent ratio under 10 µmol/L isoimperatorin in the absence or presence of 20 mmol/L TEA (A). Bar graph represents the maximal variation in the fluorescence ratio induced by isoimperatorin, TEA and isoimperatorin in the presence of TEA (B). Results are presented as mean ± SEM of 4 separate experiments; ns with Kuskal-Wallis followed by Dunn test.

As shown on Figure 51, tetraethylammonium has no additive effect on isoimperatorin-induced increase in $[Ca^{2+}]_i$. A similar profile in a single experiment was seen for imperatorin (data not shown).

Next, the effect of imperatorin on potassium current of the INS-1 cells was recorded using whole-cell patch clamp technique.

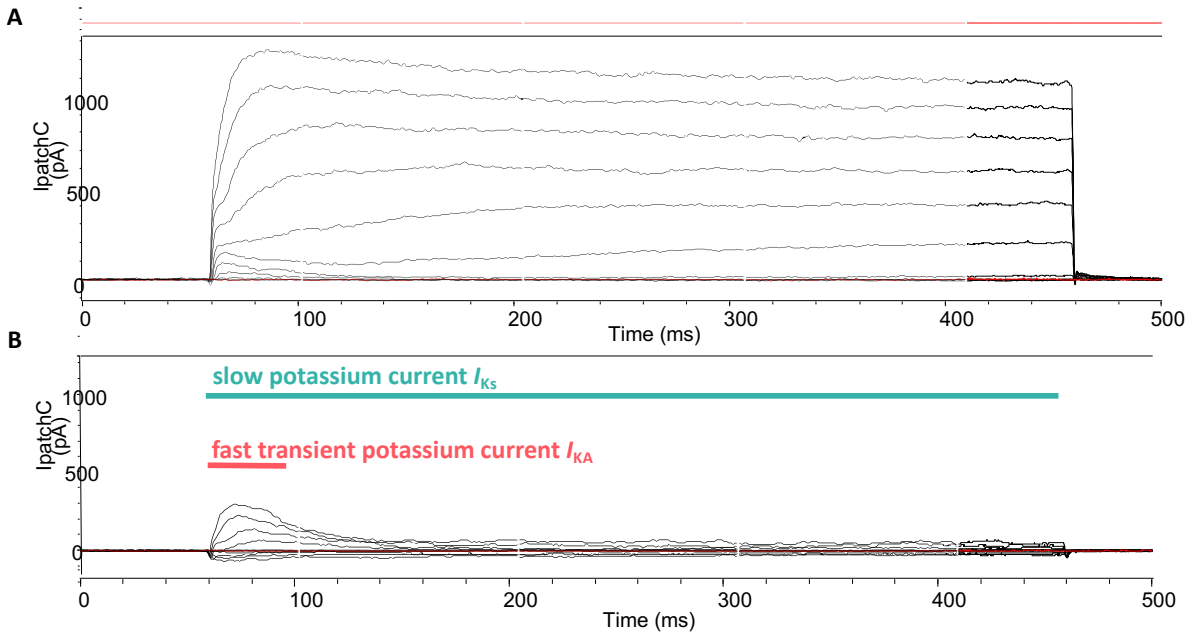

Figure 52. Imperatorin effect on slow and transient potassium current in INS-1 cells.

Typical traces of potassium current registered in the absence (A) or presence (B) of 20 µmol/L imperatorin. Voltage-gated potassium currents were elicited by depolarizing steps from −65 to +45 mV in 10 mV increments.

As shown in Figure 52, depolarization (up to 45 mV from a holding potential of -65 mV) stimulated outward voltage-gated potassium currents, which rapidly rose to a peak, followed by slow and partial inactivation. Extracellular application of 20 µmol/L imperatorin inhibited this current. This inhibition was reached within 1 minute and totally washed out. Imperatorin drastically hastened the inactivation kinetics of the potassium current and switched it into a fast transient potassium current. Inhibition of outward potassium channel unmasked in some cells an inward current due to voltage gated-calcium channels. Electrophysiological data for isoimperatorin followed the same pattern (data not shown). As potassium current is responsible for repolarization and hyperpolarization of the cell membrane, its inhibition might lead to longer action potentials and much easier depolarization and thus increase insulin secretion.

7 Discussion

Despite the advancements made in the field of anti-diabetic medications, their usage is accompanied by various undesirable side effects, including hypoglycemia, gastrointestinal issues, heart failure, weight gain, edema, impaired kidney function, pancreatitis, and genital infections. Moreover, the prevalence of diabetes is higher in low- and middle-income countries, posing an additional challenge due to limited access to modern therapies or their unaffordability for a significant portion of diabetic patients. Within this context, the exploration of plant extracts and their active components emerges as an important area for discovering new anti-diabetic treatments [91, 142]. Although hundreds of plants have been used in traditional and folk medicine to treat diabetes, the data on their efficacy is anecdotal or scarce at best [142]. Previous studies done at the Institut des Biomolécules Max Mousseron and single studies from other teams have led me to the formulation of the hypothesis that plant secondary metabolites, such as flavonoids, lignans, and coumarins, may modulate the β-cell function, possibly increasing insulin secretion, considering that this activity is based on interactions between small molecules and proteins rather than on their antioxidant potential; thus, it is highly structure-dependent.

Thus, I aimed at finding a natural source of secondary plant metabolites potentially able to protect β-cell function, induce insulin secretion in a glucose-dependent manner, and at elucidating their mechanism of action.

7.1 Flavonoids insulinotropic activity

The flavonoids were the first plant secondary metabolites group I studied on the INS-1 β-cell line. As they are widely commercially available, there was no need to isolate these plant metabolites, and instead, the library was acquired from chosen suppliers. In the previous studies at the Institut des Biomolécules Max Mousseron, multiple flavonoids have been tested for their capacity to enhance glucose-induced insulin secretion, such as quercetin, kaempferol, resokaempferol, apigenin, and chrysin [146, 147, 177, 380]. However, among this wide variety of closely related compounds, inhibitors of insulin secretion and inactive compounds were also found. The diverse pharmacological landscape of the flavonoids tested on β-cell function indicates that their activity is highly dependent on their molecular structure and is not merely a result of their antioxidative properties [381, 382]. Indeed, they rather behave as pharmacological agents and thus modulate cell processes through protein-mediated mechanisms following selective binding to targets. In their work, Saponara *et al.*

studied a variety of flavonoids to identify key structural requirements for L-type calcium current stimulatory activity. Their findings highlight the importance of the C2-C3 double bond and hydroxylation pattern in stimulatory and inhibitory activity (Figure 53) [382, 383].

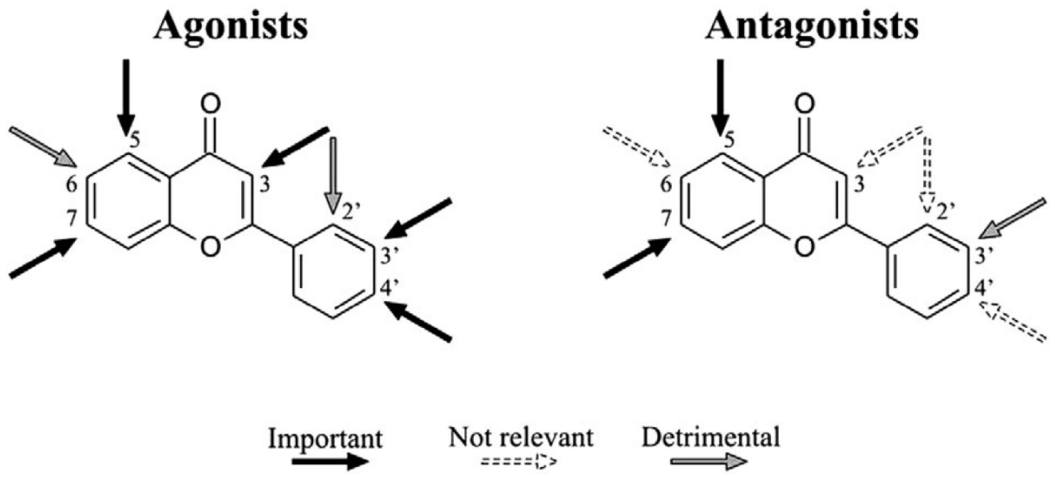

Figure 53. Outlines of the structure-activity relationship for the flavonoids investigated as $Ca_v1.2$ channel modulators [383].

As intracellular calcium has a key role in glucose-dependent insulin secretion, their finding could be partially translated into flavonoid activity towards the β-cell. However, this is not always the case, as some known $Ca_v1.2$ inhibitors were found to increase insulin secretion and vice versa. Here I tested 18 flavonoids from different subtypes, i.e., flavones, flavanones, flavonols, and flavanonols, in order to identify key structural aspects for modulation of glucose-induced insulin secretion in the β-cell (Figure 28).

In accordance with Saponara's findings on $Ca_v1.2$, the double bond between C2 and C3 was crucial to induce any (stimulatory or inhibitory activity). Incubation of INS-1 with derivatives of active compounds that had their C2-C3 double bond reduced resulted in loss of previous activity. In this context, flavanones and flavanonols are not good candidates to modulate β-cell function. Of the remaining nine compounds, four were stimulatory, one was inhibitory, and four did not induce any significant effect. All active flavonoids were hydroxylated at C5 and C7, though so were three out of the four inactive compounds. The effect was also not dependent on the overall number of hydroxyl groups, as the most hydroxylated compounds, i.e., myricetin (3,3',4',5,5',7-hexahydroxyflavone), and non-hydroxylated compound, i.e., flavone, were inactive.

Interestingly, myricetin and luteolin had stimulatory effect on $Ca_v1.2$ but none on β-cell insulin secretion, while chrysin had inhibitory effect on $Ca_v1.2$ but stimulatory on β-cell insulin secretion. These discrepancies between effect on the $Ca_v1.2$ modulation and β-cell function of studied flavonoids and lack of correlation between hydroxylation pattern and effect lead me to a conclusion that flavonoids may modulate β-cell function through different targets, not limited to $Ca_v1.2$. This is in line with the findings of Fusi *et al.*, who described flavonoids' interactions with different potassium channels (some of them also present in the β-cell) by molecular docking [384].

In this context, further mechanistic studies of active compounds are needed to elucidate possible mechanisms of action of flavonoids on β-cell insulin secretion, as it was done for quercetin [147].

7.2 Phytochemical characterization of lignan-rich extracts and isolation of lignans

Following the studies on flavonoids, I aimed at studying other secondary plant metabolites, belonging to much less described groups in the context of β-cell function modulation, i.e., lignans. These compounds were isolated here from natural sources. To this aim, sixteen plant extracts were phytochemically profiled using LC-MS/MS technique to acquire information on the presence of potentially active lignans for isolation and subsequent pharmacological examinations. *Pinus sylvestris*, *Pinus cembra*, *Pinus mugo*, *Pinus strobus*, *Pinus ×rhaetica*, *Abies alba*, *Picea abies*, *Picea glauca*, *Pseudotsuga menziesii*, *Tsuga canadensis*, *Larix decidua*, *Larix polonica*, and *Larix kaempferi* branch wood, *Arctium lappa* and *Carthamus tinctorius* fruit, and *Eleutherococcus senticosus* root methanolic extracts were studied for lignans presence.

Conifer wood and waste materials from its processing in the paper and wood industry (such as knots, bark, and branches) have been identified as a good source of many polyphenols. Willfor and his team characterized wood knots of spruces, pines, and firs, isolating many lignans in the process [321, 327, 385, 386]. More recently, Gabaston *et al.* not only characterized wood knots of *Pinus pinaster* Aiton using LC-MS/MS but also studied their antifungal activity against grapevines pathogen [344]. To the best of my knowledge, most of the wood studied here was never characterized before using LC-MS/MS techniques. This study was also the first attempt at phytochemical profiling of wood from *P. ×rhaetica* and *L. polonica*, as well as the first to compare the composition of *Pinaceae* species growing in Poland.

Referring to previous research, my study confirms that conifers from the *Pinaceae* family are rich in otherwise scarce compounds, such as lignans and stilbenes, offering a large variety of these structures (Table 5).

In this context, studied wood from the *Pinaceae* family offers a much easier-to-extract source of these polyphenols, with much fewer steps required to obtain pure compounds (directly in aglycone form with a much larger structure variety). Wood from all studied species contained detectable amounts of lignans, with silver fir being the richest source of these polyphenols. Although *A. alba* offered large quantities of lignans, especially secoisolariciresinol and lariciresinol, *P. sylvestris* was far richer than all other species in nortrachelogenin, pinoresinol, and matairesinol. This is particularly interesting as Scots pine is the most abundant and economically important tree in Europe. Another important notion from my study is the detection of a lignan (namely matairesinol) in *P. cembra*, which was previously described as the only pine not containing lignans [228].

Through my analysis, I did not detect a few lignans that have been previously found in some of the studied species. Willfor *et al.* reported the presence of matairesinol and pinoresinol in *A. alba* wood knots [321], but I did not observe any signal at expected retention times. The same study established the presence of secoisolariciresinol monomethyl ether and dimethyl ether. I cannot rule out the presence of these compounds in my samples, as pseudomolecular ions $[M-H]^-$ with expected mass for these lignans were observed. Unfortunately, no fragmentation pattern for them could be found in the literature, nor could I isolate them from the plant material.

Although it was not the main objective of this study, my analysis also contributed to the phytochemical knowledge offering insight into the stilbene, flavonoid, flavan-3-ol, and diterpene composition of conifer wood. These compounds were present in all studied samples, with differences concerning structures and their exact content. Larches and Douglas fir could be considered the richest in flavonoids and flavan-3-ols, while spruces were found to be richest in stilbenes (Table 6).

Through this analysis two conifers were chosen for subsequent isolation, based on the LC-MS signal of lignans in their methanolic extracts, i.e., *A. alba* and *P. sylvestris*. From Scots pine I was able to isolate nortrachelogenin, pinoresinol and matairesinol, about 10 mg each, while from *A. alba* 7-hydroxymatairesinol, 7-hydroxylariciresinol (two stereoisomers), todolactol, lariciresinol, cyclolariciresinol, and secoisolariciresinol. They were isolated in the amounts ranging from 4.5 mg (7-

hydroxymatairesinol) up to 1238 mg (secoisolariciresinol). In no other studied source, I was able to isolate such amounts of lignans in aglycone form.

Other sources of lignans were also evaluated in this study, i.e., *Arctium lappa* fruits, *Carthamus tinctorius* fruits, and *Eleutherococcus senticosus* roots. Metabolite profiles of their methanolic plant extracts were provided with a rich library of identified metabolites and their UV and mass spectra with fragmentation patterns.

Fruits of *Arctium lappa* were found to be a rich source of arctigenin 4-*O*-glucoside, matairesinol 4-*O*-glucoside, and their aglycones arctigenin and, to a lesser extent, matairesinol, all of which were isolated (Table 7). From this plant material, I was able to isolate the largest amount of any lignan among all isolates, i.e., 8455 mg of arctigenin 4-*O*-glucoside. The plant material also offered a rich variety of sesquilignans and dilignans, known as lappaols and arctignans, and, in the water fraction, caffeoylquinic acids.

C. tinctorius fruits have not been previously phytochemically profiled using LC-MS/MS technique. So far, lignans such as arctigenin, matairesinol, trachelogenin, secoisolariciresinol, and their glucosides have been found in safflower fruits [256]. During the analysis of the raw material, I confirmed the presence of all the above-mentioned aglycones as well as matairesinol and trachelogenin glucosides (Table 8). Among the listed lignans, trachelogenin and its glucoside are relatively rare in plant metabolites. Their presence, apart from safflower, was confirmed in the stems of *Trachelospermum* Lem. [387], in the fruits of *Cirsium* Mill. [388] and *Cynara* L. [389]. From 500 grams of raw material, I obtained a total of 339 mg of trachelogenin 4-*O*-glucoside. Although the plant material also contained the aglycone (trachelogenin), its LC-MS signal suggested amounts too small for isolation. Instead, I opted for another approach, that is the enzymatic hydrolysis of isolated glucoside, using β-glucosidase and cellulase, reaching a 77% yield of pure trachelogenin.

As it turned out, *E. senticosus* roots did not contain significant amounts of lignans (Table 9). Quantification of the most abundant lignan in this plant material, i.e., syringaresinol 4,4'-di-*O*-glucoside (eleutheroside E), carried out in the Department of Pharmaceutical Biology showed results ranging from 0.013 – 0.064 % for different sources [390]. In my study its isolation proved even more challenging, with roughly 4 mg of eleutheroside E isolated from 500 g of plant material.

The analysis of *E. senticosus* root also contributed to the better understanding of its metabolite profile. To the best of my knowledge this is the most comprehensive study to date concerning the qualitative composition of hydroxycinnamic acids in *E. senticosus* root, as most of them were not previously described in this plant material (Table 10). Moreover, the root seems to be particularly rich in these phytochemicals, to a much bigger extent than in lignans.

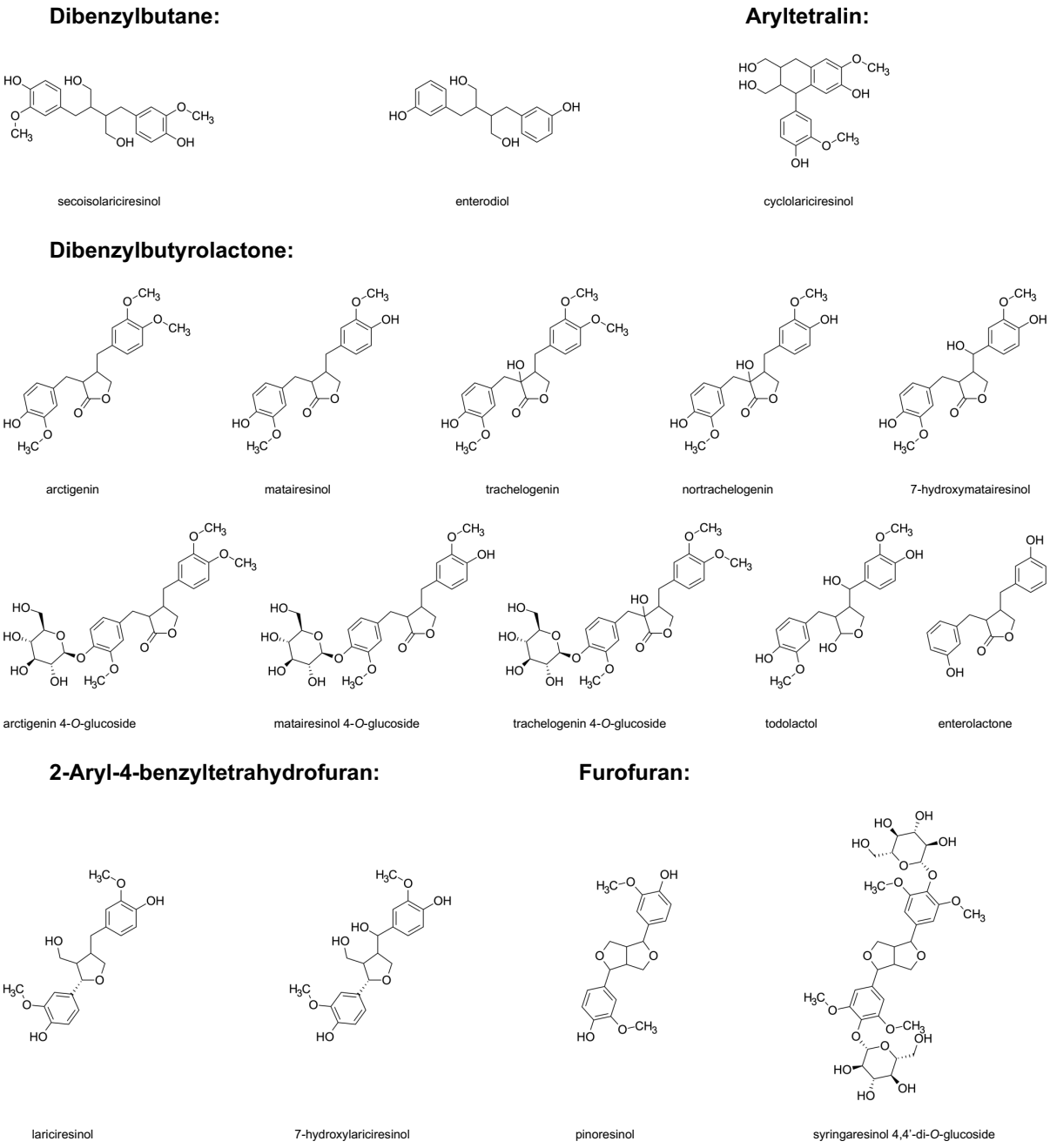

Figure 54. Structures of isolated lignans.

LC-MS analysis was a crucial step in selecting lignans for isolation. All lignans obtained during the course of this project were of purity higher than 95 %, which was deemed sufficient for pharmacological studies, and as such they formed a lignan library, which was used in this study, but that can also be used in other assays. Structures of all isolated lignans are presented in Figure 54.

7.3 Lignans effects on pancreatic β-cell

Previous reports have shown that single lignans: schisandrin C (2.5 – 5.0 μmol/L) from *Schisandra chinensis* (Turcz.) Baill. fruits and arctigenic acid (50 mg/kg, p.o.) from *Arctium lappa* L. fruits, are able to modulate the function of the pancreatic β-cell [149, 150]. The two compounds, apart from sharing a common biosynthetic pathway and the β-β' bond characteristic for lignans, have very little in common. Schisandrin C is a dibenzocyclooctadiene lignan with no free hydroxyl group, while arctigenic acid is a metabolite of arctigenin, a dibenzylbutyrolactone lignan, which due to hydrolysis opened its lactone ring to form dibenzylbutane lignan. It has two free hydroxyl groups and one carboxyl group; thus, it is more hydrophilic.

In this context, this study was the first one to assess the insulin secretagogue effect of multiple lignan structures, belonging to different subtypes, such as dibenzylbutane (secoisolariciresinol, enterodiol), dibenzylbutyrolactone (arctigenin, arctigenin 4-*O*-glucoside, matairesinol, matairesinol 4-*O*-glucoside, trachelogenin, trachelogenin 4-*O*-glucoside, nortrachelogenin, 7-hydroxymatairesinol, todolactol, enterolactone), 2-aryl-4-benzyltetrahydrofuran (lariciresinol, 7-hydroxylariciresinol), aryltetralin (cyclolariciresinol) and furofuran (pinoresinol, syringaresinol 4,4'-di-*O*-glucoside). None of the studied lignans was able to increase glucose-induced insulin secretion at the screened concentration (20 μmol/L), and three of them (arctigenin, trachelogenin, and nortrachelogenin) were found to induce toxicity in INS-1 cells leading to a decrease in insulin secretion (Figure 29). However, these results do not contradict the previous results for schisandrin C and arctigenic acid, as these compounds were not part of this study. None of the compounds belonged to the dibenzocyclooctadienes group as schisandrin C, while only lignans similar in structure to arctigenic acid, i.e., secoisolariciresinol and enterodiol, and its direct precursor arctigenin were studied. Xu *et al.*, who described the hypoglycemic effect of arctigenic acid in diabetic GK rats, did not measure insulin levels [150]. Their assumption on its insulin-secretagogue properties, which they describe as nateglinide-like, are based on structure similarity and plasma glucose levels. The authors also measured C-peptide levels in the serum, but the experiment was only designed to compare the fasting and postprandial effect of each treatment; thus, it is not clear whether arctigenic acid may indeed

modulate glucose-induced insulin secretion. As neither Xu *et al.* nor I have studied the arctigenic acid effect on insulin secretion, it is worth pursuing the path to elucidate the mechanism of action of this hypoglycemic compound.

Marrano *et al.* studied polyphenols from olive oil on β-cell function, among them one lignan, i.e., pinoresinol [391]. According to their data, and consistent with my results, pinoresinol did not modulate glucose-induced insulin secretion. It is worth noting that their studied concentration was lower (10 vs. 20 μmol/L), and the β-cell model was slightly different (INS-1E vs. INS-1). Although pinoresinol was not able to modulate glucose-induced insulin secretion, Marrano *et al.* [391] observed an increase in insulin content in the cells treated with this lignan for two subsequent 1h incubations. This might suggest that pinoresinol possesses some activity on the β-cell function.

Mellbye *et al.* studied bioactive compounds in coffee on β-cell function and glucose uptake in muscle cells. They measured glucose-induced insulin secretion in INS-1E cells after incubation with 1 pmol/L to 1 μmol/L of secoisolariciresinol but did not observe any effect [392]. This result is consistent with my observation at 20 μmol/L.

Zhai *et al*. have found that syringaresinol 4,4'-di-*O*-glucoside alleviated diabetic state in STZ mice. They reported that in STZ mice treated with 25 – 75 mg/kg (i.g.; daily for 2 weeks) syringaresinol 4,4'-di-*O*-glucoside, serum insulin levels and pancreatic insulin content was significantly higher than in control group [215]. My results did not show any effect of this lignan glycoside on glucose-induced insulin secretion in the INS-1 pancreatic β-cell model. Although it is very difficult to compare results obtained *in vitro* and *in vivo*, it is important to note that the STZ mice model is a type 1 diabetes mellitus model, where pancreatic β-cells are damaged by the cytotoxic agent. The authors did not study whether the effect of syringaresinol 4,4'-di-*O*-glucoside was a direct one on the β-cell.

To the best of my knowledge, enterodiol, arctigenin, arctigenin 4-*O*-glucoside, matairesinol, matairesinol 4-*O*-glucoside, trachelogenin, trachelogenin 4-*O*-glucoside, nortrachelogenin, 7-hydroxymatairesinol, enterolactone, lariciresinol, 7-hydroxylariciresinol, and cyclolariciresinol have not been previously studied in the context of modulation of pancreatic β-cell insulin secretion.

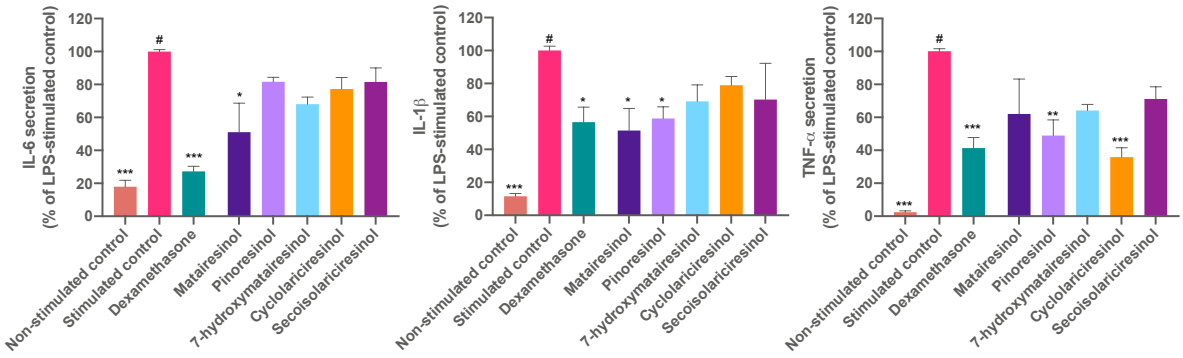

Figure 55. Modulation of pro-inflammatory cytokines secretion by lignans.

Preliminary results from a study carried out in the Department of Pharmaceutical Biology (Medical University of Warsaw) on monocytes/macrophages isolated from the human peripheral blood have shown that certain lignans reduced pro-inflammatory cytokines secretion induced by lipopolysaccharide (LPS) (Figure 55) [393]. In the context of lignans' anti-inflammatory activity, the present study assessed lignans' ability to protect the β-cell from pro-inflammatory cytokine-induced cell dysfunction and death. However, no protective effect was observed for studied lignans (Figure 33). It is possible that lignan anti-inflammatory activity targets cytokines secretion but does not influence active inflammation. The possibility that lignans could decrease pro-inflammatory cytokines secretion in chronic inflammation and thus ameliorate β-cell function is a valid goal for further explorations.

7.4 Angelica root extracts phytochemistry and insulin secretagogue properties

Angelica root extracts constitute a significant source of various traditional medicines around the northern hemisphere, from the indigenous cultures of North America to Japan. They have many uses, but T2DM is not often mentioned among them. Ethnopharmacological studies reported the use of *A. japonica var. hirsutiflora*, *A. furcijuga, A. shikokiana,* and *A. keiskei* to treat diabetes symptoms [157, 303, 394, 395]. Further reports have demonstrated insulin secretagogue activity of three angelica roots, i.e., *A. japonica var. hirsutiflora* (mouse and human islets, HIT-T15), *A. reflexa* (INS-1), and *A. dahurica* (INS-1), belonging to the species spread in East Asia (China, Korea, Japan, and Taiwan) [156-158]. The metabolite profile of all angelica roots has not been studied thoroughly. There are many reports on the phytochemical composition of *A. dahurica* roots [291, 378, 396, 397], but only a single report on *A. reflexa* [158] and only a few compounds have been isolated from *A. japonica var.*

hirsutiflora without any comprehensive study on its composition [398, 399]. However, this limited data show that all these root extracts are rich in coumarins.

For this study, angelica roots monographed in European Pharmacopeia (Ph. Eur. 11th) were chosen, i.e., *A. archangelica*, *A. dahurica*, *A. biserrata*, and *A. sinensis*. Acquired phytochemical and pharmacological data allowed me to correlate the metabolite profile with the biological activity of the extracts on insulin secretion. Obtained results confirmed that *A. dahurica* roots modulate glucose-induced insulin secretion in INS-1 cells, and additionally, for the first time, such effect was described for *A. biserrata* and *A. archangelica* roots, with the latter one being active in the lowest concentrations of the three extracts (12.5 μg/mL). The fourth studied extract, from *A. sinensis* roots, did not show any activity at the studied concentrations (1.6 to 50.0 μg/mL) (Figure 34). When considering the data on the phytochemical examination of these extracts (Table 11), it is clear that only angelica roots rich in coumarins were able to modulate insulin secretion. These results are consistent with the conclusions from previous studies on *A. dahurica*, *A. reflexa,* and *A. japonica var. hirsutiflora* roots. Therefore, this study offers data on a new activity of traditionally used angelica roots in Europe.

Furthermore, phytochemical profiling of active extracts and isolation of major (and minor) coumarin compounds from them allowed me to explore which constituents are responsible for the modulation of β-cell insulin secretion and to elucidate their mechanism of action (Figure 56).

Roots that were found to be rich in coumarins in phytochemical examinations, i.e., those of *A. archangelica*, *A. dahurica* and *A. biserrata*, were subsequently used for isolation of pure compounds, from 0.3 to 380.4 mg. From *A. archangelica* root the largest variety of coumarins was isolated. The plant offered simple *C*-prenylated coumarins: osthole (121.2 mg) and osthenol (22.1 mg), linear furanocoumarins: psoralen (5.5 mg), xanthotoxin (9.3 mg), bergapten (19.6 mg) and isopimpinellin (9.9 mg), *O*-prenylated linear furanocoumarins: oxypeucedanin hydrate (5.5 mg), imperatorin (18.0 mg), isoimperatorin (12.6 mg), phellopterin (0.8 mg), heraclenol-2'-*O*-angelate (68.2 mg), byakangelicin-2'-*O*-angelate (102.2 mg) and byakangelicin-2'-*O*-isovalerate (14.4 mg), and angular furanocoumarins: angelicin (64 mg), isoedultin (88.5 mg), vaginidiol-*O*-angelate (16.5 mg), 2'-angeloyl-3'-isovaleryl vaginate (97.2 mg) and archangelicin (110.4 mg). Dahurian angelica root had much less diverse coumarin profile, but instead offered large quantities of imperatorin (380.4 mg), isoimperatorin (148.0 mg) and cnidilin (224.5 mg), and several other linear furanocoumarins: psoralen (0.3 mg), bergapten (26.6 mg), xanthotoxin (1.2 mg), phellopterin (6.3 mg), and byakangelicin (5.5 mg). From *A. biserrata* root only 3 compounds were isolated. This is, however, not because of its poor coumarin content. As

many compounds were already isolated from the first two roots, I strived instead to isolate only those not present in the previous species. Thus, three angular furanocoumarins were isolated: columbianetin (14.2 mg), columbianetin acetate (30.7 mg) and columbianadin (108.9 mg), and one sesquiterpene: bisabolangelone (23.7 mg).

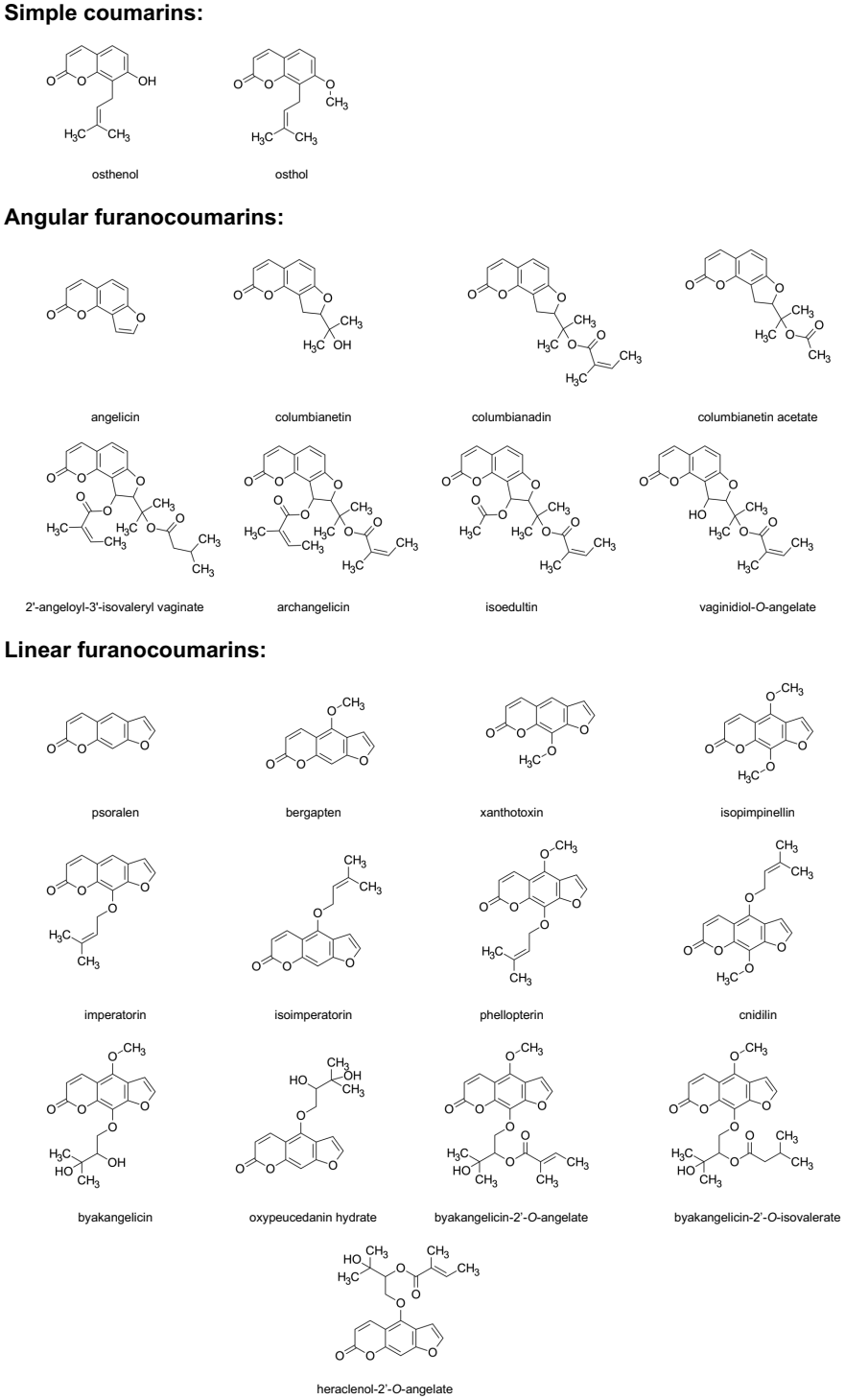

Figure 56. Structures of isolated coumarins.

All coumarins obtained during the course of this project were of purity higher than 95 %, which was deemed sufficient for pharmacological studies.

7.5 Modulation of insulin secretion by coumarins and their mechanism of action

Out of the twenty-three coumarins isolated from *A. archangelica*, *A. dahurica,* and *A. biserrata* roots, six significantly increased glucose-induced insulin secretion, i.e., isoimperatorin, imperatorin, osthenol, phellopterin, osthole, and cnidilin (Figure 35). This suggests that imperatorin, isoimperatorin, osthole, phellopterin, and osthenol are responsible for the activity of *A. archangelica*, imperatorin, isoimperatorin, cnidilin, and phellopterin are responsible for the activity of *A. dahurica*, and osthole, imperatorin, and isoimperatorin are responsible for the insulinotropic activity of *A. biserrata*. These results could also confirm previous assumptions that coumarins are responsible for this activity in other angelica roots [156-158].

Though the active compounds belonged to different coumarin subtypes (i.e., simple and linear furanocoumarins), they all shared an isoprenyl sidechain attached to the coumarin in C5 or C8 position. I suspect that insulinotropic activity is determined by this isoprenyl sidechain, as its lack or any modification led to the loss of studied function (Figure 37). This, however, must be confronted with a recent report on a similar activity of scopoletin (7-hydroxy-6-methoxycoumarin), which does not possess an isoprenyl sidechain, yet is said to increase glucose-induced insulin secretion through K_{ATP} and VGCC channels dependent pathway in INS-1 cells at concentrations below 20 µmol/L [153]. In my study, I have not studied scopoletin; thus, I cannot exclude that this and any other coumarin not studied here might fall out of the isoprenyl sidechain rule.

From the six active compounds, I selected two coumarins, i.e., isoimperatorin and imperatorin, to characterize their activity further. Both compounds have shown the highest modulatory potential in screening studies (2.6-fold increase and 1.9-fold increase of glucose-induced insulin secretion respectively) and are closely related – imperatorin is an 8-*O*-isoprenyloxypsoralen while isoimperatorin is a 5-*O*-isoprenyloxypsoralen. These efficacies are comparable within the same concentration (i.e., 20 µmol/L) as quercetin, which produced a 2.2-fold increase in 8.3 mmol/L glucose-induced insulin secretion.

Here I report that micromolar concentrations of isoimperatorin and imperatorin were necessary to generate a pharmacological action on insulin secretion. For isoimperatorin, the minimal significant effective concentration was 20 µmol/L, while for imperatorin, it was 10 µmol/L. Both compounds have shown a concentration-dependency with a rising effect for concentrations up to 40 µmol/L (Figure 38). These compounds present the same potencies that have been shown for flavonoids and are lower than those that were described for imperatorin in previous studies. Adebajo *et al.* have found that imperatorin modulated glucose-induced insulin secretion in INS-1 cells at 0.1 mg/mL (which is about 370 µmol/L) but did not show any effect at 0.01 mg/mL (equivalent to 37 µmol/L) [281]. Park *et al.* observed phellopterin and imperatorin's ability to modulate glucose-induced insulin secretion in INS-1 cells at 100 µmol/L but not at 10 µmol/L [156]. Contrary to flavonoids [384, 400], micromolar concentrations are much more likely to be reached *in vivo*, as coumarins have much better bioavailability [401].

Another important observation is that the insulinotropic activity of isoimperatorin and imperatorin is only evoked upon exposure of β-cells to a stimulating concentration of glucose, meaning that it follows a glucose-dependent pathway. This pharmacological feature of studied coumarins is particularly interesting, because it should minimize the likelihood of hypoglycemia, a common side-effect of anti-diabetic drugs present on the market (sulfonylureas) [402]. This glucose dependency may also suggest that the molecular target of isoimperatorin and imperatorin lies within the glucose-induced insulin secretion pathway. In my study, I investigated the effect of isoimperatorin and imperatorin on multiple components of this pathway.

It was found that studied coumarins have an impact on membrane potential and that they increase intracellular calcium levels ($[Ca^{2+}]_i$). The rise in $[Ca^{2+}]_i$ could come either from a release from intracellular stores (endoplasmic reticulum) or an entry from the extracellular medium. Previous reports on a coumarin scopoletin, as well as on other plant metabolites regulating β-cell insulin secretion, such as quercetin and urolithin C, have shown that their effect is mediated through the activation of the voltage-gated calcium channels, particularly through the L-type [147, 153, 155]. In this context, to study the mechanism of action, I have investigated the involvement of such channels in the pharmacological effect of imperatorin and isoimperatorin. The inhibitory effect of verapamil, an inhibitor of L-type VGCC, in coumarin-induced insulin secretion (Figure 49) and intracellular calcium increase (Figure 50) confirmed the contribution of such channels to the effect of studied coumarins. This was also confirmed by patch-clamp experiments, where a stimulatory effect was observed towards the L-type current. On the other hand, an inhibitory effect was described towards the T-type

(Figure 48). Such an effect towards the T-type channels was not described for previously studied insulin secretion modulators in the Institut des Biomolécules Max Mousseron, i.e., quercetin and urolithin C. In the β-cell, the T-type channels are responsible for slight depolarization of the cell membrane, facilitating production of action potentials, while the L-type channels are primarily responsible for the calcium influx [49, 77, 82]. Surprisingly, imperatorin was previously described as an inhibitor of L-type VGCC in vascular and intestinal smooth muscle cells [403, 404]. This discrepancy might be the result of differences in experimental conditions and cell model or the indirect character of this activity, suggesting that other pharmacological targets or mediators are involved. As for the first hypothesis, such dual (agonistic-antagonistic) activity depending on experimental conditions towards the same channel was already described for dihydropyridines [405, 406].

However, in my studies, I focused on the second possibility and searched for other targets that could indirectly modulate the L-type VGCC. Imperatorin and isoimperatorin have been previously described in transfected HEK cells as partial agonists of capsaicin receptor (TRPV1). The EC_{50} for imperatorin was 12.3 µmol/L [407]. While the TRPV1 is expressed in pancreatic β-cells, the precise mechanism by which it participates in insulin secretion is still an active area of research. It is likely that its activation might shift the membrane potential away from equilibrium, which, together with the closure of K_{ATP}, would lead to insulin secretion [60-62]. It can be noticed that the range of coumarin active concentrations towards TRPV1 activation overlaps with the one from my functional studies in the β-cell.

In another study, imperatorin was found to suppress neuronal excitability through antagonistic activity toward voltage-gated sodium channels with IC_{50} of 25 µmol/L [408]. This, however, would extinguish the action potential, not increase it, and so it is unlikely that this activity would play a role in increasing insulin secretion.

Imperatorin was also found to inhibit the K_{ATP} channels in differentiated neuronal NG108-15 cells [409]. This sulfonylureas-like activity would certainly increase insulin secretion in the β-cells, though there are two discrepancies with my findings. As stated before, the effect of imperatorin on insulin secretion is glucose-dependent, while the inhibitory effect of sulfonylureas on the K_{ATP} channels is non-glucose-dependent. Secondly, the IC_{50} for this effect reported by Wang *et al.* is greater than 100 µmol/L [409]. In this context, it is unlikely that concentrations from 10 – 40 µmol/L would induce such a strong increase in insulin secretion.

On the same neuronal cell model (NG108-15), imperatorin was found to possess inhibitory potential towards another type of potassium channel, namely the voltage-gated potassium channel. Half maximal inhibitory concentration described for $K_v1.2$ was at 32 µmol/L, and for $K_v2.1$ was at 16 µmol/L [409]; both falling within the concentration range of my study. Interestingly the $K_v2.1$ is expressed in rodent pancreatic β-cells, where they are responsible for the delayed rectifying current and cell repolarization. Thus, blocking the $K_v2.1$ channel could lead to a prolongation of action potential and an increase in insulin secretion [48]. In my study, I evaluated the possible implication of VGKC in the intracellular calcium increase induced by imperatorin and isoimperatorin using tetraethylammonium, a VGKC blocker (Figure 51). These experiments indicated the involvement of VKGC in the pharmacological action of isoimperatorin and imperatorin on the β-cell. This was subsequently confirmed by the whole-cell patch-clamp technique, which additionally allowed me to distinguish slow from fast transient potassium current and pinpoint the inhibitory effect only to the former (Figure 52).

There are other hypotheses described for imperatorin modulatory activity on the pancreatic β-cell insulin secretion involving the G protein-coupled receptors (GPCR), namely the GLP-1R, GPR-119, and TGR5 [152, 156]. Activation of GLP-1R, GPR-119, and TGR5 stimulates the production of cyclic adenosine monophosphate (cAMP) via the adenylyl cyclase pathway, leading to the PKA phosphorylation of ion channels and modulation of exocytosis process, as well as by mobilizing intracellular calcium stores and subsequently potentiating glucose-induced insulin secretion [410-412]. This theory is not contradictory with my findings, as the effect on membrane potential, $[Ca^{2+}]_i$, VGCC, and VGKC could manifest as an indirect effect through the activation of GLP-1R, GPR-119, or TGR5 [413-415]. In this context, the exact mechanism of action of imperatorin and isoimperatorin (direct or indirect) should be further evaluated, possibly using more physiological models (i.e., pancreatic islets isolated from rodents) and human cells to tackle the differences between channel expression in humans and rodents.

I have also assessed the capacity of imperatorin and isoimperatorin to ameliorate insulin secretion in β-cells whose responsiveness to glucose was impaired by glucotoxic condition (30 mmol/L glucose, 48 h); thus, in cells more closely reassembling those in a diabetic state. In this condition, glucose-induced insulin secretion was decreased by half compared to normal culturing conditions. Both imperatorin and isoimperatorin were active on such defective cells. Concentrations as little as 10 µmol/L were able to significantly increase glucose-induced insulin secretion, while at 20 µmol/L, the

insulin secretion was brought to levels characteristic of “healthy cells” (Figure 39). To the best of my knowledge, such an approach was never implemented for the study of coumarins before.

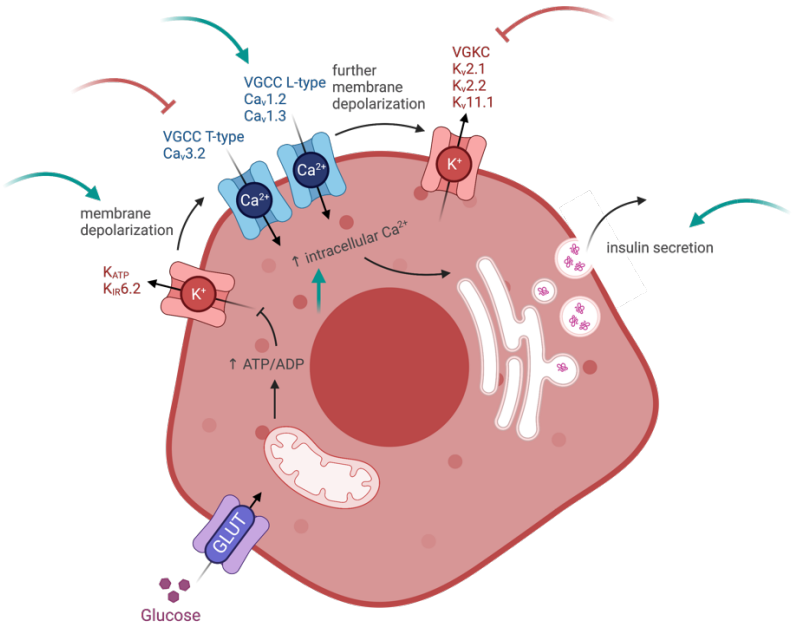

Figure 57. Modulation of β-cell function by isoprenylated coumarins.

Lastly, the ability of imperatorin and isoimperatorin to protect the β-cell from glucotoxicity and oxidative stress was assessed, but no effect was observed. Thus, studied coumarins can modulate β-cell function in healthy and dysfunctional cells but cannot protect them from insult.

These results may have implications on the traditional use of angelica roots in treating diabetes. I found insulinotropic effects of three pharmacopeial (Ph. Eur. 11th) angelica roots and corelated their metabolite profiles with pharmacological activity, identifying key structures responsible for modulation of pancreatic β-cell function, and elucidated in part their mechanism of action (Figure 57). These active coumarins may also become lead structures in the search for new anti-diabetic treatments.

Conclusions

1. **Modulation of the pancreatic β-cell function by flavonoids is highly dependent on the double bond between C2 and C3.**
    a. Loss of insulinotropic effect of quercetin, kaempferol, apigenin and chrysin was observed when the cells were incubated with their respective dihydro derivatives.
    b. Loss of inhibitory effect on insulin secretion of galangin was observed when the cells were incubated with its dihydro derivative pinobanksin.
2. **Studied lignans do not modulate insulin secretion nor do they protect the pancreatic β-cell from dysfunction and cell death.**
    a. *Abies alba* and *Pinus sylvestris* wood can be considered a valuable source of lignans.
    b. Lignan compound library was established, that can be used in other pharmacological assays.
3. **Traditionally used roots from the genus *Angelica* L. containing prenylated coumarins show insulinotropic activity in doses from 12.5 – 50 µg/mL.**
    a. *Angelica archangelica*, *Angelica dahurica* and *Angelica biserrata* roots are a rich source of isomeric coumarins with insulinotropic activity.
4. **Coumarins equipped with an isoprenyl sidechain modulate pancreatic β-cell function.**
    a. Imperatorin and isoimperatorin modulate insulin secretion in a glucose-dependent and concentration-dependent manner in micromolar range (10 – 40 µmol/L).
    b. Imperatorin and isoimperatorin effect on pancreatic β-cell function is manifested by modulation of cell membrane potential, intracellular calcium levels, activation of voltage-gated calcium channels and inhibitions of voltage-gated potassium channels.
    c. Imperatorin and isoimperatorin can restore glucose-induced insulin secretion levels in dysfunctional β-cells.
    d. Imperatorin and isoimperatorin did not protect β-cells from glucotoxic and oxidative insults.

Scientific dissemination

Papers related to the dissertation:

1. **Patyra A**, Dudek MK, Kiss AK. LC-DAD–ESI-MS/MS and NMR Analysis of Conifer Wood Specialized Metabolites. Cells 2022, 11(20), 3332. IF=6.0; MEiN=140.
2. **Patyra A**, Kołtun-Jasion M, Jakubiak O, Kiss AK. Extraction Techniques and Analytical Methods for Isolation and Characterization of Lignans. Plants 2022, 11(17), 2323. IF=4.5; MEiN=70.
3. **Patyra A**, Kołakowski M, Dudek MK, Kiss AK. Isolation of trachelogenin 4-*O*-β-D-glucoside from the fruits of *Carthamus tinctorius* L.. Prospects in Pharmaceutical Sciences 2022, 20(2), 24-30. IF=0.1; MEiN=20.
4. Gautheron G, Péraldi-Roux S, Vaillé J, **Patyra A**, Bayle M, Youl E, Omhmmed S, Cros G, Movassat J, Quignard JF, Neasta J, Oiry C. The Flavonoid Resokaempferol Improves Insulin Secretion from Healthy and Dysfunctional Pancreatic β-Cells. British Journal of Pharmacology 202#, #(#), #. IF=7.3; MEiN=140. *IN REVIEW*
5. **Patyra A**, Vaillé J, Omhmmed S, Dudek MK, Neasta J, Kiss AK, Oiry C. Pharmacological and phytochemical insights on the pancreatic β-cell modulation by *Angelica* L. roots. Journal of Ethnopharmacology 202#, #(#), #. IF=5.4; MEiN=140. *READY TO SUBMIT*
6. **Patyra A**, Kupniewska K, Dudek MK, Kiss AK. Phytochemical characterization and quality assessment of *Eleutherococci radix* herbal preparations. Phytochemical Analysis 202#, #(#), #. IF=3.3; MEiN=70. *READY TO SUBMIT*
7. **Patyra A**, Kupniewska K, Kołtun-Jasion M, Parzonko A, Kiss AK. Phytochemistry and pharmacological activities of *Eleutherococci radix*. Planta Medica 202#, #(#), #. IF=2.7; MEiN=100. *READY TO SUBMIT*
8. Kołtun-Jasion M, **Patyra A**, Dudek MK, Filipek A, Oiry C, Kiss AK. Dietary lignans effect on inflammation underlying metabolic disorders. Journal of Agricultural and Food Chemistry 202#, #(#), #. IF=6.1; MEiN=140. *READY TO SUBMIT*

Other papers:

1. Kozon K, Krzyżanowska M, Olszewski J, **Patyra A**. Spinal Muscular Atrophy – The Effectiveness of Treatment and New Therapeutic Possibilities for Selected Groups of Patients in Poland. Prospects in Pharmaceutical Sciences 2023, 21(2), 68-72. IF=0.1; MEiN=20.
2. Kołtun-Jasion M, Sawulska P, **Patyra A**, Woźniak M, Dudek MK, Filipek A, Kiss AK. Bio-Guided Isolation of Compounds from Fraxinus excelsior Leaves with Anti-Inflammatory Activity. International Journal of Molecular Sciences 2023, 24(4), 3750. IF=5.6; MEiN=140.

3. Olszewski J, Kozon K, **Patyra A**. Flozins in heart failure – a new reimbursement indication. Prospects in Pharmaceutical Sciences 2022, 20(1), 19-25. IF=0.1; MEiN=20.
4. **Patyra A**, Witkowski G. Voltage-gated sodium channels mutations and their role in epilepsy. Prospects in Pharmaceutical Sciences 2022, 20(1), 11-18. IF=0.1; MEiN=20.
5. Kiss AK, Michalak B, **Patyra A**, Majdan M. UHPLC-DAD-ESI-MS/MS and HPTLC profiling of ash leaf samples from different commercial and natural sources and their in vitro effects on mediators of inflammation. Phytochemical Analysis 2020, 31(1), 57-67. IF=3.37; MEiN=70.

Communications at scientific conferences:

1. **Patyra A**, Omhmmed S, Vaillé J, Péraldi-Roux S, Quignard JF, Kiss AK, Neasta J, Oiry C. *Angelica* L. coumarins potential to modulate glucose-induced insulin secretion and their mechanism of action. 71st International Congress and Annual Meeting of the Society for Medicinal Plant and Natural Product Research (GA), Dublin, Ireland 2023. **PLENARY SESSION TALK**
2. **Patyra A**, Omhmmed S, Vaillé J, Jakubiak O, Quignard JF, Kiss AK, Neasta J, Oiry C. Isolation of coumarins from plant material and screening for their insulinotropic effects on the β-cell. Balard Chemistry Conferences, Montpellier, France 2023. **POSTER**
3. **Patyra A**, Kołtun-Jasion M, Schwartz J, Neasta J, Kiss AK, Oiry C. Lignans effect on the pancreatic β-cell function. Annual Congress of the Société Française de Pharmacologie et de Thérapeutique, Limoges, France 2023. **POSTER**
4. **Patyra A**, Neasta J, Vaillé J, Péraldi-Roux S, Kiss AK, Oiry C. Imperatorin modulates glucose-induced insulin secretion. Annual Congress of the Société Française de Pharmacologie et de Thérapeutique, Limoges, France 2023. **POSTER**
5. **Patyra A**, Oktawia J, Kiss AK. Phytochemical analysis of coumarins in roots of the genus *Angelica* L.. Aktualne kierunki badań w naukach farmaceutycznych – FORUM MŁODYCH, Lublin, Poland 2023. **SHORT TALK**
6. **Patyra A**, Kupniewska K, Kiss AK. Phytochemical characterization of Siberian ginseng roots using LC-DAD-ESI-MS/MS. 22nd International Congress of International Society for Ethnopharmacology, Imphal, India 2023. **POSTER**
7. **Patyra A**, Kołtun-Jasion M, Schwartz J, Malle E, Kiss AK, Oiry C. Exploring the anti-diabetic and anti-inflammatory effects of lignans coming from wood waste materials. Phytochemical Society of Europe Meeting, Iasi, Romania 2022. **POSTER/FLASH TALK**

8. **Patyra A**, Schwartz J, Neasta J, Kiss AK, Oiry C. Conifer wood metabolites and their effect on the pancreatic β-cell function. Sciences Chimiques et Biologiques pour la Santé Day, Montpellier, France 2022. **SHORT TALK**
9. **Patyra A**, Herczyńska I, Kiss AK. Stilbenes in wood industry waste materials – study on composition of conifers branch wood. Interdisciplinary Conference on Drug Sciences Accord, Warsaw, Poland 2022. **POSTER**
10. **Patyra A**, Jakubiak O, Herczyńska I, Kiss AK. Phytochemical characterization of wood coming from the pine family (*Pinaceae*) species native to Poland. Trends in Natural Products Research: A PSE Young Scientists' Meeting, Kolymbari, Greece 2022. **POSTER**
11. **Patyra A**, Hubiszta M, Oiry C, Kiss AK. Isolation of pinoresinol glucoside from weeping forsythia flowers (*Forsythia suspensa* (thunb.) Vahl), its enzymatic hydrolysis and preliminary biological study. XXIV Naukowy Zjazd PTFarm, Lublin, Poland 2021. **POSTER**

Awards:

1. **Prof. Jürg Gertsch Discovery Award** for best oral presentation at the 71st International Congress and Annual Meeting of the Society for Medicinal Plant and Natural Product Research (GA). 2023.
2. **Society for Medicinal Plant and Natural Product Research (GA) Travel Grant** for young scientists. 2023.
3. **Polish Pharmaceutical Society Award** for best oral presentation at the Youth Forum. 2023.
4. **The Polish National Agency For Academic Exchange (NAWA) STER** internationalization of Doctoral Schools. 2023.
5. **Medical University of Warsaw Rector Scholarship** for best PhD students. 2022 – 2023.
6. **Medical University of Warsaw Scholarship Fund** for best PhD students. 2022 – 2023.
7. **Phytochemical Society of Europe Travel Grant** for young scientists. 2022.
8. **The Polish National Agency For Academic Exchange (NAWA) PROM** international scholarship exchange of PhD candidates and academic staff. 2023.
9. **French Government Scholarship** for double-PhD candidates realizing their thesis between Polish and French institutions. 2020 – 2023.

Scientific cooperation:

1. **Botanical Garden of the Polish Academy of Sciences, Powsin, Poland** – obtaining plant material for conifer wood analysis and lignans isolation.

2. **Botanical Garden of the University of Warsaw, Warsaw, Poland** – obtaining plant material for conifer wood analysis and lignans isolation.
3. **Centre of Molecular and Macromolecular Studies, Polish Academy of Sciences, Łódź, Poland** – NMR analysis of isolated compounds.
4. **Cardio-Thoracic Research Center of Bordeaux, Université de Bordeaux, Bordeaux, France** – electrophysiological assessments of coumarins on the pancreatic β-cell.
5. **Pharmacochemistry of Synaptic Transmission and Neuroprotection Laboratory, Université de Montpellier, Montpellier, France** – image analysis of cytoplasmatic calcium in the pancreatic β-cell.

Research projects and acquired funding:

1. The **National Science Centre**, Poland, **PRELUDIUM 20 grant** 2021/41/N/NZ7/00313 (210 000 PLN), entitled: "Wood from pine family (*Pinaceae*) native to Poland as a potent source of pharmacologically active lignans"; Principal Investigator: **Andrzej Patyra**.
2. The **Ministry of Education and Science**, Poland, **Studenckie Koła Naukowe tworzą innowacje grant** SKN/SP/533710/2022 (60 000 PLN), entitled: "Searching for new innovative drugs among compounds of natural origin"; Project Manager: Sebastian Granica; Project Executive: **Andrzej Patyra**.
3. The **Medical University of Warsaw**, Poland, **Mini-grant** FW25/1/F/MG/N/21 (8 000 PLN), entitled: "Silver fir (*Abies alba* Mill.) as a source of lignan substances"; Project Manager: Iga Herczyńska; Project Executive: **Andrzej Patyra**.
4. The **Medical University of Warsaw**, Poland, **Mini-grant** 17/F/MG/N/23 (8 000 PLN), entitled: "Do lignans protect the skin from inflammation caused by UVB radiation?"; Project Manager: Oktawia Jakubiak; Project Executive: **Andrzej Patyra**.

Training, courses, certificates:

1. **Writing in the Sciences** – University of Stanford, 2020.
2. **Statistics in Medicine** – University of Stanford, 2020.
3. **Training in Laboratory Animal Science EU Function ABD** – Mossakowski Medical Research Institute, Polish Academy of Sciences, 2020.
4. **Animal Cell Culture** – University of Warsaw, 2021.
5. **Basics of Nuclear Magnetic Resonance** – Université de Lille, 2021.
6. **Advanced NMR Spectroscopy** – Université de Lille, 2021.

7. **Fundamentals of ELISA Immunoenzymatic Technique** – Centre of Postgraduate Medical Education, 2022.
8. **Two-Dimensional Gel Electrophoresis** – Centre of Postgraduate Medical Education, 2022.
9. **Fluorescence Activated Cell Sorting** – Centre of Postgraduate Medical Education, 2022.

References

1. Da Silva Xavier G. The Cells of the Islets of Langerhans. J Clin Med 2018; 7. DOI: 10.3390/jcm7030054

2. Wierup N, Sundler F, Heller RS. The islet ghrelin cell. J Mol Endocrinol 2014; 52: R35-49. DOI: 10.1530/jme-13-0122

3. Hartig SM, Cox AR. Paracrine signaling in islet function and survival. J Mol Med (Berl) 2020; 98: 451-467. DOI: 10.1007/s00109-020-01887-x

4. Kim A, Miller K, Jo J et al. Islet architecture: A comparative study. Islets 2009; 1: 129-136. DOI: 10.4161/isl.1.2.9480

5. Steiner DJ, Kim A, Miller K et al. Pancreatic islet plasticity: Interspecies comparison of islet architecture and composition. Islets 2010; 2: 135-145. DOI: 10.4161/isl.2.3.11815

6. Bosco D, Armanet M, Morel P et al. Unique Arrangement of α- and β-Cells in Human Islets of Langerhans. Diabetes 2010; 59: 1202-1210. DOI: 10.2337/db09-1177

7. Noguchi GM, Huising MO. Integrating the inputs that shape pancreatic islet hormone release. Nature Metabolism 2019; 1: 1189-1201. DOI: 10.1038/s42255-019-0148-2

8. Folli F, La Rosa S, Finzi G et al. Pancreatic islet of Langerhans' cytoarchitecture and ultrastructure in normal glucose tolerance and in type 2 diabetes mellitus. Diabetes Obes Metab 2018; 20 Suppl 2: 137-144. DOI: 10.1111/dom.13380

9. Cabrera O, Berman DM, Kenyon NS et al. The unique cytoarchitecture of human pancreatic islets has implications for islet cell function. Proc Natl Acad Sci U S A 2006; 103: 2334-2339. DOI: 10.1073/pnas.0510790103

10. Stefan Y, Grasso S, Perrelet A et al. The pancreatic polypeptide-rich lobe of the human pancreas: definitive identification of its derivation from the ventral pancreatic primordium. Diabetologia 1982; 23: 141-142. DOI: 10.1007/bf01271177

11. Brissova M, Fowler MJ, Nicholson WE et al. Assessment of human pancreatic islet architecture and composition by laser scanning confocal microscopy. J Histochem Cytochem 2005; 53: 1087-1097. DOI: 10.1369/jhc.5C6684.2005

12. Bonner-Weir S, O'Brien TD. Islets in type 2 diabetes: in honor of Dr. Robert C. Turner. Diabetes 2008; 57: 2899-2904. DOI: 10.2337/db07-1842

13. Arntfield ME, van der Kooy D. β-Cell evolution: How the pancreas borrowed from the brain: The shared toolbox of genes expressed by neural and pancreatic endocrine cells may reflect their evolutionary relationship. Bioessays 2011; 33: 582-587. DOI: 10.1002/bies.201100015

14. Maechler P, Wollheim CB. Mitochondrial glutamate acts as a messenger in glucose-induced insulin exocytosis. Nature 1999; 402: 685-689. DOI: 10.1038/45280

15. Reetz A, Solimena M, Matteoli M et al. GABA and pancreatic beta-cells: colocalization of glutamic acid decarboxylase (GAD) and GABA with synaptic-like microvesicles suggests their role in GABA storage and secretion. Embo j 1991; 10: 1275-1284.

DOI: 10.1002/j.1460-2075.1991.tb08069.x

16. Gonoi T, Mizuno N, Inagaki N et al. Functional neuronal ionotropic glutamate receptors are expressed in the non-neuronal cell line MIN6. J Biol Chem 1994; 269: 16989-16992.

17. Henquin JC, Meissner HP. Significance of ionic fluxes and changes in membrane potential for stimulus-secretion coupling in pancreatic B-cells. Experientia 1984; 40: 1043-1052. DOI: 10.1007/bf01971450

18. Yang XJ, Kow LM, Funabashi T et al. Hypothalamic glucose sensor: similarities to and differences from pancreatic beta-cell mechanisms. Diabetes 1999; 48: 1763-1772. DOI: 10.2337/diabetes.48.9.1763

19. Sunami E, Kanazawa H, Hashizume H et al. Morphological characteristics of Schwann cells in the islets of Langerhans of the murine pancreas. Arch Histol Cytol 2001; 64: 191-201. DOI: 10.1679/aohc.64.191

20. Hebrok M, Reichardt LF. Brain meets pancreas: netrin, an axon guidance molecule, controls epithelial cell migration. Trends Cell Biol 2004; 14: 153-155. DOI: 10.1016/j.tcb.2004.02.005

21. Langley OK, Aletsee-Ufrecht MC, Grant NJ et al. Expression of the neural cell adhesion molecule NCAM in endocrine cells. J Histochem Cytochem 1989; 37: 781-791. DOI: 10.1177/37.6.2723399

22. van Arensbergen J, García-Hurtado J, Moran I et al. Derepression of Polycomb targets during pancreatic organogenesis allows insulin-producing beta-cells to adopt a neural gene activity program. Genome Res 2010; 20: 722-732. DOI: 10.1101/gr.101709.109

23. Philipson LH, Kusnetsov A, Larson T et al. Human, rodent, and canine pancreatic beta-cells express a sodium channel alpha 1-subunit related to a fetal brain isoform. Diabetes 1993; 42: 1372-1377. DOI: 10.2337/diab.42.9.1372

24. Atouf F, Czernichow P, Scharfmann R. Expression of neuronal traits in pancreatic beta cells. Implication of neuron-restrictive silencing factor/repressor element silencing transcription factor, a neuron-restrictive silencer. J Biol Chem 1997; 272: 1929-1934. DOI: 10.1074/jbc.272.3.1929

25. Cruz SA, Tseng YC, Kaiya H et al. Ghrelin affects carbohydrate-glycogen metabolism via insulin inhibition and glucagon stimulation in the zebrafish (Danio rerio) brain. Comp Biochem Physiol A Mol Integr Physiol 2010; 156: 190-200. DOI: 10.1016/j.cbpa.2010.01.019

26. Devaskar SU, Giddings SJ, Rajakumar PA et al. Insulin gene expression and insulin synthesis in mammalian neuronal cells. J Biol Chem 1994; 269: 8445-8454.

27. Leloup C, Arluison M, Lepetit N et al. Glucose transporter 2 (GLUT 2): expression in specific brain nuclei. Brain Res 1994; 638: 221-226. DOI: 10.1016/0006-8993(94)90653-x

28. Thor S, Ericson J, Brännström T et al. The homeodomain LIM protein Isl-1 is expressed in subsets of neurons and endocrine cells in the adult rat. Neuron

1991; 7: 881-889. DOI: 10.1016/0896-6273(91)90334-v

29. Vult von Steyern F, Martinov V, Rabben I et al. The homeodomain transcription factors Islet 1 and HB9 are expressed in adult alpha and gamma motoneurons identified by selective retrograde tracing. Eur J Neurosci 1999; 11: 2093-2102. DOI: 10.1046/j.1460-9568.1999.00631.x

30. Song J, Xu Y, Hu X et al. Brain expression of Cre recombinase driven by pancreas-specific promoters. Genesis 2010; 48: 628-634. DOI: 10.1002/dvg.20672

31. Pearse AG, Polak JM. Neural crest origin of the endocrine polypeptide (APUD) cells of the gastrointestinal tract and pancreas. Gut 1971; 12: 783-788. DOI: 10.1136/gut.12.10.783

32. Fujita T, Kobayashi S, Yui R. Paraneuron concept and its current implications. Adv Biochem Psychopharmacol 1980; 25: 321-325.

33. LeRoith D. Beta-cell dysfunction and insulin resistance in type 2 diabetes: role of metabolic and genetic abnormalities. Am J Med 2002; 113 Suppl 6A: 3s-11s. DOI: 10.1016/s0002-9343(02)01276-7

34. Yang J, Chi Y, Burkhardt BR et al. Leucine metabolism in regulation of insulin secretion from pancreatic beta cells. Nutr Rev 2010; 68: 270-279. DOI: 10.1111/j.1753-4887.2010.00282.x

35. Cen J, Sargsyan E, Bergsten P. Fatty acids stimulate insulin secretion from human pancreatic islets at fasting glucose concentrations via mitochondria-dependent and -independent mechanisms. Nutr Metab (Lond) 2016; 13: 59. DOI: 10.1186/s12986-016-0119-5

36. Newsholme P, Gaudel C, McClenaghan NH. Nutrient regulation of insulin secretion and beta-cell functional integrity. Adv Exp Med Biol 2010; 654: 91-114. DOI: 10.1007/978-90-481-3271-3_6

37. Winzell MS, Ahrén B. G-protein-coupled receptors and islet function-implications for treatment of type 2 diabetes. Pharmacol Ther 2007; 116: 437-448. DOI: 10.1016/j.pharmthera.2007.08.002

38. Bolea S, Pertusa JA, Martín F et al. Regulation of pancreatic beta-cell electrical activity and insulin release by physiological amino acid concentrations. Pflugers Arch 1997; 433: 699-704. DOI: 10.1007/s004240050334

39. Molina J, Rodriguez-Diaz R, Fachado A et al. Control of insulin secretion by cholinergic signaling in the human pancreatic islet. Diabetes 2014; 63: 2714-2726. DOI: 10.2337/db13-1371

40. Marchetti P, Lupi R, Bugliani M et al. A local glucagon-like peptide 1 (GLP-1) system in human pancreatic islets. Diabetologia 2012; 55: 3262-3272. DOI: 10.1007/s00125-012-2716-9

41. Nakazaki M, Crane A, Hu M et al. cAMP-activated protein kinase-independent potentiation of insulin secretion by cAMP is impaired in SUR1 null islets. Diabetes 2002; 51: 3440-3449. DOI: 10.2337/diabetes.51.12.3440

42. He LP, Mears D, Atwater I et al. Glucagon induces suppression of ATP-sensitive K+ channel activity through a

Ca2+/calmodulin-dependent pathway in mouse pancreatic beta-cells. J Membr Biol 1998; 166: 237-244. DOI: 10.1007/s002329900465

43. Nadal A, Rovira JM, Laribi O et al. Rapid insulinotropic effect of 17beta-estradiol via a plasma membrane receptor. Faseb j 1998; 12: 1341-1348. DOI: 10.1096/fasebj.12.13.1341

44. Rorsman P, Ashcroft FM. Pancreatic β-Cell Electrical Activity and Insulin Secretion: Of Mice and Men. Physiol Rev 2018; 98: 117-214. DOI: 10.1152/physrev.00008.2017

45. MacDonald PE, Rorsman P. Oscillations, intercellular coupling, and insulin secretion in pancreatic beta cells. PLoS Biol 2006; 4: e49. DOI: 10.1371/journal.pbio.0040049

46. Heimberg H, De Vos A, Pipeleers D et al. Differences in glucose transporter gene expression between rat pancreatic alpha- and beta-cells are correlated to differences in glucose transport but not in glucose utilization. J Biol Chem 1995; 270: 8971-8975. DOI: 10.1074/jbc.270.15.8971

47. Kalwat MA, Cobb MH. Mechanisms of the amplifying pathway of insulin secretion in the β cell. Pharmacol Ther 2017; 179: 17-30. DOI: 10.1016/j.pharmthera.2017.05.003

48. Jacobson DA, Shyng SL. Ion Channels of the Islets in Type 2 Diabetes. J Mol Biol 2020; 432: 1326-1346. DOI: 10.1016/j.jmb.2019.08.014

49. Braun M, Ramracheya R, Bengtsson M et al. Voltage-gated ion channels in human pancreatic beta-cells: electrophysiological characterization and role in insulin secretion. Diabetes 2008; 57: 1618-1628. DOI: 10.2337/db07-0991

50. MacDonald PE, Rorsman P. The ins and outs of secretion from pancreatic β-cells: control of single-vesicle exo-and endocytosis. Physiology 2007; 22: 113-121.

51. Lubberding AF, Juhl CR, Skovhøj EZ et al. Celebrities in the heart, strangers in the pancreatic beta cell: Voltage-gated potassium channels K(v) 7.1 and K(v) 11.1 bridge long QT syndrome with hyperinsulinaemia as well as type 2 diabetes. Acta Physiol (Oxf) 2022; 234: e13781. DOI: 10.1111/apha.13781

52. Gilon P, Chae HY, Rutter GA et al. Calcium signaling in pancreatic β-cells in health and in Type 2 diabetes. Cell Calcium 2014; 56: 340-361. DOI: 10.1016/j.ceca.2014.09.001

53. Henquin JC, Nenquin M, Ravier MA et al. Shortcomings of current models of glucose-induced insulin secretion. Diabetes, Obesity and Metabolism 2009; 11: 168-179. DOI: https://doi.org/10.1111/j.1463-1326.2009.01109.x

54. Fridlyand LE, Jacobson DA, Philipson LH. Ion channels and regulation of insulin secretion in human β-cells: a computational systems analysis. Islets 2013; 5: 1-15. DOI: 10.4161/isl.24166

55. Aguilar-Bryan L, Clement JPt, Gonzalez G et al. Toward understanding the assembly and structure of KATP channels. Physiol Rev 1998; 78: 227-245. DOI: 10.1152/physrev.1998.78.1.227

56. Tucker SJ, Gribble FM, Zhao C et al. Truncation of Kir6.2 produces ATP-sensitive K+ channels in the absence of

the sulphonylurea receptor. Nature 1997; 387: 179-183. DOI: 10.1038/387179a0

57. Aguilar-Bryan L, Nichols CG, Wechsler SW et al. Cloning of the beta cell high-affinity sulfonylurea receptor: a regulator of insulin secretion. Science 1995; 268: 423-426. DOI: 10.1126/science.7716547

58. Zhang Y, Xie L, Gunasekar SK et al. SWELL1 is a regulator of adipocyte size, insulin signalling and glucose homeostasis. Nat Cell Biol 2017; 19: 504-517. DOI: 10.1038/ncb3514

59. Remedi MS, Nichols CG. Chapter 8 - KATP Channels in the Pancreas: Hyperinsulinism and Diabetes. In: Pitt GS, ed. Ion Channels in Health and Disease. Boston: Academic Press; 2016: 199-221. DOI: https://doi.org/10.1016/B978-0-12-802002-9.00008-X

60. Drews G, Krippeit-Drews P, Düfer M. Electrophysiology of islet cells. Adv Exp Med Biol 2010; 654: 115-163. DOI: 10.1007/978-90-481-3271-3_7

61. Uchida K, Tominaga M. The role of thermosensitive TRP (transient receptor potential) channels in insulin secretion. Endocrine Journal 2011; 58: 1021-1028. DOI: 10.1507/endocrj.EJ11-0130

62. Colsoul B, Vennekens R, Nilius B. Transient Receptor Potential Cation Channels in Pancreatic β Cells. In: Amara SG, Bamberg E, Fleischmann BK et al., eds. Reviews of Physiology, Biochemistry and Pharmacology 161. Berlin, Heidelberg: Springer Berlin Heidelberg; 2011: 87-110. DOI: 10.1007/112_2011_2

63. Islam MS. TRP Channels of Islets. In: Islam MS, ed. Transient Receptor Potential Channels. Dordrecht: Springer Netherlands; 2011: 811-830. DOI: 10.1007/978-94-007-0265-3_42

64. MacDonald PE. TRP-ing down the path to insulin secretion. Diabetes 2011; 60: 28-29. DOI: 10.2337/db10-1402

65. Swayne LA, Mezghrani A, Varrault A et al. The NALCN ion channel is activated by M3 muscarinic receptors in a pancreatic beta-cell line. EMBO Rep 2009; 10: 873-880. DOI: 10.1038/embor.2009.125

66. Gilon P, Rorsman P. NALCN: a regulated leak channel. EMBO Rep 2009; 10: 963-964. DOI: 10.1038/embor.2009.185

67. Gall D, Gromada J, Susa I et al. Significance of Na/Ca exchange for Ca2+ buffering and electrical activity in mouse pancreatic beta-cells. Biophys J 1999; 76: 2018-2028. DOI: 10.1016/s0006-3495(99)77359-5

68. Rolland JF, Henquin JC, Gilon P. G protein-independent activation of an inward Na(+) current by muscarinic receptors in mouse pancreatic beta-cells. J Biol Chem 2002; 277: 38373-38380. DOI: 10.1074/jbc.M203888200

69. Miley HE, Sheader EA, Brown PD et al. Glucose-induced swelling in rat pancreatic beta-cells. J Physiol 1997; 504 (Pt 1): 191-198. DOI: 10.1111/j.1469-7793.1997.00191.x

70. Kang C, Xie L, Gunasekar SK et al. SWELL1 is a glucose sensor regulating β-cell excitability and systemic glycaemia. Nat Commun 2018; 9: 367. DOI: 10.1038/s41467-017-02664-0

71. Rorsman P, Eliasson L, Kanno T et al. Electrophysiology of pancreatic β-cells in intact mouse islets of Langerhans. Prog Biophys Mol Biol 2011; 107: 224-235. DOI: 10.1016/j.pbiomolbio.2011.06.009

72. Worley JF, 3rd, McIntyre MS, Spencer B et al. Endoplasmic reticulum calcium store regulates membrane potential in mouse islet beta-cells. J Biol Chem 1994; 269: 14359-14362.

73. Bertram R, Smolen P, Sherman A et al. A role for calcium release-activated current (CRAC) in cholinergic modulation of electrical activity in pancreatic beta-cells. Biophys J 1995; 68: 2323-2332. DOI: 10.1016/s0006-3495(95)80414-5

74. Ninomiya W, Mizobuchi K, Hayashi T et al. Electroretinographic abnormalities associated with pregabalin: a case report. Documenta Ophthalmologica 2020; 140: 279-287. DOI: 10.1007/s10633-019-09743-1

75. Alexander SPH, Mathie A, Peters JA et al. THE CONCISE GUIDE TO PHARMACOLOGY 2021/22: Ion channels. British Journal of Pharmacology 2021; 178: S157-S245. DOI: https://doi.org/10.1111/bph.15539

76. Dolphin AC. Voltage-gated calcium channels and their auxiliary subunits: physiology and pathophysiology and pharmacology. J Physiol 2016; 594: 5369-5390. DOI: 10.1113/jp272262

77. Barnett DW, Pressel DM, Misler S. Voltage-dependent Na+ and Ca2+ currents in human pancreatic islet beta-cells: evidence for roles in the generation of action potentials and insulin secretion. Pflugers Arch 1995; 431: 272-282. DOI: 10.1007/bf00410201

78. Jing X, Li DQ, Olofsson CS et al. CaV2.3 calcium channels control second-phase insulin release. J Clin Invest 2005; 115: 146-154. DOI: 10.1172/jci22518

79. Catterall WA. Sodium channels, inherited epilepsy, and antiepileptic drugs. Annu Rev Pharmacol Toxicol 2014; 54: 317-338. DOI: 10.1146/annurev-pharmtox-011112-140232

80. Zhang Q, Chibalina MV, Bengtsson M et al. Na+ current properties in islet α- and β-cells reflect cell-specific Scn3a and Scn9a expression. J Physiol 2014; 592: 4677-4696. DOI: 10.1113/jphysiol.2014.274209

81. Nica AC, Ongen H, Irminger JC et al. Cell-type, allelic, and genetic signatures in the human pancreatic beta cell transcriptome. Genome Res 2013; 23: 1554-1562. DOI: 10.1101/gr.150706.112

82. Rorsman P, Braun M. Regulation of insulin secretion in human pancreatic islets. Annu Rev Physiol 2013; 75: 155-179. DOI: 10.1146/annurev-physiol-030212-183754

83. Jacobson DA, Kuznetsov A, Lopez JP et al. Kv2.1 ablation alters glucose-induced islet electrical activity, enhancing insulin secretion. Cell Metab 2007; 6: 229-235. DOI: 10.1016/j.cmet.2007.07.010

84. Rosati B, Marchetti P, Crociani O et al. Glucose- and arginine-induced insulin secretion by human pancreatic beta-cells: the role of HERG K(+) channels in firing and release. Faseb j 2000; 14:

2601-2610. DOI: 10.1096/fj.00-0077com

85. Shepard PD, Bunney BS. Repetitive firing properties of putative dopamine-containing neurons in vitro: regulation by an apamin-sensitive Ca(2+)-activated K+ conductance. Exp Brain Res 1991; 86: 141-150. DOI: 10.1007/bf00231048

86. Jacobson DA, Mendez F, Thompson M et al. Calcium-activated and voltage-gated potassium channels of the pancreatic islet impart distinct and complementary roles during secretagogue induced electrical responses. J Physiol 2010; 588: 3525-3537. DOI: 10.1113/jphysiol.2010.190207

87. Köhler M, Hirschberg B, Bond CT et al. Small-conductance, calcium-activated potassium channels from mammalian brain. Science 1996; 273: 1709-1714. DOI: 10.1126/science.273.5282.1709

88. Pennefather P, Lancaster B, Adams PR et al. Two distinct Ca-dependent K currents in bullfrog sympathetic ganglion cells. Proc Natl Acad Sci U S A 1985; 82: 3040-3044. DOI: 10.1073/pnas.82.9.3040

89. Blodgett DM, Nowosielska A, Afik S et al. Novel Observations From Next-Generation RNA Sequencing of Highly Purified Human Adult and Fetal Islet Cell Subsets. Diabetes 2015; 64: 3172-3181. DOI: 10.2337/db15-0039

90. Henquin JC, Dufrane D, Gmyr V et al. Pharmacological approach to understanding the control of insulin secretion in human islets. Diabetes Obes Metab 2017; 19: 1061-1070. DOI: 10.1111/dom.12887

91. International Diabetes Federation. IDF Diabetes Atlas. In: 10th edn. Brussels, Belgium: International Diabetes Federation; 2021:

92. DeFronzo RA, Ferrannini E, Groop L et al. Type 2 diabetes mellitus. Nat Rev Dis Primers 2015; 1: 15019. DOI: 10.1038/nrdp.2015.19

93. Galicia-Garcia U, Benito-Vicente A, Jebari S et al. Pathophysiology of Type 2 Diabetes Mellitus. Int J Mol Sci 2020; 21. DOI: 10.3390/ijms21176275

94. Araszkiewicz A, Bandurska-Stankiewicz E, Borys S et al. 2023 Guidelines on the management of patients with diabetes - a position of Diabetes Poland. Current Topics in Diabetes 2023; 3: 1-133.

95. American Diabetes Association. 2. Classification and Diagnosis of Diabetes: Standards of Medical Care in Diabetes-2021. Diabetes Care 2021; 44: S15-S33. DOI: 10.2337/dc21-S002

96. World Health Organization. Definition and diagnosis of diabetes mellitus and intermediate and hyperglycaemia. Report of a WHO/IDF consultation. In: 2006:

97. World Health Organization. Use of Ggycated haemoglobin (HbA1c) in the diagnosis of diabetes mellitus: abbreviated report of a WHO consultation. 2011.

98. American Diabetes Association. 2. Classification and Diagnosis of Diabetes: Standards of Medical Care in Diabetes—2021. Diabetes Care 2020; 44: S15-S33. DOI: 10.2337/dc21-S002

99. Haute Autorité de Santé. Guide parcours de soins: Diabète de type 2 de

l'adulte. In: Saint-Denis La Plaine, France: 2014:

100. Narodowy Instytut Zdrowia Publicznego - Państwowy Zakład Higieny. ROZPOWSZECHNIENIE CUKRZYCY i KOSZTY NFZ ORAZ PACJENTÓW – A.D. 2017. In: Warsaw, Poland: Narodowy Instytut Zdrowia Publicznego - Państwowy Zakład Higieny,; 2017:

101. Kahn SE, Cooper ME, Del Prato S. Pathophysiology and treatment of type 2 diabetes: perspectives on the past, present, and future. Lancet 2014; 383: 1068-1083. DOI: 10.1016/s0140-6736(13)62154-6

102. Prasad RB, Groop L. Genetics of type 2 diabetes-pitfalls and possibilities. Genes (Basel) 2015; 6: 87-123. DOI: 10.3390/genes6010087

103. Zheng Y, Ley SH, Hu FB. Global aetiology and epidemiology of type 2 diabetes mellitus and its complications. Nature Reviews Endocrinology 2018; 14: 88-98. DOI: 10.1038/nrendo.2017.151

104. Stumvoll M, Goldstein BJ, van Haeften TW. Type 2 diabetes: principles of pathogenesis and therapy. Lancet 2005; 365: 1333-1346. DOI: 10.1016/s0140-6736(05)61032-x

105. Bays HE. Adiposopathy is "sick fat" a cardiovascular disease? J Am Coll Cardiol 2011; 57: 2461-2473. DOI: 10.1016/j.jacc.2011.02.038

106. Brereton MF, Rohm M, Ashcroft FM. β-Cell dysfunction in diabetes: a crisis of identity? Diabetes Obes Metab 2016; 18 Suppl 1: 102-109. DOI: 10.1111/dom.12732

107. White MG, Shaw JAM, Taylor R. Type 2 Diabetes: The Pathologic Basis of Reversible β-Cell Dysfunction. Diabetes Care 2016; 39: 2080-2088. DOI: 10.2337/dc16-0619

108. Sharma RB, Alonso LC. Lipotoxicity in the pancreatic beta cell: not just survival and function, but proliferation as well? Curr Diab Rep 2014; 14: 492. DOI: 10.1007/s11892-014-0492-2

109. Robertson RP, Harmon J, Tran PO et al. Beta-cell glucose toxicity, lipotoxicity, and chronic oxidative stress in type 2 diabetes. Diabetes 2004; 53 Suppl 1: S119-124. DOI: 10.2337/diabetes.53.2007.s119

110. Samuel VT, Petersen KF, Shulman GI. Lipid-induced insulin resistance: unravelling the mechanism. Lancet 2010; 375: 2267-2277. DOI: 10.1016/s0140-6736(10)60408-4

111. Holst JJ. The physiology of glucagon-like peptide 1. Physiol Rev 2007; 87: 1409-1439. DOI: 10.1152/physrev.00034.2006

112. Nauck MA, Meier JJ, Cavender MA et al. Cardiovascular Actions and Clinical Outcomes With Glucagon-Like Peptide-1 Receptor Agonists and Dipeptidyl Peptidase-4 Inhibitors. Circulation 2017; 136: 849-870. DOI: 10.1161/circulationaha.117.028136

113. Marzban L. New insights into the mechanisms of islet inflammation in type 2 diabetes. Diabetes 2015; 64: 1094-1096. DOI: 10.2337/db14-1903

114. Hotamisligil GS. Inflammation, metaflammation and immunometabolic disorders. Nature 2017; 542: 177-185. DOI: 10.1038/nature21363

115. Donath MY, Shoelson SE. Type 2 diabetes as an inflammatory disease. Nat Rev Immunol 2011; 11: 98-107. DOI: 10.1038/nri2925

116. Ehses JA, Böni-Schnetzler M, Faulenbach M et al. Macrophages, cytokines and beta-cell death in Type 2 diabetes. Biochem Soc Trans 2008; 36: 340-342. DOI: 10.1042/bst0360340

117. American Diabetes Association. 9. Pharmacologic Approaches to Glycemic Treatment: Standards of Medical Care in Diabetes—2021. Diabetes Care 2020; 44: S111-S124. DOI: 10.2337/dc21-S009

118. Davies MJ, D'Alessio DA, Fradkin J et al. Management of Hyperglycemia in Type 2 Diabetes, 2018. A Consensus Report by the American Diabetes Association (ADA) and the European Association for the Study of Diabetes (EASD). Diabetes Care 2018; 41: 2669-2701. DOI: 10.2337/dci18-0033

119. Foretz M, Guigas B, Viollet B. Understanding the glucoregulatory mechanisms of metformin in type 2 diabetes mellitus. Nature Reviews Endocrinology 2019; 15: 569-589. DOI: 10.1038/s41574-019-0242-2

120. Rena G, Hardie DG, Pearson ER. The mechanisms of action of metformin. Diabetologia 2017; 60: 1577-1585. DOI: 10.1007/s00125-017-4342-z

121. Foretz M, Guigas B, Bertrand L et al. Metformin: from mechanisms of action to therapies. Cell Metab 2014; 20: 953-966. DOI: 10.1016/j.cmet.2014.09.018

122. Zhou G, Myers R, Li Y et al. Role of AMP-activated protein kinase in mechanism of metformin action. J Clin Invest 2001; 108: 1167-1174. DOI: 10.1172/jci13505

123. Stephenne X, Foretz M, Taleux N et al. Metformin activates AMP-activated protein kinase in primary human hepatocytes by decreasing cellular energy status. Diabetologia 2011; 54: 3101-3110. DOI: 10.1007/s00125-011-2311-5

124. Napolitano A, Miller S, Nicholls AW et al. Novel gut-based pharmacology of metformin in patients with type 2 diabetes mellitus. PLoS One 2014; 9: e100778. DOI: 10.1371/journal.pone.0100778

125. Evia-Viscarra ML, Rodea-Montero ER, Apolinar-Jiménez E et al. The effects of metformin on inflammatory mediators in obese adolescents with insulin resistance: controlled randomized clinical trial. J Pediatr Endocrinol Metab 2012; 25: 41-49. DOI: 10.1515/jpem-2011-0469

126. Fidan E, Onder Ersoz H, Yilmaz M et al. The effects of rosiglitazone and metformin on inflammation and endothelial dysfunction in patients with type 2 diabetes mellitus. Acta Diabetol 2011; 48: 297-302. DOI: 10.1007/s00592-011-0276-y

127. Hoffmann IS, Roa M, Torrico F et al. Ondansetron and metformin-induced gastrointestinal side effects. Am J Ther 2003; 10: 447-451. DOI: 10.1097/00045391-200311000-00012

128. Ashcroft FM, Rorsman P. K(ATP) channels and islet hormone secretion: new insights and controversies. Nat Rev Endocrinol 2013; 9: 660-669. DOI: 10.1038/nrendo.2013.166

129. Holstein A, Plaschke A, Egberts EH. Lower incidence of severe hypoglycaemia in patients with type 2 diabetes treated with glimepiride versus glibenclamide. Diabetes Metab Res Rev 2001; 17: 467-473. DOI: 10.1002/dmrr.235

130. Krentz AJ, Bailey CJ. Oral antidiabetic agents: current role in type 2 diabetes mellitus. Drugs 2005; 65: 385-411. DOI: 10.2165/00003495-200565030-00005

131. Blicklé JF. Meglitinide analogues: a review of clinical data focused on recent trials. Diabetes & Metabolism 2006; 32: 113-120. DOI: https://doi.org/10.1016/S1262-3636(07)70257-4

132. Mata R, Flores-Bocanegra L, Ovalle-Magallanes B et al. Natural products from plants targeting key enzymes for the future development of antidiabetic agents. Nat Prod Rep 2023; 40: 1198-1249. DOI: 10.1039/d3np00007a

133. Deacon CF. Physiology and Pharmacology of DPP-4 in Glucose Homeostasis and the Treatment of Type 2 Diabetes. Front Endocrinol (Lausanne) 2019; 10: 80. DOI: 10.3389/fendo.2019.00080

134. Lee MMY, Sattar N. A review of current key guidelines for managing high-risk patients with diabetes and heart failure and future prospects. Diabetes Obes Metab 2023; 25 Suppl 3: 33-47. DOI: 10.1111/dom.15085

135. Chen LH, Leung PS. Inhibition of the sodium glucose co-transporter-2: its beneficial action and potential combination therapy for type 2 diabetes mellitus. Diabetes Obes Metab 2013; 15: 392-402. DOI: 10.1111/dom.12064

136. Xu B, Li S, Kang B et al. The current role of sodium-glucose cotransporter 2 inhibitors in type 2 diabetes mellitus management. Cardiovasc Diabetol 2022; 21: 83. DOI: 10.1186/s12933-022-01512-w

137. Zinman B, Wanner C, Lachin JM et al. Empagliflozin, Cardiovascular Outcomes, and Mortality in Type 2 Diabetes. N Engl J Med 2015; 373: 2117-2128. DOI: 10.1056/NEJMoa1504720

138. Olszewski J, Kozon K, Patyra A. Flozins in heart failurea new reimbursement indication. Biuletyn Wydziału Farmaceutycznego Warszawskiego Uniwersytetu Medycznego 2022; 1: 19-25.

139. Ghani U. Re-exploring promising α-glucosidase inhibitors for potential development into oral anti-diabetic drugs: Finding needle in the haystack. European Journal of Medicinal Chemistry 2015; 103: 133-162. DOI: 10.1016/j.ejmech.2015.08.043

140. Dowarah J, Singh VP. Anti-diabetic drugs recent approaches and advancements. Bioorganic and Medicinal Chemistry 2020; 28. DOI: 10.1016/j.bmc.2019.115263

141. Mushtaq A, Azam U, Mehreen S et al. Synthetic α-glucosidase inhibitors as promising anti-diabetic agents: Recent developments and future challenges. European Journal of Medicinal Chemistry 2023; 249: 115119. DOI: https://doi.org/10.1016/j.ejmech.2023.115119

142. Furman BL, Candasamy M, Bhattamisra SK et al. Reduction of blood glucose by plant extracts and their use in the treatment of diabetes

mellitus; discrepancies in effectiveness between animal and human studies. J Ethnopharmacol 2020; 247: 112264. DOI: 10.1016/j.jep.2019.112264

143. Farazi M, Houghton MJ, Murray M et al. A systematic review of the inhibitory effect of extracts from edible parts of nuts on α-glucosidase activity. Food Funct 2023; 14: 5962-5976. DOI: 10.1039/d3fo00328k

144. Bailey CJ. Metformin: historical overview. Diabetologia 2017; 60: 1566-1576. DOI: 10.1007/s00125-017-4318-z

145. Tony SK, Hassan MS, Ismail HA et al. Effect of anthocyanin-rich blackberry juice on endoplasmic reticulum stress in streptozotocin-induced diabetic rats. Environ Sci Pollut Res Int 2023; 30: 79067-79081. DOI: 10.1007/s11356-023-27827-z

146. Youl E, Bardy G, Magous R et al. Quercetin potentiates insulin secretion and protects INS-1 pancreatic beta-cells against oxidative damage via the ERK1/2 pathway. Br J Pharmacol 2010; 161: 799-814. DOI: 10.1111/j.1476-5381.2010.00910.x

147. Bardy G, Virsolvy A, Quignard JF et al. Quercetin induces insulin secretion by direct activation of L-type calcium channels in pancreatic beta cells. Br J Pharmacol 2013; 169: 1102-1113. DOI: 10.1111/bph.12194

148. Dias Soares JM, Pereira Leal AEB, Silva JC et al. Influence of flavonoids on mechanism of modulation of insulin secretion. Pharmacognosy Magazine 2017; 13: 639-646. DOI: 10.4103/pm.pm_87_17

149. Lee D, Kim YM, Kim HW et al. Schisandrin C Affects Glucose-Stimulated Insulin Secretion in Pancreatic β-Cells and Glucose Uptake in Skeletal Muscle Cells. Molecules 2021; 26. DOI: 10.3390/molecules26216509

150. Xu Z, Gu C, Wang K et al. Arctigenic acid, the key substance responsible for the hypoglycemic activity of Fructus Arctii. Phytomedicine 2015; 22: 128-137. DOI: 10.1016/j.phymed.2014.11.006

151. Xu Z, Ju J, Wang K et al. Evaluation of hypoglycemic activity of total lignans from Fructus Arctii in the spontaneously diabetic Goto-Kakizaki rats. J Ethnopharmacol 2014; 151: 548-555. DOI: 10.1016/j.jep.2013.11.021

152. Wang LY, Cheng KC, Li Y et al. The Dietary Furocoumarin Imperatorin Increases Plasma GLP-1 Levels in Type 1-Like Diabetic Rats. Nutrients 2017; 9. DOI: 10.3390/nu9111192

153. Park JE, Kim SY, Han JS. Scopoletin stimulates the secretion of insulin via a KATP channel-dependent pathway in INS-1 pancreatic beta cells. J Pharm Pharmacol 2022; 74: 1274-1281. DOI: 10.1093/jpp/rgab143

154. Ahmed S, Nur EAM, Parveen I et al. Stimulation of insulin secretion by 5-methylcoumarins and its sulfur analogues isolated from Clutia lanceolata Forssk. Phytochemistry 2020; 170: 112213. DOI: 10.1016/j.phytochem.2019.112213

155. Bayle M, Neasta J, Dall'Asta M et al. The ellagitannin metabolite urolithin C is a glucose-dependent regulator of insulin secretion through activation of L-type calcium channels. Br J

Pharmacol 2019; 176: 4065-4078. DOI: 10.1111/bph.14821

156. Park EY, Kim EH, Kim CY et al. Angelica dahurica Extracts Improve Glucose Tolerance through the Activation of GPR119. PLoS One 2016; 11: e0158796. DOI: 10.1371/journal.pone.0158796

157. Leu YL, Chen YW, Yang CY et al. Extract isolated from Angelica hirsutiflora with insulin secretagogue activity. J Ethnopharmacol 2009; 123: 208-212. DOI: 10.1016/j.jep.2009.03.027

158. Kim HS, Lee D, Seo YH et al. Chemical Constituents from the Roots of Angelica reflexa That Improve Glucose-Stimulated Insulin Secretion by Regulating Pancreatic β-Cell Metabolism. Pharmaceutics 2023; 15. DOI: 10.3390/pharmaceutics15041239

159. Dewick PM. Medicinal Natural Products: A Biosynthetic Approach. Wiley; 2011.

160. Dall'Asta M, Bayle M, Neasta J et al. Protection of pancreatic β-cell function by dietary polyphenols. Phytochemistry Reviews 2015; 14: 933-959. DOI: 10.1007/s11101-015-9429-x

161. Harborne JB. The Flavonoids: Advances in Research Since 1986. Chapman & Hall/CRC; 1999.

162. Haytowitz D, Bhagwat S, Gebhardt J. Sources of Flavonoids in the U.S. Diet Using USDA's Updated Database on the Flavonoid Content of Selected Foods. Journal of Nutrition 2007.

163. Ben Hsouna A, Sadaka C, Generalić Mekinić I et al. The Chemical Variability, Nutraceutical Value, and Food-Industry and Cosmetic Applications of Citrus Plants: A Critical Review. Antioxidants (Basel) 2023; 12. DOI: 10.3390/antiox12020481

164. Boué SM, Wiese TE, Nehls S et al. Evaluation of the Estrogenic Effects of Legume Extracts Containing Phytoestrogens. Journal of Agricultural and Food Chemistry 2003; 51: 2193-2199. DOI: 10.1021/jf021114s

165. Chun OK, Chung SJ, Song WO. Estimated Dietary Flavonoid Intake and Major Food Sources of U.S. Adults1,2. The Journal of Nutrition 2007; 137: 1244-1252. DOI: https://doi.org/10.1093/jn/137.5.1244

166. Cerezo AB, Tesfaye W, Soria-Díaz ME et al. Effect of wood on the phenolic profile and sensory properties of wine vinegars during ageing. Journal of Food Composition and Analysis 2010; 23: 175-184. DOI: https://doi.org/10.1016/j.jfca.2009.08.008

167. Vessal M, Hemmati M, Vasei M. Antidiabetic effects of quercetin in streptozocin-induced diabetic rats. Comp Biochem Physiol C Toxicol Pharmacol 2003; 135c: 357-364. DOI: 10.1016/s1532-0456(03)00140-6

168. Coskun O, Kanter M, Korkmaz A et al. Quercetin, a flavonoid antioxidant, prevents and protects streptozotocin-induced oxidative stress and beta-cell damage in rat pancreas. Pharmacol Res 2005; 51: 117-123. DOI: 10.1016/j.phrs.2004.06.002

169. Adewole SO, Caxton-Martins EA, Ojewole JA. Protective effect of quercetin on the morphology of

pancreatic beta-cells of streptozotocin-treated diabetic rats. Afr J Tradit Complement Altern Med 2006; 4: 64-74. DOI: 10.4314/ajtcam.v4i1.31196

170. Kobori M, Masumoto S, Akimoto Y et al. Dietary quercetin alleviates diabetic symptoms and reduces streptozotocin-induced disturbance of hepatic gene expression in mice. Mol Nutr Food Res 2009; 53: 859-868. DOI: 10.1002/mnfr.200800310

171. Kim JH, Kang MJ, Choi HN et al. Quercetin attenuates fasting and postprandial hyperglycemia in animal models of diabetes mellitus. Nutr Res Pract 2011; 5: 107-111. DOI: 10.4162/nrp.2011.5.2.107

172. Li JM, Wang W, Fan CY et al. Quercetin Preserves β -Cell Mass and Function in Fructose-Induced Hyperinsulinemia through Modulating Pancreatic Akt/FoxO1 Activation. Evid Based Complement Alternat Med 2013; 2013: 303902. DOI: 10.1155/2013/303902

173. Jeong SM, Kang MJ, Choi HN et al. Quercetin ameliorates hyperglycemia and dyslipidemia and improves antioxidant status in type 2 diabetic db/db mice. Nutr Res Pract 2012; 6: 201-207. DOI: 10.4162/nrp.2012.6.3.201

174. Al-Numair KS, Chandramohan G, Veeramani C et al. Ameliorative effect of kaempferol, a flavonoid, on oxidative stress in streptozotocin-induced diabetic rats. Redox Rep 2015; 20: 198-209. DOI: 10.1179/1351000214y.0000000117

175. Prasath GS, Sundaram CS, Subramanian SP. Fisetin averts oxidative stress in pancreatic tissues of streptozotocin-induced diabetic rats. Endocrine 2013; 44: 359-368. DOI: 10.1007/s12020-012-9866-x

176. Bhattacharya S, Oksbjerg N, Young JF et al. Caffeic acid, naringenin and quercetin enhance glucose-stimulated insulin secretion and glucose sensitivity in INS-1E cells. Diabetes Obes Metab 2014; 16: 602-612. DOI: 10.1111/dom.12236

177. Youl E, Magous R, Cros G et al. MAP Kinase cross talks in oxidative stress-induced impairment of insulin secretion. Involvement in the protective activity of quercetin. Fundam Clin Pharmacol 2014; 28: 608-615. DOI: 10.1111/fcp.12078

178. Dai X, Ding Y, Zhang Z et al. Quercetin and quercitrin protect against cytokine-induced injuries in RINm5F β-cells via the mitochondrial pathway and NF-κB signaling. Int J Mol Med 2013; 31: 265-271. DOI: 10.3892/ijmm.2012.1177

179. Cho JM, Chang SY, Kim DB et al. Effects of physiological quercetin metabolites on interleukin-1β-induced inducible NOS expression. J Nutr Biochem 2012; 23: 1394-1402. DOI: 10.1016/j.jnutbio.2011.08.007

180. Lee JH, Song MY, Song EK et al. Overexpression of SIRT1 protects pancreatic beta-cells against cytokine toxicity by suppressing the nuclear factor-kappaB signaling pathway. Diabetes 2009; 58: 344-351. DOI: 10.2337/db07-1795

181. Zhang Y, Liu D. Flavonol kaempferol improves chronic hyperglycemia-impaired pancreatic beta-cell viability and insulin secretory function. Eur J

Pharmacol 2011; 670: 325-332. DOI: 10.1016/j.ejphar.2011.08.011

182. Zhang Y, Zhen W, Maechler P et al. Small molecule kaempferol modulates PDX-1 protein expression and subsequently promotes pancreatic β-cell survival and function via CREB. J Nutr Biochem 2013; 24: 638-646. DOI: 10.1016/j.jnutbio.2012.03.008

183. Li Y, Zheng X, Yi X et al. Myricetin: a potent approach for the treatment of type 2 diabetes as a natural class B GPCR agonist. Faseb j 2017; 31: 2603-2611. DOI: 10.1096/fj.201601339R

184. Dubey R, Kulkarni SH, Dantu SC et al. Myricetin protects pancreatic β-cells from human islet amyloid polypeptide (hIAPP) induced cytotoxicity and restores islet function. Biol Chem 2021; 402: 179-194. DOI: 10.1515/hsz-2020-0176

185. Kappel VD, Frederico MJ, Postal BG et al. The role of calcium in intracellular pathways of rutin in rat pancreatic islets: potential insulin secretagogue effect. Eur J Pharmacol 2013; 702: 264-268. DOI: 10.1016/j.ejphar.2013.01.055

186. Lee JS. Effects of soy protein and genistein on blood glucose, antioxidant enzyme activities, and lipid profile in streptozotocin-induced diabetic rats. Life Sci 2006; 79: 1578-1584. DOI: 10.1016/j.lfs.2006.06.030

187. Fu Z, Zhang W, Zhen W et al. Genistein induces pancreatic beta-cell proliferation through activation of multiple signaling pathways and prevents insulin-deficient diabetes in mice. Endocrinology 2010; 151: 3026-3037. DOI: 10.1210/en.2009-1294

188. Elmarakby AA, Ibrahim AS, Faulkner J et al. Tyrosine kinase inhibitor, genistein, reduces renal inflammation and injury in streptozotocin-induced diabetic mice. Vascul Pharmacol 2011; 55: 149-156. DOI: 10.1016/j.vph.2011.07.007

189. Fu Z, Gilbert ER, Pfeiffer L et al. Genistein ameliorates hyperglycemia in a mouse model of nongenetic type 2 diabetes. Appl Physiol Nutr Metab 2012; 37: 480-488. DOI: 10.1139/h2012-005

190. Lee SJ, Kim HE, Choi SE et al. Involvement of Ca2+/calmodulin kinase II (CaMK II) in genistein-induced potentiation of leucine/glutamine-stimulated insulin secretion. Mol Cells 2009; 28: 167-174. DOI: 10.1007/s10059-009-0119-7

191. Kim EK, Kwon KB, Song MY et al. Genistein protects pancreatic beta cells against cytokine-mediated toxicity. Mol Cell Endocrinol 2007; 278: 18-28. DOI: 10.1016/j.mce.2007.08.003

192. Choi MS, Jung UJ, Yeo J et al. Genistein and daidzein prevent diabetes onset by elevating insulin level and altering hepatic gluconeogenic and lipogenic enzyme activities in non-obese diabetic (NOD) mice. Diabetes Metab Res Rev 2008; 24: 74-81. DOI: 10.1002/dmrr.780

193. Ae Park S, Choi MS, Cho SY et al. Genistein and daidzein modulate hepatic glucose and lipid regulating enzyme activities in C57BL/KsJ-db/db mice. Life Sci 2006; 79: 1207-1213. DOI: 10.1016/j.lfs.2006.03.022

194. Liu D, Zhen W, Yang Z et al. Genistein acutely stimulates insulin secretion in

pancreatic beta-cells through a cAMP-dependent protein kinase pathway. Diabetes 2006; 55: 1043-1050. DOI: 10.2337/diabetes.55.04.06.db05-1089

195. Panda S, Kar A. Apigenin (4',5,7-trihydroxyflavone) regulates hyperglycaemia, thyroid dysfunction and lipid peroxidation in alloxan-induced diabetic mice. J Pharm Pharmacol 2007; 59: 1543-1548. DOI: 10.1211/jpp.59.11.0012

196. Rauter AP, Martins A, Borges C et al. Antihyperglycaemic and protective effects of flavonoids on streptozotocin-induced diabetic rats. Phytother Res 2010; 24 Suppl 2: S133-138. DOI: 10.1002/ptr.3017

197. Kim EK, Kwon KB, Song MY et al. Flavonoids protect against cytokine-induced pancreatic beta-cell damage through suppression of nuclear factor kappaB activation. Pancreas 2007; 35: e1-9. DOI: 10.1097/mpa.0b013e31811ed0d2

198. Suh KS, Oh S, Woo JT et al. Apigenin attenuates 2-deoxy-D-ribose-induced oxidative cell damage in HIT-T15 pancreatic β-cells. Biol Pharm Bull 2012; 35: 121-126. DOI: 10.1248/bpb.35.121

199. Ihim SA, Kaneko YK, Yamamoto M et al. Apigenin Alleviates Endoplasmic Reticulum Stress-Mediated Apoptosis in INS-1 β-Cells. Biol Pharm Bull 2023; 46: 630-635. DOI: 10.1248/bpb.b22-00913

200. Subash-Babu P, Abdulaziz AlSedairy S, Abdulaziz Binobead M et al. Luteolin-7-O-rutinoside Protects RIN-5F Cells from High-Glucose-Induced Toxicity, Improves Glucose Homeostasis in L6 Myotubes, and Prevents Onset of Type 2 Diabetes. Metabolites 2023; 13. DOI: 10.3390/metabo13020269

201. Wu W, He S, Shen Y et al. Natural Product Luteolin Rescues THAP-Induced Pancreatic β-Cell Dysfunction through HNF4α Pathway. Am J Chin Med 2020; 48: 1435-1454. DOI: 10.1142/s0192415x20500706

202. Lin CY, Ni CC, Yin MC et al. Flavonoids protect pancreatic beta-cells from cytokines mediated apoptosis through the activation of PI3-kinase pathway. Cytokine 2012; 59: 65-71. DOI: 10.1016/j.cyto.2012.04.011

203. Sharma AK, Bharti S, Ojha S et al. Up-regulation of PPARγ, heat shock protein-27 and -72 by naringin attenuates insulin resistance, β-cell dysfunction, hepatic steatosis and kidney damage in a rat model of type 2 diabetes. Br J Nutr 2011; 106: 1713-1723. DOI: 10.1017/s000711451100225x

204. Mahmoud AM, Ashour MB, Abdel-Moneim A et al. Hesperidin and naringin attenuate hyperglycemia-mediated oxidative stress and proinflammatory cytokine production in high fat fed/streptozotocin-induced type 2 diabetic rats. J Diabetes Complications 2012; 26: 483-490. DOI: 10.1016/j.jdiacomp.2012.06.001

205. Annadurai T, Thomas PA, Geraldine P. Ameliorative effect of naringenin on hyperglycemia-mediated inflammation in hepatic and pancreatic tissues of Wistar rats with streptozotocin- nicotinamide-induced experimental diabetes mellitus. Free Radic Res 2013; 47: 793-803. DOI: 10.3109/10715762.2013.823643

206. Rodriguez-Garcia C, Sanchez-Quesada C, Toledo E et al. Naturally Lignan-Rich Foods: A Dietary Tool for Health Promotion? Molecules 2019; 24. DOI: 10.3390/molecules24050917

207. Willfor SM, Smeds AI, Holmbom BR. Chromatographic analysis of lignans. J Chromatogr A 2006; 1112: 64-77. DOI: 10.1016/j.chroma.2005.11.054

208. Holmbom B, Eckerman C, Eklund P et al. Knots in trees – A new rich source of lignans. Phytochemistry Reviews 2003; 2: 331-340. DOI: 10.1023/B:PHYT.0000045493.95074.a8

209. Ward RS. Recent Advances in the Chemistry of Lignans. In: Atta ur R, ed. Bioactive Natural Products (Part E). Elsevier; 2000: 739-798. DOI: 10.1016/s1572-5995(00)80054-x

210. Zalesak F, Bon DJD, Pospisil J. Lignans and Neolignans: Plant secondary metabolites as a reservoir of biologically active substances. Pharmacol Res 2019; 146: 104284. DOI: 10.1016/j.phrs.2019.104284

211. Adlercreutz H. Lignans and human health. Crit Rev Clin Lab Sci 2007; 44: 483-525. DOI: 10.1080/10408360701612942

212. Flower G, Fritz H, Balneaves LG et al. Flax and Breast Cancer: A Systematic Review. Integr Cancer Ther 2014; 13: 181-192. DOI: 10.1177/1534735413502076

213. DeLuca JAA, Garcia-Villatoro EL, Allred CD. Flaxseed Bioactive Compounds and Colorectal Cancer Prevention. Curr Oncol Rep 2018; 20: 59. DOI: 10.1007/s11912-018-0704-z

214. Xia M, Chen Y, Li W et al. Lignan intake and risk of cardiovascular disease and type 2 diabetes: a meta-analysis of prospective cohort studies. International Journal of Food Sciences and Nutrition 2023; 1-9. DOI: 10.1080/09637486.2023.2220985

215. Zhai L, Wang X. Syringaresinol-di-O-β-D-glucoside, a phenolic compound from Polygonatum sibiricum, exhibits an antidiabetic and antioxidative effect on a streptozotocin-induced mouse model of diabetes. Mol Med Rep 2018; 18: 5511-5519. DOI: 10.3892/mmr.2018.9580

216. Hano C, Renouard S, Molinié R et al. Flaxseed (Linum usitatissimum L.) extract as well as (+)-secoisolariciresinol diglucoside and its mammalian derivatives are potent inhibitors of α-amylase activity. Bioorg Med Chem Lett 2013; 23: 3007-3012. DOI: 10.1016/j.bmcl.2013.03.029

217. Wikul A, Damsud T, Kataoka K et al. (+)-Pinoresinol is a putative hypoglycemic agent in defatted sesame (Sesamum indicum) seeds though inhibiting α-glucosidase. Bioorg Med Chem Lett 2012; 22: 5215-5217. DOI: 10.1016/j.bmcl.2012.06.068

218. Rasouli H, Hosseini-Ghazvini SM, Adibi H et al. Differential α-amylase/α-glucosidase inhibitory activities of plant-derived phenolic compounds: a virtual screening perspective for the treatment of obesity and diabetes. Food Funct 2017; 8: 1942-1954. DOI: 10.1039/c7fo00220c

219. Barre DE, Mizier-Barre KA. Lignans' Potential in Pre and Post-onset Type 2 Diabetes Management. Curr Diabetes Rev 2019; 16: 2-11. DOI:

10.2174/1573399814666180914094520

220. Farjon A. A Handbook of the World's Conifers. Leiden, The Netherlands: Brill; 2010. DOI: 10.1163/9789047430629

221. Zajączkowski GJ, M.; Jabłoński, T.; Szmidla, H.; Kowalska, A.; Małachowska, J.; Piwnicki, J. Raport o stanie lasów w Polsce 2020. In: Warsaw, Poland: Państwowe Gospodarstwo Leśne Lasy Państwowe; 2021:

222. Farjon A, Filer D. An Atlas of the World's Conifers. Leiden, The Netherlands: Brill; 2013. DOI: 10.1163/9789004211810

223. Brus DJ, Hengeveld GM, Walvoort DJJ et al. Statistical mapping of tree species over Europe. European Journal of Forest Research 2012; 131: 145-157. DOI: 10.1007/s10342-011-0513-5

224. Rosik-Dulewska C, PWN. WN. Podstawy gospodarki odpadami. Warsaw, Poland: Wydawnictwo Naukowe PWN; 2015.

225. Mantau U. Wood flow analysis: Quantification of resource potentials, cascades and carbon effects. Biomass and Bioenergy 2015; 79: 28-38. DOI: 10.1016/j.biombioe.2014.08.013

226. Hassan MK, Villa A, Kuittinen S et al. An assessment of side-stream generation from Finnish forest industry. Journal of Material Cycles and Waste Management 2018; 21: 265-280. DOI: 10.1007/s10163-018-0787-5

227. Holmbom B, Willfoer S, Hemming J et al. Knots in Trees: A Rich Source of Bioactive Polyphenols. In: Materials, Chemicals, and Energy from Forest Biomass. American Chemical Society; 2007: 350-362. DOI: doi:10.1021/bk-2007-0954.ch022

10.1021/bk-2007-0954.ch022

228. Kumar R, Tsvetkov DE, Varshney VK et al. Chemical constituents from temperate and subtropical trees with reference to knotwood. Industrial Crops and Products 2020; 145. DOI: 10.1016/j.indcrop.2019.112077

229. Lunder M, Roskar I, Hosek J et al. Silver Fir (Abies alba) Extracts Inhibit Enzymes Involved in Blood Glucose Management and Protect against Oxidative Stress in High Glucose Environment. Plant Foods Hum Nutr 2019; 74: 47-53. DOI: 10.1007/s11130-018-0698-6

230. Huang XX, Bai M, Zhou L et al. Food Byproducts as a New and Cheap Source of Bioactive Compounds: Lignans with Antioxidant and Anti-inflammatory Properties from Crataegus pinnatifida Seeds. J Agric Food Chem 2015; 63: 7252-7260. DOI: 10.1021/acs.jafc.5b02835

231. Sammartino A, Tommaselli GA, Gargano V et al. Short-term effects of a combination of isoflavones, lignans and Cimicifuga racemosa on climacteric-related symptoms in postmenopausal women: a double-blind, randomized, placebo-controlled trial. Gynecol Endocrinol 2006; 22: 646-650. DOI: 10.1080/09513590601010722

232. Vo QV, Nam PC, Bay MV et al. Density functional theory study of the role of benzylic hydrogen atoms in the antioxidant properties of lignans. Sci

Rep 2018; 8: 12361. DOI: 10.1038/s41598-018-30860-5

233. Willför S, Reunanen M, Eklund P et al. Oligolignans in Norway spruce and Scots pine knots and Norway spruce stemwood. Holzforschung 2004; 58: 345-354. DOI: 10.1515/hf.2004.053

234. Cosentino M, Marino F, Maio RC et al. Immunomodulatory activity of the lignan 7-hydroxymatairesinol potassium acetate (HMR/lignan) extracted from the heartwood of Norway spruce (Picea abies). Int Immunopharmacol 2010; 10: 339-343. DOI: 10.1016/j.intimp.2009.12.005

235. Smeds AI, Eklund PC, Sjoholm RE et al. Quantification of a broad spectrum of lignans in cereals, oilseeds, and nuts. J Agric Food Chem 2007; 55: 1337-1346. DOI: 10.1021/jf0629134

236. Biasiotto G, Zanella I, Predolini F et al. 7-Hydroxymatairesinol improves body weight, fat and sugar metabolism in C57BJ/6 mice on a high-fat diet. Br J Nutr 2018; 120: 751-762. DOI: 10.1017/S0007114518001824

237. Nistor Baldea LA, Martineau LC, Benhaddou-Andaloussi A et al. Inhibition of intestinal glucose absorption by anti-diabetic medicinal plants derived from the James Bay Cree traditional pharmacopeia. J Ethnopharmacol 2010; 132: 473-482. DOI: 10.1016/j.jep.2010.07.055

238. Spoor DC, Martineau LC, Leduc C et al. Selected plant species from the Cree pharmacopoeia of northern Quebec possess anti-diabetic potential. Can J Physiol Pharmacol 2006; 84: 847-858. DOI: 10.1139/y06-018

239. Harbilas D, Vallerand D, Brault A et al. Larix laricina, an Antidiabetic Alternative Treatment from the Cree of Northern Quebec Pharmacopoeia, Decreases Glycemia and Improves Insulin Sensitivity In Vivo. Evid Based Complement Alternat Med 2012; 2012: 296432. DOI: 10.1155/2012/296432

240. Shang N, Guerrero-Analco JA, Musallam L et al. Adipogenic constituents from the bark of Larix laricina du Roi (K. Koch; Pinaceae), an important medicinal plant used traditionally by the Cree of Eeyou Istchee (Quebec, Canada) for the treatment of type 2 diabetes symptoms. J Ethnopharmacol 2012; 141: 1051-1057. DOI: 10.1016/j.jep.2012.04.002

241. D'Andrea G. Pycnogenol: a blend of procyanidins with multifaceted therapeutic applications? Fitoterapia 2010; 81: 724-736. DOI: 10.1016/j.fitote.2010.06.011

242. Shimada T, Tokuhara D, Tsubata M et al. Flavangenol (pine bark extract) and its major component procyanidin B1 enhance fatty acid oxidation in fat-loaded models. Eur J Pharmacol 2012; 677: 147-153. DOI: 10.1016/j.ejphar.2011.12.034

243. Poussard S, Pires-Alves A, Diallo R et al. A natural antioxidant pine bark extract, Oligopin(R), regulates the stress chaperone HSPB1 in human skeletal muscle cells: a proteomics approach. Phytother Res 2013; 27: 1529-1535. DOI: 10.1002/ptr.4895

244. Benković ET, Grohar T, Žigon D et al. Chemical composition of the silver fir (Abies alba) bark extract Abigenol® and its antioxidant activity. Industrial Crops

and Products 2014; 52: 23-28. DOI: 10.1016/j.indcrop.2013.10.005

245. Skowrońska W, Granica S, Dziedzic M et al. Arctium lappa and Arctium tomentosum, Sources of Arctii radix: Comparison of Anti-Lipoxygenase and Antioxidant Activity as well as the Chemical Composition of Extracts from Aerial Parts and from Roots. Plants (Basel) 2021; 10. DOI: 10.3390/plants10010078

246. Chan YS, Cheng LN, Wu JH et al. A review of the pharmacological effects of Arctium lappa (burdock). Inflammopharmacology 2011; 19: 245-254. DOI: 10.1007/s10787-010-0062-4

247. Yan L, Li Y. Effects of extract from Fructus Arctii on blood glucose and immune function in mice. Northwest Pharm J 1993; 8: 75-78.

248. Xu Z, Li T, Deng Y et al. Studies on hypoglycemic activity of a Chinese herbal medicine–Fructus Arctii. Chin Tradit Herbal Drugs 2005; 36: 1043-1045.

249. Xu Z, Wang X, Zhou M et al. The antidiabetic activity of total lignan from Fructus Arctii against alloxan-induced diabetes in mice and rats. Phytotherapy Research 2008; 22: 97-101. DOI: https://doi.org/10.1002/ptr.2273

250. Annunziata G, Barrea L, Ciampaglia R et al. Arctium lappa contributes to the management of type 2 diabetes mellitus by regulating glucose homeostasis and improving oxidative stress: A critical review of in vitro and in vivo animal-based studies. Phytotherapy Research 2019; 33: 2213-2220. DOI: https://doi.org/10.1002/ptr.6416

251. Tousch D, Bidel LP, Cazals G et al. Chemical analysis and antihyperglycemic activity of an original extract from burdock root (Arctium lappa). J Agric Food Chem 2014; 62: 7738-7745. DOI: 10.1021/jf500926v

252. Tang X, Zhuang J, Chen J et al. Arctigenin efficiently enhanced sedentary mice treadmill endurance. PLoS One 2011; 6: e24224. DOI: 10.1371/journal.pone.0024224

253. Zhang JY, Mei JW, Wang HY et al. Chromatographic fingerprint combined with quantitative analysis of multi-components by single-marker for quality control of total lignans from Fructus arctii by high-performance liquid chromatography. Phytochem Anal 2022; 33: 1214-1224. DOI: 10.1002/pca.3172

254. Asgarpanah J, Kazemivash N. Phytochemistry, pharmacology and medicinal properties of Carthamus tinctorius L. Chin J Integr Med 2013; 19: 153-159. DOI: 10.1007/s11655-013-1354-5

255. Delshad E, Yousefi M, Sasannezhad P et al. Medical uses of Carthamus tinctorius L. (Safflower): a comprehensive review from Traditional Medicine to Modern Medicine. Electron Physician 2018; 10: 6672-6681. DOI: 10.19082/6672

256. Zhang LL, Tian K, Tang ZH et al. Phytochemistry and Pharmacology of Carthamus tinctorius L. Am J Chin Med 2016; 44: 197-226. DOI: 10.1142/s0192415x16500130

257. Zafari M, Ebadi A, Jahanbakhsh S et al. Safflower (Carthamus tinctorius) Biochemical Properties, Yield, and Oil

Content Affected by 24-Epibrassinosteroid and Genotype under Drought Stress. J Agric Food Chem 2020; 68: 6040-6047. DOI: 10.1021/acs.jafc.9b06860

258. Qian XJ, Jin YS, Chen HS et al. Trachelogenin, a novel inhibitor of hepatitis C virus entry through CD81. J Gen Virol 2016; 97: 1134-1144. DOI: 10.1099/jgv.0.000432

259. Moura AF, Lima KSB, Sousa TS et al. In vitro antitumor effect of a lignan isolated from Combretum fruticosum, trachelogenin, in HCT-116 human colon cancer cells. Toxicol In Vitro 2018; 47: 129-136. DOI: 10.1016/j.tiv.2017.11.014

260. Yoo HH, Park JH, Kwon SW. An anti-estrogenic lignan glycoside, tracheloside, from seeds of Carthamus tinctorius. Biosci Biotechnol Biochem 2006; 70: 2783-2785. DOI: 10.1271/bbb.60290

261. Huang Y.H. LJT, Zan K., Wang J., Fu Q. The traditional uses, secondary metabolites, and pharmacology of Eleutherococcus species. Phytochemistry Reviews 2021. DOI: https://doi.org/10.1007/s11101-021-09775-z

262. Davydov M. KAD. Eleutherococcus senticosus (Rupr. & Maxim.) Maxim. (Araliaceae) as an adaptogen: a closer look. Journal of Ethnopharmacology 2000; 72: 345–393.

263. Huang L. ZH, Huang B., Zheng C., Peng W., Qin L. . Acanthopanax senticosus: review of botany, chemistry and pharmacology Pharmazie 2011; 83-97.

264. Shi X. YY, Ren H., Sun S., Mu L.T., Chen X., Wang Y., Zhang Y., Wang L.H., Sun C. Identification of multiple components in deep eutectic solvent extract of Acanthopanax senticosus root by ultra-high-performance liquid chromatography with quadrupole orbitrap mass spectrometry. Phytochemistry Letters 2020; 35: 175-185.

265. Huang L.Z. HBK, Ye Q., Qin L.P. Bioactivity-guided fractionation for anti-fatigue property of Acanthopanax senticosus. Journal of Ethnopharmacology 2011; 133: 213–219.

266. Jia A. ZY, Gao H., Zhang Z., Zhang Y., Wang Z., Zhang J., Deng B., Qiu Z., Fu C. . A review of Acanthopanax senticosus (Rupr and Maxim.) Harms: From ethnopharmacological use to modern application. Journal of Ethnopharmacology 2021 Mar 25.

267. Zhang L, Li BB, Li HZ et al. Four new neolignans isolated from Eleutherococcus senticosus and their protein tyrosine phosphatase 1B inhibitory activity (PTP1B). Fitoterapia 2017; 121: 58-63. DOI: 10.1016/j.fitote.2017.06.025

268. Panossian A. Understanding adaptogenic activity: specificity of the pharmacological action of adaptogens and other phytochemicals. Ann N Y Acad Sci 2017; 1401: 49-64. DOI: 10.1111/nyas.13399

269. Panossian A, Wagner H. Stimulating effect of adaptogens: an overview with particular reference to their efficacy following single dose administration. Phytother Res 2005; 19: 819-838. DOI: 10.1002/ptr.1751

270. Panossian A, Wikman G. Evidence-based efficacy of adaptogens in

fatigue, and molecular mechanisms related to their stress-protective activity. Curr Clin Pharmacol 2009; 4: 198-219. DOI: 10.2174/157488409789375311

271. Community herbal monograph on Eleutherococcus senticosus (Rupr. et Maxim.) Maxim. r. In: EMA/HMPC/680618/2013:

272. Park JY, Ji HD, Lee WM et al. Anti-diabetic effects of fermented Acanthopanax senticosus extracts on rats with streptozotocin-induced type 1 diabetic mellitus. J Med Plants Res 2013; 7: 1994-2000. DOI: 10.5897/JMPR12.784

273. Hong JH, Cha YS, Rhee SJ. Effects of the Cellcultured Acanthopanax senticosus Extract on Antioxidative Defense System and Membrane Fluidity in the Liver of Type 2 Diabetes Mouse. J Clin Biochem Nutr 2009; 45: 101-109. DOI: 10.3164/jcbn.08-263

274. Maria João M, Lourdes S, Eugenio U et al. Coumarins — An Important Class of Phytochemicals. In: Rao AV, Leticia GR, eds. Phytochemicals. Rijeka: IntechOpen; 2015: Ch. 5. DOI: 10.5772/59982

275. Hu Y, Wang B, Yang J et al. Synthesis and biological evaluation of 3-arylcoumarin derivatives as potential anti-diabetic agents. J Enzyme Inhib Med Chem 2019; 34: 15-30. DOI: 10.1080/14756366.2018.1518958

276. Channa Basappa V, Hamse Kameshwar V, Kumara K et al. Design and synthesis of coumarin-triazole hybrids: biocompatible anti-diabetic agents, in silico molecular docking and ADME screening. Heliyon 2020; 6: e05290. DOI: 10.1016/j.heliyon.2020.e05290

277. Sepehri N, Mohammadi-Khanaposhtani M, Asemanipoor N et al. Synthesis, characterization, molecular docking, and biological activities of coumarin-1,2,3-triazole-acetamide hybrid derivatives. Arch Pharm (Weinheim) 2020; 353: e2000109. DOI: 10.1002/ardp.202000109

278. Kumar V, Ahmed D, Verma A et al. Umbelliferone β-D-galactopyranoside from Aegle marmelos (L.) corr. an ethnomedicinal plant with antidiabetic, antihyperlipidemic and antioxidative activity. BMC Complement Altern Med 2013; 13: 273. DOI: 10.1186/1472-6882-13-273

279. Ramu R, P SS, S NS et al. Assessment of In Vivo Antidiabetic Properties of Umbelliferone and Lupeol Constituents of Banana (Musa sp. var. Nanjangud Rasa Bale) Flower in Hyperglycaemic Rodent Model. PLoS One 2016; 11: e0151135. DOI: 10.1371/journal.pone.0151135

280. Vinayagam R, Xu B. 7, 8-Dihydroxycoumarin (daphnetin) protects INS-1 pancreatic beta-cells against streptozotocin-induced apoptosis. Phytomedicine 2017; 24: 119-126. DOI: 10.1016/j.phymed.2016.11.023

281. Adebajo AC, Iwalewa EO, Obuotor EM et al. Pharmacological properties of the extract and some isolated compounds of Clausena lansium stem bark: anti-trichomonal, antidiabetic, anti-inflammatory, hepatoprotective and antioxidant effects. J Ethnopharmacol 2009; 122: 10-19. DOI: 10.1016/j.jep.2008.11.015

282. Kaur A, Bhatti R. Understanding the phytochemistry and molecular insights to the pharmacology of Angelica

archangelica L. (garden angelica) and its bioactive components. Phytother Res 2021; 35: 5961-5979. DOI: 10.1002/ptr.7206

283. Wszelaki N, Paradowska K, Jamroz MK et al. Bioactivity-guided fractionation for the butyrylcholinesterase inhibitory activity of furanocoumarins from Angelica archangelica L. roots and fruits. J Agric Food Chem 2011; 59: 9186-9193. DOI: 10.1021/jf201971s

284. Lewis D, Jordan A. Creek Indian Medicine Ways: The Enduring Power of Mvskoke Religion. University of New Mexico Press; 2002.

285. Dexter DF, Martin K, Travis L. Prehistoric Plant Use at Beaver Creek Rock Shelter, Southwestern Montana, U.S.A. Ethnobotany Research and Applications 2014; 12: 355-384.

286. Moerman DE. Native American Ethnobotany. Timber Press; 1998.

287. Raal A, Jaama M, Utt M et al. The Phytochemical Profile and Anticancer Activity of Anthemis tinctoria and Angelica sylvestris Used in Estonian Ethnomedicine. Plants (Basel) 2022; 11. DOI: 10.3390/plants11070994

288. Malik K, Ahmad M, Zhang G et al. Traditional plant based medicines used to treat musculoskeletal disorders in Northern Pakistan. European Journal of Integrative Medicine 2018; 19: 17-64. DOI: https://doi.org/10.1016/j.eujim.2018.02.003

289. Kumar P, Rana V, Singh AN. Angelica glauca Edgew. – A comprehensive review. Journal of Applied Research on Medicinal and Aromatic Plants 2022; 31: 100397. DOI: https://doi.org/10.1016/j.jarmap.2022.100397

290. Ikram A, Zahra N, Shinwari Z et al. Ethnomedicinal Review of Folklore Medicinal Plants Belonging to Family Apiaceae of Pakistan. Pakistan Journal of Botany 2015; 47: 1007-1014.

291. Zhao H, Feng YL, Wang M et al. The Angelica dahurica: A Review of Traditional Uses, Phytochemistry and Pharmacology. Front Pharmacol 2022; 13: 896637. DOI: 10.3389/fphar.2022.896637

292. Jeong SY, Kim HM, Lee KH et al. Quantitative analysis of marker compounds in Angelica gigas, Angelica sinensis, and Angelica acutiloba by HPLC/DAD. Chem Pharm Bull (Tokyo) 2015; 63: 504-511. DOI: 10.1248/cpb.c15-00081

293. Wei WL, Zeng R, Gu CM et al. Angelica sinensis in China-A review of botanical profile, ethnopharmacology, phytochemistry and chemical analysis. J Ethnopharmacol 2016; 190: 116-141. DOI: 10.1016/j.jep.2016.05.023

294. Alqethami A, Aldhebiani AY, Teixidor-Toneu I. Medicinal plants used in Jeddah, Saudi Arabia: A gender perspective. J Ethnopharmacol 2020; 257: 112899. DOI: 10.1016/j.jep.2020.112899

295. Kusuma WA, Habibi ZI, Amir MF et al. Bipartite graph search optimization for type II diabetes mellitus Jamu formulation using branch and bound algorithm. Front Pharmacol 2022; 13: 978741. DOI: 10.3389/fphar.2022.978741

296. He Y, Hou P, Fan G et al. Authentication of Angelica anomala Avé-Lall cultivars

through DNA barcodes. Mitochondrial DNA 2012; 23: 100-105. DOI: 10.3109/19401736.2012.660924

297. Wang R, Yu C, Wang N et al. Angelicae Pubescentis Radix (Umbelliferae): Systematic review of traditional Chinese medicine for treating rheumatoid arthritis, including traditional usage, chemical components, active components, related inflammatory factors. Phytomedicine Plus 2023; 3: 100389. DOI: 10.1016/j.phyplu.2022.100389

298. Ma J, Huang J, Hua S et al. The ethnopharmacology, phytochemistry and pharmacology of Angelica biserrata - A review. J Ethnopharmacol 2019; 231: 152-169. DOI: 10.1016/j.jep.2018.10.040

299. Zhao D, Islam MN, Ahn BR et al. In vitro antioxidant and anti-inflammatory activities of Angelica decursiva. Arch Pharm Res 2012; 35: 179-192. DOI: 10.1007/s12272-012-0120-0

300. Kim H, Song MJ. Analysis and recordings of orally transmitted knowledge about medicinal plants in the southern mountainous region of Korea. J Ethnopharmacol 2011; 134: 676-696. DOI: 10.1016/j.jep.2011.01.024

301. Leu YL, Chen YW, Yang CY et al. Extract isolated from Angelica hirsutiflora with insulin secretagogue activity. Journal of Ethnopharmacology 2009; 123: 208-212. DOI: https://doi.org/10.1016/j.jep.2009.03.027

302. Aulifa DL, Adnyana IK, Sukrasno S et al. Inhibitory activity of xanthoangelol isolated from Ashitaba (Angelica keiskei Koidzumi) towards α-glucosidase and dipeptidyl peptidase-IV: in silico and in vitro studies. Heliyon 2022; 8: e09501. DOI: 10.1016/j.heliyon.2022.e09501

303. Mira A, Tanaka A, Tateyama Y et al. Comparative biological study of roots, stems, leaves, and seeds of Angelica shikokiana Makino. J Ethnopharmacol 2013; 148: 980-987. DOI: 10.1016/j.jep.2013.06.008

304. Yoshikawa M, Nishida N, Ninomiya K et al. Inhibitory effects of coumarin and acetylene constituents from the roots of Angelica furcijuga on D-galactosamine/lipopolysaccharide-induced liver injury in mice and on nitric oxide production in lipopolysaccharide-activated mouse peritoneal macrophages. Bioorg Med Chem 2006; 14: 456-463. DOI: 10.1016/j.bmc.2005.08.038

305. Harvey AL, Edrada-Ebel R, Quinn RJ. The re-emergence of natural products for drug discovery in the genomics era. Nature Reviews Drug Discovery 2015; 14: 111-129. DOI: 10.1038/nrd4510

306. Kingston DGI. Modern Natural Products Drug Discovery and Its Relevance to Biodiversity Conservation. Journal of Natural Products 2011; 74: 496-511. DOI: 10.1021/np100550t

307. Newman DJ, Cragg GM. Natural Products as Sources of New Drugs over the Nearly Four Decades from 01/1981 to 09/2019. J Nat Prod 2020; 83: 770-803. DOI: 10.1021/acs.jnatprod.9b01285

308. Schwikkard SL, Mulholland DA. Useful methods for targeted plant selection in the discovery of potential new drug candidates. Planta Med 2014; 80:

1154-1160. DOI: 10.1055/s-0034-1368549

309. Irondi EA, Oboh G, Akindahunsi AA et al. Phenolics composition and antidiabetic property of Brachystegia eurycoma seed flour in high-fat diet, low-dose streptozotocin-induced type 2 diabetes in rats. Asian Pacific Journal of Tropical Disease 2015; 5.

310. Kahn SE. Clinical review 135: The importance of beta-cell failure in the development and progression of type 2 diabetes. J Clin Endocrinol Metab 2001; 86: 4047-4058. DOI: 10.1210/jcem.86.9.7713

311. Kasole R, Martin HD, Kimiywe J. Traditional Medicine and Its Role in the Management of Diabetes Mellitus: "Patients' and Herbalists' Perspectives". Evid Based Complement Alternat Med 2019; 2019: 2835691. DOI: 10.1155/2019/2835691

312. Toubal S, Oiry C, Bayle M et al. Urolithin C increases glucose-induced ERK activation which contributes to insulin secretion. Fundam Clin Pharmacol 2020; 34: 571-580. DOI: 10.1111/fcp.12551

313. Curtis MJ, Alexander SPH, Cirino G et al. Planning experiments: Updated guidance on experimental design and analysis and their reporting III. Br J Pharmacol 2022; 179: 3907-3913. DOI: 10.1111/bph.15868

314. Peraldi-Roux S, Bayle M, M'Kadmi C et al. Design and characterization of a triazole-based growth hormone secretagogue receptor modulator inhibiting the glucoregulatory and feeding actions of ghrelin. Biochem Pharmacol 2022; 202: 115114. DOI: 10.1016/j.bcp.2022.115114

315. Jaiswal R, Jayasinghe L, Kuhnert N. Identification and characterization of proanthocyanidins of 16 members of the Rhododendron genus (Ericaceae) by tandem LC-MS. J Mass Spectrom 2012; 47: 502-515. DOI: 10.1002/jms.2954

316. Shen Z, Haslam E, Falshaw CP et al. Procyanidins and polyphenols of Larix gmelini bark. Phytochemistry 1986; 25: 2629-2635. DOI: 10.1016/s0031-9422(00)84524-0

317. Yeap Foo L, Karchesy JJ. Procyanidin dimers and trimers from Douglas fir inner bark. Phytochemistry 1989; 28: 1743-1747. DOI: 10.1016/s0031-9422(00)97836-1

318. Strack D, Heilemann J, Wray V et al. Structures and accumulation patterns of soluble and insoluble phenolics from norway spruce needles. Phytochemistry 1989; 28: 2071-2078. DOI: 10.1016/s0031-9422(00)97922-6

319. Sut S, Baldan V, Faggian M et al. The Bark of Picea abies L., a Waste from Sawmill, as a Source of Valuable Compounds: Phytochemical Investigations and Isolation of a Novel Pimarane and a Stilbene Derivative. Plants (Basel) 2021; 10. DOI: 10.3390/plants10102106

320. Pietarinen SP, Willför SM, Ahotupa MO et al. Knotwood and bark extracts: strong antioxidants from waste materials. Journal of Wood Science 2006; 52: 436-444. DOI: 10.1007/s10086-005-0780-1

321. Willför S, Nisula L, Hemming J et al. Bioactive phenolic substances in industrially important tree species. Part 2: Knots and stemwood of fir

species. Holzforschung 2004; 58: 650-659. DOI: 10.1515/hf.2004.119

322. Dellus V, Mila I, Scalbert A et al. Douglas-fir polyphenols and heartwood formation. Phytochemistry 1997; 45: 1573-1578. DOI: 10.1016/s0031-9422(97)00245-8

323. Suprun AR, Dubrovina AS, Aleynova OA et al. The Bark of the Spruce Picea jezoensis Is a Rich Source of Stilbenes. Metabolites 2021; 11: 714.

324. Ivanova SZ, Babkin VA. Polyphenolic compounds from Larix gmelinii phloem. Chemistry of Natural Compounds 2011; 47: 124-125. DOI: 10.1007/s10600-011-9853-0

325. Wu L, Li YL, Li SM et al. Systematic phytochemical investigation of Abies spectabilis. Chem Pharm Bull (Tokyo) 2010; 58: 1646-1649. DOI: 10.1248/cpb.58.1646

326. Yashunsky DV, Men´shov VM, Tsvetkov DE et al. Analysis of content of (–)-secoisolariciresinol and related polyphenols in different morphological parts and anatomical structures of larch wood from Siberia. Russian Chemical Bulletin 2015; 63: 2571-2576. DOI: 10.1007/s11172-014-0780-7

327. Willför S, Hemming J, Reunanen M et al. Phenolic and Lipophilic Extractives in Scots Pine Knots and Stemwood. Holzforschung 2003; 57: 359-372. DOI: 10.1515/hf.2003.054

328. Fang J-M, Su W-C, Cheng Y-S. Flavonoids and stilbenes from armand pine. Phytochemistry 1988; 27: 1395-1397. DOI: 10.1016/0031-9422(88)80201-2

329. Mbakidi-Ngouaby H, Pinault E, Gloaguen V et al. Profiling and seasonal variation of chemical constituents from Pseudotsuga menziesii wood. Industrial Crops and Products 2018; 117: 34-49. DOI: 10.1016/j.indcrop.2018.02.069

330. Razgonova M, Zakharenko A, Pikula K et al. LC-MS/MS Screening of Phenolic Compounds in Wild and Cultivated Grapes Vitis amurensis Rupr. Molecules 2021; 26: 3650. DOI: 10.3390/molecules26123650

331. Abdelghffar EA, Obaid WA, Alamoudi MO et al. Thymus fontanesii attenuates CCl(4)-induced oxidative stress and inflammation in mild liver fibrosis. Biomed Pharmacother 2022; 148: 112738. DOI: 10.1016/j.biopha.2022.112738

332. Tsimogiannis D, Samiotaki M, Panayotou G et al. Characterization of flavonoid subgroups and hydroxy substitution by HPLC-MS/MS. Molecules 2007; 12: 593-606. DOI: 10.3390/12030593

333. Bibi Sadeer N, Sinan KI, Cziáky Z et al. Towards the Pharmacological Validation and Phytochemical Profiling of the Decoction and Maceration of Bruguiera gymnorhiza (L.) Lam.—A Traditionally Used Medicinal Halophyte. Molecules 2022; 27: 2000.

334. Koulis GA, Tsagkaris AS, Aalizadeh R et al. Honey Phenolic Compound Profiling and Authenticity Assessment Using HRMS Targeted and Untargeted Metabolomics. Molecules 2021; 26: 2769. DOI: 10.3390/molecules26092769

335. Parisi V, Vassallo A, Pisano C et al. A Herbal Mixture from Propolis, Pomegranate, and Grape Pomace Endowed with Anti-Inflammatory Activity in an In Vivo Rheumatoid Arthritis Model. Molecules 2020; 25: 2255. DOI: 10.3390/molecules25092255

336. Wu H, Cao Y, Qu Y et al. Integrating UPLC-QE-Orbitrap-MS technology and network pharmacological method to reveal the mechanism of Bailemian capsule to relieve insomnia. Nat Prod Res 2022; 36: 2554-2558. DOI: 10.1080/14786419.2021.1900176

337. Mena P, Calani L, Dall'Asta C et al. Rapid and comprehensive evaluation of (poly)phenolic compounds in pomegranate (Punica granatum L.) juice by UHPLC-MSn. Molecules 2012; 17: 14821-14840. DOI: 10.3390/molecules171214821

338. Mercolini L, Protti M, Saracino MA et al. Analytical Profiling of Bioactive Phenolic Compounds in Argan (Argania spinosa) Leaves by Combined Microextraction by Packed Sorbent (MEPS) and LC-DAD-MS/MS. Phytochem Anal 2016; 27: 41-49. DOI: 10.1002/pca.2585

339. Eklund PC, Backman MJ, Kronberg LA et al. Identification of lignans by liquid chromatography-electrospray ionization ion-trap mass spectrometry. J Mass Spectrom 2008; 43: 97-107. DOI: 10.1002/jms.1276

340. Voronin KS, Fenin AA, Zhevlakova AK et al. Polyphenolic Profile of Larch Knotwood. Pharmaceutical Chemistry Journal 2021; 55: 781-786. DOI: 10.1007/s11094-021-02494-x

341. Stella L, De Rosso M, Panighel A et al. Collisionally induced fragmentation of [M-H](-) species of resveratrol and piceatannol investigated by deuterium labelling and accurate mass measurements. Rapid Commun Mass Spectrom 2008; 22: 3867-3872. DOI: 10.1002/rcm.3811

342. Flamini R, De Rosso M, De Marchi F et al. An innovative approach to grape metabolomics: stilbene profiling by suspect screening analysis. Metabolomics 2013; 9: 1243-1253. DOI: 10.1007/s11306-013-0530-0

343. Buiarelli F, Coccioli F, Jasionowska R et al. Analysis of some stilbenes in Italian wines by liquid chromatography/tandem mass spectrometry. Rapid Commun Mass Spectrom 2007; 21: 2955-2964. DOI: 10.1002/rcm.3174

344. Gabaston J, Richard T, Cluzet S et al. Pinus pinaster Knot: A Source of Polyphenols against Plasmopara viticola. J Agric Food Chem 2017; 65: 8884-8891. DOI: 10.1021/acs.jafc.7b04129

345. Yeo SC, Luo W, Wu J et al. Quantification of pinosylvin in rat plasma by liquid chromatography-tandem mass spectrometry: application to a pre-clinical pharmacokinetic study. J Chromatogr B Analyt Technol Biomed Life Sci 2013; 931: 68-74. DOI: 10.1016/j.jchromb.2013.05.023

346. Manville JF. Juvabione and its Analogs. Juvabione and Δ4' -Dehydrojuvabione Isolated from the Whole Wood of Abiesbalsamea, have the R,R Stereoconfigurations, not the R,S. Canadian Journal of Chemistry 1975; 53: 1579-1585. DOI: 10.1139/v75-223

347. Brunswick P, Blajkevitch O, Chow L et al. Trace analysis of resin acids in surface waters by direct injection liquid chromatography time of flight mass spectrometry and triple quadrupole mass spectrometry. J Chromatogr A 2021; 1656: 462558. DOI: 10.1016/j.chroma.2021.462558

348. Schymanski EL, Ruttkies C, Krauss M et al. Critical Assessment of Small Molecule Identification 2016: automated methods. J Cheminform 2017; 9: 22. DOI: 10.1186/s13321-017-0207-1

349. Clifford MN, Johnston KL, Knight S et al. Hierarchical scheme for LC-MSn identification of chlorogenic acids. J Agric Food Chem 2003; 51: 2900-2911. DOI: 10.1021/jf026187q

350. Jaiswal R, Deshpande S, Kuhnert N. Profiling the chlorogenic acids of Rudbeckia hirta, Helianthus tuberosus, Carlina acaulis and Symphyotrichum novae-angliae leaves by LC-MS(n). Phytochem Anal 2011; 22: 432-441. DOI: 10.1002/pca.1299

351. Jaiswal R, Muller H, Muller A et al. Identification and characterization of chlorogenic acids, chlorogenic acid glycosides and flavonoids from Lonicera henryi L. (Caprifoliaceae) leaves by LC-MSn. Phytochemistry 2014; 108: 252-263. DOI: 10.1016/j.phytochem.2014.08.023

352. Jaiswal R, Sovdat T, Vivan F et al. Profiling and characterization by LC-MSn of the chlorogenic acids and hydroxycinnamoylshikimate esters in mate (Ilex paraguariensis). J Agric Food Chem 2010; 58: 5471-5484. DOI: 10.1021/jf904537z

353. Jaiswal R, Kuhnert N. Identification and characterization of five new classes of chlorogenic acids in burdock (Arctium lappa L.) roots by liquid chromatography/tandem mass spectrometry. Food Funct 2011; 2: 63-71. DOI: 10.1039/c0fo00125b

354. Lin LZ, Harnly JM. Identification of hydroxycinnamoylquinic acids of arnica flowers and burdock roots using a standardized LC-DAD-ESI/MS profiling method. J Agric Food Chem 2008; 56: 10105-10114. DOI: 10.1021/jf802412m

355. Elboutachfaiti R, Molinie R, Mathiron D et al. Secondary Metabolism Rearrangements in Linum usitatissimum L. after Biostimulation of Roots with COS Oligosaccharides from Fungal Cell Wall. Molecules 2022; 27: 2372. DOI: 10.3390/molecules27072372

356. Li M, Huang Z-Y, Yuan Y-L-L et al. Characterization of chemical components and the potential anti-influenza mechanism of Fructus Arctii by a strategy integrating pharmacological evaluations, chemical profiling, serum pharmacochemistry, and network pharmacology. New Journal of Chemistry 2022; 46: 18426-18446. DOI: 10.1039/D2NJ02799B

357. Gu J, Wu W, Huang M et al. Application of High-Performance Liquid Chromatography Coupled with Linear Ion Trap Quadrupole Orbitrap Mass Spectrometry for Qualitative and Quantitative Assessment of Shejin-Liyan Granule Supplements. Molecules 2018; 23. DOI: 10.3390/molecules23040884

358. Huh J, Lee CM, Lee S et al. Comprehensive Characterization of Lignans from Forsythia viridissima by

UHPLC-ESI-QTOF-MS, and Their NO Inhibitory Effects on RAW 264.7 Cells. Molecules 2019; 24. DOI: 10.3390/molecules24142649

359. Jo AR, Han HS, Seo S et al. Inhibitory effect of moschamine isolated from Carthamus tinctorius on LPS-induced inflammatory mediators via AP-1 and STAT1/3 inactivation in RAW 264.7 macrophages. Bioorg Med Chem Lett 2017; 27: 5245-5251. DOI: 10.1016/j.bmcl.2017.10.035

360. Tian X, Guo S, He K et al. Qualitative and quantitative analysis of chemical constituents of Ptychopetalum olacoides Benth. Nat Prod Res 2018; 32: 354-357. DOI: 10.1080/14786419.2017.1354187

361. Zhang HL, Nagatsu A, Watanabe T et al. Antioxidative compounds isolated from safflower (Carthamus tinctorius L.) oil cake. Chem Pharm Bull (Tokyo) 1997; 45: 1910-1914. DOI: 10.1248/cpb.45.1910

362. Wang S, Cao J, Deng J et al. Chemical characterization of flavonoids and alkaloids in safflower (Carthamus tinctorius L.) by comprehensive two-dimensional hydrophilic interaction chromatography coupled with hybrid linear ion trap Orbitrap mass spectrometry. Food Chem X 2021; 12: 100143. DOI: 10.1016/j.fochx.2021.100143

363. Saleem H, Zengin G, Khan KU et al. New insights into the phytochemical composition, enzyme inhibition and antioxidant properties of desert cotton (Aerva javanica (Bum.f) Shult. - Amaranthaceae). Nat Prod Res 2021; 35: 664-668. DOI: 10.1080/14786419.2019.1587427

364. Liu X-T, Wang X-G, Xu R et al. Qualitative and Quantitative Analysis of Lignan Constituents in Caulis Trachelospermi by HPLC-QTOF-MS and HPLC-UV. Molecules 2015; 20: 8107-8124.

365. Sulaiman CT, Balachandran I. Chemical Profiling of an Indian Herbal Formula Using Liquid Chromatography Coupled with Electro Spray Ionization Mass Spectrometry. Spectroscopy Letters 2014; 48: 222-226. DOI: 10.1080/00387010.2013.872670

366. Kurkin VA, Evstratova RI, Zapesochnaya GG. Phenolic compounds of the bark of Eleutherococcus senticosus. Chemistry of Natural Compounds 1992; 28: 512-513. DOI: 10.1007/bf00630671

367. Sanz M, de Simon BF, Cadahia E et al. LC-DAD/ESI-MS/MS study of phenolic compounds in ash (Fraxinus excelsior L. and F. americana L.) heartwood. Effect of toasting intensity at cooperage. J Mass Spectrom 2012; 47: 905-918. DOI: 10.1002/jms.3040

368. Mekky RH, Contreras MdM, El-Gindi MR et al. Profiling of phenolic and other compounds from Egyptian cultivars of chickpea (Cicer arietinum L.) and antioxidant activity: a comparative study. RSC Advances 2015; 5: 17751-17767. DOI: 10.1039/c4ra13155j

369. Sun H, Liu J, Zhang A et al. Characterization of the multiple components of Acanthopanax Senticosus stem by ultra high performance liquid chromatography with quadrupole time-of-flight tandem mass spectrometry. J Sep Sci 2016; 39: 496-502. DOI: 10.1002/jssc.201500915

370. Filipek A, Wyszomierska J, Michalak B et al. Syringa vulgaris bark as a source of compounds affecting the release of inflammatory mediators from human neutrophils and monocytes/macrophages. Phytochemistry Letters 2019; 30: 309-313. DOI: 10.1016/j.phytol.2019.02.008

371. EDQM. Eleutherococci radix. In: European Pharmacopoeia 10th ed. Strasbourg, France: Council of Europe; 2019: 1423.

372. Slacanin I. MA, Hostettmann K. The Isolation of Eleutherococcus senticosus Constituents by Centrifugal Partition Chromatography and Their Quantitative Determination by High Performance Liquid Chromatography. Phytochemical Analysis 1991; 2: 137-142.

373. Grzegorczyk-Karolak I, Kuźma Ł, Lisiecki P et al. Accumulation of phenolic compounds in different in vitro cultures of Salvia viridis L. and their antioxidant and antimicrobial potential. Phytochemistry Letters 2019; 30: 324-332. DOI: 10.1016/j.phytol.2019.02.016

374. Emad AM, Rasheed DM, El-Kased RF et al. Antioxidant, Antimicrobial Activities and Characterization of Polyphenol-Enriched Extract of Egyptian Celery (Apium graveolens L., Apiaceae) Aerial Parts via UPLC/ESI/TOF-MS. Molecules 2022; 27: 698. DOI: 10.3390/molecules27030698

375. He Y, Wang Y, Zhang X et al. Chemical characterization of small-molecule inhibitors of monoamine oxidase B synthesized from the Acanthopanax senticosus root with affinity ultrafiltration mass spectrometry. Rapid Commun Mass Spectrom 2020; 34: e8694. DOI: 10.1002/rcm.8694

376. Li Z, Li B-B, Xiu M-X et al. DGAT inhibitory three new lignans from the stem of Eleutherococcus senticosus. Phytochemistry Letters 2020; 40: 67-71. DOI: 10.1016/j.phytol.2020.09.002

377. Tian Z, Sun L, Chi B et al. Affinity ultrafiltration and UPLC-HR-Orbitrap-MS based screening of neuraminidase inhibitors from Angelica pubescens. J Chromatogr B Analyt Technol Biomed Life Sci 2022; 1208: 123398. DOI: 10.1016/j.jchromb.2022.123398

378. Shi H, Chang YQ, Feng X et al. Chemical comparison and discrimination of two plant sources of Angelicae dahuricae Radix, Angelica dahurica and Angelica dahurica var. formosana, by HPLC-Q/TOF-MS and quantitative analysis of multiple components by a single marker. Phytochem Anal 2022; 33: 776-791. DOI: 10.1002/pca.3129

379. Wang B, Liu X, Zhou A et al. Simultaneous analysis of coumarin derivatives in extracts of Radix Angelicae pubescentis (Duhuo) by HPLC-DAD-ESI-MSn technique. Anal Methods 2014; 6: 7996-8002. DOI: 10.1039/c4ay01468e

380. Gautheron G. Effects and mechanisms of action of quercetin-like compounds on pancreatic β-cells functions. Montpellier, France: Université de Montpellier; 2021.

381. Yokoyama T, Kosaka Y, Mizuguchi M. Structural Insight into the Interactions between Death-Associated Protein Kinase 1 and Natural Flavonoids. J Med Chem 2015; 58: 7400-7408. DOI: 10.1021/acs.jmedchem.5b00893

382. Fusi F, Spiga O, Trezza A et al. The surge of flavonoids as novel, fine regulators of cardiovascular Ca(v) channels. Eur J Pharmacol 2017; 796: 158-174. DOI: 10.1016/j.ejphar.2016.12.033

383. Saponara S, Carosati E, Mugnai P et al. The flavonoid scaffold as a template for the design of modulators of the vascular Ca(v) 1.2 channels. Br J Pharmacol 2011; 164: 1684-1697. DOI: 10.1111/j.1476-5381.2011.01476.x

384. Fusi F, Trezza A, Tramaglino M et al. The beneficial health effects of flavonoids on the cardiovascular system: Focus on K(+) channels. Pharmacol Res 2020; 152: 104625. DOI: 10.1016/j.phrs.2019.104625

385. Willför S, Nisula L, Hemming J et al. Bioactive phenolic substances in industrially important tree species. Part 1: Knots and stemwood of different spruce species. Holzforschung 2004; 58: 335-344. DOI: 10.1515/hf.2004.052

386. Willför S, Hemming J, Reunanen M et al. Lignans and Lipophilic Extractives in Norway Spruce Knots and Stemwood. Holzforschung 2003; 57: 27-36. DOI: 10.1515/hf.2003.005

387. Tan XQ, Chen HS, Liu RH et al. Lignans from Trachelospermum jasminoides. Planta Med 2005; 71: 93-95. DOI: 10.1055/s-2005-837761

388. Boldizsár I, Kraszni M, Tóth F et al. Complementary fragmentation pattern analysis by gas chromatography-mass spectrometry and liquid chromatography tandem mass spectrometry confirmed the precious lignan content of Cirsium weeds. J Chromatogr A 2010; 1217: 6281-6289. DOI: 10.1016/j.chroma.2010.08.018

389. Graikou K, Kourti PM, Zengin G et al. Chemical Characterisation-Biological Evaluation of Greek Cultivar Cardoon Seeds (Cynara cardunculus). A By-product with Potential High Added Value. Planta Med 2021; 87: 1025-1031. DOI: 10.1055/a-1472-6336

390. Kupniewska K. Quality evaluation of dietary supplements containing root of Eleutherococcus senticosus with microscopic and chromatographic methods. Warsaw, Poland: Medical University of Warsaw; 2023.

391. Marrano N, Spagnuolo R, Biondi G et al. Effects of Extra Virgin Olive Oil Polyphenols on Beta-Cell Function and Survival. Plants (Basel) 2021; 10. DOI: 10.3390/plants10020286

392. Mellbye FB, Jeppesen PB, Hermansen K et al. Cafestol, a Bioactive Substance in Coffee, Stimulates Insulin Secretion and Increases Glucose Uptake in Muscle Cells: Studies in Vitro. J Nat Prod 2015; 78: 2447-2451. DOI: 10.1021/acs.jnatprod.5b00481

393. Patyra A, Kołtun-Jasion M, Schwartz J et al. Exploring the anti-diabetic and anti-inflammatory effects of lignans coming from wood waste materials. Phytochemical Society of Europe Meeting; 2022; Iasi, Romania.

394. Kim DW, Curtis-Long MJ, Yuk HJ et al. Quantitative analysis of phenolic metabolites from different parts of Angelica keiskei by HPLC-ESI MS/MS and their xanthine oxidase inhibition. Food Chem 2014; 153: 20-27. DOI: 10.1016/j.foodchem.2013.12.026

395. Oh HA, Lee H, Park SY et al. Analysis of plasma metabolic profiling and evaluation of the effect of the intake of Angelica keiskei using metabolomics and lipidomics. J Ethnopharmacol 2019; 243: 112058. DOI: 10.1016/j.jep.2019.112058

396. Tian Y, Shi R, Gao M et al. Differentiation of Furanocoumarin Isomers with Ratio of Relative Abundance of Characteristic Fragment Ions and Application in Angelicae dahuricae Radix. Chromatographia 2017; 80: 1401-1410. DOI: 10.1007/s10337-017-3348-5

397. Li B, Zhang X, Wang J et al. Simultaneous Characterisation of Fifty Coumarins from the Roots of Angelica dahurica by Off-line Two-dimensional High-performance Liquid Chromatography Coupled with Electrospray Ionisation Tandem Mass Spectrometry. Phytochemical Analysis 2014; 25: 229-240. DOI: https://doi.org/10.1002/pca.2496

398. Wang C-C, Lai J-E, Chen L-G et al. Inducible nitric oxide synthase inhibitors of Chinese herbs. Part 2: Naturally occurring furanocoumarins. Bioorganic & Medicinal Chemistry 2000; 8: 2701-2707. DOI: https://doi.org/10.1016/S0968-0896(00)00200-5

399. Pan T-L, Wang P-W, Aljuffali IA et al. Coumarin derivatives, but not coumarin itself, cause skin irritation via topical delivery. Toxicology Letters 2014; 226: 173-181. DOI: https://doi.org/10.1016/j.toxlet.2014.02.009

400. Williamson G, Kay CD, Crozier A. The Bioavailability, Transport, and Bioactivity of Dietary Flavonoids: A Review from a Historical Perspective. Compr Rev Food Sci Food Saf 2018; 17: 1054-1112. DOI: 10.1111/1541-4337.12351

401. Deng M, Xie L, Zhong L et al. Imperatorin: A review of its pharmacology, toxicity and pharmacokinetics. Eur J Pharmacol 2020; 879: 173124. DOI: 10.1016/j.ejphar.2020.173124

402. Perreault L, Skyler JS, Rosenstock J. Novel therapies with precision mechanisms for type 2 diabetes mellitus. Nat Rev Endocrinol 2021; 17: 364-377. DOI: 10.1038/s41574-021-00489-y

403. Zhang Y, Cao Y, Wang Q et al. A potential calcium antagonist and its antihypertensive effects. Fitoterapia 2011; 82: 988-996. DOI: 10.1016/j.fitote.2011.05.016

404. Mendel M, Skalicka-Woźniak K, Chłopecka M et al. Effect of Imperatorin on the Spontaneous Motor Activity of Rat Isolated Jejunum Strips. Evid Based Complement Alternat Med 2015; 2015: 614849. DOI: 10.1155/2015/614849

405. Hockerman GH, Peterson BZ, Johnson BD et al. Molecular determinants of drug binding and action on L-type calcium channels. Annu Rev Pharmacol Toxicol 1997; 37: 361-396. DOI: 10.1146/annurev.pharmtox.37.1.361

406. Lacinová L. Voltage-dependent calcium channels. Gen Physiol Biophys 2005; 24 Suppl 1: 1-78.

407. Chen X, Sun W, Gianaris NG et al. Furanocoumarins Are a Novel Class of Modulators for the Transient Receptor Potential Vanilloid Type 1 (TRPV1) Channel*. Journal of Biological

Chemistry 2014; 289: 9600-9610. DOI: https://doi.org/10.1074/jbc.M113.536862

408. Wu KC, Chen YH, Cheng KS et al. Suppression of voltage-gated Na(+) channels and neuronal excitability by imperatorin. Eur J Pharmacol 2013; 721: 49-55. DOI: 10.1016/j.ejphar.2013.09.056

409. Wang YW, Yang CT, Chen YH et al. Inhibitory effects of imperatorin on voltage-gated K(+) channels and ATP-sensitive K(+) channels. Pharmacol Rep 2015; 67: 134-139. DOI: 10.1016/j.pharep.2014.08.015

410. Liu Y, Zhong X, Ding Y et al. Inhibition of voltage-dependent potassium channels mediates cAMP-potentiated insulin secretion in rat pancreatic β cells. Islets 2017; 9: 11-18. DOI: 10.1080/19382014.2017.1280644

411. Chu ZL, Jones RM, He H et al. A role for beta-cell-expressed G protein-coupled receptor 119 in glycemic control by enhancing glucose-dependent insulin release. Endocrinology 2007; 148: 2601-2609. DOI: 10.1210/en.2006-1608

412. Yang JW, Kim HS, Choi YW et al. Therapeutic application of GPR119 ligands in metabolic disorders. Diabetes Obes Metab 2018; 20: 257-269. DOI: 10.1111/dom.13062

413. Gromada J, Dissing S, Bokvist K et al. Glucagon-like peptide I increases cytoplasmic calcium in insulin-secreting beta TC3-cells by enhancement of intracellular calcium mobilization. Diabetes 1995; 44: 767-774. DOI: 10.2337/diab.44.7.767

414. Holz GG, Leech CA, Heller RS et al. cAMP-dependent mobilization of intracellular Ca2+ stores by activation of ryanodine receptors in pancreatic beta-cells. A Ca2+ signaling system stimulated by the insulinotropic hormone glucagon-like peptide-1-(7-37). J Biol Chem 1999; 274: 14147-14156. DOI: 10.1074/jbc.274.20.14147

415. Britsch S, Krippeitdrews P, Lang F et al. Glucagon-like Peptide-1 Modulates Ca2+ Current But Not K+ATP Current in Intact Mouse Pancreatic B-Cells. Biochemical and Biophysical Research Communications 1995; 207: 33-39. DOI: https://doi.org/10.1006/bbrc.1995.1149

Abstracts

Titre : Effets et mécanisme d'action de métabolites secondaires des plantes sur la régulation de la sécrétion d'insuline

Le diabète de type 2 (DT2) est une maladie associant résistance à l'insuline et dysfonction des cellules β pancréatiques. Basées sur la compréhension actuelle de la physiopathologie de cette maladie, différentes approches thérapeutiques ont été développées afin d'améliorer le contrôle glycémique et de ralentir la progression de la maladie. Néanmoins, elles présentent une efficacité limitée et de nombreux effets indésirables. Dans ce contexte, les extraits végétaux et leurs constituants actifs sont considérés comme un domaine important pour la recherche de nouveaux traitements antidiabétiques.

Cette thèse avait pour objectif de trouver une source naturelle de métabolites secondaires végétaux potentiellement capables de protéger la fonction des cellules β, d'induire la sécrétion d'insuline de façon gluco-dépendante, et de caractériser le mécanisme d'action des molécules actives.

Vingt extraits de plantes ont été profilés phytochimiquement à l'aide de LC-MS, conduisant à l'identification et l'isolement de 39 composés purifiés. Les flavonoïdes, les lignanes et les coumarines ont été testés pour leur capacité à moduler la fonction des cellules β sur le modèle cellulaire INS-1. Certains flavonoïdes et coumarines ont augmenté la sécrétion d'insuline induite par le glucose, tandis qu'aucun effet n'a été observé avec les lignanes. Le mécanisme d'action des métabolites actifs a ensuite été étudié en évaluant leurs effets sur l'activité électrique des cellules, les niveaux de calcium intracellulaire et les courants calciques et potassiques. De plus, l'activité insulino-sécrétoire a été confirmée dans des extraits pharmacopéiques contenant des coumarines.

Ces découvertes pourraient avoir des implications sur l'utilisation traditionnelle des racines d'angélique dans le traitement du DT2. Des effets insulinotropes de trois racines d'angélique pharmacopéiques ont été identifiés et leurs profils de métabolites ont été corrélés à l'activité pharmacologique, avec des structures clés responsables de la modulation de la sécrétion d'insuline. Pour certaines métabolites le mécanisme d'action a été étudié. Les métabolites végétaux actifs pourraient ainsi devenir des structures de référence dans la recherche de nouveaux traitements antidiabétiques, qui devraient être plus amplement évalués.

Mots clés : diabète de type 2, fonctionnalité cellule beta pancréatique, mécanisme d'action, coumarines, flavonoïdes, lignanes.

Tytuł: Wpływ wtórnych metabolitów roślinnych na regulację wydzielania insuliny i mechanizm leżący u jej podstaw

Cukrzyca typu 2 jest chorobą, która wiąże insulinooporność z dysfunkcją komórek β trzustki. W oparciu o obecną wiedzę na temat patofizjologii tej choroby opracowano wiele terapii przeciwcukrzycowych, mających na celu poprawę kontroli glikemii i spowolnienia postępu choroby. Niemniej jednak mają one ograniczoną skuteczność i liczne skutki uboczne. W tym kontekście wyciągi roślinne i ich aktywne składniki są uważane za ważny obszar poszukiwań nowych terapii przeciwcukrzycowych.

Niniejsza praca miała na celu znalezienie naturalnego źródła wtórnych metabolitów roślinnych potencjalnie zdolnych do ochrony funkcji komórek β, stymulowania wydzielania insuliny w sposób zależny od glukozy oraz wyjaśnienia mechanizmu ich działania.

Dwadzieścia ekstraktów roślinnych sprofilowano fitochemicznie za pomocą LC-MS, co doprowadziło do identyfikacji i izolacji 39 czystych związków. Flawonoidy, lignany i kumaryny zostały przebadane pod kątem zdolności do modulowania funkcji komórek β na modelu komórkowym INS-1. Niektóre z badanych flawonoidów i kumaryn zwiększały wydzielanie insuliny indukowane glukozą, podczas gdy dla lignanów nie zaobserwowano takiego efektu. Następnie zbadano mechanizm działania aktywnych metabolitów, oceniając ich wpływ na aktywność elektryczną komórek, stężenia wapnia wewnątrzkomórkowego oraz śladowe prądy kanałów wapniowych i potasowych. Aktywność potwierdzono również dla ekstraktów farmakopealnych zawierających kumaryny.

Odkrycia te mogą mieć wpływ na tradycyjne stosowanie korzeni dzięgli w leczeniu cukrzycy typu 2. Stwierdzono działanie insulinotropowe trzech farmakopealnych korzeni dzięgli, a ich profil metaboliczny skorelowano z aktywnością farmakologiczną, zidentyfikowano kluczowe struktury odpowiedzialne za modulację wydzielania insuliny. Zbadano mechanizm działania wybranych aktywnych metabolitów. Aktywne metabolity roślinne mogą również stać się wiodącymi strukturami w poszukiwaniu nowych terapii przeciwcukrzycowych.

Słowa kluczowe: cukrzyca typu 2, funkcja komórek beta trzustki, mechanizm działania, kumaryny, flawonoidy, lignany.

Title: Effects and underlying mechanism of plant secondary metabolites on insulin secretion regulation

Type 2 diabetes mellitus (T2DM) is a disease that associates insulin resistance and pancreatic β-cell dysfunction. Based on the current understanding of the pathophysiology of this disease, multiple anti-diabetic therapies have been developed to improve glycemic control and slow disease progression. Nevertheless, they have limited effectiveness and numerous side effects. In this context, plant extracts and their active constituents are considered an important area of seeking new anti-diabetic treatments.

This thesis aimed to find a natural source of secondary plant metabolites potentially able to protect β-cell function, induce insulin secretion in a glucose-dependent manner, and elucidate their mechanism of action.

Twenty plant extracts were phytochemically profiled using LC-MS, leading to identification and isolation of 39 pure compounds. Flavonoids, lignans and coumarins were screened for their ability to modulate β-cell function on INS-1 cell model. Some of the flavonoids and coumarins increased glucose-induced insulin secretion, while no such effect was observed for lignans. The mechanism of action of active metabolites was then investigated, by assessing their effects on cell electrical activity, intracellular calcium levels, and trace currents of calcium and potassium channels. The activity was also confirmed for pharmacopeial extracts containing coumarins.

These findings may have implications on the traditional use of angelica roots in treating T2DM. Insulinotropic effects of three pharmacopeial angelica roots were found and their metabolite profiles were correlated with pharmacological activity, with key structures responsible for modulation of insulin secretion identified. Mechanism of action of chosen metabolites was studied. Active plant metabolites may also become lead structures in the search for new anti-diabetic treatments, which should be further evaluated.

Keywords: type 2 diabetes, pancreatic beta-cell function, mechanism of action, coumarins, flavonoids, lignans.